DEVELOPMENT AND ASSESSMENT OF SUSTAINED RELEASE STAVUDINE LOADED MICROPARTICLES

A Thesis Submitted to Rhodes University in

Fulfilment of the Requirements for the Degree of

MASTER OF SCIENCE (PHARMACY)

By

Chiedza Cathrine Zindove

February 2014

Faculty of Pharmacy
Rhodes University
Grahamstown
South Africa

ABSTRACT

Stavudine (D4T) has been used as first line treatment for HIV/AIDS and is part of highly active anti-retroviral treatment (HAART). It is an affordable medicine and its use is beneficial in resource limited settings. However D4T exhibits dose dependent side effects that may lead to non-adherence in patients. This study was undertaken to formulate, develop and manufacture a dosage form that could reduce dose dependent side effects by decreasing the dose of D4T but still exhibit antiretroviral (ARV) activity. The use of sustained release (SR) formulations of D4T that ensure constant levels of the D4T in the body would not only optimize therapy but also reduce the incidence of side effects thereby increasing patient adherence. SR microparticles containing 30mg D4T were manufactured and loaded into size 3 hard gelatine capsules prior to analysis.

The D4T microparticles were manufactured by microencapsulation using non-aqueous oil-in-oil solvent evaporation approach. D4T-excipient, excipient-excipient interactions and D4T purity were assessed using Infrared Spectroscopy (IR), Differential Scanning Calorimetry (DSC) and Thermogravimetric Analysis (TGA). Copolymers synthesized from acrylic and methacrylic acid esters viz., Eudragit® RSPO and S100 were used as rate retardant materials and the effect of microcrystalline cellulose (Avicel® PH102) on the microparticles was also investigated. Magnesium stearate was used as a droplet stabilizer and n-hexane was added to harden the microspheres formed in a liquid paraffin continuous phase. The microparticles were optimized using a Box Behnken design and Response Surface Methodology (RSM). The microparticles were characterized in terms of their flow properties and encapsulation efficiency (% EE), in addition to visualization of the surface morphology with Scanning Electron Microscopy. *In vitro* D4T release studies were performed using USP Apparatus III in media of different pH and the samples were analysed using a validated High Performance Liquid Chromatographic (HPLC) method with ultraviolet (UV) detection that had been developed and optimized using a Central Composite Design (CCD). The method was validated according to ICH guidelines.

The IR spectra and DSC thermographs revealed that D4T exhibited thermal stability and there was no evidence of D4T-excipient and excipient-excipient interactions. The microparticles that were produced were white, free flowing and were obtained in a high yield with high encapsulation efficiency. Scanning Electron Microscopy studies revealed that the

microparticles were spherical and porous in nature. *In vitro* D4T release extended to 12 hours and the mechanism of release was established using model dependent methods by fitting the data to a Zero-order, First order, Higuchi and Hixson Crowell model. It was observed that the mechanism of D4T release was diffusion-controlled and that the data was best fitted to the Higuchi model with correlation coefficients > 0.9. The release mechanism was confirmed using the Korsmeyer-Peppas model that revealed that most of the formulations exhibited anomalous transport kinetics with the release exponent, n, ranging from $0.5<n<1.0$. These data suggest that diffusion was not the only mechanism controlling D4T release and that swelling and/or polymer relaxation may contribute to the release. Model-independent analysis for comparison of dissolution profiles was undertaken and the f_1 and f_2 difference and similarity factor were calculated. The optimized formulation, Batch BB-018 was found to be similar to two batches (BB-005 and BB-016). The dissolution profiles were evaluated to establish which of the batches exhibited D4T release that was appropriate for SR dosage forms.

In conclusion polymethacrylate copolymers were successfully used to produce SR D4T microparticles that have the potential to be used for a twice a day dosing of D4T.

ACKNOWLEDGEMENTS

First and foremost I would like to acknowledge the Almighty God for his constant divine protection, his favour, for his constant faithfulness, his promises that do not return to him void and his everlasting love. I thank the Almighty God for being my guide and making this degree possible!!

I would like to express my sincere gratitude to the following:

My supervisor, the Head and Dean of Pharmacy Professor R. B. Walker for giving me the opportunity to be a member of his research group. I thank you for your support, motivation, inspiration, continuous words of encouragement, guidance and expertise throughout my studies. Even when I thought there was no more hope for me and I was about to give up I thank you for your continuous faith in me.

My co-supervisor Dr S. M. M. Khamanga for his patience and constant support, I thank you for helping with response surface methodology. For always encouraging me to go on and that all would be well, I am forever thankful.

Dr Kasongo wa Kasongo for his support and guidance.

My colleagues in the Biopharmaceutics research institute for the constant motivation and friendship throughout my studies.

Aspen Pharmacare (Port Elizabeth, South Africa) for the donation of stavudine and zidovudine.

Mr Tich Samkange for always being there when I needed your technical assistance and for always being reliable and dependable, I thank you.

Mr L. Purdon, Mr C. Nontyi, and Mr D. Morley for technical assistance, I thank you.

My Mum, I would not have done this without your constant support and sweet words of motivation and always offering an ear to listen and try to understand pharmaceutics even when it did not make sense to you. I thank you for the financial support throughout my studies. I would not have done it without you, I love you mama and you are special to me.

My father and my sisters Emma and Vongai, I thank you for your prayers and support.

My friends and all those who prayed for me, made me laugh and made life worth living I would like to express my sincere gratitude.

STUDY OBJECTIVES

The HIV/AIDS epidemic is one of the greatest challenges to the well-being of society globally. Presently there is no cure for HIV/AIDS and continued research and development is required to assist people living with HIV/AIDS to lead manageable lives. D4T is a potent ARV compound that is commonly used in first-line combination therapy to treat HIV infection. It is affordable in comparison to other ARV intended for the same use in resource limited settings where public health issues are prevalent. However D4T exhibits serious dose dependent side effects including lipodystrophy, peripheral neuropathy and lactic acidosis. These side effects are debilitating and patients on D4T therapy tend to default taking medication. The dose dependent nature of the side effects may be as a result of dose dumping as all commercially available D4T products are immediate release technologies. Lowering the dose through the use of a SR formulation to maintain constant levels in the body could be beneficial and improve patient adherence thereby improving the quality of life of patients treated with D4T.

The objectives of this study were:

1. To develop, validate and optimize a simple, sensitive, accurate and precise HPLC method with UV detection using RSM for the quantitation of D4T in pharmaceutical dosage forms.
2. To identify polymers and excipients for use in developing SR D4T microparticles.
3. To elucidate possible D4T-excipient and excipient-excipient interactions in addition to the purity of D4T using IR, DSC and TGA.
4. To use RSM to develop and optimize SR microparticle formulations.
5. To assess D4T microparticles in terms of cumulative % D4T released, surface morphology, encapsulation efficiency and flow properties.
6. To elucidate the mechanisms of D4T release from microparticles.

TABLE OF CONTENTS

LIST OF TABLES

LIST OF FIGURES

CHAPTER 1

STAVUDINE

1.1 INTRODUCTION

Human Immuno-Deficiency Virus (HIV) and Acquired Immuno Deficiency Syndrome (AIDS) commonly referred to as HIV/AIDS constitute one of the most serious infectious disease challenges to public health globally [1]. HIV/AIDS has had a crippling effect internationally and particularly in sub-Saharan Africa [1]. The HIV retrovirus has specificity and targets helper/inducer T-cells leading to their depletion *in vivo*. Depletion of these cells leads to immuno-suppression which predisposes HIV patients to life-threatening opportunistic infection(s) [2]. There is no cure for HIV and drug discovery and product development studies have been undertaken in an attempt to decrease viral load, improve quality of life of patients and where appropriate, provide prophylaxis at an affordable cost for all infected with the virus. Nucleoside reverse transcriptase inhibitors (NRTI) have been effectively used in HAART and significantly reduce viral load in patients treated for prolonged periods [3].

D4T is a potent ARV compound that is commonly used in first-line combination therapy to treat HIV infection. It is a NRTI that has been approved by Food and Drug Administration (FDA), Medicines Control Council (MCC), Center for Drug Evaluation and Research (CDER) and several other regulatory agencies for the treatment of HIV infection. At high doses D4T has the potential to cause significant and potentially life-threatening adverse reactions including lactic acidosis, lipo-dystrophy and peripheral neuropathy [4, 5]. The mechanism of action that causes toxicity is not known but it has been hypothesized that defective mitochondrial DNA replication resulting from inhibition of mitochondrial DNA polymerase by nucleoside analogues is implicated in the toxicity [6-10]. Most industrialized countries no longer recommend D4T as a first-line option for ARV therapy due to its toxicity. However, in many low- and middle-income countries D4T remains an important component of first-line ARV therapy. Despite significant advances that have been made in understanding the modes of action of HIV infection and identifying treatment approaches, the search for optimum treatment strategies for HIV and AIDS remains a major challenge [1].

Studies have shown that novel drug delivery systems present an opportunity to overcome the many challenges associated with difficult therapeutic strategies [1]. The use of microparticles

as drug delivery systems may be appropriate to reduce toxicity by sustaining drug release and reducing the need for frequent dosing and further, permits administration of lower doses thereby potentially improving quality of life [11]. D4T has an elimination half-life of 1.5 hours and the fact that it has a short half-life makes it suitable for inclusion in a SR dosage form [12]. D4T is commercially available as 15, 20, 30, 40 mg immediate release capsules and as a 1mg/ml powder for reconstitution for use as an oral solution [12].

The brand names of D4T products commercially available in South Africa include Zerit®, Aspen Stavudine®, Auro-Stavudine®, Sonke-Stavudine®, Stavir® [12].

1.2 PHYSICO-CHEMICAL PROPERTIES

1.2.1 Description

D4T is a NRTI that is a nucleoside pyrimidine analogue. It is chemically known as 1-[(2R,5S)-5-(hydroxymethyl)-2,5-dihydrofuran-2-yl]-5-methylpyrimidine-2,4(1H,3H)-dione, 1-(2,3-dideoxy-β-D-glycero-pent-2-enofuranosyl)-5-methylpyrimidine-2,4(1H,3H)-dione(D4T) and 2',3'-didehydro-3'-deoxythymidine [13-16]. D4T exists in one of two polymorphic forms, of which Form 1 is stable, as a hydrate and in several solvate forms. The two polymorphic forms are mono-tropic and are related [17]. The chemical structure of the most stable polymorph of D4T is depicted in Figure 1.1.

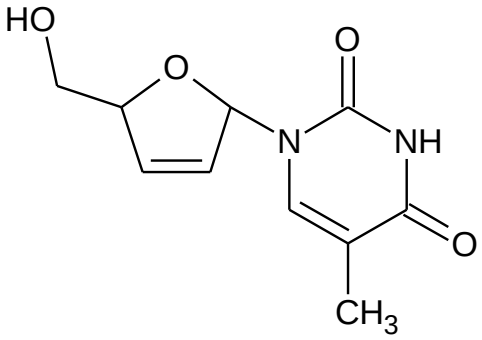

Figure 1.1 Structure of D4T

D4T occurs as a white to almost white powder and has a molecular weight of 224 daltons. It contains not less than 97.0 % and not more than 102.0% $C_{10}H_{12}N_2O_4$ calculated with reference to the anhydrous form [13, 14].

1.2.2 Solubility

The pH–solubility profile of D4T at 37.0 ± 0.5°C was determined in 0.01 N HCl, acetate buffer at pH 4.5 and phosphate buffer at pH 6.8 [18]. The solubility of D4T as a function of pH is depicted in Figure 1.2. D4T showed the highest solubility in acetate buffer,

intermediate solubility in HCl acid and lowest solubility in phosphate buffer [18]. This information is important and helpful when predicting bioavailability, developing analytical methods and for dissolution method development. A summary of the solubility of D4T in a variety of solvents is shown in Table 1.1. D4T has high aqueous solubility compared to other solvents and this is important to know as it is vital in determining potential *in vitro* and *in vivo* performance in addition to establishing the formulation design.

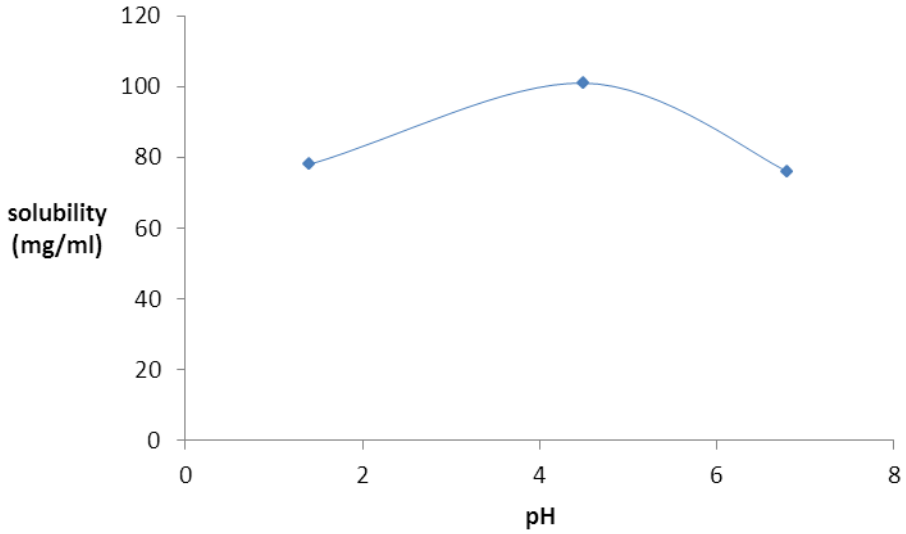

Figure 1. 2 Solubility of D4T as a function of pH

Table 1. 1 Solubility of D4T

Solvent	Solubility	Reference
Water	83mg/ml (freely soluble)	19
Propylene glycol	30mg/ml (sparingly soluble)	16
Ethanol	Slightly soluble	16
Methanol	Slightly soluble	16
Isopropanol	Slightly soluble	16
Acetone	Sparingly soluble	16

1.2.3 Partition coefficient

The n-octanol/water partition coefficient of D4T at 23° C is 0.144 [20]. This is a measure of how hydrophilic or hydrophobic D4T is. The low value shows that D4T is very hydrophilic and the information is essential in determining the *in vitro* and *in vivo* performance.

1.2.4 Dissociation constant (pKa)

D4T is non-ionized at physiological pH and the pKa of the molecule is 10. The pH of a 1µg/ml aqueous solution of D4T is 4.5- 6.1. The molecule is weakly acidic and is absorbed

throughout the GIT. It is important to know the pKa during formulation development in order to determine the type of dosage form to be manufactured [20].

1.2.5 Hygroscopicity

D4T is extremely hygroscopic and must be stored appropriately [16].

1.2.6 Melting range

The melting point of D4T is 159-160°C [15].

1.2.7 Infrared absorption spectrum (IR)

Infrared spectroscopy is a sensitive, rapid and simple technique used to assist the structural elucidation of organic molecules [21]. The approximate position of an infrared absorption band is determined by a vibrating mass and the type of bond, the exact position of electron withdrawing or donating effects of intra- and inter-molecular environments coupled with other existing vibrations. The strength of the absorption band increases as the polarity of the vibrating bonds increases [21]. The IR spectrum of D4T was determined in the range 4000-600cm^{-1} using a Perkin-Elmer® Precisely FT-IR Spectrometer Spectrum 100 (Perkin-Elmer® Pty Ltd, Beaconsfield, England). The IR spectrum of D4T is depicted in Figure 1.3 and the relevant band assignments are summarized in Table 1.2.

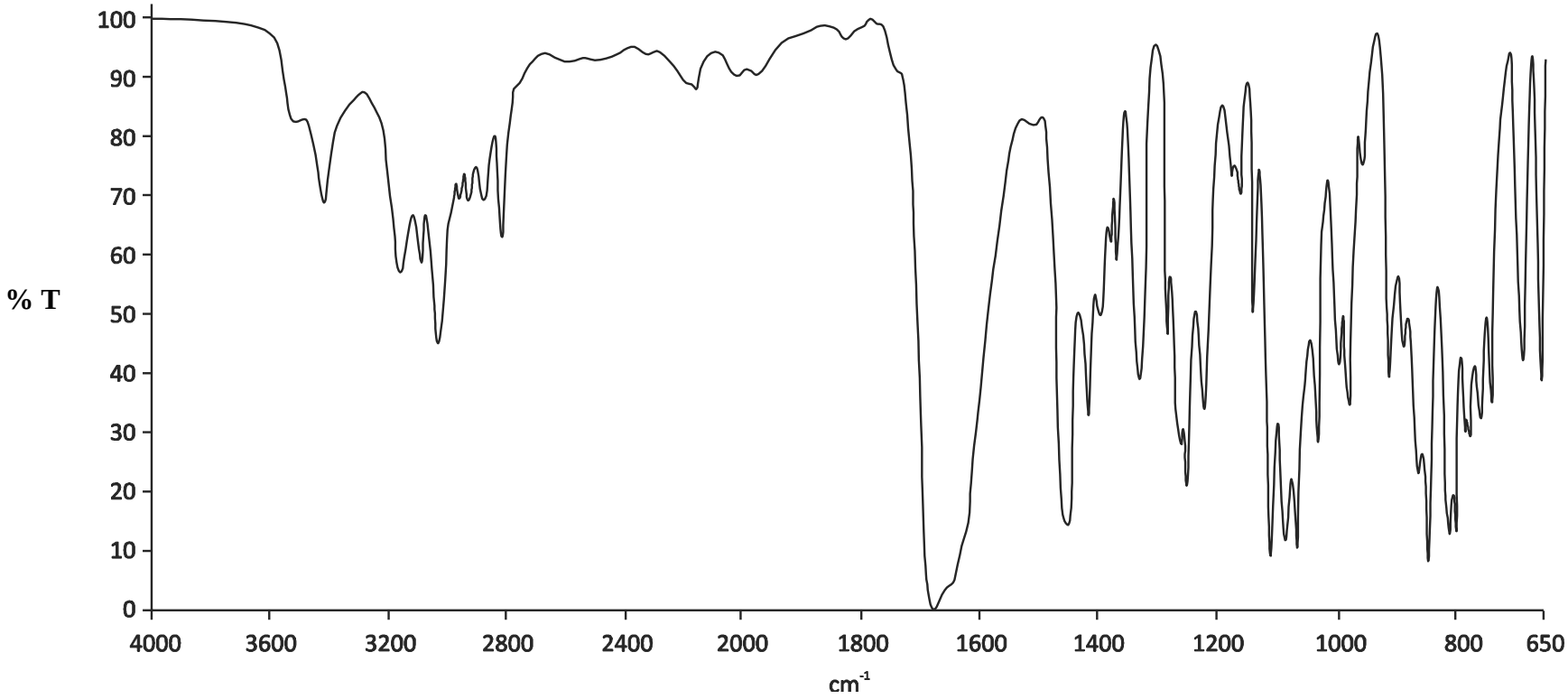

Figure 1. 3 Infrared absorption spectrum of D4T

Table 1. 2 IR band assignments for D4T

Major band frequencies (cm^{-1})	Assignment
3422	OH stretch of hydroxyl group
3161	NH stretching of secondary amine
3039	CH stretch
2875	CH stretching of CH_3 group
1691	C=O stretching of aromatic structure
1113	C-C stretch
1088	C-H scissoring and bending
848	NH bend

The principal peaks for D4T are found at wave numbers 3422, 3161, 3039, 2875, 1691, 1457, 1113, 1088, 848cm^{-1} and are similar to the values reported in the literature [21, 22]. It is important to know the principal peaks of D4T in order to establish whether interactions or incompatibilities are likely to occur during formulation development studies.

1.2.8 Ultraviolet absorption spectrum (UV)

The ultraviolet absorption spectrum of D4T in a solution of methanol and water in a ratio of 35.5:64.5 v/v at a concentration of 25µg/ml is shown in Figure 1.4. The spectrum was generated using a double beam Model GBC 916 UV VIS spectrophotometer (GBC Scientific Equipment Pty Ltd, Melbourne, Victoria, Australia). The wavelength of maximum absorption (λ_{max}) for D4T was 265.9 nm with a corresponding absorbance value of 0.8588. The λ_{max} is similar to values quoted following the use of compendial methods for the quantitation of D4T in pharmaceutical dosage forms and was used for the analysis of D4T using a validated RP-HPLC method that was developed and validated as reported in Chapter 2 *vide infra* [13, 14].

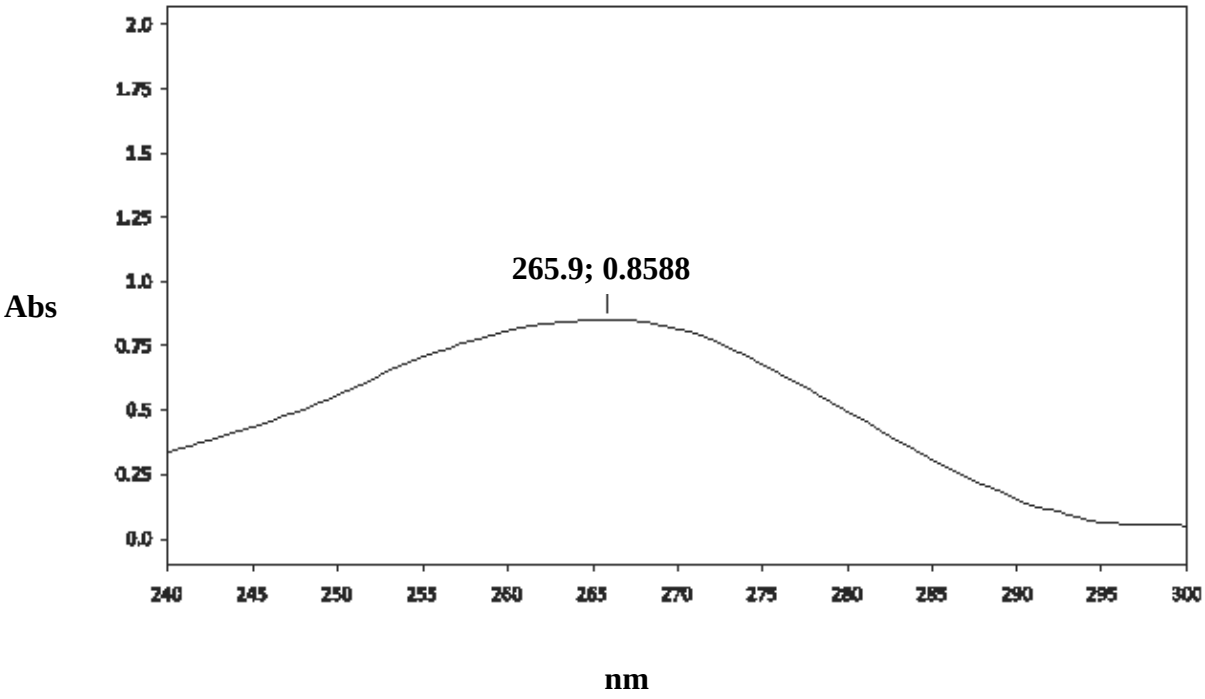

Figure 1. 4 Ultraviolet absorption spectrum of D4T in a solution of methanol and water in a ratio of 35.5:64.5 v/v

1.3 SYNTHESIS

1.3.1 Synthetic pathway

Perusal of the literature reveals that only a few methods for the synthesis of D4T have been reported and in general these are tedious, not economically feasible as they require expensive reagents, result in low yields and are therefore not viable for large scale synthesis of D4T. The synthesis of D4T by two different methods was first reported by Horwitz *et al* [23]. The first synthetic route involves subjecting the 3', 5'-anhydro derivative of thymidine to an elimination reaction under strongly basic conditions [24]. The second route involves subjecting the 5'-O-protected 2, 3'-anhydro nucleoside derivative of thymidine to a ring-opening elimination reaction under basic conditions followed by de-protection to yield D4T. Both methods involve the use of a strong base and polar solvents such as dimethyl sulfoxide (DMSO) and dimethyl formamide (DMF) and require the use of a high vacuum and temperatures of approximately 0.01 mmHg and 0°-50° C respectively to distil the solvents from the reaction mixture [23].

Following discovery of the potency of D4T as an anti-HIV agent, a process which permitted 2', 3'-dideoxy-2', 3'-didehydronucleosides, including D4T to be synthesized relatively cheaply and on a large scale was necessary. The Horwitz route of synthesis that produces D4T from the 3', 5'-anhydro compound was not feasible due to prolonged exposure to basic

conditions at high temperatures, which in turn leads to decomposition of D4T by cleavage of the glycosidic bond, resulting, in the formation of thymine, which is undesired and a decreased overall yield and purity of the final product. To overcome these challenges an improved process suitable for large-scale production of 2',3'-didehydro-3'-deoxythymidine (D4T) had to be developed to produce high yields and purity without the use of hazardous reactions or reagents [2, 23-25].

Mansuri *et al*., attempted to improve the synthesis of D4T by producing the potassium salt of D4T as an oily solid by dilution of the DMSO reaction mixture with toluene prior to further processing [26]. However the volumes of material to be used on a large scale were unmanageable and generated large volumes of waste solvents, which were difficult to recover. Furthermore the salt was sensitive to moisture and required excessive drying [25-29].

The Mansuri process was modified by Starrett *et al.* [2] in an attempt to overcome these drawbacks. Their approach involved subjecting the 3', 5'anhydro intermediate of thymidine to an elimination reaction using a strong base in polar solvents such as DSMO/DMF at room temperature (22˚C), followed by precipitation of the resulting potassium salt of D4T by addition of solvents such as toluene, acetone and/or ethyl acetate [27, 28]. The resultant salt was then dissolved in a minimum quantity of water, neutralized with acid and recrystallized from acetone [2, 26].

Despite the fact that the method proposed by Starrett *et al.* was an improvement, there are still a number of drawbacks. The isolation of the potassium salt is tedious and the neutralisation process of the potassium salt is an exothermic process that can lead to the decomposition of D4T to form thymine [24].

A different approach used to minimize product decomposition involves replacement of KOt- in the reaction process with hexamethylphosphoric triamide (HMPA) and sodium hydroxide. This approach eliminates decomposition since the HMPA solvent can be removed from aqueous solution as a chloroform complex. However, the use of highly toxic agents such as HMPA and chloroform that are reputed to be carcinogens may be a hazard when used on a large scale and should be avoided [30]. A route of synthesis using phenylselenyl thymidine derivative was reported by Cosford *et al* [25, 31].

A two-step synthetic process for the production of D4T on a large scale in high yields and acceptable purity has been reported [24] and is depicted in Figure 1.5. The process incorporates a number of improvements on previously reported approaches involving the use of inexpensive reagents and non-hazardous solvents such as acetone rather than solvents reported for other synthetic processes. Furthermore this approach uses relatively mild bases such as KOH and *t*-BuOH as solvent [24]. In addition, the process can be conveniently applied for use on an industrial scale.

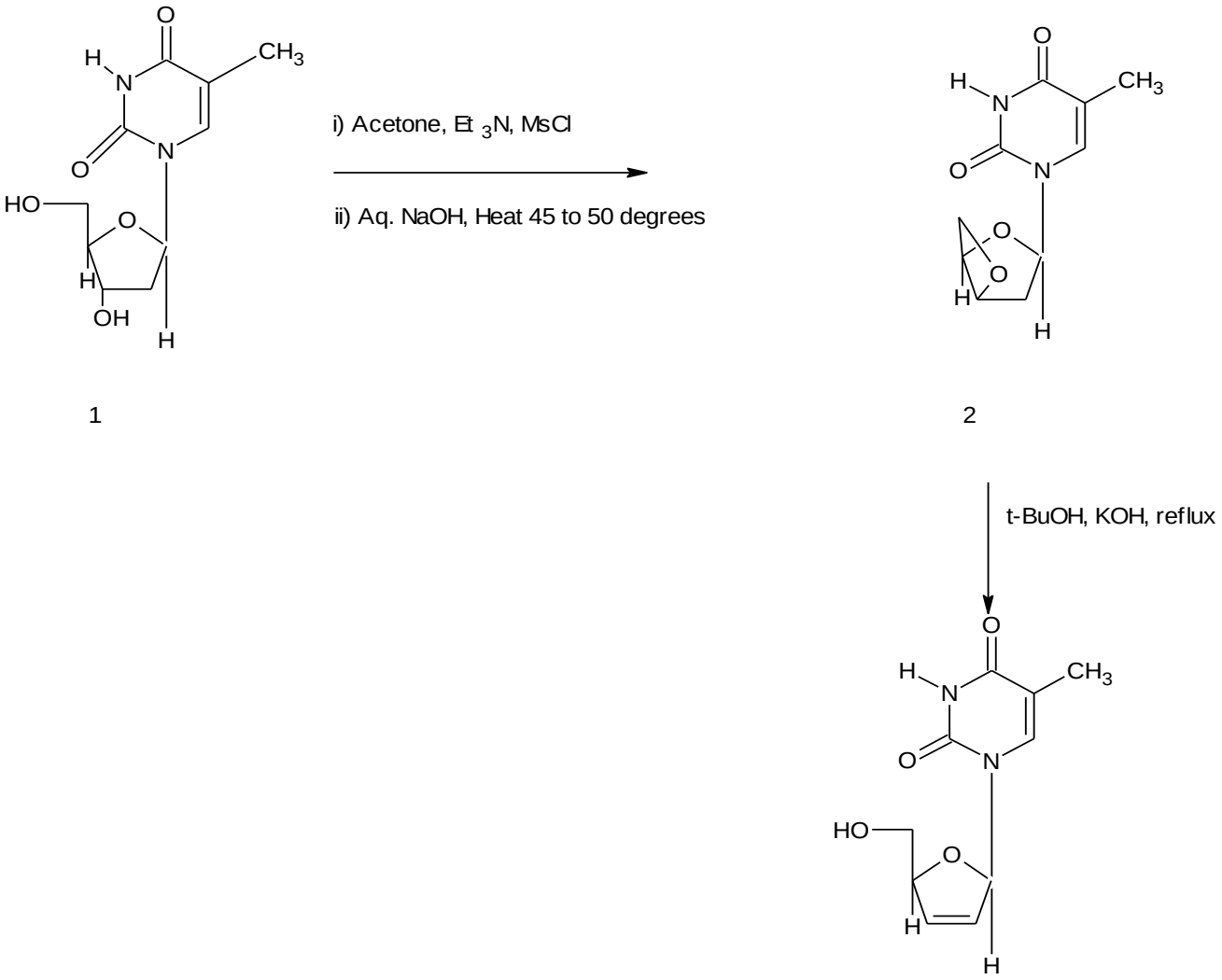

1 2

Figure 1. 5 A two-step synthetic process for the production of D4T on a large scale in high yields [24].

During the initial step of the process (1) thymidine is converted to the intermediate dimesylated thymidine (2) by reacting thymidine and mesyl chloride. Improvements in this step involve the use of a polar solvent acetone and about 2 to 4 equivalents of an organic base stronger than pyridine but weaker than triethylamine, N-methylmorpholine [29]. Following concentration of the solvent the reaction mass is treated with aqueous sodium hydroxide to obtain a reactive intermediate viz., 3', and 5'-anhydrothymidine, which chemically is an oxetane. During conversion of the dimesylated thymidine to 3',5'-anhydrothymidine the primary mesylate undergoes base hydrolysis and subsequently displaces the secondary mesylate through an intramolecular nucleophilic substitution reaction [24].

The second step of the process involves subjecting the oxetane to an elimination reaction by treatment with potassium hydroxide in *t*-butanol and following completion of the reaction, methanol is added. The mixture is then neutralised with HCl as a gas in isopropyl alcohol and the potassium chloride precipitate is removed by filtration. Following concentration of the solvent the product is recrystallized from acetone to yield D4T via an elimination mechanism [24].

1.3.2 Structure activity relationships

All NRTI are nucleoside pyrimidine analogues that share the same structural skeleton consisting of deoxyribose and thymine, commonly known as thymidine and is depicted in Figure 1.6. Nucleosides are converted into nucleotides in cells and are the molecular building blocks for viral DNA by a process of phosphorylation of the 5' hydroxyl group of the deoxyribose sugar. Modification of the 5' hydroxyl group markedly reduces the antiviral activity of such compounds [32]. NRTI compete with natural deoxynucleotides for incorporation into growing viral DNA chains. However unlike natural deoxynucleotides substrates NRTI lack a 3'-hydroxyl group on the deoxyribose moiety and following incorporation of an NRTI the next incoming deoxynucleotide cannot form a 5'-3' phosphodiester bond that is needed to extend the DNA chain [33]. Therefore incorporation of an NRTI results in the cessation of viral DNA synthesis by a process known as chain termination. The first NRTI reported to show antiviral activity was observed by substitution of the 3' hydroxyl functional group with an azido (N_3) functional moiety to produce 3'-azido-3-deoxythymidine, further modified by inclusion of a double bond between positions 2' and 3' resulting in the production of D4T. This molecule showed sufficient potency and the antiviral activity was significantly enhanced compared to that observed following azido

substitution. Substitution at position C-5 with chains > 2 carbons in length or including bromovinyl substitution reduces antiviral activity as shown in figure 1.6 [32, 33].

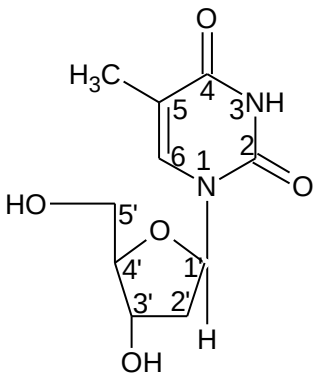

Figure 1. 6 Structure of thymidine

The presence of thymine in the molecular structure is essential for competitive inhibition to take place in the viral cell as the reverse transcriptase enzyme will recognise the moiety and consequently bind to it.

1.4 STABILITY

D4T degrades to form thymine when exposed to solutions in the pH range 1-9 and also undergoes oxidative degradation. A degradation study of D4T conducted under ICH prescribed conditions revealed that D4T decomposed under hydrolytic conditions with an order of sensitivity of acid > neutral > alkali and this is depicted in Figure 1.7. Approximately 50% D4T was oxidised in 30% v/v H_2O_2 after 3 days of exposure. D4T samples stored in 0.01 M HCl, 0.1 M NaOH and in water were exposed to light in a photostability chamber Model KBF 240 Binder (Germany) [34]. The light conditions were 6000 Iux fluorescent and 0.7W/m2 UV light and the samples were analysed 15 days following the commencement of irradiation. All samples showed a similar extent of degradation whether stored in light or dark conditions. It was concluded that light had no effect on the degradation of D4T [34].

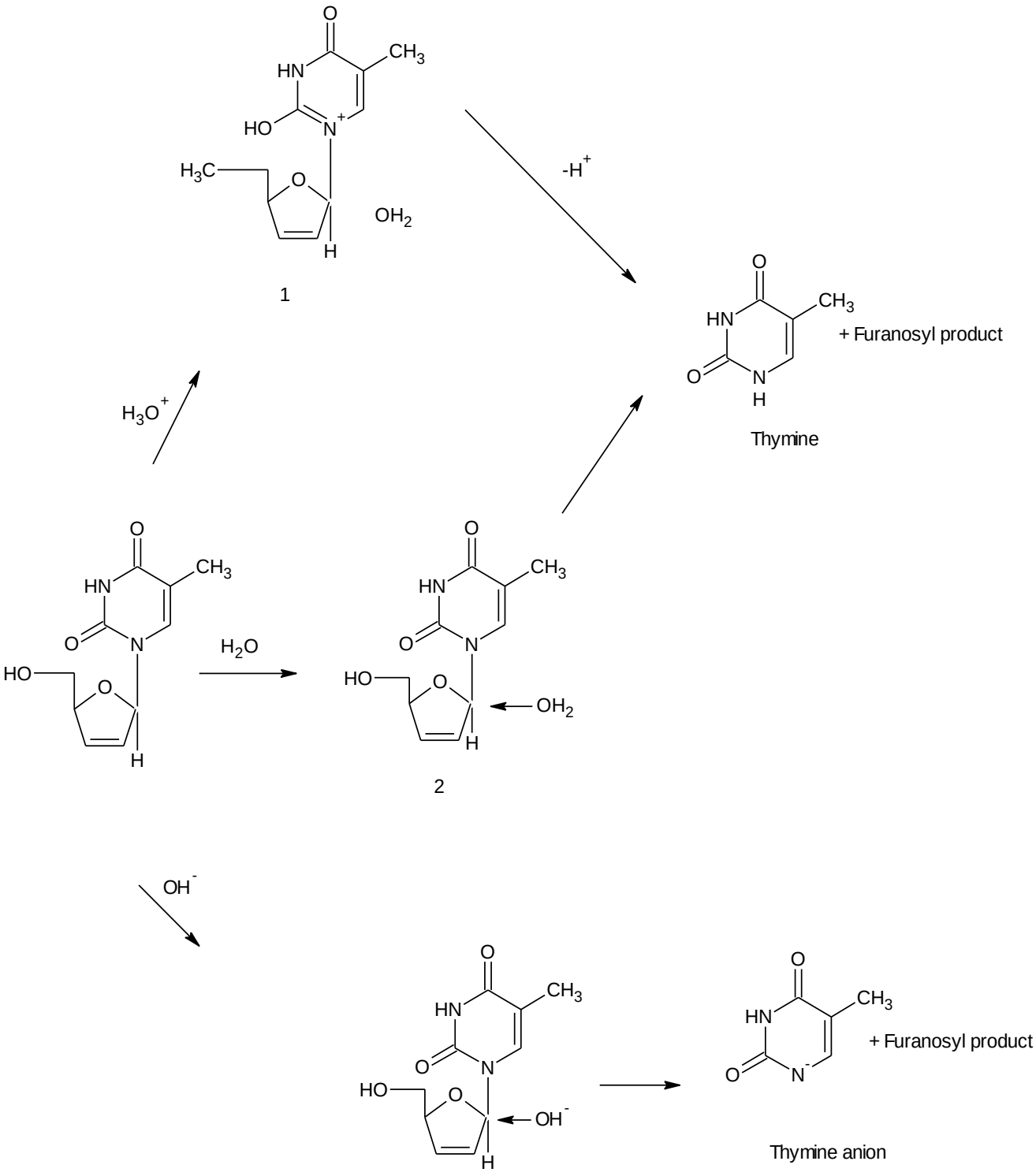

Figure 1. 7 Mechanism of hydrolytic decomposition of D4T [34]

HPLC was used to analyse all samples under all stress conditions where decomposition was observed and decomposition peaks were evident. Analysis of pure thymine confirmed that it was a product formed during hydrolysis and during oxidative degradation of D4T [34].

An important structural feature of D4T that is considered the point for hydrolytic cleavage to form thymine under acidic, neutral and alkaline conditions is the aminal functional group located at C1' shown in Figure 1.8[34]. The aminal nitrogen carries a positive charge under acidic conditions and protonation of the thymine moiety results in the formation of an enol (I) which acts as a leaving group, thereby promoting hydrolytic cleavage. The absence of a positive charge on the aminal nitrogen under neutral conditions results in the thymine moiety being a relatively ineffective leaving group, resulting in a reduced rate of hydrolysis compared to that observed under acidic conditions. In alkaline conditions the liberated thymine anion undergoes electrostatic destabilization resulting in a reduced rate of reaction compared to that observed under acid or neutral conditions, thereby explaining the order of the sensitivity to hydrolysis of acid > neutral > alkali.

It is postulated that in the presence of hydrogen peroxide, the double bond in D4T undergoes oxidation to form an epoxide III as shown in Figure 1.8 [34].

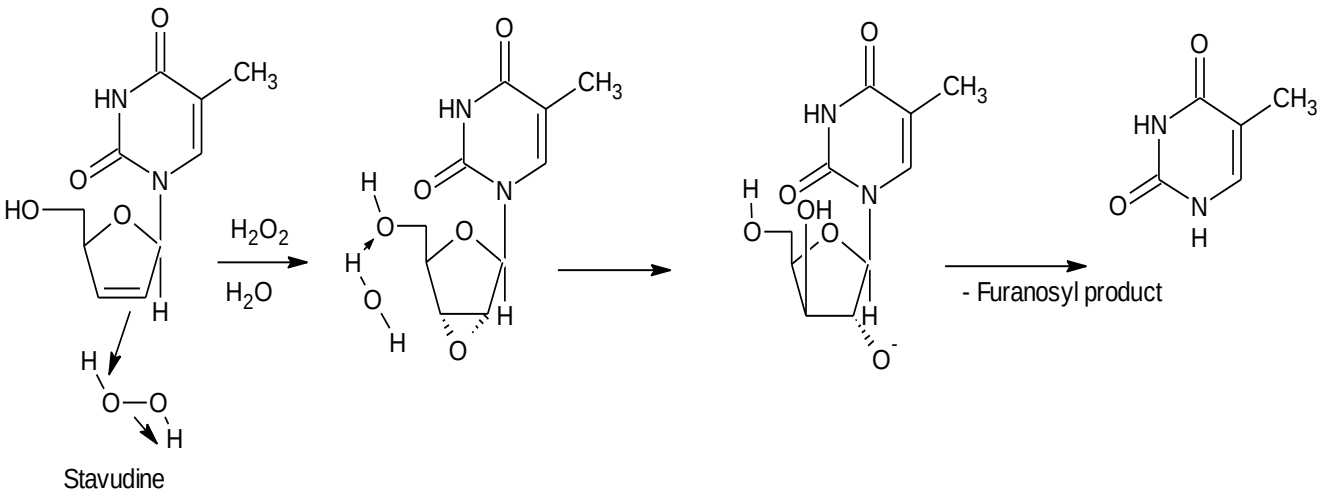

Figure 1.8 Postulated mechanisms for the decomposition of D4T in 30% v/v H_2O_2 [34]

1.5 CLINICAL PHARMACOLOGY

1.5.1 Mechanism of action

D4T enters viral cells rapidly by simple diffusion, with a linear rate of influx in respect to concentration [35]. Following three phosphorylation reactions, D4T is converted intracellularly to 5'-monophosphate, 5'-diphosphate and 5'-triphosphate. The presence of the triphosphate form halts DNA synthesis of retroviruses, including HIV, through competitive inhibition of HIV-encoded reverse transcriptase (RT). Subsequent incorporation into the DNA chain leads to termination of DNA chain elongation as the 3'-hydroxyl function that is required for the formation of the ester linkage with α-phosphate of the next nucleotide is not present (Figure 1.9) [33, 36, 37]. D4T triphosphate also inhibits cellular DNA beta and gamma polymerases and markedly reduces the synthesis of mitochondrial DNA [24, 38-40].

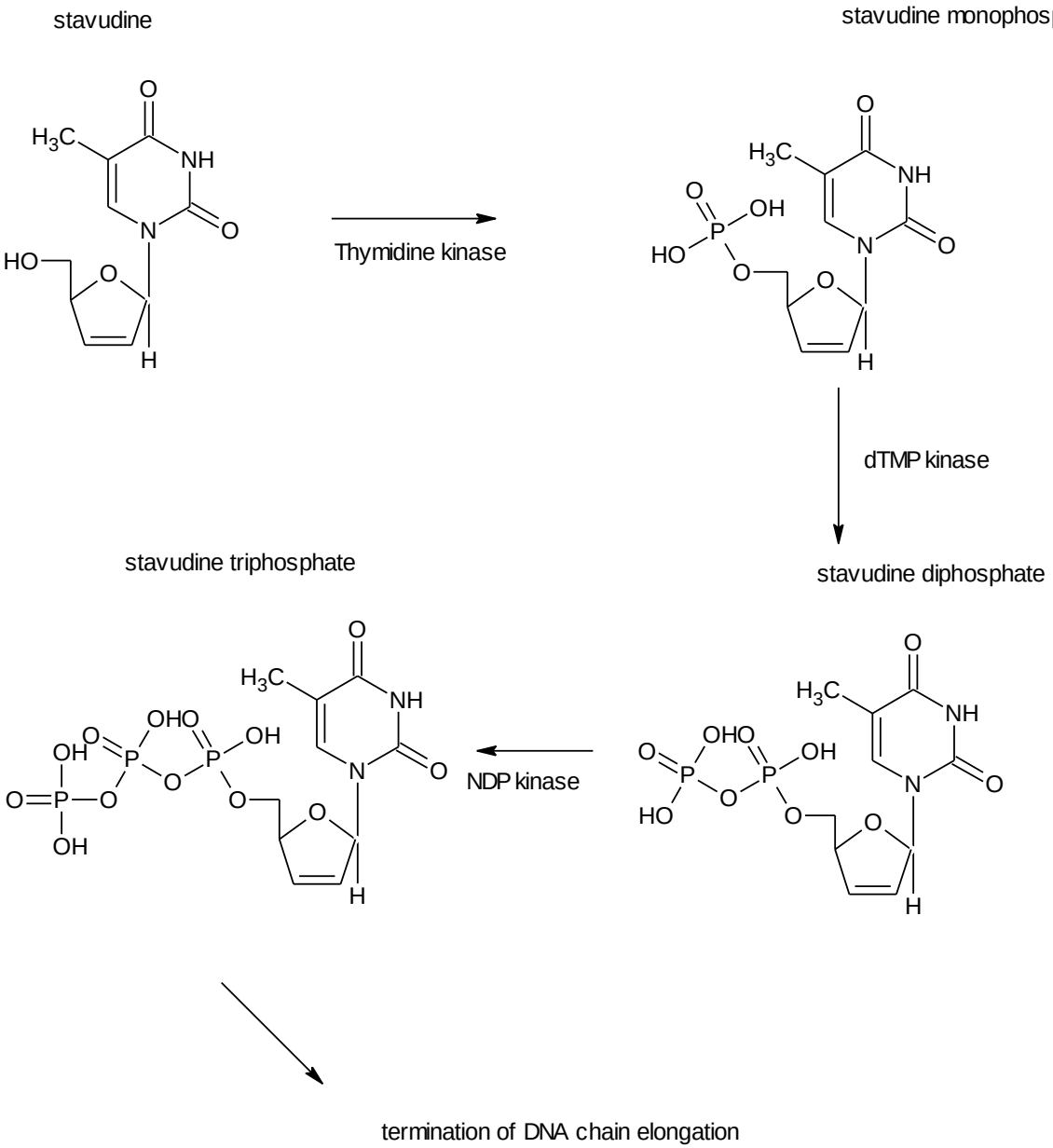

Figure 1. 9 Mechanism of action of D4T [40]

1.5.2 Resistance

The biochemical mechanism of HIV RT resistance to NRTI is due, in many cases, to decreased binding of RT that has mutated to respective NRTI-triphosphate (NRTI-TP) [40, 41]. The emergence of resistance due to mutation in HIV infected patients receiving ARV treatment is one of the most important causes of ARV treatment failure [42]. Whilst NRTI are effective at terminating DNA synthesis and HIV replication, the HIV eventually develops mechanisms that make the virus resistant to these compounds. HIV RT does not have proof-reading activity and combined with selective pressure from the therapy leads to mutations in RT that makes the virus less susceptible to NRTI [41]. Aspartate residues 110, 185, and 186 in the RT polymerase domain are important for the binding and incorporation of nucleotides.

The side chains of residues K65, R72, and Q151 interact with the next incoming nucleotide. Also important is L74 which interacts with the template strand to position it for base pairing with the nucleotide. Mutation of these key amino acids results in reduced incorporation of therapeutic analogues [41].

There are two major mechanisms of NRTI resistance. The first is due to reduced incorporation of the nucleotide analogue into DNA over a normal nucleotide. This results from mutation in the N-terminal polymerase domain of RT that reduces the affinity or ability of the enzyme to bind to the drug. Another well characterized set of mutations occurs in the Q151M complex found in multi-drug resistant HIV which decreases the efficiency of RT to incorporate NRTI but does not affect the incorporation of natural nucleotides [42].

The second mechanism of resistance is the excision or hydrolytic removal of incorporated drug. This is the reverse of the polymerase reaction in which the pyrophosphate/PPI released during nucleotide incorporation reacts with the monophosphate drug, resulting in the release of triphosphate drug. The result is that the DNA chain is 'unblocked', allowing it to be extended and replication to continue. Excision enhancement mutations, typically M41L, D67N, K70R, L210W, T215Y/F, and K219E/Q are selected for by thymidine analogues such as D4T and are therefore called thymidine analogue mutations (TAM) [42].

1.5.3 Indications

D4T is indicated for the treatment of HIV infection in combination with other ARV agents. D4T is also used for prophylaxis and the prevention of opportunistic infections. If you treat with D4T the viral load is reduced and therefore immune-suppression is not realised and therefore opportunistic infections do not manifest [12, 15, 16, 20].

1.5.4 Contra-indications

D4T is contradicted in patients with known hypersensitivity to the drug or to any of the components contained in the formulation [12, 20].

1.5.5 Drug interactions

The intracellular phosphorylation of D4T and hence its antiviral effect may be competitively inhibited by Zidovudine [20]. *In vitro* data indicate that phosphorylation of D4T is inhibited at relevant concentrations by doxorubicin. The clinical significance of this interaction is unknown and concomitant use of D4T with doxorubicin should therefore be undertaken with caution [20]. *In vitro* data indicate that ribavirin reduces phosphorylation of D4T and the clinical significance of the interaction with D4T is unknown, therefore concomitant use of

D4T with ribavirin should be undertaken with caution [12, 20]. Concurrent administration of D4T with other drugs known to cause pancreatitis, such as, intravenous pentamidine or peripheral neuropathy, such as metronidazole, isoniazid and vincristine, should be avoided [20].

1.5.6 Precautions and warnings

Lactic acidosis/ severe hepatomegaly with steatosis, including fatal cases, have been reported with the use of nucleoside analogues when used alone or in combination. Particular caution should be exercised when administering D4T to any patient with known risk factors for liver disease, however cases of lactic acidosis have also been reported in patients presenting with no known risk factors. Generalized fatigue, digestive symptoms including nausea, vomiting, abdominal pain and unexplained weight loss, respiratory symptoms such as tachypnea and dyspnoea or neurologic symptoms, including motor weakness, might be indicative of the development of symptomatic hyperlactatemia or lactic acidosis syndrome [20].

D4T should be used with caution in patients with a history of peripheral neuropathy, and treatment should be suspended if peripheral neuropathy develops. If symptoms resolve on withdrawal of D4T it may be resumed at doses 50% of those previously administered. Dose adjustment should be considered if the levels of liver enzymes are significantly raised. Patients with a history of pancreatitis should also be carefully monitored for signs of pancreatitis during treatment. D4T should also be used with caution in patients with renal impairment [12, 20].

1.5.6.1 Fat Redistribution

Redistribution and/or accumulation of body fat including central obesity, dorsocervical fat enlargement (buffalo hump), peripheral wasting, facial wasting, breast enlargement and a ‘cushingoid appearance’ have been observed in patients on ARV therapy. Patients receiving D4T should be monitored for symptoms or signs of lipo-atrophy or lipo-dystrophy and medical consultation should include questions about body changes related to lipo-atrophy or lipo-dystrophy [12, 20].

1.5.6.2 Immune reconstitution syndrome

Immune reconstitution syndrome has been reported in patients treated with combination ARV therapy that includes D4T. During the initial phase of combination therapy the immune system of some patients responds and they may develop an inflammatory response to residual opportunistic infections such as *Mycobacterium-avium*, cytomegalovirus, *Pneumocystis*

carinii pneumonia (PCP) or tuberculosis which will necessitate further evaluation and treatment.

Autoimmune disorders such as Graves' disease, polymyositis, and Guillain-Barré syndrome have also been reported to occur in the setting of immune reconstitution, however the time to onset is more variable and can occur many months after the initiation of therapy [20].

1.5.7 Adverse Effects

Major adverse effects of D4T include dose-related peripheral neuropathy which is characterised by numbness, tingling or pain in the hands and/or feet. Raised liver enzyme levels may also be observed during treatment. Lactic acidosis is also a major side effect of D4T and symptoms include unexplained weight loss, abdominal discomfort, nausea, vomiting, fatigue, dyspnoea and motor weakness.

Other adverse effects include asthenia, chest pain, hypersensitivity reactions, an influenza-like syndrome including dizziness, headache, insomnia and abdominal pain, anorexia, constipation, diarrhoea, nausea, vomiting, neutropenia, thrombocytopenia, arthralgia and myalgia, mood changes, dyspnoea, pruritus and rashes, lymphadenopathy and neoplasms. Pancreatitis has rarely been reported [12, 19, 20].

1.5.8 High Risk Groups

1.5.8.1 Geriatric patients

There are insufficient clinical data relating to the use of D4T in patients aged > 65 years to determine whether they respond differently to therapy in comparison with younger patients. Greater sensitivity of some older individuals to the effects of D4T cannot be ruled out and further studies are needed to establish whether there are likely to be therapeutic challenges in geriatric patients [12, 20].

1.5.8.2 Pregnancy

D4T is listed in the Pregnancy Category C list and healthcare providers caring for HIV-infected pregnant women receiving D4T should be alert to the possibility of lactic acidosis and/or hepatic steatosis syndrome. Fatal lactic acidosis has been reported in pregnant women who were treated with a combination of D4T and didanosine with other antiretroviral agents, and the combination should be used with caution during pregnancy and is recommended only if the benefits of use clearly outweigh the potential risk of use [12, 15, 20].

1.5.8.3 Lactation

Nursing mothers should be instructed not to breastfeed when treated with D4T due to the potential for postnatal HIV transmission. Studies in lactating rats have demonstrated that D4T is excreted in breast milk. Although it is not known whether D4T is excreted in human breast milk there exists the potential for adverse effects due to D4T transmission [12, 20].

1.5.8.4 Renal impairment

Data from two studies in which adults were dosed with D4T indicated that the apparent oral clearance of D4T decreased, the terminal elimination half-life increased and creatinine clearance decreased. Based on these observations it is recommended that the dosage of D4T be modified in patients with a reduced creatinine clearance and in patients on maintenance haemodialysis [12, 20].

1.6 PHARMACOKINETICS

1.6.1 Dosage and Administration

The recommended dosage interval for D4T is 12 hourly or twice daily. D4T may be taken with or without food. The recommended adult dosage of D4T is based on body weight, and patients weighing < 60kg should take 30mg every 12 hours. Those weighing at least 60kg should take 40mg every 12 hours. The recommended paediatric dosage for new-borns from birth to 13 days is 0.5mg/kg every 12 hours. Paediatric patients at least 14 days old and weighing <30 kg should be administered 1 mg/kg every 12 hours, and paediatric patients weighing at least 30 kg should be treated with the recommended adult dose. Dosage adjustment is necessary in the case of renal impairment since urinary excretion is the major route of elimination of D4T [12, 20].

1.6.1.1 Overdosage

Adults treated with 12 to 24 times the recommended daily dosage presented with no acute toxicity. Complications of chronic overdosage include peripheral neuropathy and hepatic toxicity. D4T can be removed by haemodialysis and the mean reported haemodialysis clearance of D4T is 120 ± 18 mL/min. Clearance of D4T following peritoneal dialysis has not been studied [12, 20].

1.6.2 Absorption

D4T is rapidly absorbed following oral administration and has a reported bioavailability of approximately 86% in adults and 76.9% in paediatric patients, with peak plasma

concentrations reported to occur within 1 hour following dosing. Administration with food delays but does not reduce the extent of absorption [12, 15].

1.6.3 Distribution

D4T is able to cross the blood brain barrier and produces a CSF: plasma ratio of about 0.4 approximately 4 hours following administration. The volume of distribution in adults is reported to be 46 L and is 0.73 L/kg in paediatric patients. Protein binding of D4T is negligible. The drug distributes into total body water and appears to enter cells by simple diffusion or passive transport and distributes equally between red blood cells and plasma [12, 15, 16, 20].

1.6.4 Metabolism

Metabolism appears to play a limited role in the clearance of D4T. It is metabolised intra-cellularly by the sequential action of thymidine kinase and dTMP kinase to form the active D4T triphosphate. Minor metabolites include oxidized D4T, glucuronide conjugates of D4T and associated oxidized metabolite and an N-acetylcysteine conjugate of the ribose that occurs following glycosidic cleavage suggesting that thymine is a metabolite of D4T. D4T does not appear to be metabolised to any great extent in the liver [12, 20].

1.6.5 Elimination

The elimination half-life of D4T following administration of a single dose is reported to be 1 to 1.5 hours in adults and 0.96 hours in children between 5 weeks and 15 years of age. The intracellular half-life of D4T triphosphate has been estimated to be 3.5 hours *in vitro*. Approximately 40% of the administered dose of D4T is excreted in the urine between 6 and 24 hours following oral administration. D4T elimination occurs via the kidneys and approximately 40% of the administered dose is excreted unchanged. The renal clearance of D4T is 237 mL/min [12, 15, 16, 20].

1.7 CONCLUSIONS

D4T is a potent antiviral compound that is used for treatment of HIV and prophylaxis to prevent opportunistic infections. The main challenge with the use of D4T is the occurrence of dose dependent side effects following prolonged use and in many countries with unlimited resources the clinical use of D4T has been discontinued. Despite these challenges it is necessary to continue research with D4T due to the fact that it is stable, potent due to structural modification of thymidine, affordable and still has the potential for use in middle- and low- income countries and in sub-Saharan Africa for example.

Newer and more recently developed antiretroviral drugs also present challenges, for example tenofovir, a clinical substitute for D4T, is expensive and is highly nephrotoxic. In reality D4T has potential for use in the future as a means of improving the quality of life of HIV patients.

Stability studies on D4T are essential so as to predict the behaviour of the API when exposed to different conditions when incorporated into formulations, and the short half-life of D4T makes it a suitable agent for incorporation into a SR formulation manufactured by microencapsulation. Sustained drug release has the potential advantage of decreasing side effects, dosing frequency and thereby improve patient adherence to therapy.

CHAPTER TWO

DEVELOPMENT AND VALIDATION OF AN HPLC METHOD FOR THE ANALYSIS OF STAVUDINE

2.1 INTRODUCTION

2.1.1 Principles of HPLC

High Performance Liquid Chromatography (HPLC) is a dynamic adsorption process and is the fastest developing analytical technique for analyzing pharmaceutical formulations [43]. Rapid progress in the use of HPLC has been facilitated by the development of dependable, reasonably priced equipment and efficient columns [44, 45]. HPLC closely resembles gas chromatography (GC) and complements GC as it can be used to analyse substances that are not volatile, have a high degree of polarity, of large molecular weight, display thermal instability or are ionised in solution [46]. HPLC is defined as a separation of compounds encompassing mass transfer of an analyte between a stationary and liquid mobile phase that may be a binary, ternary or quaternary mixture of solvents [44]. The interaction of an analyte with the mobile and/or stationary phases can be manipulated through selection of different solvents and stationary phases [46, 47]. Monitoring a separation is achieved by using a suitable detection system and the response is usually recorded on a computer, integrator or strip chart recorder so as to facilitate the calculation of peak height or peak area [43, 45, 47]. HPLC analysis provides rapid and high resolution separations using stainless steel or glass columns usually 4.6 mm in diameter, packed with particles of 3, 5 or 10μm in diameter [47].

Mixtures of small molecules can be analysed using HPLC and samples can be classified as ionic or neutral. Ionic samples can be further classified as weakly acidic or basic, amphoteric or salts [47, 48]. A number of different modes of HPLC exist and are classified according to the phases used for the separation, such as liquid-liquid chromatography (LLC) or liquid-solid chromatography (LSC), or by the mechanism of retention such as ion-exchange or size exclusion chromatography. LSC is often called adsorption chromatography, and generally in adsorption chromatography the compounds are eluted in reverse order of polarity and a separation can only be achieved using particles with a high surface area [44, 47, 48]. The difference in affinity of the solutes for the surface of the stationary phase facilitates the separation [48, 49].

The stationary phase can be non-polar or polar and the polarity of the mobile phase used is different from that of the stationary phase. If the stationary phase is non-polar and the mobile-phase is polar the separation is termed Reversed-phase Partition Chromatography (RPC) [47, 49].

High performance RPC columns are efficient, stable and reproducible and analyte separation is easily attained due to the nature of the solvents used [47, 49, 50]. In all types of HPLC the polarity of the mobile phase plays a major role in a separation that can be achieved using isocratic or gradient chromatographic conditions [49, 50]. The mobile phase in HPLC has an impact on the retention of solutes and the separation of the components of a sample mixture.

When selecting a mobile phase certain characteristics must be considered when determining the constituents of the mobile phase. These include viscosity, UV-cutoff, and polarity, amongst others [51]. A large number of carbon atoms in the solvent results in a viscous mobile phase and decreased system efficiency [47]. The principal constituent of RP mobile phases is water and water miscible solvents that modify the polarity of the mobile phase [51]. Solvents commonly used include methanol and acetonitrile, and the removal of dissolved gases is important to achieve a robust separation [46, 47, 51].

Column packing materials can be manufactured using irregular or spherical particles. Irregular particles give rise to high operating pressures [52]. The particles may or may not be porous, but most columns are based on a silica backbone with a wide range of porosity. The particle size of the packing material has a major effect on the resolution of a separation and as a general rule, particles of 5-10µm are used for quantitative analytical procedures [53]. Since organic moieties are generally long-chain hydrocarbons the mobile phases are generally polar. More polar solutes elute early, whereas non-polar compounds are retained for longer on the column [46, 49].

For HPLC analysis the ideal detector should have high sensitivity, produce reproducible and predictable responses and respond to an analyte monitored in that separation. It should have a linear response over a wide range of sample concentration and the detector should be rugged and not sensitive to temperature changes or mobile phase composition [49, 54]. UV detectors are commonly used for pharmaceutical analysis. The light source for UV detection is typically a deuterium lamp that provides a suitable light intensity in the wavelength range 190 to 400nm [50].

The mechanism of retention in RPC includes solute transfer from a mobile phase into or onto a stationary phase. Many theoretical studies concerning retention mechanism(s) of RP-HPLC have been undertaken [55-57]. The nature of hydrophobic binding interactions is an issue of debate since there are many factors that determine the mechanism of retention that include the process used to manufacture the silica, the type of alkyl ligand bonded to the stationary phase, the type and composition of the mobile phase and the properties of the solute molecule under investigation [50, 55].

Conventional knowledge assumes an association of a solute with a stationary phase that can involve partitioning and/or adsorption or can be explained using solvophobic theory which focuses on the role of the mobile phase only on retention and not difference in properties of the stationary phase [58, 59]. The theory of adsorption offers a better basis for explaining retention mechanism(s) in LC, since column packing materials are composed of solid porous particles with a high surface area and are impermeable to the analyte and molecules of the eluent [60]. In summary HPLC is a dependable analytical tool with the potential for the separation and quantitation of many substances [49]. It is versatile as non-ionic, ionic and ionisable compounds can be separated using a single column and mobile phase.

2.2 EXPERIMENTAL

2.2.1 HPLC apparatus

A modular isocratic RP-HPLC system was used for method development and consisted of a Thermo Separation Products® P100 solvent delivery module (San Jose, USA), a Spectra-PHYSICS® SP8780 auto sampler (San Jose, USA), a Linear® UVIS 200 detector (Reno, USA) and a Spectra-PHYSICS® Data Jet-CH2 integrator (San Jose, USA). The mobile phase was degassed prior to use with an Eyela A-35 Aspirator (Tokyo, Japan). The separation was achieved using a Phenomenex® 150mm x 4.6mm i.d. stainless steel column packed with 5µm ODS (C_{18}) material (Phenomenex®, Torrance, CA, USA).

2.2.2 Chemicals and reagents

D4T and the internal standard (IS), AZT were donated by Aspen Pharmacare (Port Elizabeth, South Africa). HPLC grade MeOH-215 far UV Romil-SpS® Super Purity Solvent (Romil® Ltd, Waterbeach, Cambridge) was used as the organic modifier. HPLC grade water was prepared by reverse osmosis, using a Milli-RO® water purification system (Millipore®, Bedford, MA, USA) consisting of a Super-C carbon cartridge, two Ion-X® ion-exchange

cartridges and an Organex-Q® cartridge. The water was filtered through a 0.22µm Millipak® stack filter (Millipore®, Bedford, MA, USA) prior to use and the mobile phase was vacuum degassed and filtered through a 0.45µm Millipore® HVLP membrane filter (Millipore®, Bedford, MA, USA).

2.2.3 Preparation of stock solution

Standard stock solutions of D4T (100µg/ml) and 100µg/ml IS were prepared by accurately weighing approximately 10mg of D4T and AZT and dissolving in 100ml mobile phase in A-grade volumetric flasks. The stock solutions were sonicated for 10 minutes using a Branson® B12 sonicator (Branson® Inc., Shelton, CN, USA) to aid dissolution. The stock solution was serially diluted with HPLC water to produce D4T solutions of 1, 2, 5, 30 and 60µg/ml. All working standards were prepared with the IS, AZT at a concentration of 40µg/ml. The solutions were stable when stored at room temperature (22ºC) for a day. The stock and standard solutions were prepared on a daily basis and were stored in a refrigerator until used. All working solutions were used on the day that they were prepared.

2.2.4 Preparation of mobile phase

The initial mobile phase used comprised of MeOH:H_2O in a ratio of 30:70 v/v. The mobile phase was prepared daily, degassed and filtered through a 0.45µm HVLP membrane filter prior to use. The mobile phase was recycled during extended analysis.

2.3 METHOD DEVELOPMENT

2.3.1 Introduction

Prior to HPLC method development the properties of D4T were studied. These included the chemical structure of compounds, molecular weight, pKa , UV absorption spectra, concentration range and solubility, amongst others [44, 47]. The initial chromatographic conditions are usually selected based on literature reports, followed by manipulation of process variables, such as mobile phase composition, temperature and flow rate.

The conditions published for the analysis of D4T are summarised in Table 2.1. The initial conditions used in these studies were based on data summarized in Table 2.1.

Table 2. 1 Summary of the analytical conditions for D4T

Analyte	IS	Matrix	Column	Mobile phase	R_t min	Flow rate ml/min	λ nm	Ref
D4T	AZT	Human plasma	C_{18}	Acetate buffer: acetonitrile pH 6.5 , 10mM	11.7	1.0	265	61
D4T	-	Tablets	Inertsil ODS C_{18} (250 x 4.6mm, 5µm)	Methanol:1% O.P.A : acetonitrile (40:50:10)	6.8	1.2	267	62
D4T, 3TC, NVP	-	Tablet	Thermo Hypersil Gold C_{18} (150 mm x 4.6 mm, 5 µm)	Phosphate buffer 20mM: methanol	7.8	1.0	265	63
D4T, 3TC, NVP	FTC	Plasma	Hypersil BDS (250 mm x 4.6 mm, 5 µm)	Acetate buffer pH 6, 10mM : methanol (93:7)	15.6	1.0	270	64
D4T, 3TC, NVP	-	Capsule	C_{18}	Methanol: water (30:70)	9	0.8	270	65
D4T	-	Capsule	C_{18}	Methanol: water (10:90)	12.3	1.0	265	66
3TC, D4T, AZT, ABC, DDI	-	Plasma	C_{18}	Acetate buffer pH 4.6, 20mM: acetonitrile (95:5)	6.1	1.0	260	67
D4T	-	Tablets	C_{18} ODS Hypersil (250 mm x 4.6 mm, 5 µm)	Sodium phosphate buffer pH 3.5,20mM: acetonitrile (4:1)	2.85	1.0	266	68
D4T	-	Rat plasma	C_{18}	Methanol: water: acetic acid (23:77:0.2)	3	1.0	265	69
D4T	-	Capsule	C_{18}	Acetate buffer pH3.5, 20mM :methanol (80:20)	8.8	0.6	270	70
D4T	-	Capsule	C_{18}	Methanol: acetate buffer pH6, 10mM (40:60)	3.85	1.0	265	71
D4T	-	Tablet	C_{18}	Methanol: water (80:20)	7.49	1.5	266	72
D4T	-	Tablet	C_{18}	Acetate buffer pH3.5, 10mM: methanol (90:10)	6.09	1.0	265	73
D4T	-	Tablet	C_{18} (250 mm× 4.6 mm,5 µm)	Methanol: water (20:80)	10	0.6	280	74
D4T	-		C_{18}	Acetonitrile: acetate buffer (25:75)	12.5	2.0	254	13

2.3.2 Column selection

To develop a rugged, reproducible HPLC method, a stable, high-performance column is essential and column to column reproducibility is non-negotiable [48]. Reproducibility can be assessed by undertaking column suitability tests, including determination of theoretical plate number (N) for a specific value of k, peak symmetry (A_s), selectivity (α), back pressure, retention (k), reproducibility and column stability [47]. When selecting a column it is essential to know the MW, chemistry of the analyte and sample and the range of solubility of the compounds [44, 45, 48].

Most column packing materials used for HPLC separations make use of a silica particle backbone with bonded organic surface layers of C_8 or $C_{18,}$ amongst others [58]. Several particle types exist for HPLC applications, and 3 or 5µm totally porous microspheres are commonly used as they are efficient, robust, convenient and readily obtainable [60, 75].

Due to the high mechanical strength of silica particles, the formation of efficient packed beds stable under high operating pressures for long periods give rise to columns with high efficiency. The surface of the silica support can be chemically modified with a large variety of bonded phases. Silica-based packing materials are compatible with water and all organic solvents [50].

A Phenomenex® (150mm x 4.6mm) packed with 5µm ODS C_{18} material (Phenomenex®, Torrance, CA, USA) column was selected for the HPLC separation to be developed in these studies. The performance of the column was assessed based on (N), a measure of the number of peaks that can be located per unit run-time of a chromatogram, (A_s), a resolution and capacity factor which is a measure of where the peak of interest is located with respect to the elution time of non-retained components of a sample matrix [76].

2.3.4 Method of detection

Methods of detection used in conjunction with HPLC for the analysis of D4T mainly involve ultraviolet (UV) detectors and UV detection at a wavelength of 265nm was selected for the analysis of D4T.

2.3.5 Effect of Mobile phase composition

The ideal retention time for the analysis of D4T using AZT has been reported as ≥ 4 minutes and ≤ 10 minutes, as retention times below 4 minutes may result in interference with the solvent front or void. Methanol in a concentration of 10% v/v was selected as the solvent as it has been commonly used in published methods of analysis (Table 2.1) [66]. An increase in the concentration of methanol from 10-50 % v/v resulted in a decrease in the retention time of both D4T (blue) and AZT (red) from 9.8 minutes and 20 minutes to 4.4 minutes and 4.8 minutes respectively (Figure 2.1).

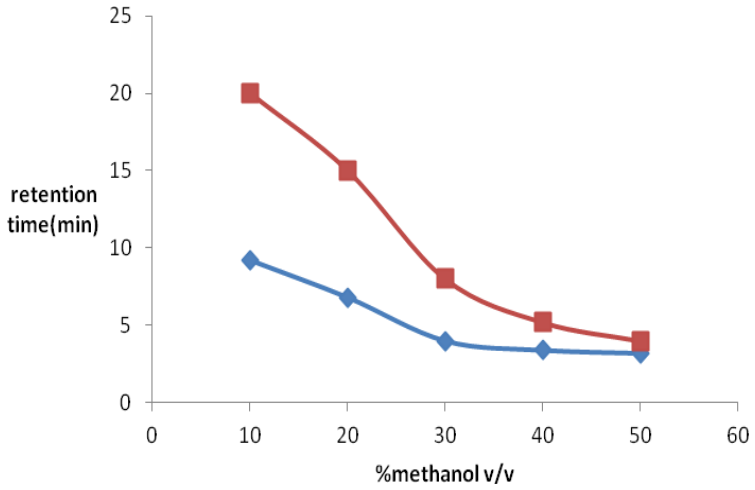

Figure 2. 1 Effect of mobile phase composition on retention time of D4T and AZT

2.3.6 Effect of flow rate

The effect of flow rate was investigated over a range of 0.7ml/min to 1.1ml/min, and it was observed that an increase in the flow rate resulted in a decrease in the retention time for both D4T (blue) and AZT (red) (Figure 2.2). Effect of flow rate was investigated because high flow rates lead to an increase in column pressure and this would lead to a shorter column life. An initial flow rate of 1ml/min was selected.

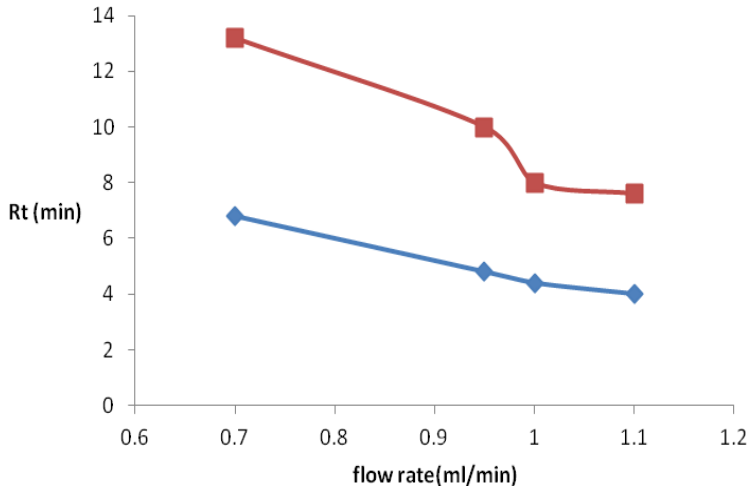

Figure 2. 2 Effect of flow rate on retention time of D4T and AZT

2.3.7 Internal standard

The IS approach is used in analyses in order to account for changes in sample volume or concentration due to instrumental or analyst variability [50]. The IS selected is usually a compound similar in terms of physico-chemical characteristics to the analyte of interest but should be well resolved from the peak(s) of interest, have a similar retention time, be absent from original sample, be prepared in the same way as the analyte, not necessarily be chemically similar to the analyte, be available in high purity, be stable, should not react with sample or mobile phase and have a detector response similar to the analyte [76].

The IS is added to the sample to be analysed prior to an extraction procedure or sample manipulation and facilitates quantitation by establishing a response factor for the analyte relative to the IS, for example a ratio for peak areas or peak heights [48].

2.4 INITIAL CHROMATOGRAPHIC CONDITIONS

Acetonitrile was also evaluated as a potential organic modifier but methanol was selected as the organic modifier for the purpose of this study since it produced suitable retention times for both D4T and AZT and it is affordable. A summary of the initial chromatographic conditions used is shown in Table 2.2.

Table 2. 2 Initial chromatographic conditions for quantitation of D4T

Column	Phenomenex® (150mm x 4.6mm), 5µm C_{18} material (Phenomenex®, Torrance, CA, USA)
Pump	Thermo Separation Products® P100 solvent delivery module pump (San Jose, USA)
Injector	Spectra-Physics® SP8780 autosampler, (San Jose, USA)
Detector	Linear® UVIS 200 detector (Reno, USA)
Detection wavelength	265nm
Sensitivity	0.2 AUFS
Recorder	Spectra-Physics®, Data Jet CH2 Integrator (, San Jose, USA)
Integrator speed	0.25cm/min
Flow rate	1ml/min
Injection volume	20µL
Temperature	Ambient 22ºC
Column pressure	800-1200 psi
Mobile phase composition	MeOH: H_2O (30:70v/v)

The selected chromatographic conditions revealed a good separation for D4T (60µg/ml) and the AZT (40µg/ml) and no decomposition of D4T was observed during analysis. The capacity factor for this separation was within the acceptable limits of >2 for the initial peak and <1 for the second peak. The symmetry factor was within the limits established in the FDA guideline of between 0.95 and 1.1 [76]. The resolution of the two peaks was therefore within acceptable limits and the separation was considered appropriate for the analysis.

2.5 METHOD OPTIMIZATION

2.5.1 Introduction

HPLC method optimization is essential to establish a set of adequate analytical conditions that yield a separation in a short time with minimum effort through the selection of a suitable column and mobile phase combination that results in baseline separation [49]. Traditionally optimization has been based on changing and monitoring one variable at a time and keeping all other variables constant. The disadvantage of this approach is that it does not include an assessment of the interactive effects of the variables under investigation, and as a result the technique does not illustrate the complete effects of a parameter on a response [77].

Multivariate statistical techniques such as Response Surface Methodology (RSM) provide an alternate approach for optimization and facilitates the evaluation of interactive effects of variables on a response. RSM uses mathematical and statistical techniques centred on the fit of polynomial equations to experimental data obtained in relation to an experimental design [78]. RSM involves selection of independent variables for the main effects on a system through screening studies, and the selection of an appropriate experimental design, after

which the experiments are conducted according to an experimental matrix. Examples of experimental designs include Box-Behnken (BBD), Central Composite (CCD) and Doehlert designs, statistical handling of experimental data through fitting polynomial functions, evaluation of the fitness of a model and obtaining optimum values for each variable studied. The aim of this approach is to optimize responses. An essential assumption is that the independent variables are continuous and controllable with negligible error [79].

Since RSM measures the relationship between independent variables and dependant response(s), it was used in this study based on a CCD to establish individual and interactive effects of identified independent variables on retention time and peak symmetry, for the purposes of identifying optimum conditions for analysis of D4T. CCD is the most popular second order experimental design used and is an efficient approach to provide sufficient amounts of information to test the fitness of a model [80]. CCD does not require many experiments and the number of experiments usually contains three sets including (i) full factorial or fractional factorial runs (2^{k-1} where k is the number of factors) to study factors at -1 (minimum) and +1(maximum) level, (ii) centre point runs examining factors at the centre point of the design space that facilitates an understanding of curvature and replicating them to evaluate pure errors and (iii) axial or star point runs (2k) setting all factors to 0 (i.e., the center point) [77, 81, 82]. Replicates at the centre are important as they provide an independent estimate of experimental error. For three variables the recommended number of experiments at the centre is six and the total number of experiments for three independent variables is $2^3 + (2 \times 3) + 6 = 20$ [78, 80, 82].

Initially a series of experiments was designed and a mathematical model of second order response surface that best fitted the data was identified. The optimal set of experimental parameters that produced a maximum and minimum value for a response was identified and the direct and interactive effects of process parameters were depicted graphically.

A number of HPLC methods involving the use of acidic buffer systems and other complex systems for the analysis of D4T have been reported and these had analytical run times > 10 minutes [13, 61, 64, 66, 70, 83]. Difficulties with baseline stabilization has been reported and can be solved by maintaining the temperature of the column as even small changes in column temperature can cause baseline drift. Column temperature was selected as an independent variable [84]. In RPC an increase in column temperature results in a decrease in retention

time, an increase in column efficiency, improved sample capacity and an increase in column permeability [59].

Initially the levels for design parameters were established using a trial and error approach based on literature data, and only a single parameter was modified at a time [81, 85, 86]. CCD statistical approaches have been used to optimize HPLC methods but to our knowledge CCD has not been used for the optimization of analytical methods for D4T. The experiments were performed in a random sequence to minimize the effect of uncontrolled factors and bias. On completion of experiments the data were fitted to a second-order polynomial equation by multiple regression and the resultant empirical model is shown in Equation 2.1.

$$\mathbf{Y = \beta_0 + \beta_1 A + \beta_2 B + \beta_3 C + \beta_{12} AB + \beta_{23} BC + \beta_{13} AC + \beta_{11} A^2 + \beta_{22} B^2 + \beta_{33} C^2}$$

Equation 2.1

Where,

Y = experimental response to be optimized
β_0 = a constant term
β_1, β_2, and β_3 = linear coefficients
β_{11}, β_{22}, and β_{33} = squared coefficients
β_{12}, β_{13}, and β_{23} = coefficients of the interaction between the factors under investigation [68, 87].
A = mobile phase concentration (%v/v)
B = column temperature (ºC)
C = flow rate of the mobile phase

2.5.2 Experimental design for HPLC separation optimization

Twenty experiments were conducted using the conditions summarized in Table 2.3, and the levels used are described in Table 2.4. Minimum and maximum values of the mobile phase composition (% v/v) (X_1) were fixed as 20 and 40, respectively. Similarly minimum and maximum values for column temperature (X_2) and flow rate (X_3) were selected as 20ºC and 30ºC and 0.8 and 1.1 respectively. The retention time for the last eluting peak and peak symmetry were the responses monitored for these studies.

Table 2. 3 Summary of experiments with coded values for factor levels for CCD

Experiment (run)	standard run number	Type	(A) Mobile phase (%)	(B) Column temperature (ºC)	(C) Flow rate (ml/min)
1	2	Fact	1	-1	-1
2	7	Fact	-1	1	1
3	5	Fact	-1	-1	1
4	14	Axial	0	0	1.68
5	12	Axial	0	1.68	0
6	0	Centre	0	0	0
7	1	Fact	-1	-1	-1
8	8	Fact	1	1	1
9	6	Fact	1	-1	1
10	13	Axial	0	0	-1.68
11	10	Axial	1.68	0	0
12	11	Axial	0	-1.68	0
13	4	Fact	1	1	-1
14	0	Centre	0	0	0
15	0	Centre	0	0	0
16	0	Centre	0	0	0
17	3	Fact	-1	1	-1
18	0	Centre	0	0	0
19	9	Axial	-1.68	0	0
20	0	Centre	0	0	0

Table 2. 4 Experimental factors and levels used for CCD of D4T

Factor	Level (-1)	Level (0)	Level (+1)
Independent			
% MeOH (A)	20	30	40
Column TºC (B)	20	25	30
Flow rate (C)	0.8	0.95	1.1
Dependant			
Y_1= Retention time			
Y_2= Peak symmetry			

2.5.3 Results and discussion

On the basis of the quadratic polynomial equation for the response surface, the present model and data analysis not only permitted the definition of optimum conditions for retention time but also showed the interactive effects of independent variables such as mobile phase composition (% v/v), column temperature (ºC) and flow rate (ml/min) on this response as shown in Equation 2.2

$$\mathbf{Y_1\ (retention\ time) = 4.43 - 1.92*A - 0.22*B - 1.4*C + 0.2*A*B + 0.3*A*C + 0.1*B*C + 1.22*A^2 + 0.3*B^2 + 0.58*C^2}$$

Equation 2.2

The contour plots (Figures 2.3-2.5) and Equation 2.2 reveal that the mobile phase composition and flow rate had an antagonistic effect on retention time, whereas column temperature had an antagonistic effect to a less extent that was not significant. The value of the coefficient in Equation 2.2 depicts the magnitude of the effect and the sign is an indication of whether the variables had a synergistic or antagonistic effect on retention time.

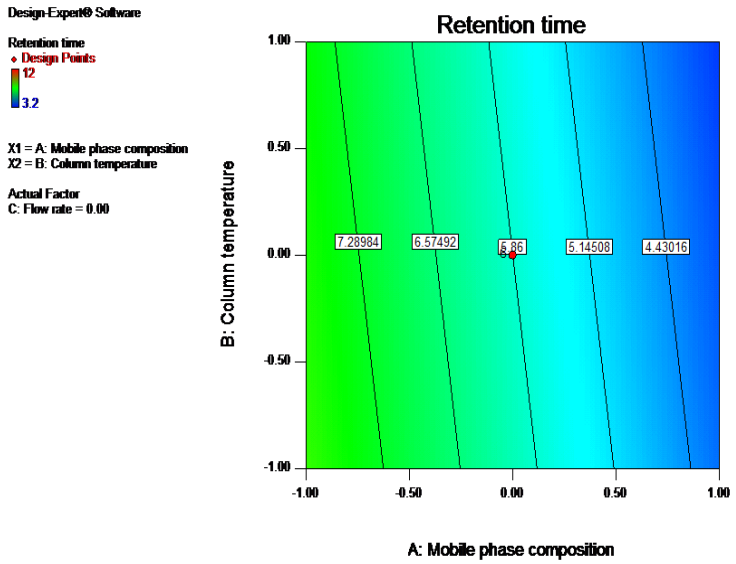

Figure 2. 3 Contour plot for retention time as a function of mobile phase composition and column temperature

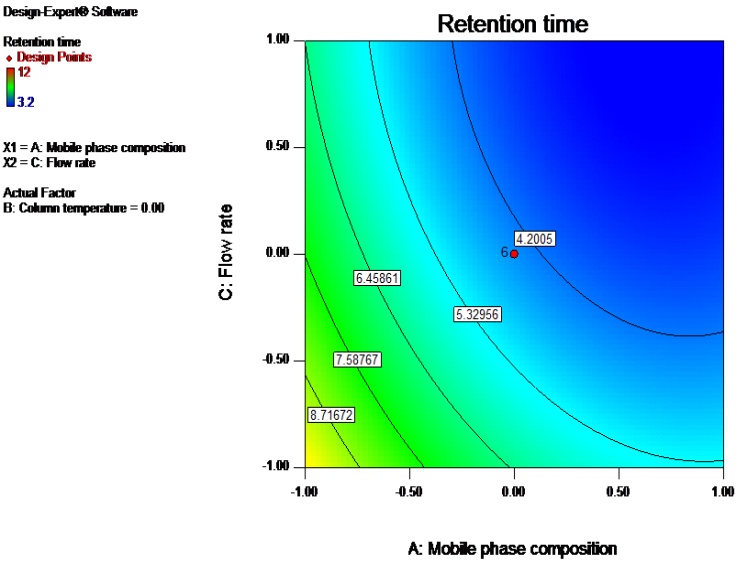

Figure 2. 4 Contour plot for retention time as a function of mobile phase composition and flow rate

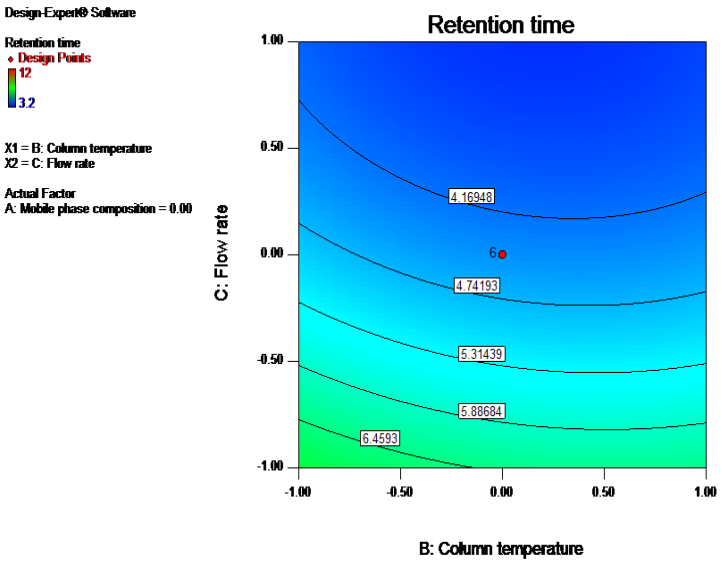

Figure 2. 5 Contour plot for retention time as a function of column temperature and flow rate

Figure 2.3 reveals that an increase in the concentration of the mobile phase composition of methanol at a constant column temperature resulted in a decrease in retention time, whereas if the methanol composition was held constant and the column temperature increased, no significant effect was observed. A decrease in retention time was observed when flow rate was increased with constant mobile phase composition (Figure 2.4) and a decrease in retention time was observed with an increase in flow rate at constant column temperature (Figure 2.5).

The model was validated using Analysis of Variance (ANOVA) and Design Expert software version 8.0.7.1 Stat-Ease, Inc. (Minneapolis, USA). Fischer's *F*- test was used to measure the significance of the model with respect to the variance of all terms and included an error term at p = 0.05 (Table 2.7). The model F-value of 13.06 implied that the model was significant. Values of "Prob > F" < 0.05 indicate significant model terms and in this case A, C, A^2, C^2 were significant model terms. The "Predicted R-Squared" of 0.4092 was not close to the "Adjusted R-Squared" of 0.8510, indicating a large block effect or that there is a possible problem with the model and/or data (Table 2.5).

Table 2. 5 ANOVA for the Response Surface quadratic model for retention time

Source	Sum of squares	df	Mean square	F-value	p-value Prob>F	
Model	**103.60**	**9**	**11.51**	**13.06**	**0.0002**	**Significant**
A-MPC	**50.33**	**1**	**50.33**	**57.11**	**<0.0001**	**Significant**
B-CT	0.69	1	0.69	0.78	0.3966	
C-FR	**26.74**	**1**	**26.74**	**30.34**	**0.0003**	**Significant**
AB	0.32	1	0.32	0.36	0.5602	
AC	0.72	1	0.72	0.82	0.3873	
BC	0.08	1	0.08	0.091	0.7694	
A^2	**21.36**	**1**	**21.36**	**24.24**	**0.0006**	**Significant**
B^2	1.28	1	1.28	1.45	0.2556	
C^2	**4.87**	**1**	**4.87**	**5.52**	**0.0407**	**Significant**
Residual	8.81	10	0.88			
Lack of fit	8.68	5	1.74	65.10	0.0002	
Pure error	0.13	5	0.027			
Corr total	1124	19				
Std. Dev	0.94	**R^2**	0.9216			
Mean	5.86	**Adjusted R^2**	0.8510			
C.V. %	16.02	**Predicted R^2**	0.4092			
PRESS	66.41	**Adequate precision**	11.554			

Since some model terms were not significant, model reduction was performed in an attempt to improve the model. A linear model was selected for this purpose and the resulting ANOVA data are summarized in Table 2.6. The results clearly indicate that the model was significant with a "Predicted R-Squared" of 0.5078, which was in reasonable agreement with the "Adjusted R-Squared" of 0.6340. Adequate Precision measures the signal to noise ratio, and a ratio > 4 is desirable. A ratio of 10.77 was observed for this model and an adequate signal suggests that the model was adequate to navigate the design space.

Table 2. 6 ANOVA for the Response Surface model for retention time (model reduction)

Source	Sum of squares	df	Mean square	F-value	p-value Prob>F
Model	**77.61**	**3**	**25.92**	**11.97**	**0.0002**
A-MPC	**50.33**	**1**	**50.33**	**23.24**	**0.0002**
B-CT	0.69	1	0.69	0.32	0.5799
C-FR	**26.74**	**1**	**26.74**	**12.35**	**0.0029**
Residual	34.65	16	2.17		
Lack of fit	34.51	11	3.14	117.66	<0.0001
Pure error	0.13	5	0.027		
Corr total	112.4	1			
Std. Dev.	1.47	**R^2**	0.6918		
Mean	5.86	**Adjusted R^2**	0.6340		
C.V. %	25.11	**Predicted R^2**	0.5078		
PRESS	55.33	**Adequate precision**	10.77		

The model that has been developed can be used to predict the retention time of D4T within the limits of the experiments undertaken. The normal probability plot of residuals and the plot of actual versus the predicted response for the retention time are shown in Figures 2.6 and 2.7. These plots are important and are required to check the normality assumption in a fitted model. If points on a normal probability plot follow a straight line this is an indication that the residuals or difference between the observed and predicted values follow a normal distribution and the model is adequate for data analysis [81].

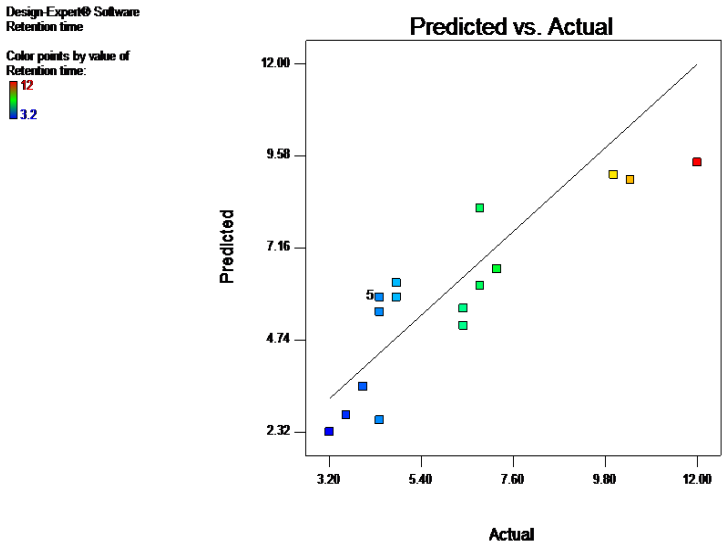

Figure 2. 6 Plot of residuals versus predicted response for retention time

The plot depicted in Figure 2.7 reveals that the data fitted the model as the errors are distributed normally as the residuals fall on the line. Normality plots are essential as they ensure that the model provides an adequate approximation of the optimization process. It is also clear that the points for residuals versus the predicted response plot generally lie along the straight line and are evenly distributed above and below the X-axis, indicating that the model is satisfactory [81].

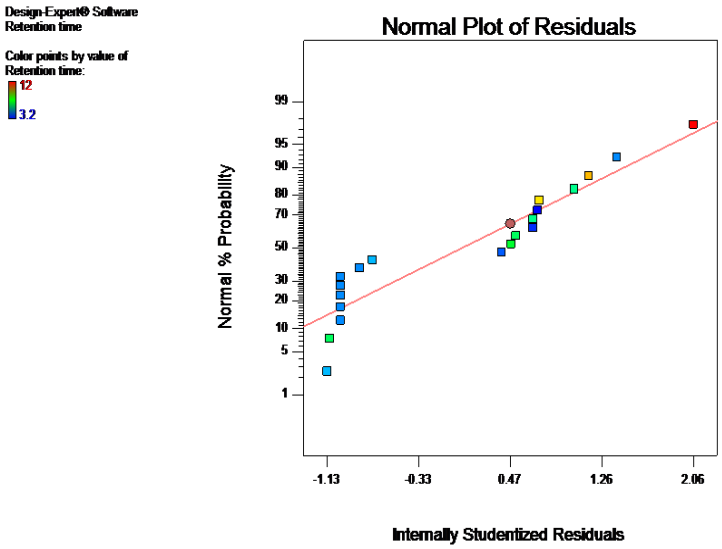

Figure 2.7 Normal probability plot of residuals for retention time

The peak symmetry factor was calculated by initially plotting a line through the peak of interest following analysis of samples at 10% of the peak height. The peak symmetry factor was calculated by dividing the length at 10% height of the right half of the peak by the length of the left side [72, 73]. The peak symmetry using the optimized chromatographic conditions was 1, which was deemed suitable for this method. The same procedure was used to establish the effect of variables on retention time. The mathematical relationship in the form of polynomial equations for the measured response Y_2 is shown in equation 2.3,

$$\mathbf{Y_2 = 0.99 - 0.05*A - 0.02*B - 0.05*C + 3.8e^{-016}\,A*B - 0.05*A*C + 4.07e^{-016}*B*C + 0.09*A^2 + 0.03*B^2 + 0.07*C^2}$$

Equation 2.3

ANOVA analysis revealed that the model was significant, with a model F-value of 3.68 and values of "Prob > F" less than 0.05. A and C were significant model terms. The p-value was 0.0273; confirming that the model was significant and both variables had an antagonistic effect on peak symmetry. The Adequate Precision value which measures the signal to noise ratio, was 5.392. A ratio greater than 4 is desirable, therefore the model was deemed adequate. A summary of the results for the responses and the predicted vs observed are depicted in appendix four.

2.6 OPTIMIZED CHROMATOGRAPHIC CONDITIONS

Following CCD the optimized chromatographic conditions that were obtained were used for future analytical studies. The MeOH content was 35.5%v/v and the separation was undertaken with a column temperature of 22ºC and a flow rate of 0.9ml/min

A typical chromatogram of the separation using a standard solution of D4T (60 µg/ml) and AZT (40 µg/ml) is depicted in Figure 2.8.

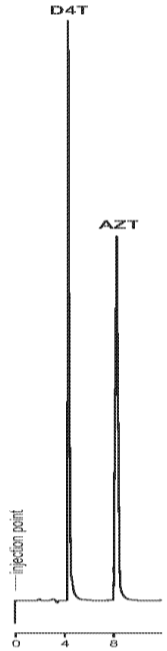

Figure 2. 8 Typical chromatogram of D4T (60µg/ml) and AZT (40µg/ml) using the optimized separation conditions

2.7 METHOD VALIDATION

2.7.1 Introduction

Validation of an HPLC method is required for any new or amended analytical method to ensure that it is capable of producing reproducible and dependable results when used by other operators using the same equipment in the same or different laboratories [14]. Typical parameters evaluated in method validation include an assessment of linearity, range, accuracy, precision, ruggedness, selectivity, specificity, limits of detection and quantitation [14].

2.7.2 Linearity

If a method is linear, results obtained should be directly proportional to the concentration of an analyte within a specific range [19]. A linear relationship can be calculated by use of least

squares linear regression and the results can provide a mathematical estimate of the degree of linearity [76]. The correlation coefficient, y-intercept, slope of the regression line and residual sum of squares and a plot of the data should be provided. A minimum of five (5) concentrations is recommended for an estimation of linearity [88].

Linearity across the concentration range of 1-60µg/ml was investigated. The mean peak height ratios (MPHR) of D4T/AZT were plotted against concentration of D4T to produce the calibration curve. Each sample was analysed in replicates of six to ensure reproducibility at each concentration level. The method was found to be linear over the concentration range studied with a representative linear equation of y = 0.0302x and a regression coefficient (R^2 value) of 0.9998. A typical calibration curve is depicted in Figure 2.9.

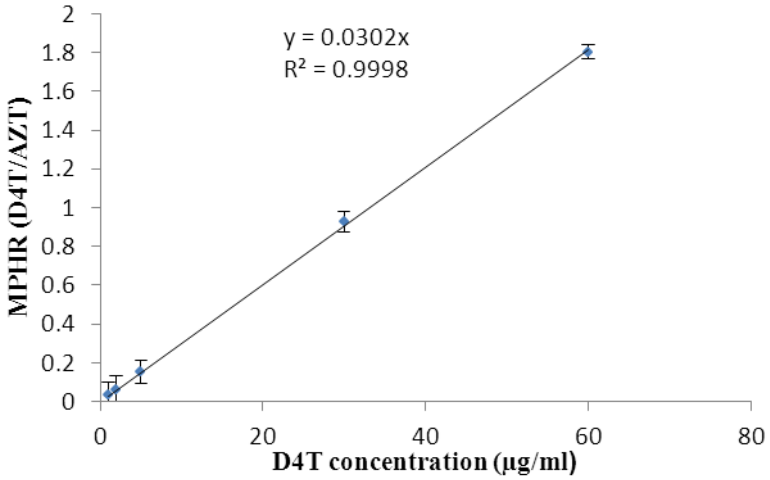

Figure 2. 9 Typical calibration curve constructed following linear regression analysis of a plot of peak height ratio versus concentration

2.7.3 Range

The range of a method is defined as the interval between the upper and lower levels of an analyte that have been determined with acceptable precision, accuracy and linearity [76].

2.7.4 Precision

Precision is a measure of the reproducibility of an analytical method under normal operating conditions. The standard deviation (SD) and relative standard deviation (RSD) should be reported for each type of precision investigated [89]. The precision was considered at two (2) levels viz., repeatability (intra-assay precision) and intermediate (inter-day precision). The precision was reported as the % RSD of a set of responses and was set at a limit of ≤ 5%.

2.7.4.1 Intra-assay precision (Repeatability)

Repeatability expresses the precision of a method under the same operating conditions over a short interval of time. Repeatability should be assessed using a minimum of 9 determinations covering the specified range for the procedure (e.g. 3 concentrations/ 3 replicates each) and a minimum of six (6) determinations at 100% of the test concentration [88].

2.7.4.2 Inter-day precision (intermediate precision)

Intermediate precision expresses within-laboratory variations such as analysing samples on different days or use of different analysts or different equipment [48, 50]. The results of precision studies are summarized in Tables 2.7-2.8. The method was found to be repeatable and precise as the % RSD was <5%.

Table 2. 7 Intra-assay precision data for the analysis of D4T

Concentration (µg/ml)	MPHR	Standard deviation	%RSD
2	0.089490	0.0008	0.94
30	1.334113	0.0053	0.40
60	2.649462	0.0141	0.53

Table 2. 8 Inter-day precision data for the analysis of D4T

	Concentration (µg/ml)	MPHR	Standard deviation	%RSD
Day 1	2	0.071990	0.0003	0.47
	30	0.975001	0.0028	0.29
	60	1.957173	0.0105	0.54
Day 2	2	0.073803	0.0004	0.48
	30	1.028249	0.0025	0.02
	60	1.999907	0.0058	0.29
Day 3	2	0.073339	0.0001	0.14
	30	1.016022	0.0020	0.97
	60	1.983848	0.0011	0.06

2.7.5 Accuracy and bias

Accuracy is a measure of the closeness of test results generated to the true value for the test sample. Accuracy is determined by applying the method to a minimum of three (3) samples across the specified range to which known amounts of analyte have been added with a minimum of 9 determinations. Accuracy should be reported as the percent recovery of a known amount of analyte that has been added to a sample [76, 89]. A tolerance of 5% was set for % RSD for accuracy. The bias of a method is an indication of the influence of an analyst on the performance of a method [88]. Accuracy and bias were assessed by replicate measurement of three (3) samples of different concentration and the results are summarized in Table 2.9. The % RSD values were < 5% for all samples, suggesting that the method was accurate.

Table 2. 9 Accuracy data for the analysis of D4T

Theoretical concentration (µg/ml)	Mean concentration (µg/ml)	% RSD	% Recovery	% Bias
1.5	1.48	1.19	98.7	1.35
35	34.6	0.25	98.8	1.20
55	54.4	0.54	98.9	1.10

2.7.6 Specificity and selectivity

The selectivity of a method to accurately and specifically measure the analyte in the presence of constituents that may be expected to be present in a sample matrix must be established [88]. Specificity is used to denote the response for a single analyte and was established by dissolving commercially available D4T capsules in mobile phase. The peaks observed in the chromatograms (Figure 2.10) were well resolved from the solvent front and no other peaks were observed on the chromatogram, indicating that the method is specific for D4T.

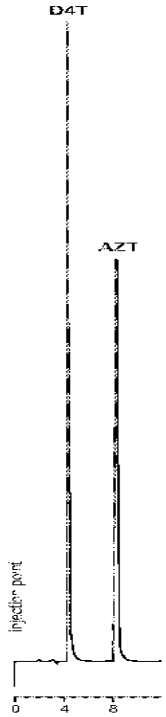

Figure 2. 10 Typical chromatogram of D4T (60µg/ml) showing specificity of D4T

2.7.7 Limits of Quantitation (LOQ) and Detection (LOD)

The LOQ of a method is the lowest concentration of an analyte in a sample that can be determined with acceptable precision and accuracy. The LOQ can be determined by visual evaluation for non-instrumental methods but may also be used with instrumental methods [76]. The LOQ is generally determined by analysis of samples of known concentration of

analyte and by establishing the minimum level at which the analyte can be quantified with acceptable accuracy and precision [89]. A Signal-to-Noise Approach can only be applied to analytical procedures that exhibit baseline noise [88].

The LOD is the lowest concentration of an analyte in a sample that can be detected but not necessarily quantitated under the stated experimental conditions. The LOD is important for impurity testing and for the assays of products containing low API levels or for placebo products [88]. At low levels, assurance is needed that the detection and quantitation limits are achievable for the test method [19, 76, 89].

The LOQ and LOD of the method developed for the analysis of D4T were established using a precision of ≤ 5%. The LOQ was found to be 1µg/ml and LOD was established by convention as one third the LOQ to produce a value of 0.3µg/ml.

2.8. FORCED DEGRADATION STUDIES

2.8.1 Introduction

Forced degradation studies are undertaken to demonstrate the specificity of a method when developing stability-indicating methods, particularly if little information is available about potential degradation products [90]. These studies also offer information about the degradation pathway and degradation products that could form on product storage. Forced degradation studies may enable pharmaceutical development in areas such as formulation development, manufacturing and packaging in which knowledge of chemical behaviour can be used to improve a drug product [91]. The purpose of stability testing is to provide evidence of the quality of an API or drug product over time under the influence of a variety of environmental factors such as temperature, humidity and light, and to establish a re-test period for the API or the shelf life for the drug product under recommended storage conditions [92].

2.8.2 Temperature stress studies

The ICH guideline recommends that temperature stress studies be undertaken at 10°C increments above the temperatures that are usually used for accelerated stability studies (e.g. 50°C, 60°C, 70°C.) [90]. For the purposes of our studies it was necessary to determine if D4T would degrade at 50, 60, 70, 80, 90 and 100°C and to establish whether any potential degradation products were present, and if so whether they were resolved from the peak for D4T when using the validated method. 30µg/ml samples of D4T were prepared and subjected to the different conditions maintained at the specified test temperature using a Colora®

Model ND-34980 Ultra-Thermostat water bath (Colora®, Lorch, Germany) for four hours. The samples were cooled to room temperature (22°C) before injecting into the HPLC system. The results of these studies are summarized in Table 2.10. A typical chromatogram (Figure 2.11) reveals that a degradation peak (I) was present and was resolved from the D4T peak.

Table 2. 10 Summary of the effect of different temperatures on D4T

Temperature (°C)	Time (hr)	Observations	Comments
50	4	D4T peak was resolved at 4.0min. no extra peak	Degradation absent
60	4	D4T peak was resolved at 4.0min. no extra peak	Degradation absent
70	4	D4T peak was resolved at 4.0min. no extra peak	Degradation absent
80	4	D4T peak was resolved at 4.0min. no extra peak	Degradation absent
90	4	D4T peak was resolved at 4.0min. Extra peak at 3.2min	Possible degradation
100	4	D4T peak was resolved at 4.0min. Extra peak at 3.2min	Possible degradation

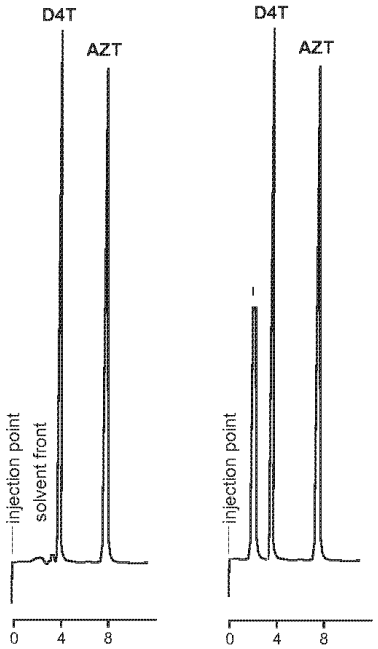

Figure 2. 11 Typical chromatogram showing degradation of D4T (30µg/ml) after exposure to 80° and 90°C

All samples of D4T stored at temperatures < 80°C appeared to be stable, whereas at temperatures of 90-100°C an additional peak (I) that was fully resolved from D4T and the IS

was observed at 3.2 min. This peak may be a degradation product of D4T which might have been thymine. Analysis of pure thymine could help confirm this.

2.8.3 Photostability studies

The photostability of a material on exposure to light and energy of 200W h/m^2 UV minimum should be undertaken to establish whether an API can be considered photostable[93]. Photostability is an essential part of forced degradation studies since a number of compounds are photolabile [92]. The photostability of D4T was established by exposing 30µg/ml solutions of D4T in a Model CPS+ SUNTEST Weathering unit (Atlas Material Testing Technology, Linsengericht, Germany, for 24 hours. The solution was analysed using HPLC. No degradation was observed and 100% D4T was recovered in these studies (Figure 2.12).

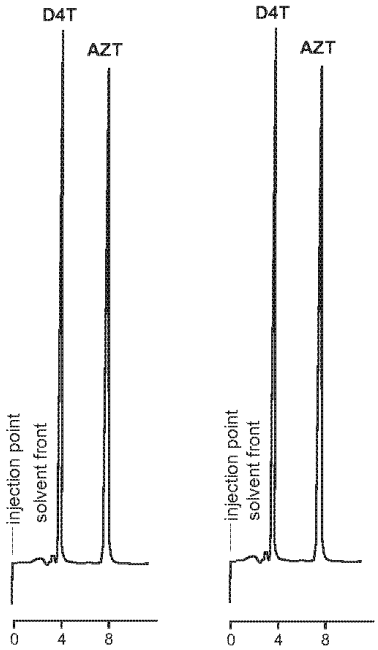

Figure 2. 12 Typical chromatogram of D4T (30µg/ml) showing absence of degradation following exposure to a photochamber at a temperature of 80°C at t=0 and 24 hours

2.8.4 Alkali degradation studies

Alkali degradation can be studied by refluxing an API in 0.1M NaOH solutions for eight hours or weaker or stronger solution depending on whether or not degradation occurs in the specified time [93]. For the purposes of these studies 50ml 0.1M NaOH was mixed with 30ml of a 100µg/ml stock solution to produce a final concentration of D4T of 30µg/ml. The solution was refluxed at 80°C for four hours. HPLC analysis revealed the presence of an additional peak at 3.0 minutes (I) and alkali degradation of D4T was assumed to have occurred (Figure 2.13).

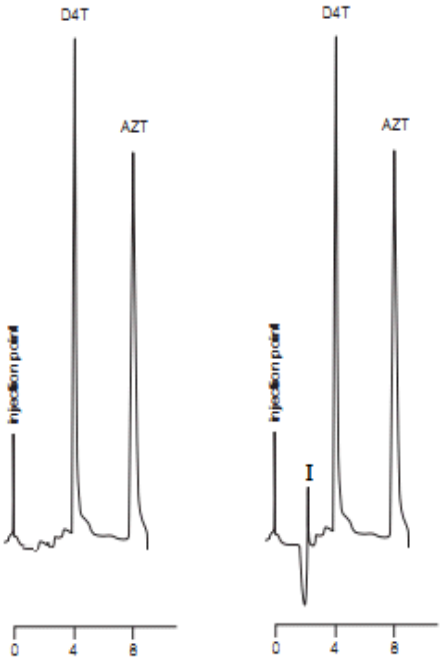

Figure 2. 13 Typical chromatogram of D4T (30µg/ml) showing degradation following exposure to 0.1M NaOH at a temperature of 80°C at t=0 and 4 hours

2.8.5 Acid degradation studies

Acid degradation studies can be undertaken by refluxing an API in 0.1M HCl for eight hours, [93]. For the purposes of these studies 50ml 0.1M HCl was mixed with 30ml of a 100µg/ml stock solution to produce a final concentration of 30µg/ml and was refluxed at 80°C for four hours and a degradation peak (I) was observed (Figure 2.14).

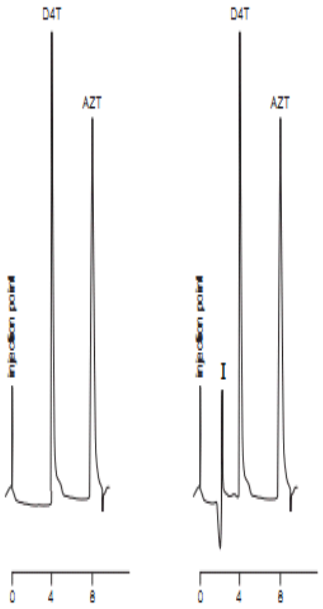

Figure 2. 14 Typical chromatogram of D4T (30µg/ml) showing degradation following exposure to 0.1M HCl at a temperature of 80°C for four hours

2.8.6 Neutral hydrolysis

Degradation under neutral conditions can be achieved by refluxing API solutions in water. A 30ml aliquot of a 100µg/ml stock solution was added to water to produce a solution with a final concentration of 30µg/ml of D4T and was refluxed at 80°C for four hours. No additional peaks were observed and it was assumed that no degradation of D4T had taken place (Figure 2.15).

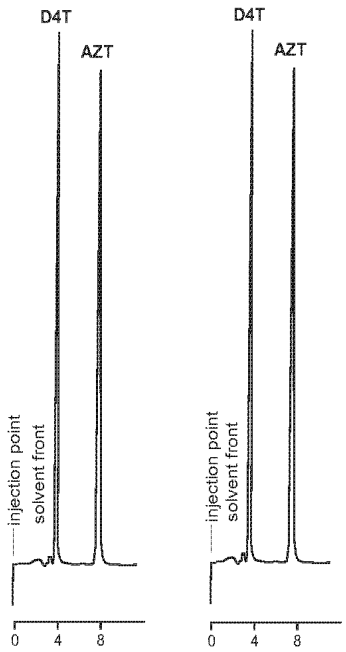

Figure 2. 15 Typical chromatogram of D4T (30µg/ml) showing absence of degradation following exposure to neutral hydrolysis at a temperature of 80°C at t=0 and 4 hours

2.8.7 Oxidation studies

Oxidation studies are to be performed using hydrogen peroxide in the concentration range of 3-30% v/v [93]. A hydrogen peroxide concentration of 10%v/v was selected for use in these studies and 50ml of H_2O_2 was mixed with 30ml of 100µg/ml of D4T stock solution to produce a solution of final concentration of 30µg/ml. The solution was refluxed at 80°C for four hours and analysed using HPLC. An extra peak (I) was observed at 3 minutes and it was concluded that degradation had occurred (Figure 2.16).

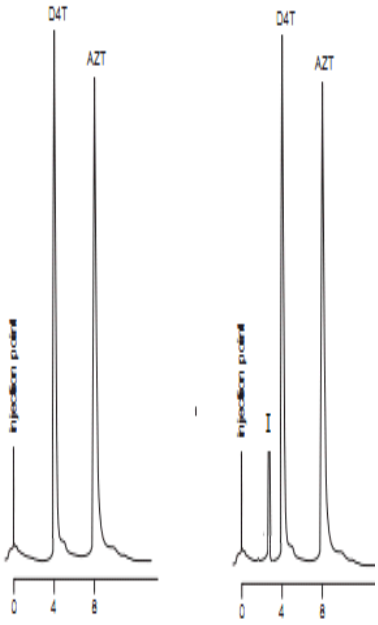

Figure 2. 16 Typical chromatogram of D4T (30µg/ml) showing degradation following exposure to 10% v/v H_2O_2 at a temperature of 80°C at t=0 and 4 hours

2.8.8 Dry heat degradation

Approximately 5g of D4T powder was stored in an oven at 80°C for four hours. A stock solution was prepared using D4T powder and was further diluted with mobile phase to produce a solution of 30µg/ml. The solution was analysed using HPLC. No degradation was observed (Figure 2.17).

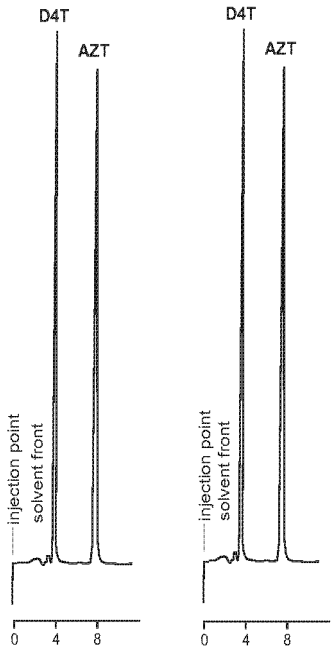

Figure 2. 17 Typical chromatogram of D4T (30µg/ml) showing absence of degradation following exposure to dry heat at a temperature of 80°C at t=0 and 4 hours

2.9 ASSAY OF COMMERCIAL STAVUDINE

To establish the applicability of the method for the analysis of D4T in dosage forms, two commercially available pharmaceutical products, Aspen-Stavudine® and Sonke-Stavudine®, were purchased from a local pharmacy and subjected to analysis. Twenty capsules were weighed, opened and blended with a mortar and pestle. An accurately weighed amount of powder equivalent to 30mg of D4T was extracted using 100ml of mobile phase by sonicating for 10min to ensure complete dissolution. The solution was filtered into a 100ml volumetric flask using a HVLP 0.45µm filter and made to volume with distilled water and mixed well. The API content was found to be within the pharmacopoeial limits for this product. There was no interference from excipients as the samples were filtered initially and no additional peaks were observed. The percentage recovery ranged between 97% and 102% and the % RSD values were < 5% (Table 2.11).

Table 2. 11 Assay results for commercially available D4T products

Analyte label claim (30mg)	Theoretical (mg)	Actual (mg/tablet)	Recovery (%)	% RSD
Aspen-Stavudine®	30	29.5±0.2	98.3	1.03
Sonke-Stavudine®	30	30.37±0.6	101.2	2.54

2.10 CONCLUSIONS

A stability indicating RP-HPLC method with UV detection has been developed and validated according to ICH guidelines for the analysis of D4T and has been applied to the analysis of commercially available D4T containing dosage forms. The method was optimized by the use of RSM using a CCD approach to establish the optimum mobile phase composition, flow rate and column temperature. The chromatographic conditions yielded sharp, symmetrical peaks with a high degree of resolution. AZT was selected as the IS and was used throughout the application of the analytical method. D4T and AZT were well separated, with R_t of 4 and 8 minutes, respectively. The linearity of D4T/AZT mean peak height ratio versus D4T concentration was demonstrated over a concentration range of 1-60µg/ml.

To our knowledge this is not only the most rapid method of analysis for D4T but it is also affordable and has a mobile phase that does not contain acidic buffer systems or other components. Furthermore the method is an improvement on that reported in the monograph in the British Pharmacopoeia [13] that reports the need for an acetate buffer and acetonitrile which is more expensive in comparison to methanol. In addition there are no methods for D4T analysis in which optimization was achieved using a CCD.

A simple, rapid, linear, precise and accurate stability indicating HPLC method for the in-vitro quantitation of D4T has been developed, validated and used for the analysis of commercially available D4T products.

CHAPTER THREE

PREFORMULATION AND COMPATIBILITY STUDIES

3.1 INTRODUCTION

Prior to the development of a dosage form it is essential to have a fundamental knowledge of the physical and chemical properties of the API under investigation. Such information will assist in deciding an appropriate approach for formulation development and product manufacture [94]. Preformulation involves the application of biopharmaceutical principles to the physicochemical parameters of an API with the goal of designing an optimum drug delivery system [95] and requires consideration of the therapeutic category and anticipated dose of a compound in addition to the nature of a formulation [95]. The successful development of a stable and effective solid oral dosage form depends on the careful selection of excipients that are added to a formulation to facilitate the administration, manufacture, control of release, bioavailability and stability of the API. Thermal analysis can be used to investigate and predict any potential physicochemical interactions between components of a formulation and can therefore be used to facilitate the selection of suitable chemically compatible excipients for a dosage form [94, 96].

Preformulation studies include but are not limited to the determination of solubility of an API at different pH using simulated gastric and intestinal fluids, as for absorption to occur an API should generally be in solution. The determination of solubility of an API in manufacturing vehicles/solvents is also essential [95] as is the establishment of the existence of polymorphs that can be achieved using thermal analysis approaches such as, Differential Scanning Calorimetry (DSC), Thermogravimetric Analysis (TGA) and Differential Thermal Analysis (DTA) [97]. The stability of the API in media of different pH and compatibility with excipients using DSC and Infrared Spectroscopy (IR) are also critical to ensure the successful development of formulations.

3.2. THERMAL ANALYSIS

Thermal analysis encompasses techniques that measure heat flow of an API as a function of temperature [97]. DSC is a popular and useful thermal technique since the results of DSC analysis can provide detailed information about the physical and energetic properties of a substance [98, 99]. DSC measures endothermic and exothermic transitions of compounds as a function of temperature and time and is easy to use in terms of sample preparation and

experimental setup. DSC has been used to characterize polymeric and other pharmaceutical materials, organic and inorganic compounds [98, 100, 101]. The response of pharmaceutical dosage forms to thermal stress is an integral part of the development of a stable formulation [102, 103].

3.2.1 Differential Scanning Calorimetry (DSC)

DSC is used to study thermal transitions involving energy or heat capacity changes such as melting, glass transition, recrystallization, mesomorphic transition temperatures, corresponding entropy and enthalpy changes and exothermic decomposition of different materials with a high level of sensitivity [97]. Qualitative measurements of these processes have many applications and include identification of materials, studies of purity, polymorphism, quantitative and qualitative degradation, glass transition temperature identification and compatibility of materials [97, 98, 104].

In DSC there are two sample positions, one for the material under investigation and a reference pan. The pans are generally made of nonreactive materials such as aluminium, quartz glass, platinum, stainless steel or nickel amongst others [98, 102, 105]. The pans are sealed with a lid that is crimped in place and both pans are maintained at temperatures predetermined by isothermal or gradient programming [97, 106, 107].

A platinum resistance thermometer is used to measure the temperature differential between the pans and these data are converted to energy flow via mathematical manipulation [105, 106]. In order to ensure reliable and reproducible results for DSC testing the instrument must be calibrated routinely as part of a quality assurance programme [107]. The sample and reference pans are heated electrically and the temperature increases at a specific heating rate in an inert atmosphere of nitrogen gas, purged at constant pressure. The amount of heat or energy supplied or removed to maintain a zero temperature differential between the sample and reference is recorded and produces exothermic or endothermic peaks on the resultant thermogram. The area under the curve is proportional to the total enthalpic change of the material(s) under investigation [98].

The accuracy of results generated by DSC is dependent on the use of high purity calibration standards and clean DSC sensors. Calibration standards include metals such as indium, tin, bismuth and lead [108]. DSC has been used for the rapid screening of excipients in API-excipient compatibility studies since no long term storage is required prior to analysis and only small amounts of API are required [108]. During rapid screening of excipients using DSC it is assumed that the thermal properties of blends or mixtures of excipients and API are

the sum of the individual components in the mixture, if no interaction between the components exists.

3.2.2 Thermogravimetric Analysis (TGA)

TGA measures the amount and rate of change in weight of a material as a function of temperature or time in a controlled atmosphere. Measurements are used primarily to determine the composition of materials and to predict their thermal stability at temperatures up to 1000°C [109]. TGA is the act of heating a mixture to a high enough temperature so that one of the components of that mixture decomposes to form a gas that vaporises into the air. TGA is a process that uses heat and stoichiometry ratios to determine the percent by mass ratio of a solute that is tested. If the compound(s) in a mixture that remain are known then the percentage by mass can be determined using the weight of the remaining material and the initial mass [98]. The advantage of TGA includes the determination of the composition of multi-component systems, thermal and oxidative stability of compounds, and estimated life time of a product and decomposition kinetics of materials. TGA can also be used to determine the effect of reactive and corrosive atmospheres on compounds in addition to an estimation of moisture and volatile content(s) of a compound [108].

3.3 SPECTROSCOPIC ANALYSIS

3.3.1 Infrared spectroscopy (IR)

IR is a commonly used, rapid, convenient and non-destructive technique that requires limited sample preparation for the identification of unknown materials [96]. IR provides structural information about a material at a molecular level and permits the determination of the amount of the components in a mixture in addition to identification of materials for the purposes of quality control [21]. IR relies on the measurement of light absorbed by a sample in the IR region of the electromagnetic spectrum to identify functional groups in a molecule [110]. The absorption intensity depends on the efficiency with which the energy of an electromagnetic wave is transferred to the atoms involved in that vibration. Atoms in a functional group can vibrate in symmetrical and asymmetrical stretching, scissoring, rocking, wagging and twisting configurations. An IR spectrum is generated when a sample absorbs energy and results in a transition between two vibrational energy levels from a ground to an excited state [21].

IR photon absorption data are reported as wave numbers (cm^{-1}) that are defined as number of waves per unit length. The mid-IR region has a wave number range of 4000–400 cm^{-1} and is

the most commonly reported data for IR spectroscopy analysis since spectral fingerprints for organic molecules are generated if they are IR active [111].

When a beam of IR light is directed at an organic compound and the frequency of a specific vibration is equal to the frequency of the IR radiation directed at the molecule, the molecule absorbs radiation [110]. The remaining photons pass through the molecule and strike a detector that sends a signal to a data capture system for spectrum generation indicating which photons were absorbed or transmitted by the compound thereby permitting identification of the functional groups of the compound [110]. The vibrational spectrum of a molecule is considered to be a unique physical property of the material and is characteristic of that molecule [112].

A set of absorption band tables (Table 3.1) have been reported that vary from compound to compound but are generally consistent [112]. During preformulation studies the use of IR has been important as the spectrum of an API is generated initially, after which spectra of mixtures of API and potential excipients can be compared to establish whether the compounds are compatible or not. The principal absorption bands of an API should be evident following mixing with excipients should the materials be compatible. However the use of IR alone is not sufficient to make conclusive decisions in this respect and usually a second analytical technique such as thermal analysis is often used to provide additional information [110, 111].

Table 3. 1 Summary of absorption bands for IR [112]

STRETCHING VIBRATIONS		**BENDING VIBRATIONS**	
FUNCTIONAL GROUP	**FREQUENCY (cm^{-1})**	**ALKENES**	**FREQUENCY (cm^{-1})**
RO-H	3200-3600	$RC=CH_2$ (terminal)	910 and 990
COO-H (carboxylic acid)	2500-3600	$R_2C=CH_2$ (terminal)	885-895
Sp^3 C-H	2850-3000	*cis*-RCH=CHR	665-730
Sp^2 C-H	3000-3100	*trans*-RCH=CHR	960-980
Sp C-H	~3300	Trisubstituted alkene	790-840
Sp^3 C-O	1000-1200	**BENZENE RINGS**	**FREQUENCY (cm^{-1})**
Sp^2 C-O	1100-1200	Mono-sub	~700 and ~750
C=C	1575-1650	Meta-disub	~710 and ~775
C=O	1600-1800	Ortho-sub	~750
C≡C	2100-2200	Para-sub	~800
C≡N	2240-2260		
N=H	3300-3500		
Aldehyde C-H	2695-2830		

During preformulation studies Fourier Transform Infrared (FTIR) spectroscopy was used as it is a rapid non-destructive, inexpensive and sensitive high resolution technique. FTIR is widely used for the analysis of solid materials that are prepared using one of several different methods [113-117]. In pharmaceutical research FTIR is used to identify and analyze the structure of drugs, excipients and polymorphism [96].

For the purposes of this study spectroscopic and thermal analysis approaches were used to evaluate D4T alone and in combination with Eudragit® RSPO, Eudragit® RLPO, Eudragit® EPO, Eudragit® S100, Methocel®K4M, Klucel®, Avicel® PH102, Kollidon® VA64 and magnesium stearate.

3.4 METHOD

Homogenous, binary mixtures of D4T and the excipients to be tested were prepared by weighing 0.5g of each component and mixing in 1:1 ratios using a mortar and pestle. A 3mg sample of the powder was then weighed and TGA studies were performed under a dry nitrogen atmosphere in platinum crucibles with an empty platinum crucible as reference. DSC studies were performed under a dry nitrogen atmosphere using aluminium crucibles. D4T and excipient blends were manufactured and tested without further treatment.

3.4.1 Differential scanning calorimetry

DSC thermograms were developed using a Model DSC-7 Perkin Elmer Differential Scanning Calorimeter (Perkin Elmer AG, USA). Pyris® Software for Windows was used to analyse the data. Approximately 3mg of D4T, 1:1 binary mixtures of D4T and excipients and a mixture of D4T with all excipients were weighed and placed directly into aluminium DSC pans and hermetically sealed prior to analysis. The samples were placed directly onto the microscopic hot stage DSC and the temperature of the microscopy cell was monitored using a central processor. The heating rate of the DSC assembly was controlled at 10°C/min over the temperature range 50-250°C. A nitrogen atmosphere was maintained during testing at a rate of 25ml/min.

3.4.2 Thermogravimetric analysis

TGA was conducted using a Model TGA 7 Perkin Elmer Thermogravimetric Analyzer (Norwalk, CT, USA) fitted with a platinum sample holder. Pyris® Software was used for data analysis. Approximately 3 mg of D4T was placed in a platinum crucible. Measurements were performed in a nitrogen atmosphere at a flow rate of 25ml/min and a heating rate of 10°C/min over the temperature range 25-400°C was used for the analysis.

3.4.3 Infrared spectroscopy

The IR absorption spectra of D4T and potential excipients were generated using a Spectrum 100 FT-IR ATR Spectrophotometer (Perkin Elmer® Ltd, Beaconsfield, United Kingdom). The spectra were generated from 1:1 binary mixtures of D4T and each excipient in addition to a mixture of all excipients and API. Samples of the binary mixture were prepared by weighing approximately 0.5g of each component and gently blending the powders in a mortar and pestle. Approximately 3mg of the mixture was placed onto a diamond crystal, pressure was applied and the samples were analysed in the range 400-4000cm^{-1}at a resolution of 4cm^{-1}.

3.5 EXCIPIENTS

All excipients that were used in these studies are generally recognised as safe (GRAS) and appear in the FDA Inactive Ingredients for general use and inclusion in oral formulations [118].

3.5.1 Klucel® (Hydroxypropyl cellulose (HPC))

Klucel® is a white to slightly yellow coloured odourless and tasteless powder that is partially substituted poly hydroxypropyl ether of cellulose. It is commercially available in a variety of grades that have a different viscosity when in solution. The molecular weight range of Klucel® is 50000-1250000 daltons and the viscosity ranges between 75-6500mPa [118]. Klucel® is widely used in oral and topical formulations as an extended release matrix forming material, a binder and as a film forming coating material. Klucel® has also been used for microencapsulation processes and as a thickening agent in transdermal patches and ophthalmic products. Klucel® is soluble in ethanol, dichloromethane, methanol, propanol, acetone and propylene glycol. The Klucel® grade used can have a marked effect on the quality of solution in some organic solvents. Klucel® is a stable material but hygroscopic material after it is dried. It is safe and is generally regarded as a non-toxic and non-irritant material [118]. Klucel® has been successfully used in microencapsulation processes [119, 119-121].

3.5.2 Avicel® PH102 (Microcrystalline cellulose (MCC))

Avicel® PH102 is purified, partially depolymerised cellulose that occurs as a white, odourless, tasteless, crystalline powder composed of porous particles. It is commercially available in different particle size and moisture grades that possess different properties and are used for different applications. Avicel® PH102 is widely used in pharmaceutical products

as an adsorbent, anti-adherent, binder, disintegrant or diluent in tablets, capsules and microparticles. Avicel® PH 102 has a bulk density of 0.28-0.33g/cm^3, a tapped density of 0.478g/cm^3 and a melting point of 260-270°C. Avicel® PH102 is stable but hygroscopic and is slightly soluble in a 5% w/v sodium hydroxide solution, is practically insoluble in water, dilute acids and most organic solvents. Avicel® PH102 is incompatible with strong oxidizing materials and is a relatively nontoxic and non-irritant material. It is not absorbed systemically following oral administration and thus has a low toxicity potential [118, 122].

3.5.3 Polymethacrylate and Methacrylic acid copolymers

Methacrylic acid copolymers are generally described as fully polymerized copolymers of methacrylic acid and an acrylic or methacrylic ester. Three main types of copolymers exist *viz.*, Types A, B and C that vary in methacrylic acid content and viscosity of solution. Type A and B polymers are also known as ammonio-methacrylate copolymers and consist of fully polymerized copolymers of acrylic and methacrylic acid esters with low quaternary ammonium functional group substitution and different numbers of ammonio-methacrylate block units [118, 123]. This property enables them to be used in SR formulations and to facilitate pH dependent drug release [124]. Typical molecular weights of these materials are ≥ 100 000 and can be cationic or anionic. These polymers are commercially available as dry powders, granules, aqueous dispersions or organic solutions in a mixture of acetone and propan-2-ol. Dry powder blends are stable at temperatures < 30^{0}C for approximately 3 years. They are generally regarded as non-toxic, non-irritant and are primarily used in capsule and tablet formulations for oral use and for film coating materials [124, 125]. The type of polymer used has an impact on the manufacture of films of different solubility and permeability characteristics [118].

The polymethacrylates copolymers used in this research included Eudragit® S100, EPO, RSPO and RLPO. Eudragit® S100 is an anionic copolymer based on methacrylic acid and methyl methacrylate in a 1:2 ratio of free carboxylic acid functional groups to the ester. It is a white powder with a faint characteristic odour and is used for enteric coating of dosage forms that target drug release to the colon. It is soluble in solutions of pH > 7 and is resistant to gastric fluid. Eudragit® EPO is soluble in gastric fluids of pH < 5 and is usually used as a film forming material. Eudragit® RLPO and RSPO are also referred to as ammonio-methacrylate copolymers and occur as fine, white powders with a slight amine-like odour that are synthesized from acrylic acid and methacrylic acid esters. Eudragit® RLPO is 10% quatenary ammonium functional group substituted whereas Eudragit® RSPO is 5% quatenary

ammonium functional group substituted. The ammonium groups are present as salts and result in pH independent permeability of the polymeric materials. Both polymers are insoluble in water but are permeable to water and Eudragit® RSPO exhibits lower permeability than Eudragit® RLPO [118, 123].

3.5.4 Methocel® K4M (Hydroxymethylpropyl cellulose (HPMC))

Methocel® K4M is an odourless, tasteless, white or creamy-white fibrous or granular powder that is a partly O-methylated and O-2-hydroxypropylated cellulose derivative. Methocel® K4M is available in a number of different grades that vary in viscosity of solution and the extent of methyl substitution [118]. Methocel® K4M has been primarily used as a coating material, controlled release and viscosity increasing agent and for microencapsulation [122, 126]. Methocel® K4M is soluble in cold water and mixtures of dichloromethane with ethanol and/or methanol. Some grades are soluble in aqueous solutions of acetone. Methocel® K4M is stable but is hygroscopic after drying. It is incompatible with some oxidizing agents and is non-toxic and non-irritating although excessive oral consumption may have a laxative effect [118].

3.5.5 Magnesium Stearate

Magnesium stearate is a fine, light white precipitated or milled impalpable powder of low density that has a faint odour of stearic acid with a characteristic taste. It is widely used in pharmaceuticals, cosmetics and foods and is primarily a lubricant in capsule and tablet formulations when used at concentrations between 0.25% and 5%w/w. Magnesium stearate is generally regarded as non-toxic following oral administration. It has a bulk density of 0.159g/cm^3 and a tapped density of 0.286g/cm^3 and is very stable. Commercial samples have a melting range of 117-150°C and are practically insoluble in ethanol, ether and water and are only slightly soluble in warm benzene and/or ethanol. It is incompatible with strong acids, alkalis and iron salts [118].

3.5.6 Kollidon® VA64 (Copovidone)

Kollidon® VA64 is a white to yellowish-white amorphous powder. It is typically spray dried to a relatively fine particle size and has a slight odour and a faint taste. Kollidon® VA64 has a molecular weight ranging between 45000-70000 mass units. It is used as a film-forming agent and in direct compression and wet granulation to produce controlled release formulations [127]. Kollidon® VA64 is stable, soluble in most organic solvents and compatible with most organic and inorganic pharmaceutical excipients and is generally regarded as safe [118, 128].

3.6 RESULTS AND DISCUSSION

3.6.1 Differential Scanning Calorimetry

The DSC thermograms for D4T alone, in a mixture with all excipients and as 1:1 binary mixtures are depicted in Figures 3.1-3.11. The figures reveal typical endothermic heat flow curves *versus* temperature generated in DSC experiments. D4T exhibits a melting endotherm between 171 and 178°C for all mixtures studied and the DSC thermogram for pure D4T (Figure 3.1) shows a sharp endothermic peak at 175.5°C which is in agreement with that reported in previous DSC studies [129-134]. It can be concluded that the bulk D4T that was used in the preformulation studies and for the manufacture of microparticles was pure. In all cases the melting endotherm of D4T did not appear to be significantly affected by the presence of excipients with only slight changes in the peak, through broadening or a peak shift towards lower or higher temperatures. These slight changes may be due to mixing of D4T and the excipients which in turn could lower the purity of each component in the mixture. The responses observed do not indicate incompatibility as interactions are indicated by significant changes in the melting point of a material or by the appearance of new peaks or complete disappearance of the peaks of interest.

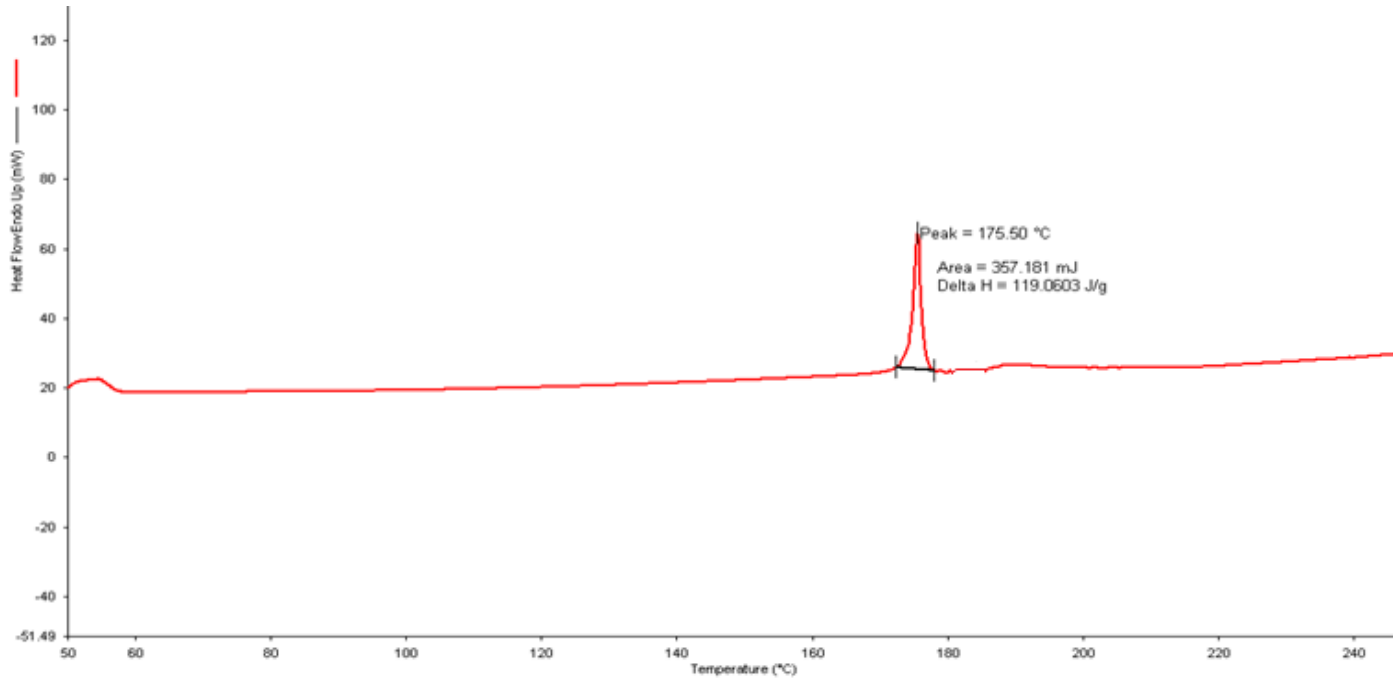

Figure 3. 1 Typical DSC thermogram for D4T determined at a heating rate of 10°C/min

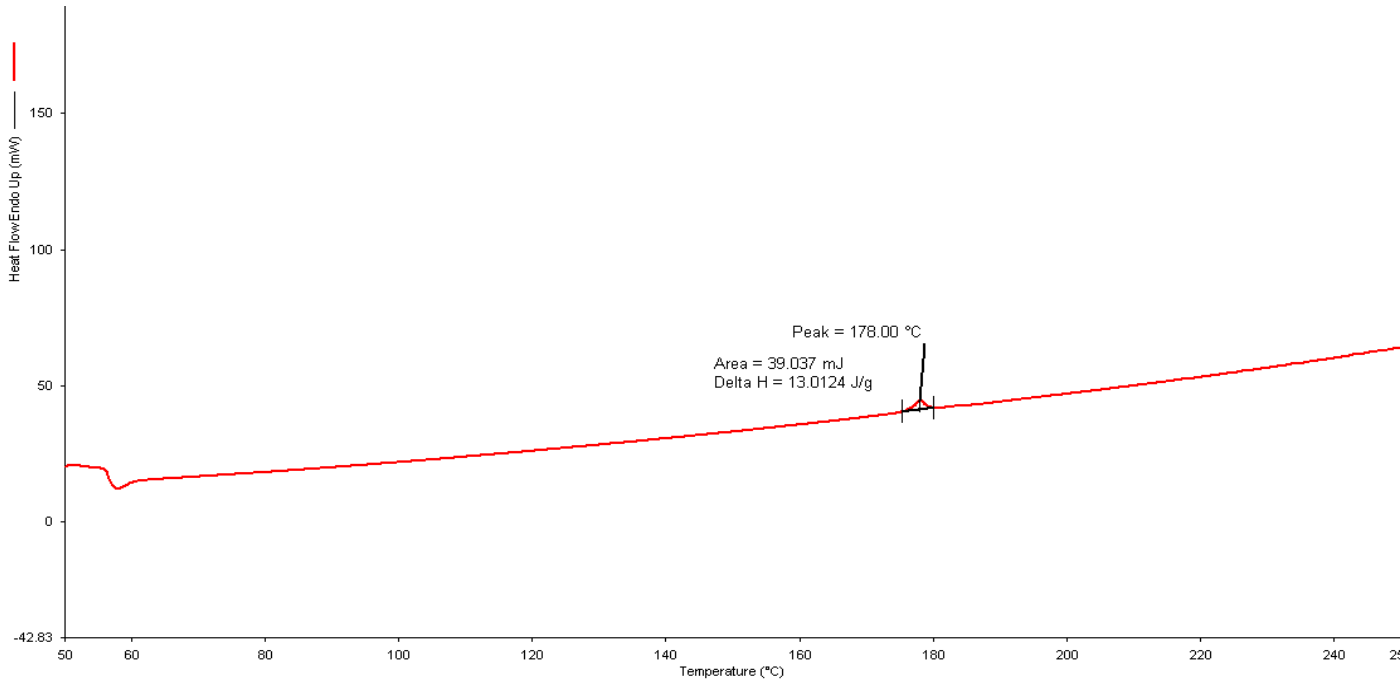

Figure 3. 2 Typical DSC thermogram for a 1:1 mixture of D4T and Klucel® determined at a heating rate of 10°C/min

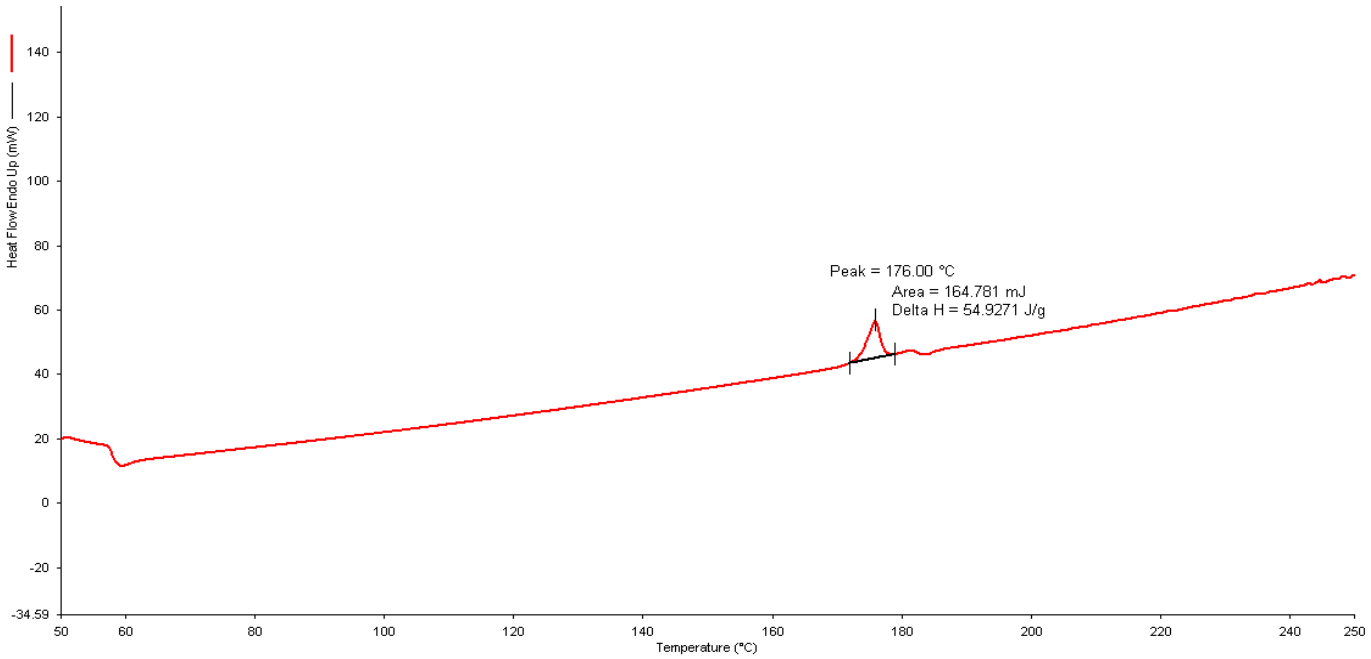

Figure 3. 3 Typical DSC thermogram for a 1:1 mixture of D4T and Avicel® PH102 determined at a heating rate of 10°C/min

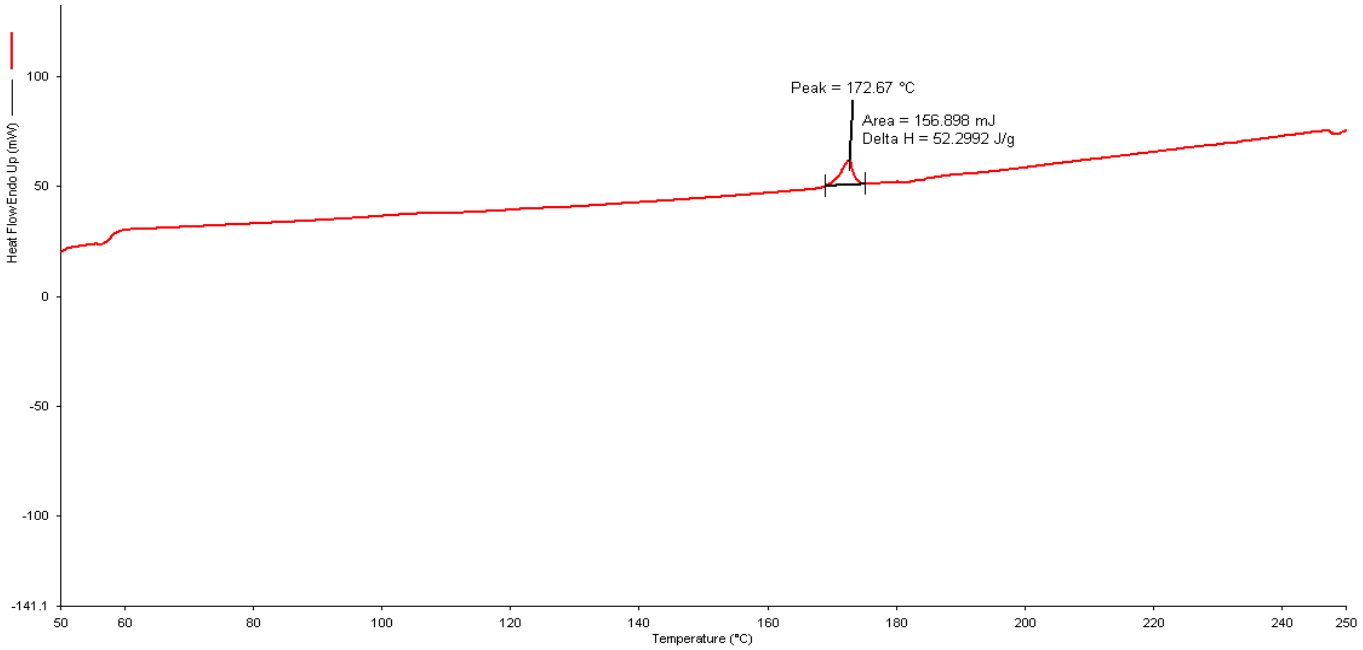

Figure 3. 4 Typical DSC thermogram for a 1:1 mixture of D4T and magnesium stearate determined at a heating rate of 10°C/min

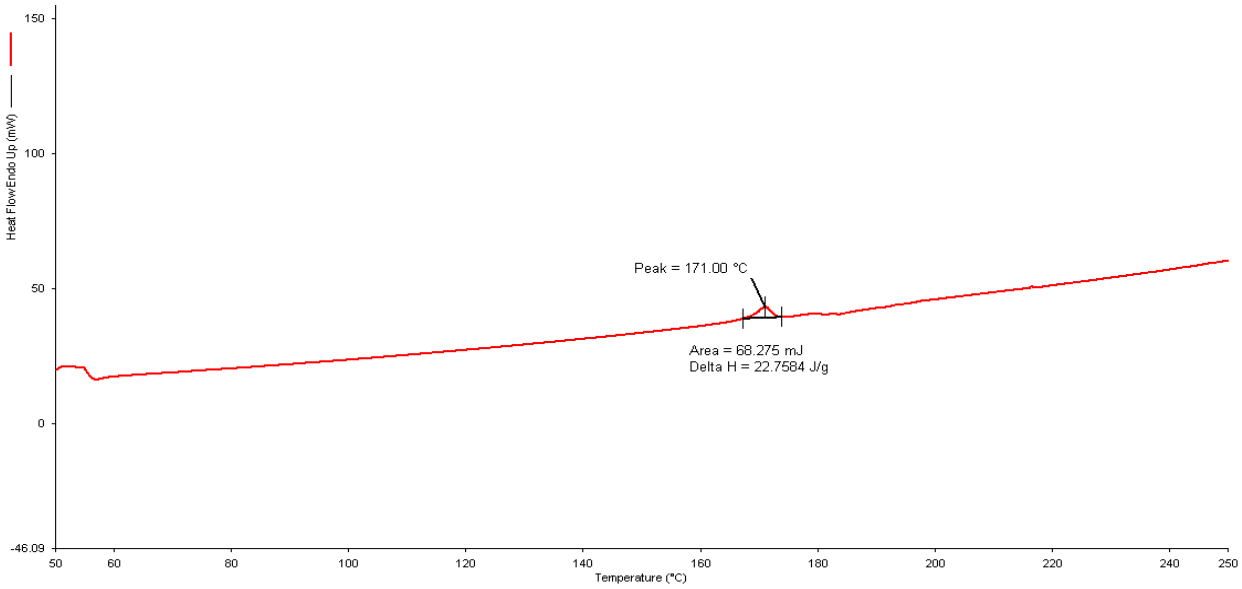

Figure 3. 5 Typical DSC thermogram for a 1:1 mixture of D4T and Eudragit® RSPO determined at a heating rate of 10°C/min

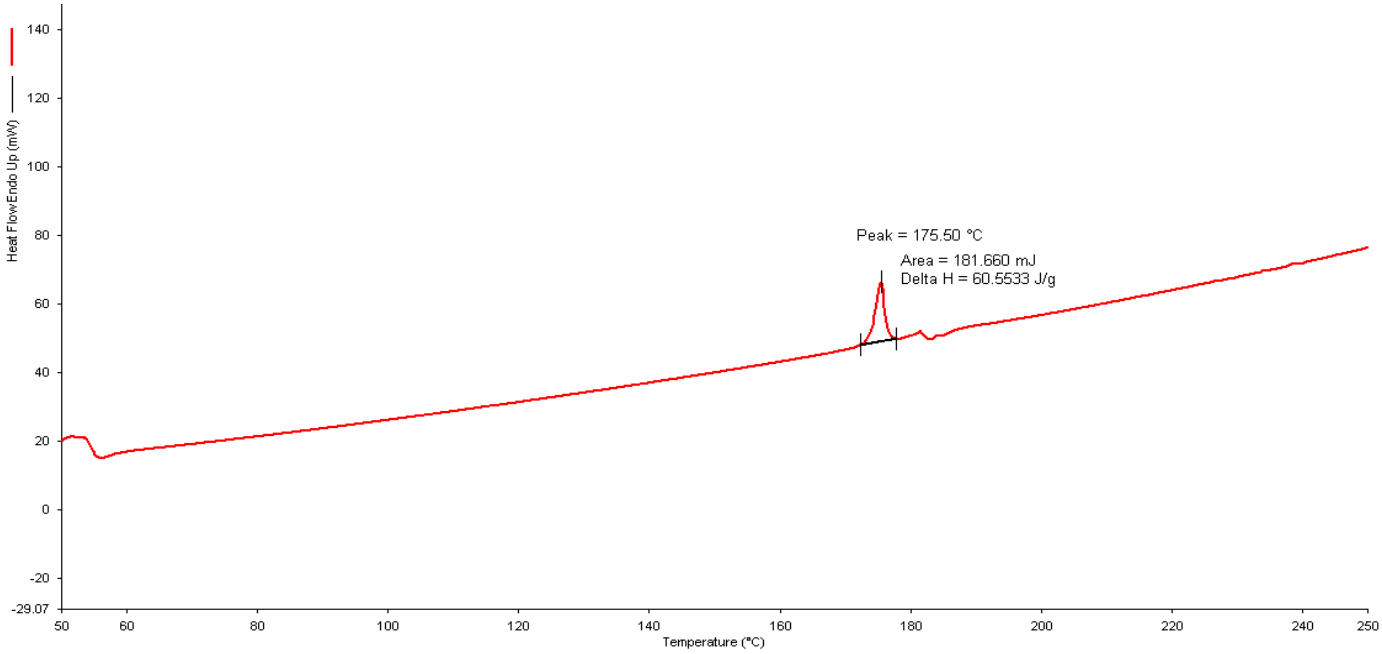

Figure 3. 6 Typical DSC thermogram for a 1:1 mixture of D4T and Eudragit® EPO determined at a heating rate of 10°C/min

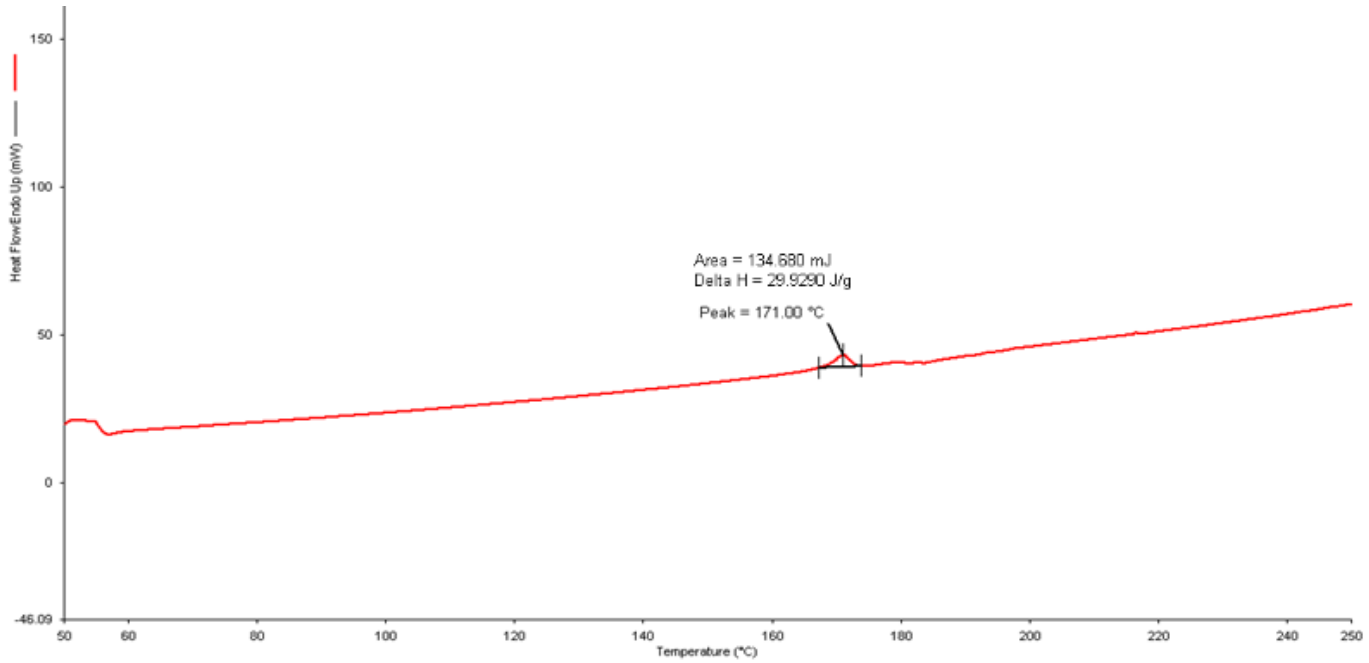

Figure 3. 7 Typical DSC thermogram for a 1:1 mixture of D4T and Eudragit® S100 determined at a heating rate of 10°C/min

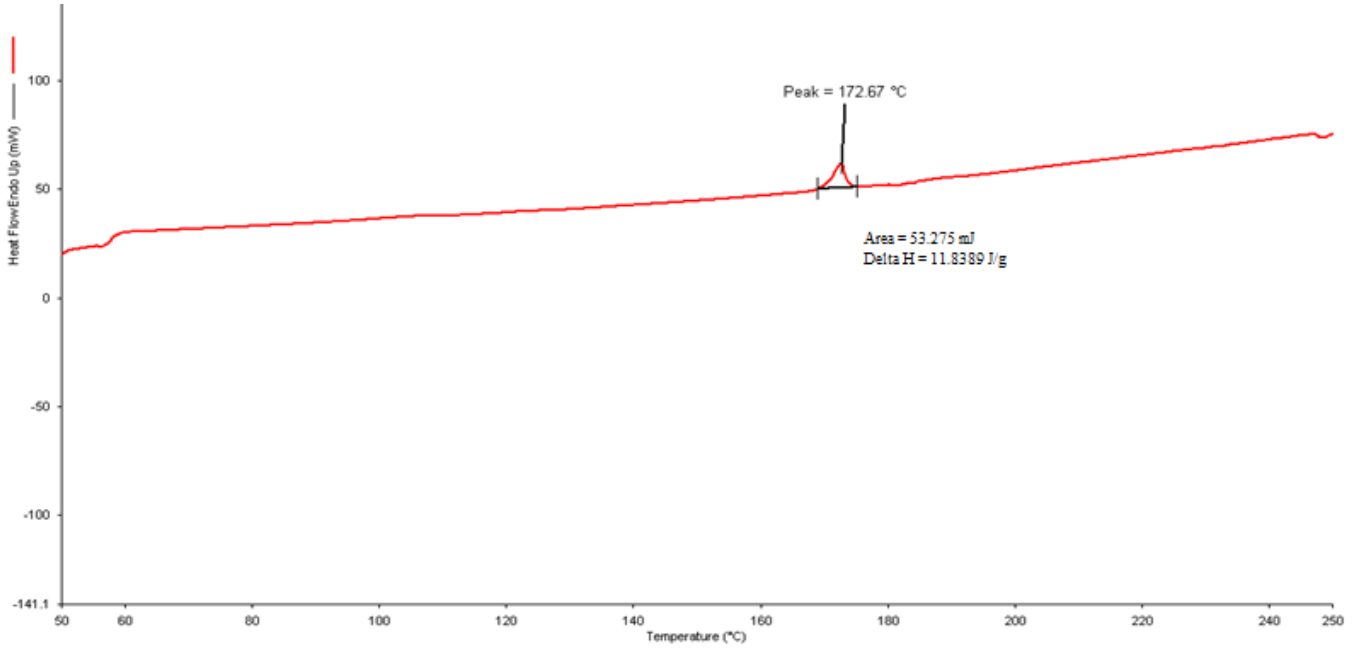

Figure 3. 8 Typical DSC thermogram for a 1:1 mixture of D4T and Eudragit® RLPO determined at a heating rate of 10°C/min

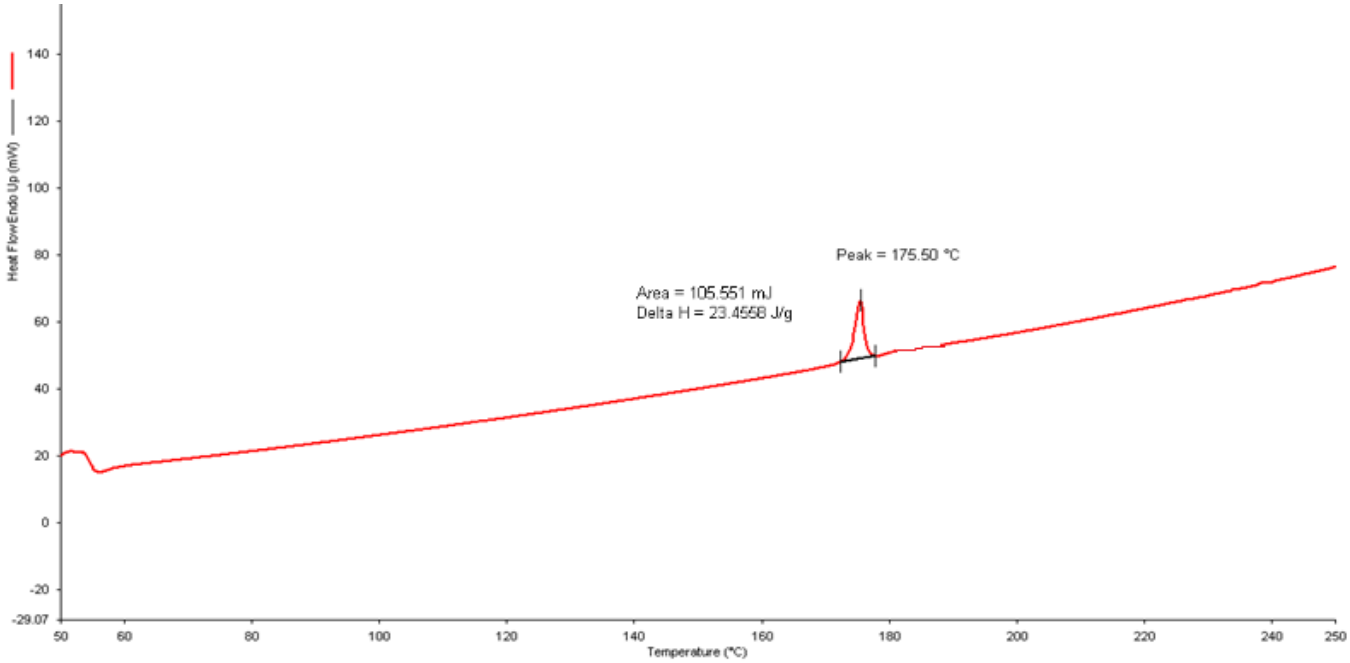

Figure 3. 9 Typical DSC thermogram for a 1:1 mixture of D4T and Kollidon® VA64 determined at a heating rate of 10°C/min

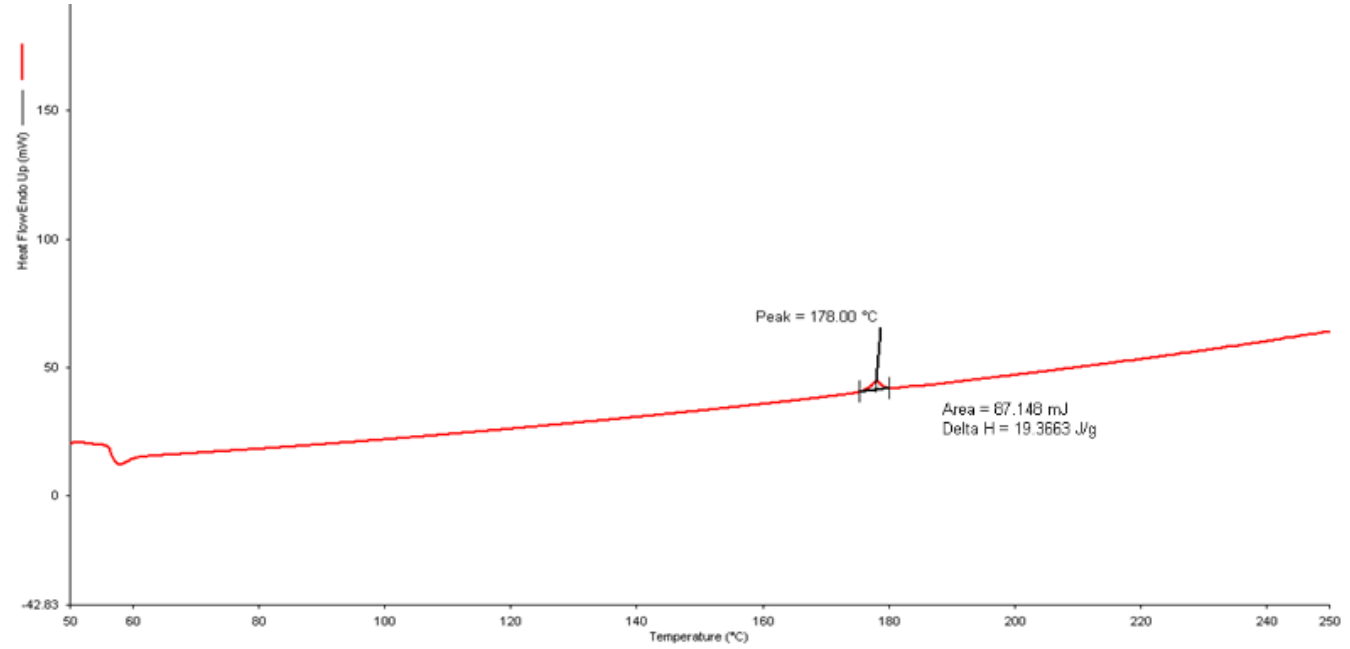

Figure 3. 10 Typical DSC thermogram for a 1:1 mixture of D4T and Methocel® K4M determined at a heating rate of 10°C/min

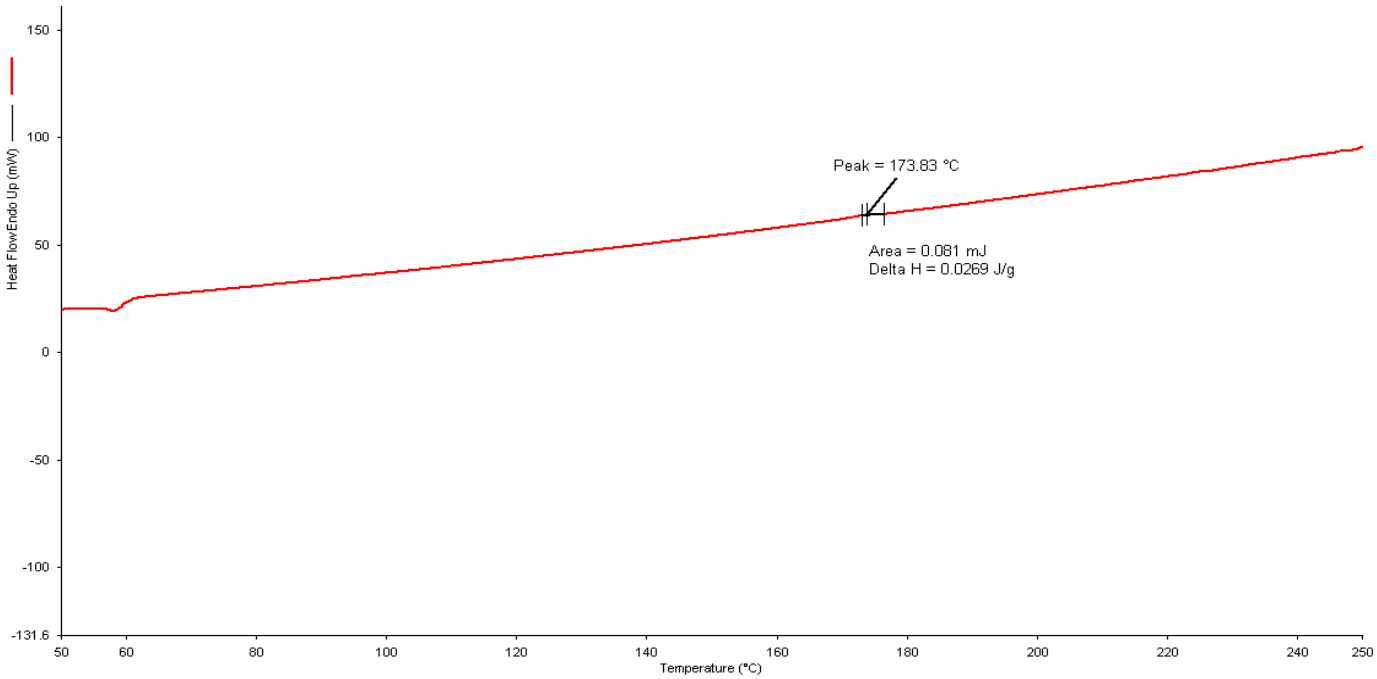

Figure 3. 11 Typical DSC thermogram for a mixture of D4T with all excipients determined at a heating rate of 10°C/min

No new peaks and significant thermal events were observed in the thermograms for mixtures of D4T and excipients. These results were expected as most of the excipients do not melt in the temperature range used for DSC studies and it was concluded that there were no interactions as only the D4T endothermic peak was evident in the thermogram. Some minor changes in the peak shape of the melting endotherm for D4T that was observed may have been due to the quantity of material used. Dilution of the API with excipients may have resulted in the shift and therefore the presence of incompatibility may not be evident. Infrared spectroscopy was used to confirm the absence of interactions. This narrow range of temperatures was used since during formulation development D4T and the excipients would not be subjected to temperatures higher than the range tested.

3.6.2 Infrared Spectroscopy

IR studies revealed that all characteristic bands for D4T were present in all spectra generated for all combinations tested. The IR spectra for D4T, mixture of all excipients and API, 1:1 binary mixtures of API and excipient are depicted in Figures 3.12-3.22 and reveal no new bands or shifts in the characteristic peaks that were present for pure D4T. A summary of the significant peaks for the IR spectrum of D4T depicted in Figure 3.12 and the peaks observed are consistent with those previously reported [131-135].

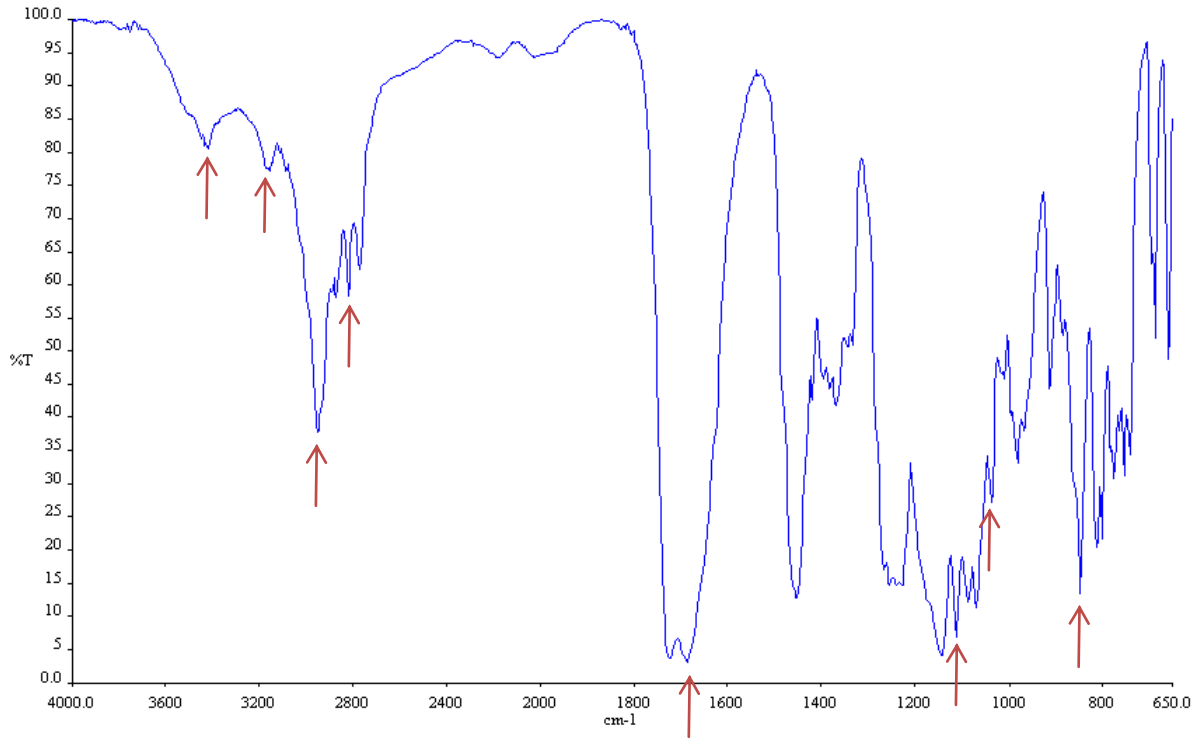

Figure 3. 12 Infrared absorption spectrum of D4T

The peak at 3422cm^{-1} is representative of the OH stretching of the hydroxyl group in the D4T molecular structure. Another important peak is that observed for NH stretching of the secondary amine at a wave number of 3161cm^{-1}. The band observed at 1691cm^{-1} represents C=O stretching of the aromatic structure. C-H stretching of the CH_3 bond and a C-C stretch are evident at wavenumbers 2875 and 1113 cm^{-1}, respectively. Scissoring and bending of the C-H bond and N-H of D4T are evident at 1088 and 848 cm^{-1} and a summary of these assignments is listed in Table 3.2.

Table 3. 2 IR absorption band assignments for D4T

Major band frequencies cm^{-1}	**Assignment**
3422	OH stretch of hydroxyl group
3161	NH stretching of secondary amine
3039	CH stretch
2875	CH stretching of CH_3 group
1691	C=O stretching of aromatic structure
1113	C-C stretch
1088	C-H scissoring and bending
848	NH bend

The FT-IR absorption spectra for D4T and excipients indicate that the characteristic bands of D4T and those of the polymers and excipients are evident in all spectra as indicated by the

arrows (Figures 3.13 to 3.21). The mixture of all excipients and API reveals similar results (Figure 3.22). It was therefore concluded that there was no evidence of incompatibility confirming the observations from DSC studies. However a slight shift in bands and the intensity of the bands was observed and this could have been due to dilution of the API with the excipients and does not necessarily imply any incompatibility. However, long term stability studies are needed in order to be able to state categorically that there are no interactions or compatibility issues.

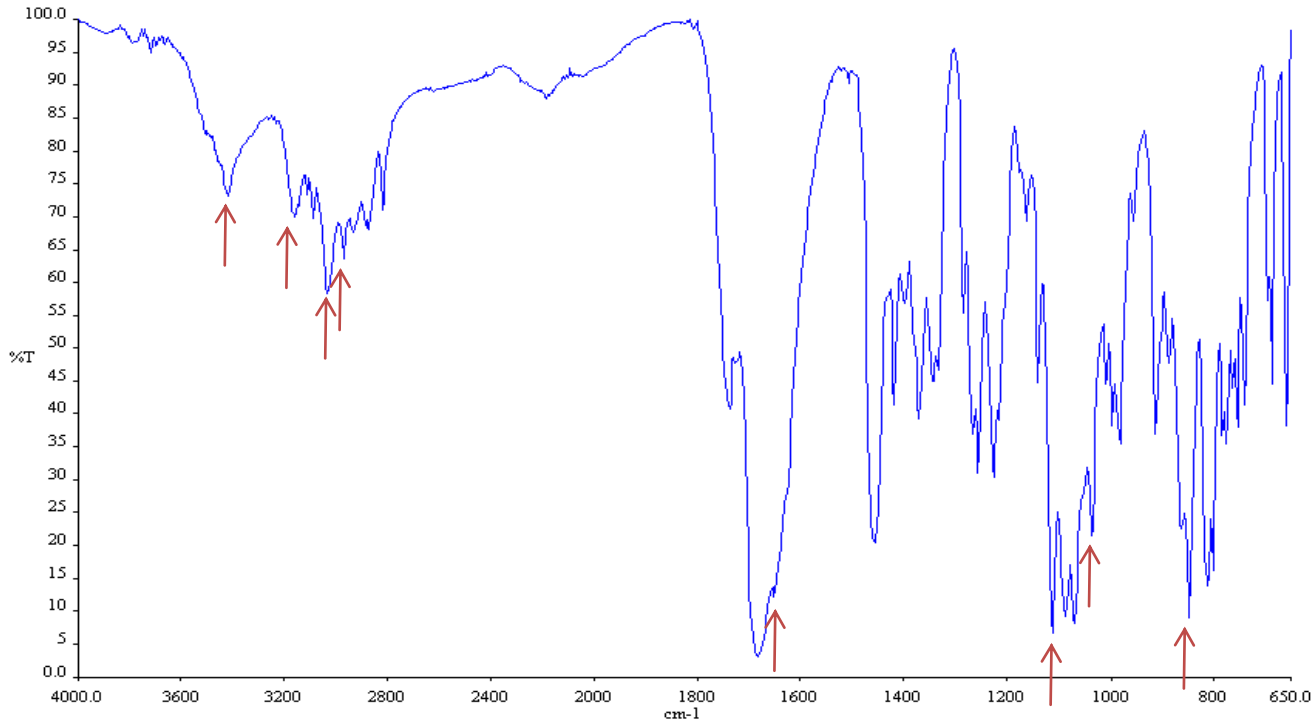

Figure 3. 13 Infrared spectrum of a 1:1 ratio of D4T and Klucel®

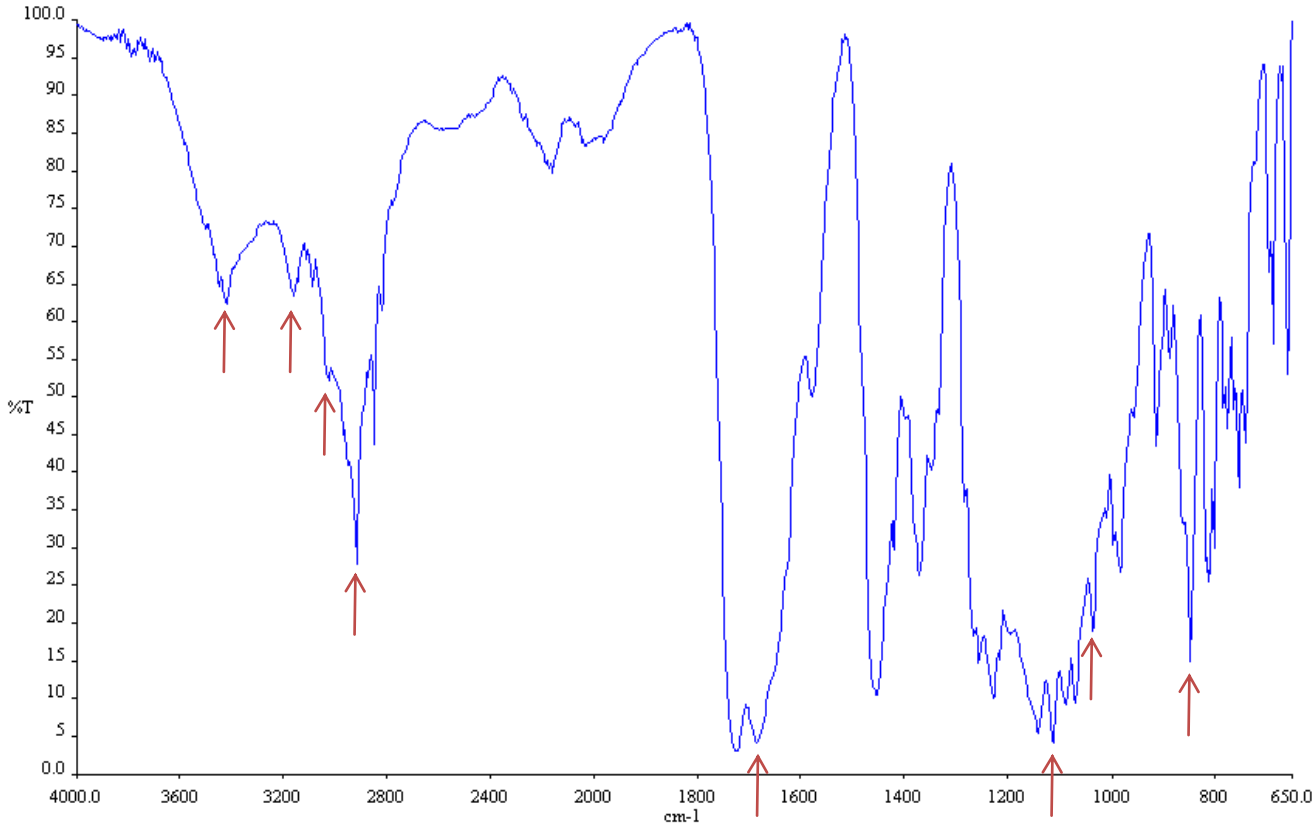

Figure 3. 14 Infrared spectrum of a 1:1 ratio of D4T and Avicel® PH102

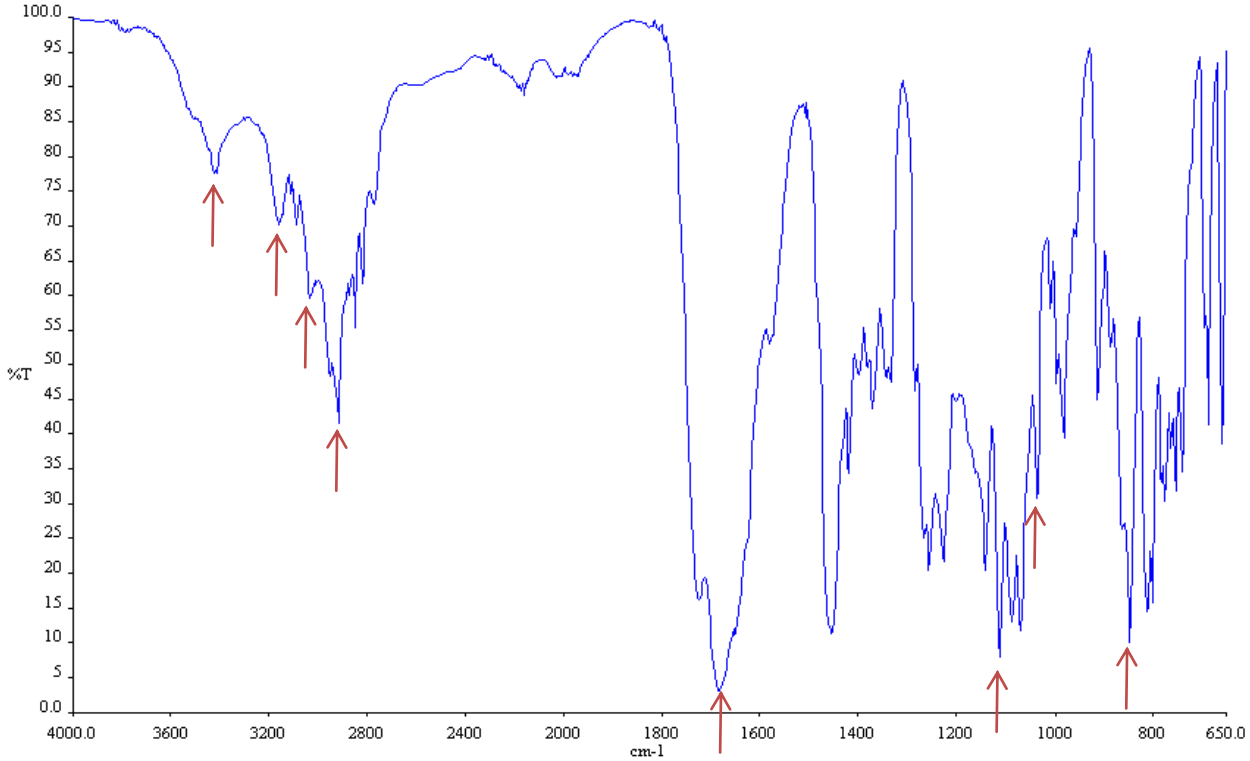

Figure 3. 15 Infrared spectrum of a 1:1 ratio of D4T and magnesium stearate

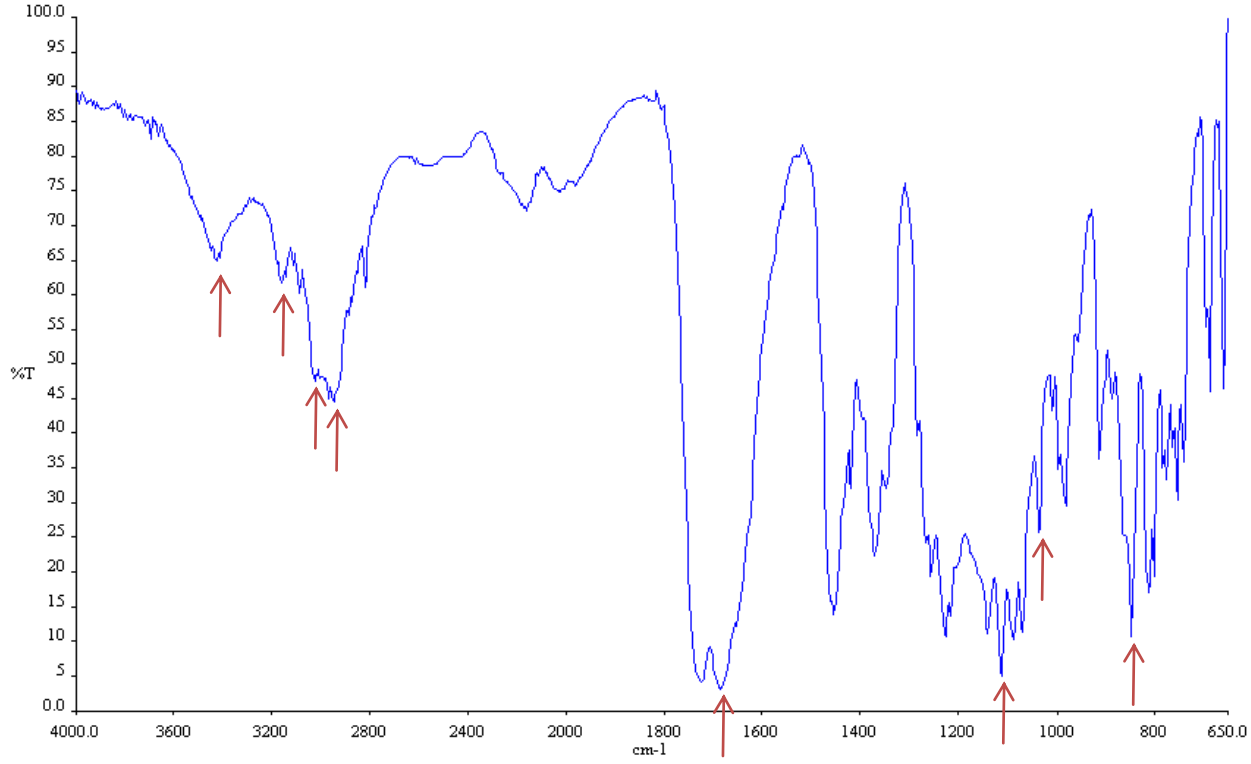

Figure 3. 16 Infrared spectrum of a 1:1 ratio of D4T and Eudragit® RSPO

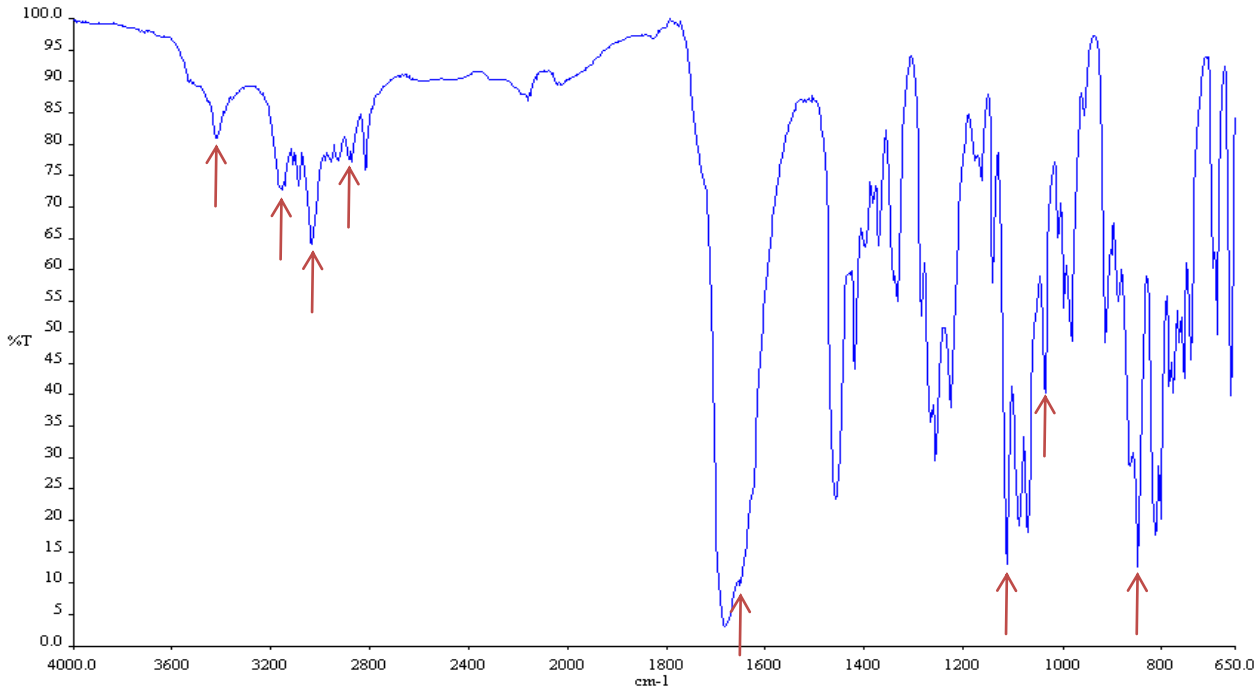

Figure 3. 17 Infrared spectrum of a ratio of D4T and Eudragit® EPO

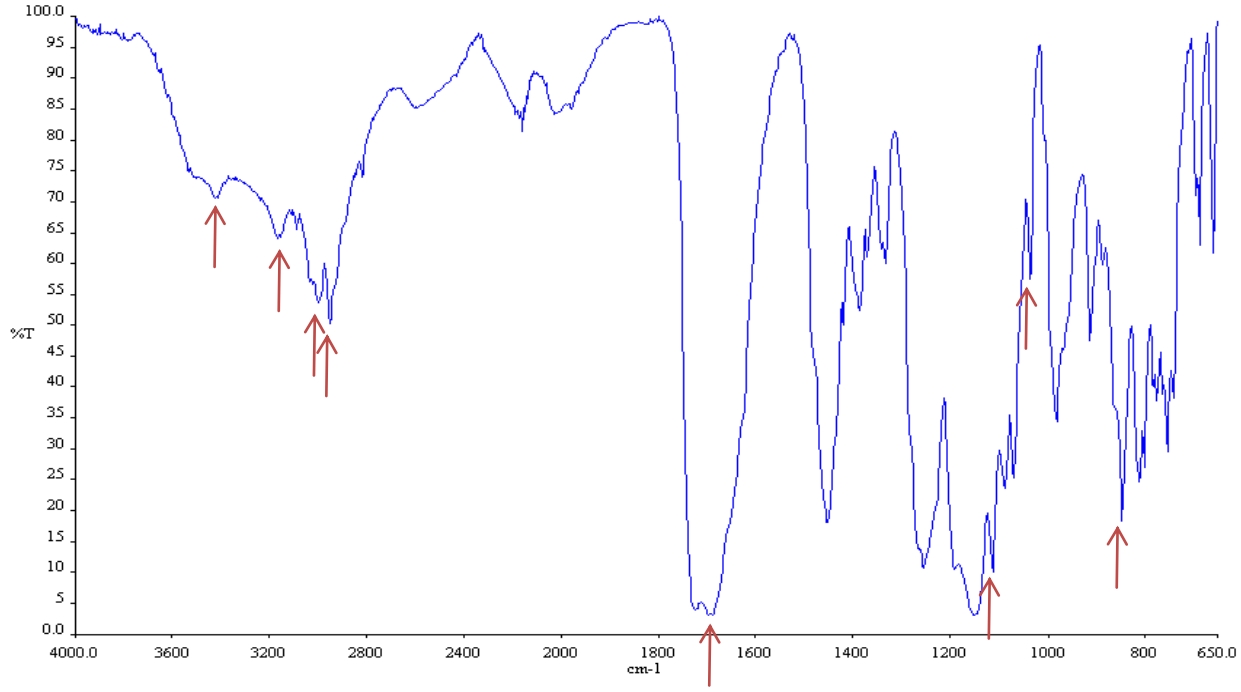

Figure 3. 18 Infrared spectrum of a 1:1 ratio of D4T and Eudragit® S100

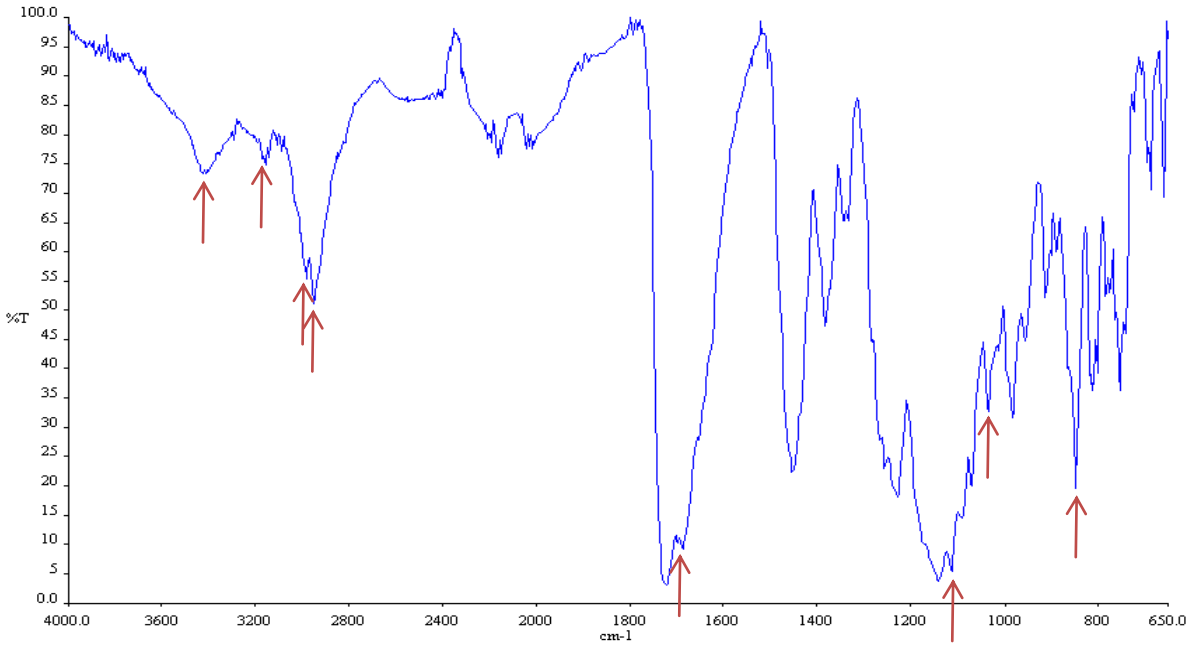

Figure 3. 19 Infrared spectrum of a 1:1 ratio of D4T and Eudragit® RLPO

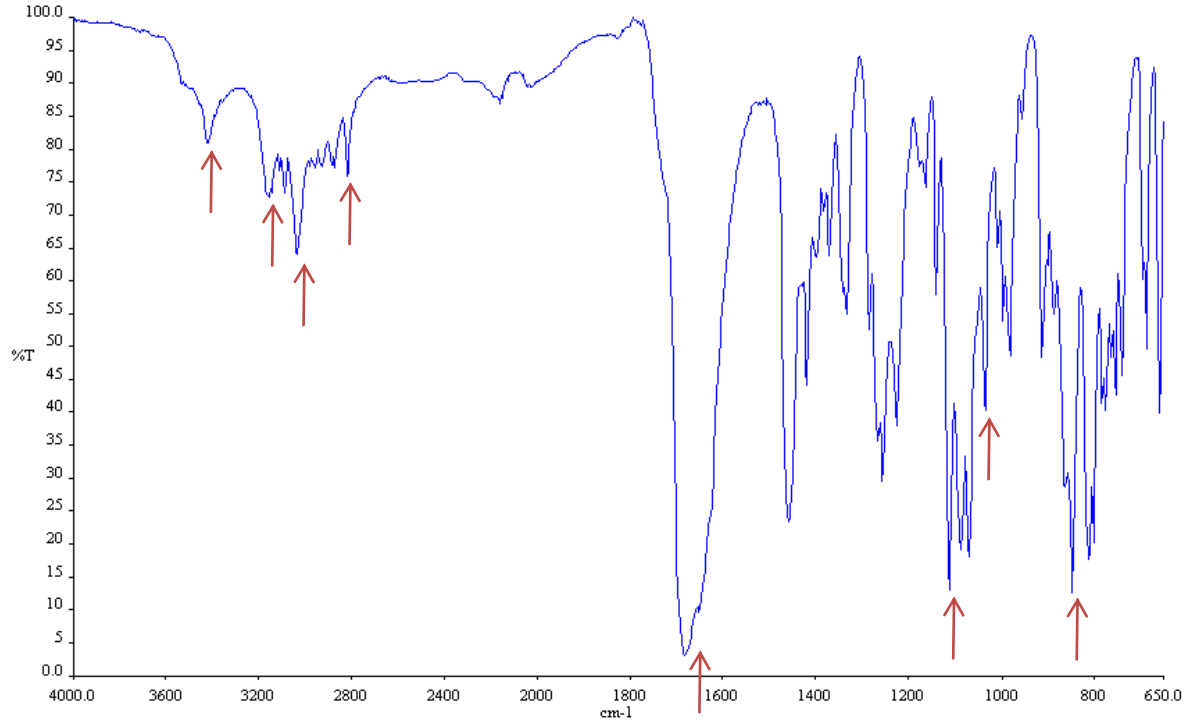

Figure 3. 20 Infrared spectrum of a 1:1 ratio of D4T and Kollidon® VA 64

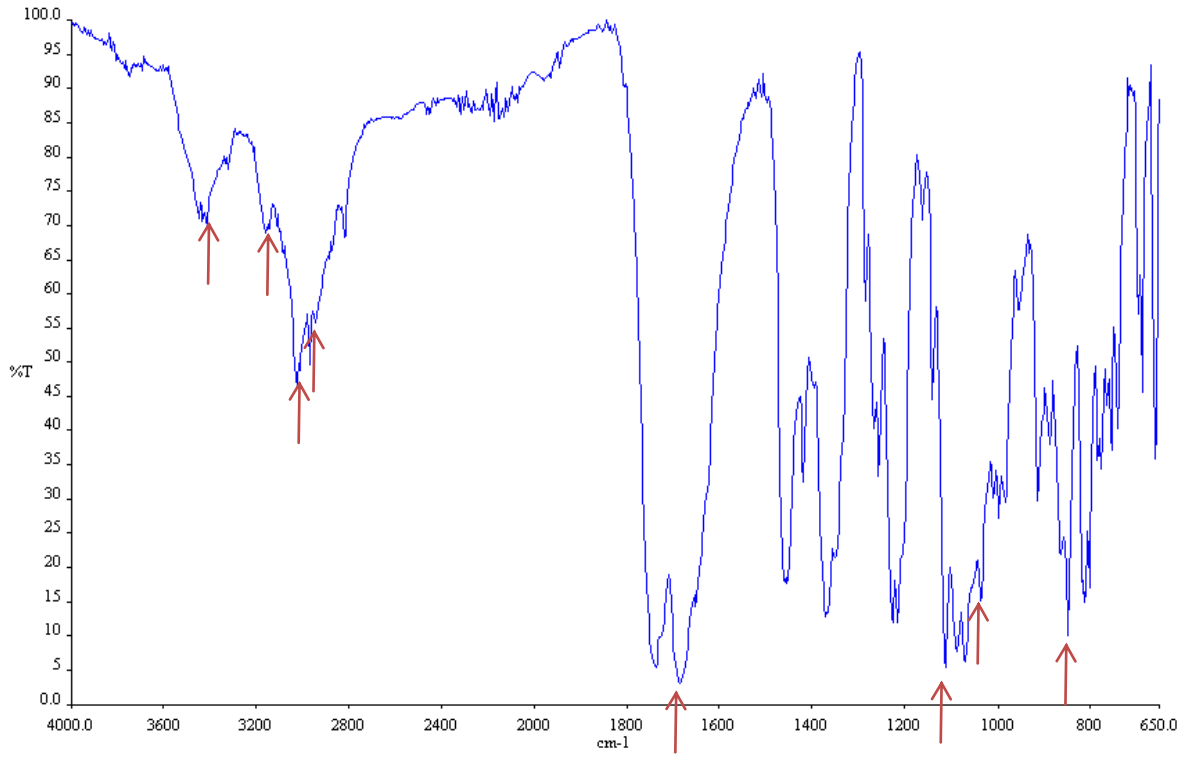

Figure 3. 21 Infrared spectrum of a 1:1 ratio of D4T and Methocel® K4M

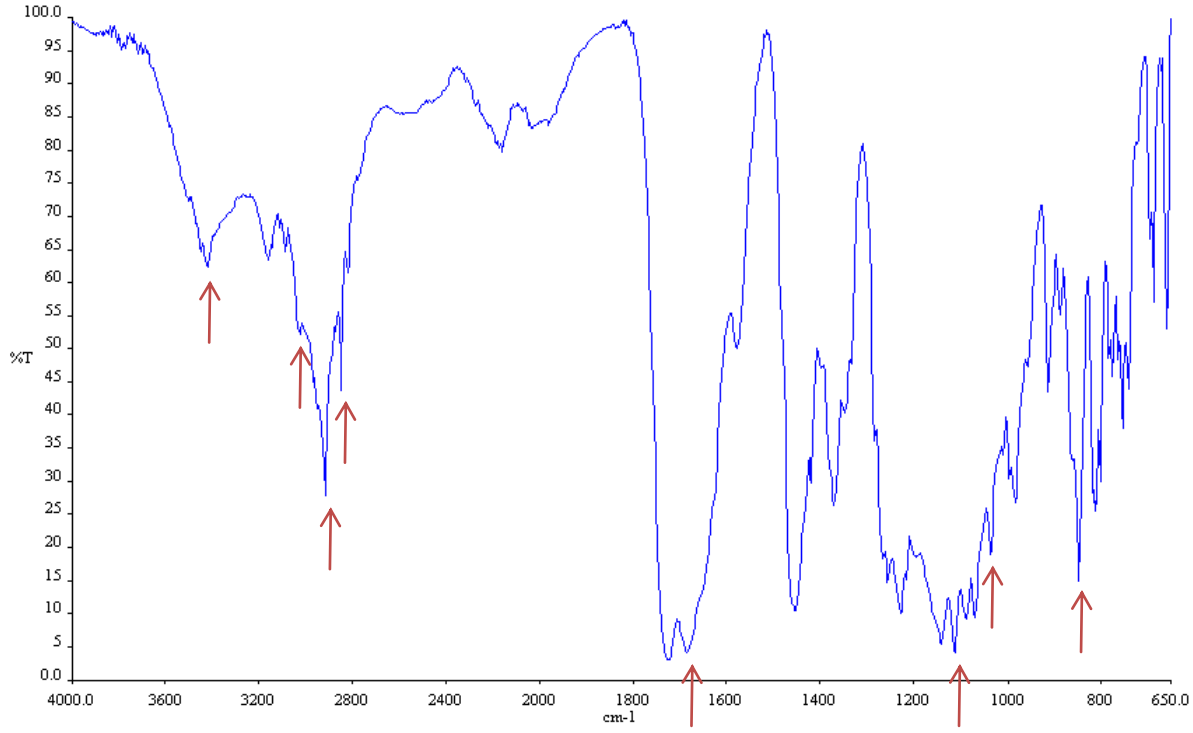

Figure 3. 22 Infrared spectrum of a 1:1 ratio of D4T and all excipients

3.6.3 Thermogravimetric analysis

Thermogravimetric analysis of D4T reveals that the molecule is stable up to a temperature of approximately 190°C and then it decomposes in three distinct steps (Figure 3.23). The first decomposition starts at 190-220°C with an associated loss of 40% by weight. The next step starts at 220-270°C with a further 20% loss in weight and the last residue completely degrades at approximately 300°C with no residue observed at the end of the TG experiment. The decomposition could be due to the fact that D4T exists as 3 different polymorphic forms and decomposition occurs in three steps from the stable form to the least stable polymorph until complete degradation is observed.

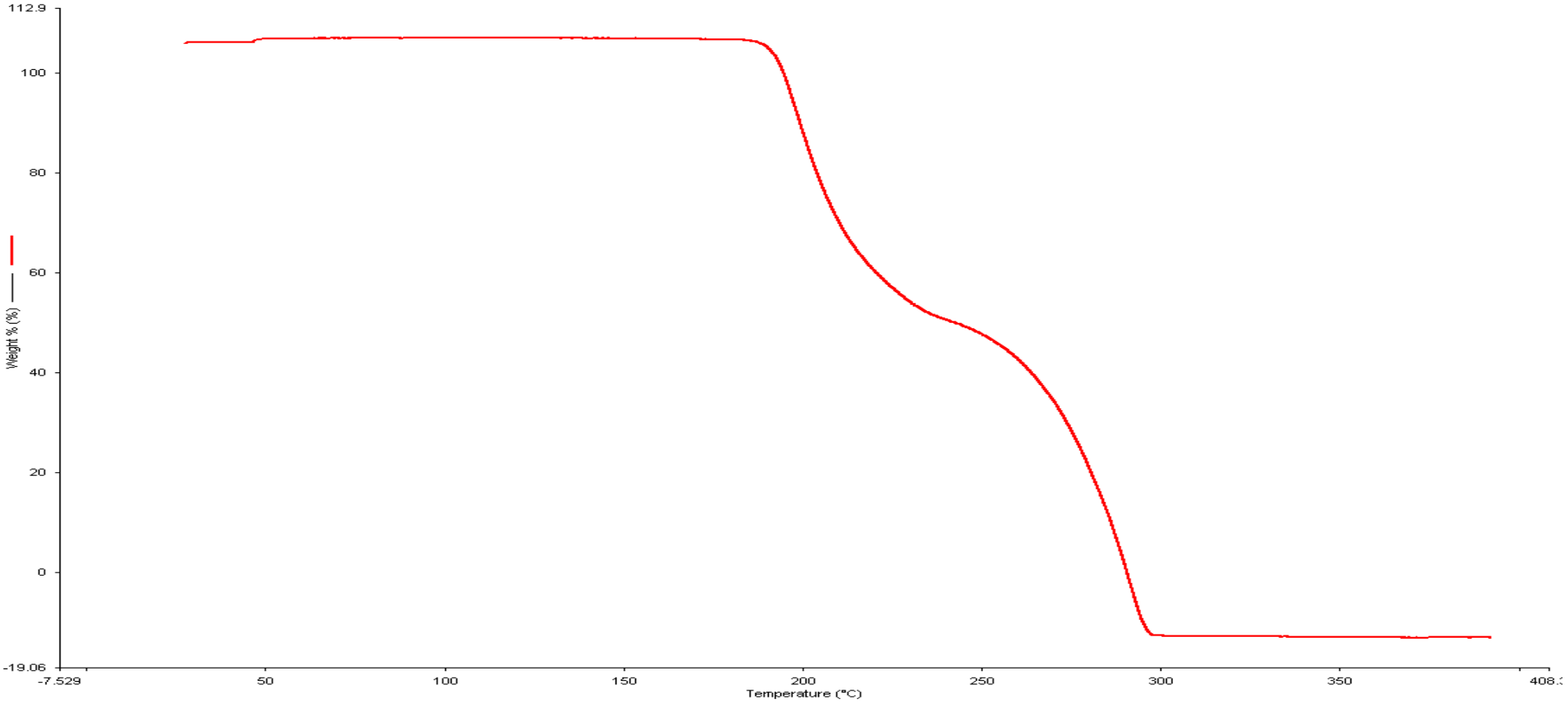

Figure 3. 23 TGA plot for D4T

3.7. CONCLUSIONS

Formulation studies involve the development of dosage forms that are stable, of high quality, safe, effective and must be acceptable to patients. Dosage forms contain a number of excipients and preformulation studies must be performed to ensure that the API is compatible with these materials. Although excipients are generally considered pharmaceutically inert they often initiate or participate in chemical and physical interactions with an API to form degradation products thereby reducing the amount of API available to exert a therapeutic effect and possibly compromising the safety of the product. In order to formulate a suitable dosage form, formulation scientists have to develop an extensive scientific understanding of the physical characteristics of the API and the manner in which it interacts with the adjuvants that may be used or present in a product. Investigations were undertaken using DSC, TGA and results were confirmed using IR. The results observed in these studies indicate that there is no evidence of incompatibility between the potential excipients to be used and D4T and it was concluded that these adjuvants could be explored for microencapsulation studies.

The DSC thermogram of D4T revealed a melting endotherm at 175.5°C which corresponds to the melting point of the stable polymorph of D4T which is consistent with what has been reported [131-134]. DSC analysis of combinations of D4T in 1:1 ratio with excipients revealed no evidence of any interaction as no new peaks were observed and a single peak for D4T was evident. This was further confirmed by IR spectroscopic analysis that revealed the presence of all principal bands for the binary mixtures of API and excipient. The presence of an interaction is usually revealed by the absence or appearance of frequency bands. TGA was also undertaken to establish whether D4T undergoes degradation and it was noted that the molecule degrades in three distinct steps in different temperature ranges with the initial degradation commencing at a temperature of approximately 190°C leaving no residue after a temperature of 300^0C. D4T exists in three different polymorphic forms and degrades to the least stable polymorph at temperatures higher than 190°C. TGA is important tool for predicting whether an API is likely to degrade under manufacturing conditions. As the temperature of manufacture of microparticles is likely to be under 100^0C we can conclude that D4T is unlikely to degrade under normal operating conditions.

In summary preformulation studies are essential for establishing the potential composition of a final formulation in addition to determining the relevant storage conditions and precautions to be taken for manufacture and storage of a final product. IR and DSC are useful analytical

tools in formulation development studies; however it is important to use several techniques as data from one approach may not permit conclusive decisions to be taken in respect of the stability and or incompatibility of an API or product.

CHAPTER FOUR

DEVELOPMENT AND ASSESSMENT OF SUSTAINED RELEASE STAVUDINE MICROPARTICLES

4.1 INTRODUCTION

D4T is a virustatic drug that has a short half-life of 1.5 hours and therefore requires frequent dosing for effective therapy [136]. It is initially well tolerated, however patients treated with D4T develop lipodystrophy, peripheral neuropathy and lactic acidosis on long term therapy [136, 137]. The side effects are dose dependent and a reduction of the total administered dose may reduce the severity of toxicity and still suppress the viral load [138, 139]. Attempts to reduce the frequency of administration and to improve patient adherence by decreasing the incidence of side effects through the use of a SR formulation of D4T to maintain constant drug levels in the body and avoid dose dumping have been reported [138, 140]. D4T is affordable in comparison to other ARV and presents with fewer serious side effects such as renal disease [141, 142]. The majority of patients on ARV are supplied by public health facilities and to meet demand the use of affordable drugs like D4T is beneficial [140].

The use of novel technologies has become popular for the development of SR dosage forms. A sustained, constant drug concentration at therapeutic levels is required to treat a number of pathological conditions [143]. Therefore the manufacture of controlled and/or targeted drug delivery systems is an important task for pharmaceutical technology [1, 143]. One such approach is microencapsulation, a process by which small droplets or particles of liquid, solid or gaseous material are surrounded, enclosed or coated with a continuous film of a polymeric material [144]. The unique nature of microencapsulation lies in the small size of the coated particles, their subsequent use and adaptation to use in a wide variety of dosage forms [145].

Microencapsulation is a well-designed controlled drug delivery approach that can be used to achieve maximum therapeutic efficacy. Microparticles deliver drugs to target tissues in the desired amount, at an appropriate rate, in the right time without toxicity and with minimal side effects [144]. Ideal microparticles should have a particle size ranging between 1µm and 3mm and should incorporate reasonably high concentrations of drug, be stable with an acceptable shelf life, release the drug with control over a wide time scale, biocompatible with controllable biodegradability and not be susceptible to chemical modification.

Microencapsulation may lead to a decrease in the incidence of side effects that occur due to dose dumping and this approach therefore improves patient adherence [144, 146].

A microparticle consists of two parts viz., the core and coating materials. The core material(s) is defined as the material to be coated and may be liquid or solid. The core can be a mixture of API, stabilizers, diluents and rate retarding compounds [145, 146]. The coating material should stabilize the core material, be inert and must control the release of API under specific conditions. Moreover it must be a film-forming, pliable, tasteless, stable, non-hygroscopic, economical and soluble material [146].

The different methods of microencapsulation can be classified into mechanical and physico-chemical encapsulation processes. In these studies D4T microparticles were manufactured using a solvent evaporation technique that has gained much attention due to its ease of use without compromising the activity of the API [144, 146].

4.1.1 Solvent evaporation

Solvent evaporation is a technique performed in a liquid vehicle that is prepared by agitation of two immiscible liquids. There are various methods of performing microencapsulation using solvent evaporation. The ideal approach is one that provides efficient API encapsulation and is dependent on the hydrophilicity or hydrophobicity of the API [147]. The oil- in- water method (o/w) is frequently used for insoluble or poorly soluble drugs. This is the simplest approach and other methods are derived from it. However this method is not suitable for the encapsulation of water soluble or hydrophilic drugs simply because hydrophilic drugs do not dissolve in organic solvents or will diffuse into the continuous aqueous phase during emulsion formation, leading to loss of API and low encapsulation efficiencies [147, 148]. There are four methods that have been proposed for the encapsulation of hydrophilic molecules and include the w/o/w double emulsion, o/w co-solvent, o/w dispersion and o/o non-aqueous solvent evaporation where the aqueous phase is replaced by mineral oil [148].

For the purposes of this study an o/o non-aqueous solvent evaporation method was selected for the encapsulation of D4T. The approach is comprised of four major steps (Figure 4.1) [125].

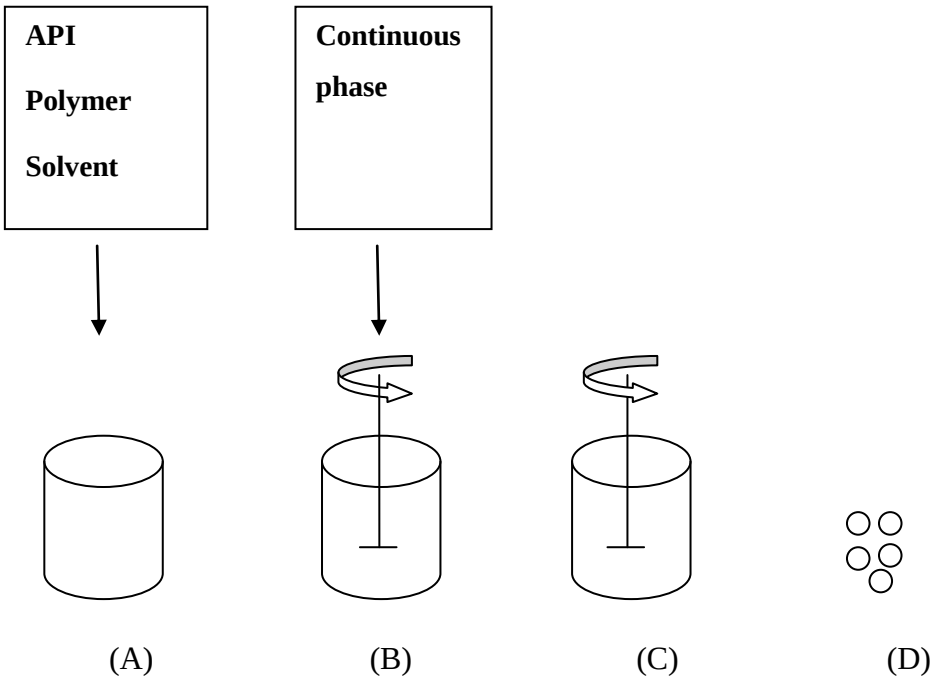

Figure 4. 1 Basic steps of microencapsulation using solvent evaporation

Initially the hydrophilic API is dissolved in a suitable organic solvent (A) containing polymer and any other excipients such as droplet stabilizers and/or diluents. Emulsification (B), of the organic phase in suitable oil and a continuous phase that can consist of hexane to aid with the hardening of the microparticles is then undertaken. Extraction of solvent from the dispersed phase by the continuous phase (C) is accompanied by solvent evaporation, transforming droplets of dispersed phase into solid particles. Following recovery and drying of microparticles to eliminate the residual solvent the product is harvested (D).

When selecting materials for use in the solvent evaporation approach a number of specific criteria have to be met. The polymer used must be biodegradable or biocompatible as this is an essential property for use in pharmaceutical applications [148]. Non-biodegradable polymers such as the polymethyl methacrylates with biocompatible properties may be used as drug carriers [148].

The selection of organic solvents for obtaining a good yield and advantageous characteristics of a product is mainly restricted by their residual toxicity. ICH guidelines classify solvents into 3 classes according to their toxicity and potential to harm humans [149]. Class 1 organic solvents are to be avoided in pharmaceutical manufacturing since they are known human carcinogens. Class 2 organic solvents use is limited since they are possible causative agents of irreversible conditions such as neurotoxicity or teratogenicity. Class 3 organic solvents

have a low toxic potential to humans and no health-based exposure limit is required. An example of Class 3 solvents include acetone which was used as the solvent for the purposes of this study [149]. Other constituents can be added to the dispersed phase and magnesium stearate has been used as a droplet stabilizer whilst microcrystalline cellulose as a diluent. Operating conditions and other process parameters have a significant impact on the properties of microparticles and these are summarised in Table 4.1 [124, 147, 148, 150-154].

Table 4. 1 Summary of operating conditions and parameters affecting microparticle quality and integrity

Factors		Impact on properties of microparticles		
		Size	**Surface morphology**	**Encapsulation efficiency**
Viscosity	Increased viscosity of dispersed phase	larger diameter	Smoother surface	Increased efficiency, slower drug release
Ratio of dispersed to continuous phase	Increased volume fraction of dispersed phase to continuous phase	Decrease in diameter or no influence	-	Increased efficiency
API content	Increased quantity of drug in the dispersed phase	-	More porous and irregular	Low efficiency when the quantity of drug is too high due to the formation of big pores
Operating conditions	Increased temperature	larger diameter	Coarser surface	Decreased efficiency
	Increased agitation rate	Smaller diameter and small size distribution	-	-

4.1.2 Aim

The object of this work was to develop and evaluate SR D4T microparticles. Initial manufacturing studies included screening important factors that may have significant effects on D4T encapsulation and release.

4.2 EXPERIMENTAL

4.2.1 Materials

D4T was donated by Aspen Pharmacare (Port Elizabeth, South Africa). Microcrystalline cellulose (Avicel® 102) was purchased from FMC (Philadelphia, USA). Eudragit® RSPO and EPO was donated by Rohm Pharma (GmbH, Darmstadt, Germany). Liquid paraffin was supplied by ADC laboratories (Durban, South Africa). Acetone was purchased from Associated Chemical Enterprises (Southdale, South Africa). *n*-Hexane was purchased from Burdick and Jackson Laboratories (Michigan, USA).

4.2.2 Methods

4.2.2.1 Formulation composition

Ten formulations were prepared by o/o non-aqueous solvent evaporation using different polymers and polymer concentrations for screening purposes. The formulations were assessed in terms of flowability using the Hausner ratio (HR), Carr's Index (CI) and angle of repose (AOR), cumulative % D4T released using USP Apparatus 1, % yield and encapsulation efficiency (%EE). The best formulation in terms of % D4T released, % EE, % yield, flowability and surface morphology was selected for further optimization. A summary of the formulation composition is listed in Table 4.2. The micraparticles were filled into size 3 gelatine capsules before dissolution testing. For all preliminary formulations 10% w/v D4T and 1% w/v magnesium stearate were used and all experiments were performed on a laboratory scale in triplicate.

Table 4. 2 Screening formulation compositions

Batch number	Eudragit® EPO	Eudragit® RSPO	Eudragit® RLPO	Eudragit® S100	Kollidon® VA64	Klucel®	Methocel® K4M	Avicel® 102
ST-001	30	-	-	-	-	-	-	59
ST-002	-	30	-		-	-	-	59
ST-003	-	-	30	-	-		-	59
ST-004	-	-	-	30	-	-		59
ST-005	-		-	-	30	-	-	59
ST-006	-	-		-	-	30	-	59
ST-007	-	-	-	-		-	30	59
ST-008	-	45	-	-	-	-	-	44
ST-009		45	15	-	-	-	-	29
ST-010		45	-	15	-	-	-	29

4.2.2.2 Manufacture of microparticles

The manufacture of microparticles involved dissolving a polymer(s) in acetone to produce a microparticle coating solution. A diagrammatic representation of the manufacture of microparticles is depicted in Figure 4.2.

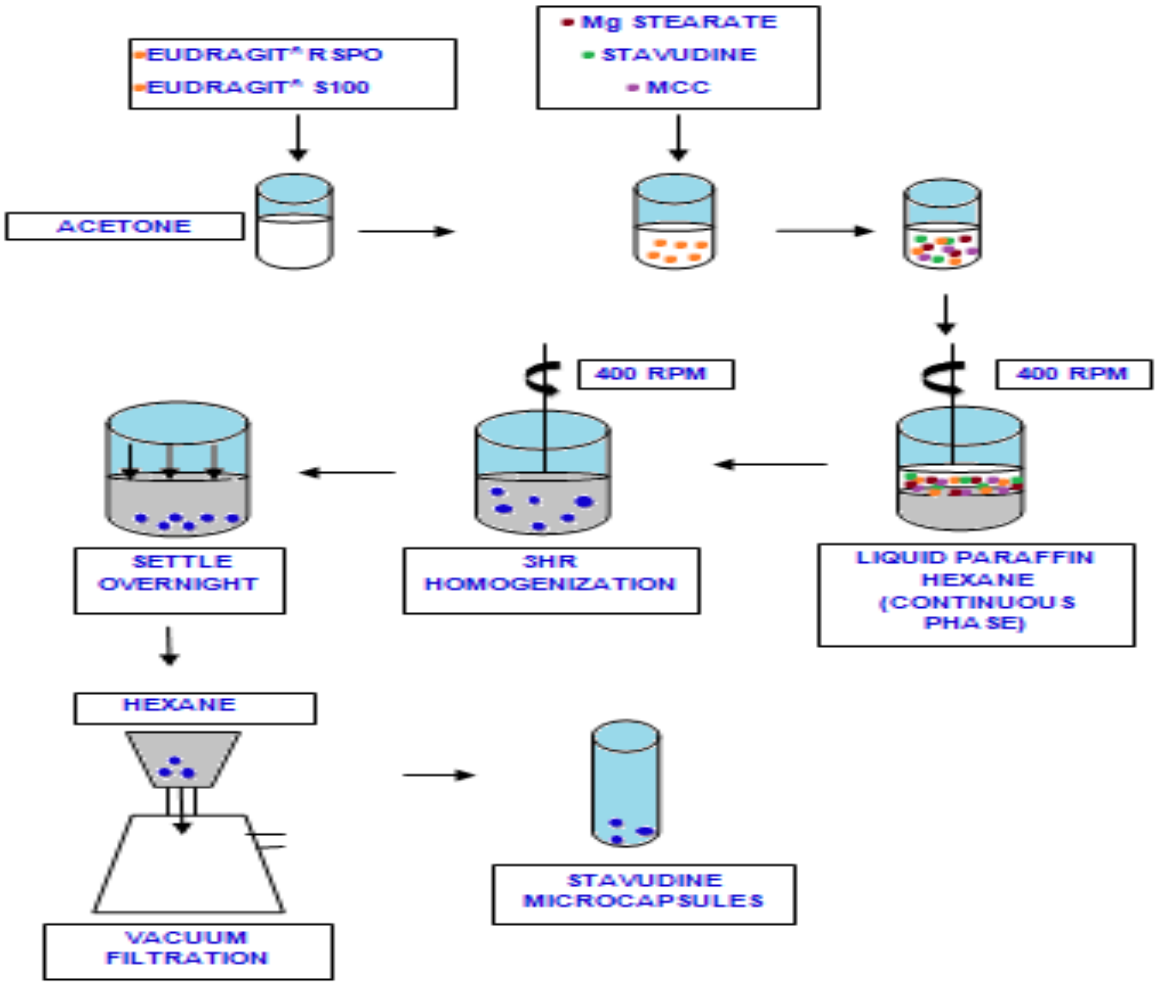

Figure 4. 2 Schematic representation of the manufacture of D4T microparticles

D4T, Avicel®PH102 and magnesium stearate were added to the polymer solution and constituted the dispersed phase. D4T and coating material mixture was dispersed with agitation at 400rpm using a homogenizer fitted with a four-blade "butterfly" propeller of 50 mm diameter (Virtis ® Company, USA) in the liquid paraffin which also contained hexane. Hexane was added to harden the microparticles and to facilitate the formation of microparticles. Agitation of the system was continued for a further 3hours until the acetone had partitioned into the continuous phase. The solvent, removed by evaporation, resulted in the formation of hardened microparticles containing D4T. The microparticles were left to settle overnight and the hardened microparticles were filtered through a 125mm diameter filter paper (Whatman International Ltd, Maidstone, England), collected using a funnel and washed with hexane to remove excess liquid paraffin. The microparticles were then harvested and left to dry at room temperature (22°C) and were stored in well-closed containers. The microparticles were assessed in terms of particle size, flowability, D4T release, surface morphology and encapsulation efficiency.

4.2.2.3 Flowability

The flowability of microparticles is essential in order for them to be conveniently filled into hard capsules. Some of the methods used for measuring flowability include, but are not limited to measurement of the AOR, determination of CI and HR that are calculated using the bulk and tapped density of the microparticles [155].

4.2.2.3.1 Angle of repose

The AOR (θ) for each batch was measured by placing 3g of the microparticles in a funnel (with orifice and base diameters of 1.0 and 5.0 cm, respectively). The tip of the orifice of the funnel was set at a fixed height (30cm) from a horizontal surface and the microparticles were allowed to flow under only the force of gravity. The AOR was calculated using Equation 4.1 and the experimental considerations of the AOR are shown in Table 4.3 [155]. For the purpose of this study an AOR < 40° was considered acceptable with values of < 35° being the most desirable and defined good flow properties.

$$\tan \theta = \frac{h}{r}$$

Equation 4.1

Where,

h = height of the pile of microcapsules, and
r = the radius of the base of the cone.

Table 4. 3 Experimental conditions for the angle of repose [14]

Flow property	Angle of repose (^{0})
Excellent	25-30
Good	31-35
Fair	36-40
Poor	>40

4.2.2.3.2 Bulk and tapped bulk density

The bulk and tapped bulk density of the microparticles were calculated using the initial and final volumes for a fixed mass of microparticles prior to and after tapping. The microparticles were weighed and carefully transferred to a measuring cylinder and the initial volume recorded. Each sample was poured slowly and gently into a 10ml measuring cylinder. The cylinder was lightly tapped to dislodge residual powders from the wall of the measuring cylinder. The cylinder was then tapped using a Model SVM 203 tapped density tester (Erweka GmbH, Heueastamm, Germany) at 220taps/min for 2 minutes. The percent compressibility of the microparticles was expressed using CI calculated using Equation 4.2. This equation describes the relationship between the degree of volume reduction of the powder column and the pressure applied to the powder. A CI greater than 25 is considered to be an indication of poor flowability and < 15, of good flowability and these limits were used for the purposes of this study [155].

$$\mathbf{CI} = \left(\frac{\rho tapped - \rho bulk}{\rho tapped}\right) \mathbf{X100}$$

Equation 4.2

Where,

CI = Carr's compressibility index,
ρ_{tap} = tapped density, and
ρ_{bulk} = bulk density

4.2.2.3.3 Hausner ratio (HR)

The HR is the ratio of the tapped and bulk densities of a material and is calculated using Equation 4.3. A HR > 1.25 is considered to be an indication of poor flowability [155].

$$\mathbf{HR} = \frac{\rho tapped}{\rho bulk}$$

Equation 4.3

Where,

ρ_{tapped} =tapped density
ρ_{bulk} = bulk density

4.2.2.4 Encapsulation Efficiency

Approximately 3g of the microparticles were crushed and powdered using a mortar and pestle. Approximately 300mg of the crushed microparticles was accurately weighed and dissolved in 100ml of mobile phase (methanol: water 35.5:64.5v/v) with sonication for 20minutes using a Branson® B12 sonicator (Branson® Inc., Shelton, CN, USA). The solution was then filtered through a 0.45µm PVDF Millipore® Millex-HV filter paper (Bedford, MA, USA). A 1ml aliquot was withdrawn from this solution and diluted to 10ml with water and analysed using the validated HPLC method described in Chapter 2, to determine the D4T content of microparticles. The % EE was calculated using equation 4.4 [155]. A target %EE > 70% was desirable.

$$\mathbf{\%\ EE} = \frac{\text{actual loaded drug}}{\text{theoretical loaded drug}} \mathbf{X\ 100}$$

Equation 4.4

4.2.2.5 Scanning electron microscopy (SEM)

The shape, surface morphology and particle size of the microparticles was investigated using SEM (Tescan, VEGA LMU, Czechoslovakia Republic). The microparticles were mounted onto a double-sized carbon stub that was placed onto a sample disc carrier (3mm height, 10mm diameter) and were sputter coated with gold under high vacuum with a sputter coater (Balzers Union Ltd, Balzers, Lichtenstein).

4.2.2.6 D4T release studies

Dissolution is defined as the process by which a solid substance enters a solvent to yield a solution and is controlled by the affinity of the solvent for the solid. API release rate determination for SR oral dosage forms adds a level of sophistication to the concept of dissolution testing and requires setting acceptance criteria at multiple time points [156].

The *in vitro* dissolution test serves as a guide to estimating the amount of API released per unit time in a dissolution medium and is a sensitive and in some cases reliable predictor of *in vivo* performance [157]. *In vitro* dissolution testing of pharmaceutical dosage forms has emerged as the single most important test that ensures the quality of a product and is considered one of the most important quality control tools to use when assessing the efficacy of a product *in vitro* [156]. Dissolution testing is also used to ensure batch-to-batch equivalence in respect of quality and is an aid to assess performance when screening formulations during product development studies. *In vitro* dissolution testing should be designed in a way so as to mimic as closely, biological conditions a product might be exposed to [157].

Ideally the dissolution profile of a test formulation should be similar to that of a commercially available product. However in cases where no modified release dosage form is commercially available guidelines from USP, FIP, and FDA for SR dosage forms should be used and these generally state that at 25% of the dosing interval a range of 20-50% of the labelled content should be released. At 50% of the interval 45-75% of the labelled content should be released and at least 75% drug should be released at the full dosing interval [156, 158]. These guidelines were followed for the purposes of this study. In addition SRdosage forms should be tested over the entire physiological pH range (pH 1-7.8) in order to simulate *in vivo* conditions. However there are difficulties in determining the time interval related to a particular pH segment of *in vivo* condition since the time a dosage form is exposed to certain segments is influenced by factors such as the presence of food, body position, gastric emptying time and pH of the GIT fluid [157].

Several dissolution test apparatus have been reported for use in the determination of the dissolution rate of different dosage forms and dissolution media are generally simulated gastric or intestinal fluids maintained at 37°C [156]. A device for agitating the dissolution fluid and product at a fixed speed and a screen for separating disintegrated particles from bulk product is necessary. The time interval, composition of dissolution fluid, type of agitator and mesh size of the screen are variables that are specific for each method 157]. The main

USP dissolution test devices that have been reported include the rotating basket apparatus (USP Apparatus 1), paddle apparatus (USP Apparatus 2), Bio-dis® reciprocating cylinder apparatus (USP Apparatus 3) and the flow-through cell (USP Apparatus 4) [156-158].

For the purposes of this study the USP Apparatus 1 was used for preliminary studies and USP Apparatus 3 was used for testing the optimized formulations. USP Apparatus 3 has several advantages over USP Apparatus 1 in that it can be used to simulate gastro-intestinal conditions with simple programming that permits *in vitro* dissolution pH profiling with biorelevant agitation rates. Through use of this apparatus it is possible to test a variety of samples that are transported sequentially from one medium to the next without operator intervention and the dissolution test can be optimized using different mesh sizes and agitation rates [156, 159].

4.2.2.6.1 USP Apparatus 1 (rotating basket)

The USP/NF rotating basket apparatus for dissolution testing essentially consists of stainless steel 40-mesh wire basket that is rotated at a constant speed ranging between 25 and 150rpm. The basket is usually immersed in 900ml of dissolution medium held in a flask of 1000ml capacity. The basket is centred within 2mm of the centreline of the vessel and the temperature of the medium is maintained at 37 ± 0.5°C. Sample aliquots are withdrawn midway between the surface of the dissolution medium and the bottom of the vessel and midway between the cylindrical edge of the basket and the wall of the dissolution vessel. The USP specifies the use of six baskets at a time that are lowered into the vessels simultaneously [157].

The dissolution behaviour of D4T from microparticles was assessed using a fully automated Hanson Research SR 8 PLUS (Chartsworth, CA, USA) dissolution apparatus fitted with an Autoplus™ Multifill™ and Maximizer Syringe Fraction Collector (Chatsworth, CA, USA). The release studies were performed at 37 ± 0.5°C using USP Apparatus 1 fitted with 8 baskets (40-mesh) rotated at 75rpm. All dosage forms were placed in baskets that were then lowered into 900ml of degassed phosphate buffer (0.1M, pH 7.2) which was prepared by adding approximately 12ml of orthophosphoric acid and then transferring into a 1000ml A-grade volumetric flask and made up to volume with distilled water. The pH of the medium was adjusted using 0.1N NaOH. The cumulative percent D4T released after 12 hours was monitored. Five (5) ml aliquots were withdrawn and replaced with 5ml of fresh medium that had been automatically filtered through a Hanson Research 10µm,1/8in membrane filter

(Chatsworth, CA, USA). The samples were collected at predetermined time intervals 1, 2, 4, 6, 8, and 12 hours after commencing dissolution testing.

4.2.2.6.2 USP Apparatus 3 (Bio-Dis®)

The International Pharmaceutical Federation (FIP) drew attention to acute problems associated with dissolution testing results obtained through use of USP Apparatus 1 and 2 and inspired the concept of the USP Apparatus 3 [158, 160]. USP Apparatus 3 has inner tubes that mechanically transverse six rows of corresponding media filled outer tubes. Six of the tubes are usually for testing drug product while the seventh is used for blank media or standard solutions [156]. The reciprocating cylinder apparatus consists of cylindrical flat bottomed glass tubes fitted with top and bottom caps containing screens. These are designed to contain the drug product under investigation and have corresponding sets of reciprocating cylinders. A motor and a drive assembly reciprocate the cylinders vertically inside the vessels [160]. The cylinders are allowed to move from row to row to expose undissolved drug product to solutions of different pH. After the programmed time for each row expires the inner tubes rise above the vessels, drain for a predetermined period and then move automatically to the next row of fluid and the process is repeated [156, 160, 161].

For the purposes of this study a VanKel® Bio-dis® dissolution tester (VanKel® Industries, New Jersey, USA) was used for dissolution testing of the microparticles manufactured as described in Chapter 5. A model VK 750D digitally controlled water circulation/ heater (VanKel® industries, New Jersey, USA) was used to maintain the temperature of dissolution media at 37 ± 0.5°C. Samples were collected at 1, 2, 4, 6, 8, and 12 hours following commencement of dissolution testing and diluted prior to analysis using HPLC. The micraparticles were filled into size 3 gelatine capsules before dissolution testing.The dissolution conditions used for these studies are depicted in Table 4.4.

Table 4. 4 Summary of dissolution conditions for USP Apparatus 1 and 3

Parameter	USP Apparatus I	USP Apparatus III
Dissolution medium	Buffer (pH 1.6 and 7.2) at 0.1M	Buffers (pH 1.6, 3.4, 4.7, 6.8, 7.2) at 0.1M
Temperature	37 ± 0.5^{0}C	37 ± 0.5^{0}C
Initial volume	900ml	250ml
Basket/dip speed	75rpm	10dpm
Screen size	-	405 µm top/ 177 µm bottom
Filter size	0.45 µm	0.45 µm
Volume withdrawn	5ml	2.5ml and diluted
Dissolution time	1h in pH 1.6 and 11h in pH 7.4	1h pH 1.6 and 3.4, 2h in pH 4.7 and 6.8 and 4h in pH 7.2

4.3 RESULTS AND DISCUSSION

All 10 screening experiments were performed on a trial and error or modification of one factor at a time basis. Initially a range of possible polymers were used and this was determined on the basis of whether or not the polymers were soluble in acetone since the solvent evaporation technique was used to manufacture the microparticles. Solvent evaporation involves dissolving the polymer of interest in an organic solvent. Eudragit® EPO, Eudragit® RSPO, Eudragit® RLPO, Eudragit® S100, Kollidon® VA64, Klucel® and Methocel® K4M were polymers initially considered suitable for these studies . The D4T load and magnesium stearate content were held constant. Microparticles manufactured using Kollidon® VA64, Klucel®, Methocel® K4M (Figures 4.3-4.5) were irregular shaped, rough, had a dough like appearance, aggregated, porous and exhibited poor flow properties that may have been due to their limited solubility in acetone. A summary of the acceptable limits used for this study is depicted in Table 4.5.

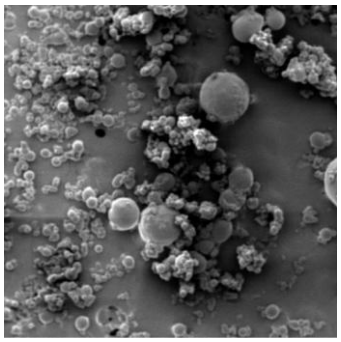

Figure 4. 3 SEM of a microparticle manufactured using Kollidon® VA 64 (ST-005)

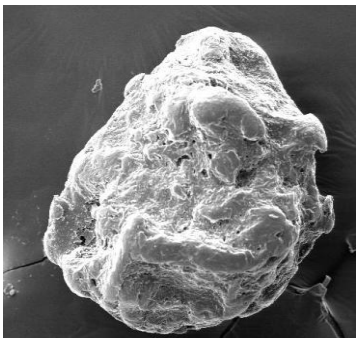

Figure 4. 4 SEM of a microparticle manufactured using Klucel® (ST-006)

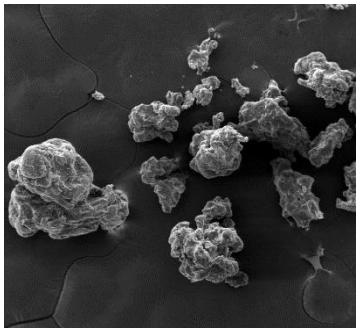

Figure 4. 3 SEM of a microparticle manufactured using Methocel® K4M (ST-007)

Table 4. 5 Summary of acceptable limits for this study

Parameter	Specification
HR	<1.25
CI	<25
AOR	<35
%EE	>70
Cumulative % D4T released after (12h)	≥75

In terms of sphericity, surface morphology, flowability, % EE and particle size the microparticles manufactured using Eudragit® EPO, RSPO, RLPO, S100 were considered acceptable (Table 4.5). The microparticles had reasonable flow properties, were almost spherical and discrete as can be seen in Figures 4.6-4.9 that depict microparticles manufactured using Eudragit® EPO, RSPO, RLPO, S100.

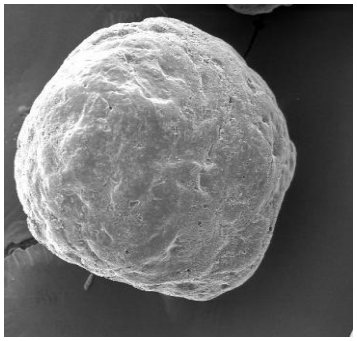

Figure 4.6 SEM of a microparticle manufactured using Eudragit® EPO (ST-001)

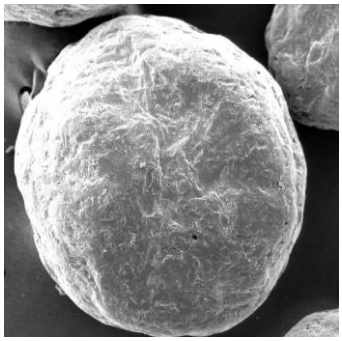

Figure 4.7 SEM of a microparticle manufactured using Eudragit® RSPO (ST-002)

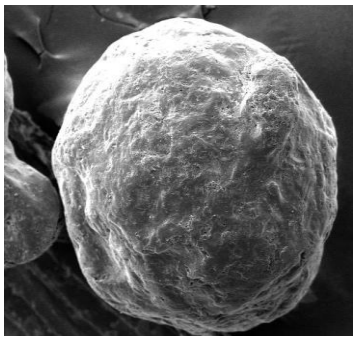

Figure 4.8 SEM of a microparticle manufactured using Eudragit® RLPO (ST-003)

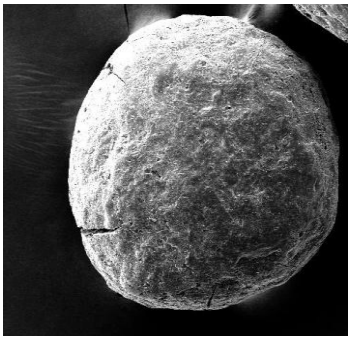

Figure 4.9 SEM of a microparticle manufactured using Eudragit® S100 (ST-004)

Most manufactured microparticles had high EE ranging between 69-90.4% (Table 4.6) which may be a result of the non-aqueous o/o technique that was used since D4T is hydrophilic and no API was lost to the lipophilic manufacturing liquid. The reason the %EE values were <100% is most likely due to the fact that some D4T loss occurred when the acetone evaporated and dispersed phase droplets were transformed into solid microparticles.

Table 4. 6 Summary of %EE, %yield, HR, CI and AOR for preliminary formulations

Formulation	%EE	%Yield	HR	CI	AOR (^{0})
ST-001	80.0	91.5	1.15	13	23
ST-002	79.0	93.6	1.18	19	25
ST-003	79.6	97.8	1.20	23	27
ST-004	85.6	86.4	1.16	15	23
ST-005	78.6	79.6	1.27	32	38
ST-006	69.0	79.8	1.29	36	40
ST-007	83.6	98.6	1.31	38	42
ST-008	73.5	93.0	1.18	19	25
ST-009	83.0	95.4	1.17	16	27
ST-010	90.4	94.6	1.10	10	21

The microparticles that exhibited poor flow properties (Table 4.6) and surface morphology were not evaluated further. Microparticles with good flow properties, %EE and surface morphology were further evaluated using *in vitro* release studies.

Despite the good flow properties, high %EE and surface morphology of Eudragit® EPO microparticles there was limited SR of D4T as the polymer is soluble at pH< 5 and 80% D4T was released after the first 2hrs of testing (Figure 4.10). At 30%w/w Eudragit® RSPO, RLPO and S100 exhibited a sustained release effect. The SR observed for Eudragit® RLPO microparticles was less pronounced than that of Eudragit® RSPO and this was likely due to Eudragit® RLPO containing 10% quaternary ammonium groups whereas Eudragit® RSPO

has only 5% rendering the former more permeable. The ammonium groups are present as salts and result in pH independent permeability [118, 154]. Microparticles manufactured using Eudragit® S100 exhibited a pronounced SR effect as it is soluble in solutions of pH> 7. The material is usually used for delayed release and colon targeted delivery applications and dissolution profiles for D4T from several formulations using USP Apparatus 1 are shown in Figure 4.10.

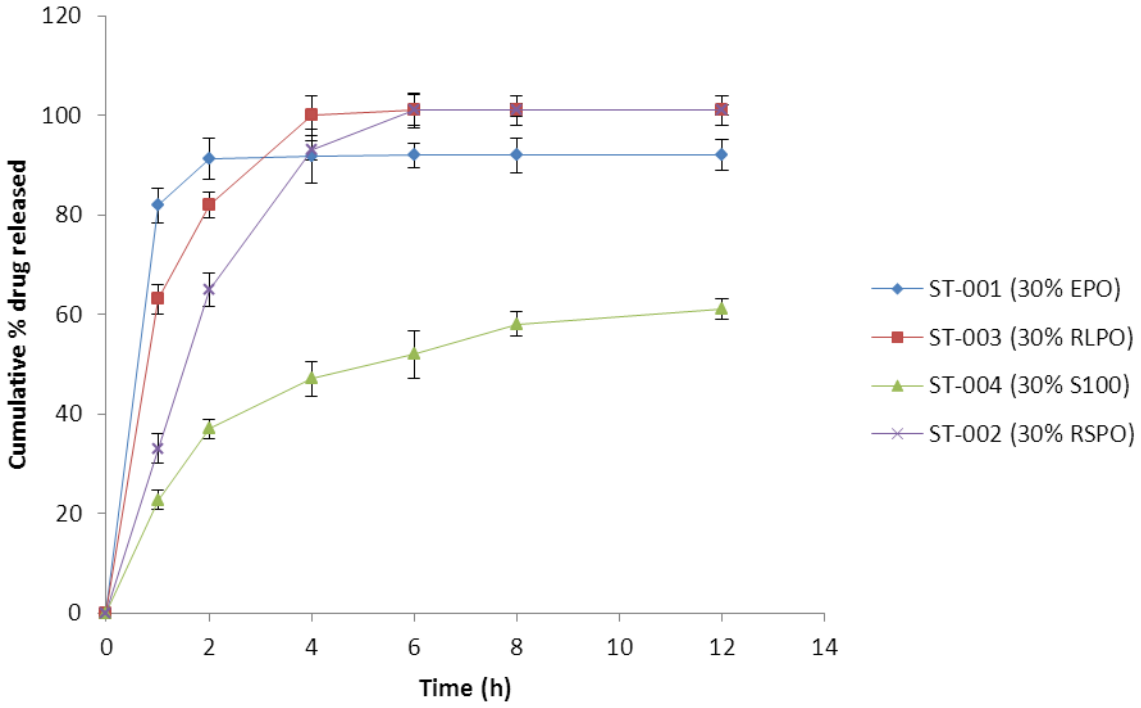

Figure 4. 4 Cumulative % D4T released using dispersions of 30% w/w Eudragit® RSPO, RLPO, EPO and S100 using USP Apparatus 1

In an attempt to investigate the effects of increasing the amount of Eudragit® RSPO from 30% to 45%w/w a more SR effect was observed but was not adequate to reach the desired target (Figure 4.11).

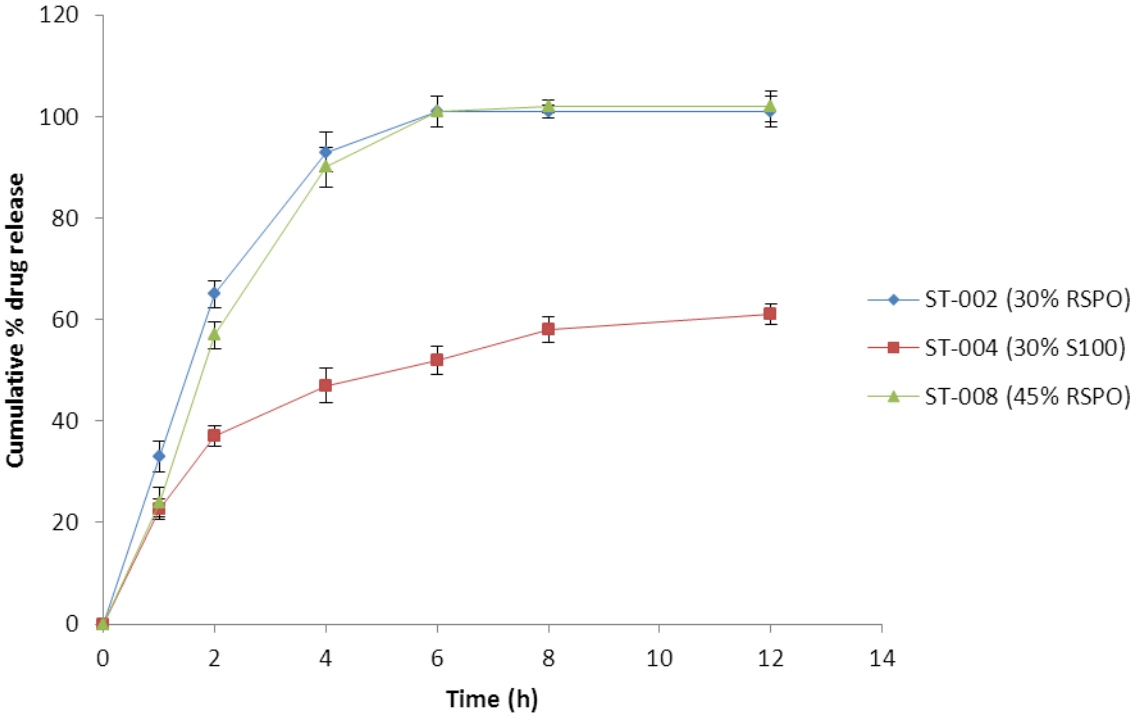

Figure 4. 5 Cumulative % D4T released for 30% w/w Eudragit® RSPO and S100 and 45% w/w Eudragit® RSPO using USP Apparatus 1

Possible combinations of polymers were also evaluated and a combination of Eudragit® RSPO and S100 was found to be suitable to sustain D4T release (Figure 4.12) and produced spherical microparticles with good flow properties and a high %EE.

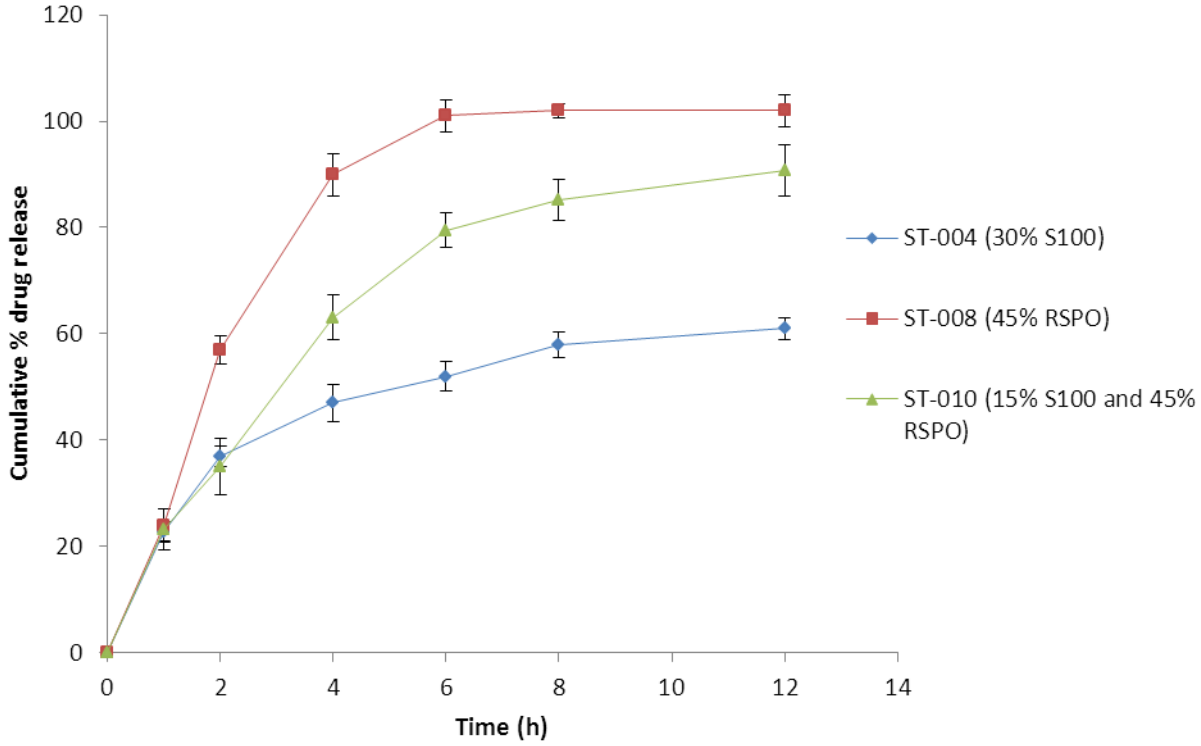

Figure 4. 6 Cumulative %D4T released from a 45% w/w Eudragit® RSPO and 15% w/w Eudragit® S100 dispersion, a 45% w/w Eudragit® RSPO and 30% w/w Eudragit® S100 using USP Apparatus 1

Following a series of trial and error screening experiments a formulation containing 10% D4T was found to be most appropriate with respect to %EE (90.4%), flow properties (HR = 1.1, CI=10, AOR=21°) and D4T release characteristics (90.8% after 12 hours). This formulation was therefore selected for further optimization using Response Surface Methodology and the dissolution behaviour was assessed using USP Apparatus 3. The composition of the formulation to be optimized is listed in Table 4.7.

Table 4. 7 Formulation to be optimized

Excipient	%w/w
D4T	10
Eudragit® RSPO	45
Eudragit® S100	15
Avicel® PH102	29
Magnesium stearate	1

4.4 CONCLUSIONS

Microencapsulation technology using oil in oil non-aqueous solvent evaporation approach was successfully used to produce SR D4T microparticles with a high yield, %EE and good flowability characteristics. Polymethacrylate copolymers resulted in the production of microparticles with appropriate surface morphology, %EE and the potential to sustain D4T release. Kollidon® VA64, Klucel® and Methocel® K4M were evaluated and they produced microparticles that had poor surface morphology and flow properties. Microparticles manufactured using Eudragit® RSPO at 30% w/w revealed potential for sustaining D4T release. The concentration was further increased to 45% w/w and the difference was not significant which led to the conclusion that a combination of polymers would produce the desired effect.

Microparticles manufactured using Eudragit® S100 exhibited a marked sustained effect. A combination of Eudragit® S100 and Eudragit® RSPO gave the desired dissolution profile according to the regulatory guidelines which state that at 25% of the dosing interval a range of 20-50% of the labelled content should be released. At 50% of the interval 45-75% of the labelled content should be released and at least 75% drug should be released at the full dosing interval. This combination of materials resulted in 90.8 % D4T release after 12 hours. The microparticles were spherical, discrete, had a %EE of 90.4% and exhibited good flow properties. This formulation was further optimized as it produced a suitable initial dissolution profile.

A combination of polymers, solvent, diluents and stabilizers produced quality microparticles. The method was efficient for the manufacture of microparticles. USP Apparatus I was used for dissolution studies for quality control purposes. Dissolution is an important parameter to measure since drug absorption from solid dosage forms following oral administration is based on the release of API from the product, dissolution rate of the API in physiological conditions and permeability across the gastrointestinal tract. One of the major challenges in pharmaceutical sciences is that dissolution is the rate limiting step for bioavailability. In addition in the development of SR dosage forms, especially for oral administration *in vitro* release must be maintained in physiologic conditions to produce an approximation of *in vivo* performance.

CHAPTER FIVE

OPTIMIZATION OF STAVUDINE MICROPARTICLES MANUFACTURED USING OIL IN OIL SOLVENT EVAPORATION

5.1 EXPERIMENTAL DESIGN FOR RESPONSE SURFACE MORPHOLOGY (RSM)

Optimization of product and/or processes using factorial based designs and analysis of response surfaces is a powerful, efficient and systematic approach that shortens timelines for dosage form development [162, 163]. This approach permits an evaluation of the interactive effects between input variables or factors on measured responses. If there are significant interactive effects between factors, optimization by the approach of changing one variable at a time will produce results that are different from those resolved by multivariate optimization [164]. The effect of changing one variable at a time, which may be dependent on the level of other variables in an optimization process does not permit multivariate optimization in which the levels of all variables are changed simultaneously [165, 166]. Such designs include Central Composite (CCD), Box-Behnken (BBD) and Doehlert matrix designs [77]. For the purposes of this study a BBD was used.

BBD are a class of rotatable or nearly rotatable second-order designs based on a three-level incomplete factorial designs [167, 168]. A comparison between BBD and other response surface designs viz., CCD, Doehlert and three-level full factorial design, has demonstrated that the BBD is slightly more efficient than the CCD and much more efficient than three-level full factorial designs [169]. The number of experiments (N) required for the development of BBD is defined using Equation 5.1 [78, 170]

$$\mathbf{N = 2k\,(k - 1) + C_0}$$

Equation 5.1

Where,

k = number of factors

C_o= number of central points

A BBD approach requires fewer experiments to be performed than CCD, as it does not contain combinations for which all factors are simultaneously at their highest or lowest levels [167]. Therefore these designs are useful and avoid conducting experiments performed under

extreme conditions and for which, unsatisfactory results might occur [164, 171]. In summary, a BBD is a good design for RSM since it permits the estimation of parameters of a quadratic model, building of sequential designs, detection of lack of fit and use of blocks [172].

RSM was used to investigate the impact of Avicel® PH102, Eudragit® RSPO and Eudragit® S100 content on microparticle formation. A BBD approach was used to generate the number of experiments to be performed and to code the different levels to be investigated. The variables and their coded levels are listed in Table 5.1.

Table 5. 1 Coded levels for independent variables used in BBD

Factor	Coded X_i	Coded level		
		-1	0	+1
Eudragit® RSPO	X_1	40%	45%	50%
Eudragit® S100	X_2	10%	15%	20%
Avicel® 102	X_3	24%	29%	34%

5.2 METHODS

5.2.1 Manufacture of microparticles

To produce the microparticles a solvent evaporation technique was used, based on the method described in § 4.2.2.2. The representative formulations used to manufacture the microparticles are listed in Table 5.2, and for all 17 experiments 10% w/w D4T and 1% w/w magnesium stearate were used.

Table 5. 2 Formulations used to manufacture microparticles

Experiment (run)	Standard run number	(A) Eudragit® RSPO	(B) Eudragit® S100	(C) Avicel® 102
		%	%	%
1	5	40	15	24
2	2	50	10	29
3	15	45	15	29
4	9	45	10	24
5	12	45	20	34
6	3	40	20	29
7	16	45	15	29
8	4	50	20	29
9	17	45	15	29
10	8	50	15	34
11	14	45	15	29
12	1	40	10	29
13	10	45	20	24
14	11	45	10	34
15	13	45	15	29
16	6	50	15	24
17	7	40	15	34

5.3 RESULTS AND DISCUSSION

Optimization was performed using Design Expert version 8.0.7.1 (Stat-Ease, Inc. software, Minneapolis, USA) using a BBD that generated 17 experiments for the three independent variables under investigation. All experiments were performed in a randomized fashion in order to minimize the effects of uncontrolled factors that may introduce bias [164]. The data were evaluated using the software and a suitable statistical model that best described a particular response was selected for further evaluation. The model selected can be used to establish whether transformation is required and the absence of a need for transformation indicates that the model was adequate for data analysis. The appropriate nature of the model is confirmed using a p-value < 0.05, normal probability plots, predicted vs actual residual plots and Box-Cox plots. Residuals are the difference between observed and predicted responses [77]. If the model is adequate the points of a normal probability plot and a plot of residuals should fall on a straight line. Most statistical tests are based on an assumption of normality as this approach simplifies analyses. Box-Cox plots of normality are applied when transformation of data is required to increase the applicability and usefulness of a model or statistical technique [77].

The coefficients for the second order polynomial model were estimated by least squares regression. The different models selected for the responses were validated by Analysis of Variance (ANOVA) using Design Expert Software. ANOVA analysis indicates that a model

is significant and is desired. A p-value < 0.05 indicates significant model terms. The Fischer F-ratio is used to measure the significance of the model under investigation with respect to the variance of all terms included in the model. Precision is used to compare the range of predicted values generated at the points of the experimental design, to the average prediction error. Values for this ratio > 4 indicate that there is adequate model discrimination. Following analysis a desired set of values was selected, an optimized formulation was elucidated and a batch of microparticles was manufactured. The cumulative % D4T released and %EE were responses selected for discussion, and data for all other responses are summarized in Appendix 3. The ANOVA table for the Response Surface Quadratic Model for cumulative % D4T released after 12hours is summarized in Table 5.3.

5.3.1 Cumulative % D4T released after 12h

Table 5. 3 ANOVA Table for Response Surface Quadratic Model for % D4T released after 12 hours

Source	Sum of squares	Df	Mean square	f-value	p-value prob>F	
MODEL	**1394.07**	**9**	**154.90**	**4.15**	**0.0370**	**Significant**
A:RSPO	0.061	1	0.061	1.641E-003	0.9688	
B:S100	**905.25**	**1**	**905.25**	**24.25**	**0.0017**	**Significant**
C:MCC	3.38	1	3.38	0.091	0.7722	
AB	0.12	1	0.12	3.281E-003	0.9559	
AC	0.090	1	0.090	2.411E-003	0.9622	
BC	**302.76**	**1**	**302.76**	**8.11**	**0.0248**	**Significant**
A2	124.49	1	124.49	3.33	0.1106	
B2	13.45	1	13.45	0.36	0.5672	
C2	29.85	1	29.85	0.80	0.4009	
Residual	261.33	7	37.33			
Lack of fit	260.33	3	86.78	347.11	<0.001	
Pure error	1.00	4	0.25			
Cor total	1655.40	16				
Std dev.	6.11					
Mean	86.05					
C.V %	7.10					
Press	4166.88					
R^2	0.8421					
Adj R^2	0.6392					
Pred R^2	-1.5171					
Adeq precision	8.253					

Adequate precision is used to measure the signal to noise ratio. A ratio for adequate precision > 4 is desirable. In this case the ratio of 8.23 indicates that an adequate signal was obtained, hence the model can be used to interpret the data and navigate the design space. The R^2 value was close to 1 indicating a high degree of correlation between observed and predicted data. The percent coefficient of variation (CV) of 7.10 indicates the degree of precision with which

the experiments were performed. The reliability of an experiment is indicated by a % CV < 10 [77]. The normal probability and predicted vs actual plot reveals that the points lie on a straight line, which further confirms the adequacy of the model (Figure 5.1-5.2).

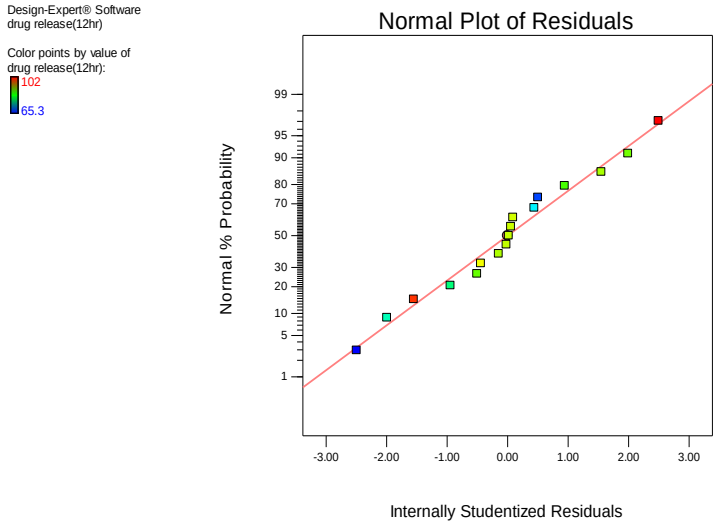

Figure 5. 1 Normal plot of residuals for D4T release

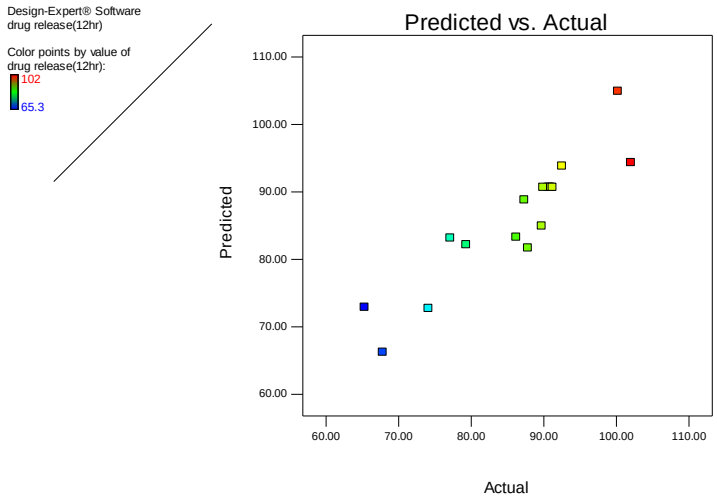

Figure 5. 2 Predicted versus actual plot for D4T release

The Model F-value of 4.15 implies that the model is significant. Values of "Prob > F" < 0.0500 indicate that the model terms are significant. In this case the terms B (Eudragit® S100) and BC (Eudragit® S100 and Avicel® PH102) were significant model terms for % D4T released, as summarised in Equation 5.2 for cumulative % D4T released and listed in Table 5.4.

Table 5. 4 Summary of equations for all responses

Cumulative % D4T released (Y_1)

$$Y_1 = - 262.53 + 19.28*A – 10.39*B + 0.82*C – 7E\text{-}003*A*B – 6E\text{-}003*A*C + 0.35*B*C – 0.22*A^2 - 0.07*B^2 + 0.11*C^2$$

Equation 5.2

Encapsulation efficiency ($Y_{2)}$

$$Y_2= -80.11+3.22*A+8.80*B-0.34*C-0.07*A*B+0.012*A*C-0.034*B*C-0.02*A^2-0.09*B^2+9.9E\text{-}003*C^2$$

Equation 5.3

Yield (Y_3)

$$Y_3= +81.02+0.36*A+1.09*B+7.50*C-5.60*A*B+7.78*A*C+4.32*B*C+2.36*A^2-2.69*B^2+4.94*C^2$$

Equation 5.4

Particle size (Y_4)

$$Y_4= +634.4-15.3*A+22.9*B-7.34*C-79*A*B-78.5*A*C-3.25*B*C+34.7*A^2-47.6*B^2+51.9*C^2$$

Equation 5.5

HR (Y_5)

$$Y_5= +1.16-0.04*A-0.02*B-0.02*C$$

Equation 5.6

CI (Y_6)

$$Y_6= +13.72-0.14*A-0.28*B-0.26*C$$

Equation 5.7

AOR (Y_7)

$$Y_7= +28.24-4.5*A-3.25*B-3.25*C+1.75*A*B+2.75*A*C+1.25*B*C$$

Equation 5.8

The signs for the terms in the equation indicate whether that factor has an antagonistic or synergistic effect on D4T release. The coefficient denotes the magnitude or extent of the effect. Evaluation of Equation 5.2 indicates that Eudragit® S100 has an antagonistic effect on D4T release and that a combination of Eudragit® S100 and Avicel® PH102 has a synergistic effect on D4T release. This can be confirmed by evaluating the contour and 3D plots that suggest that Eudragit® S100 is the primary polymer modulating D4T release. An increase in Eudragit® S100 content results in a decrease in D4T release when the Eudragit® RSPO content is constant (Figures 5.3-5.4).

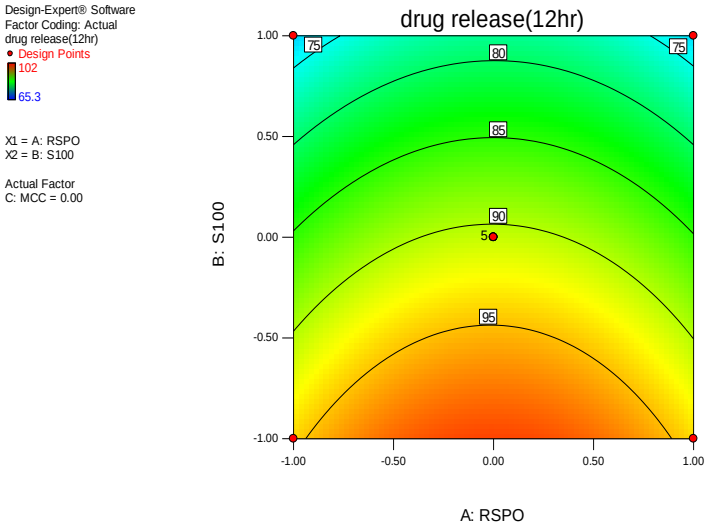

Figure 5. 3 Contour plot showing the effect of Eudragit® S100 and Eudragit® RSPO on D4T release

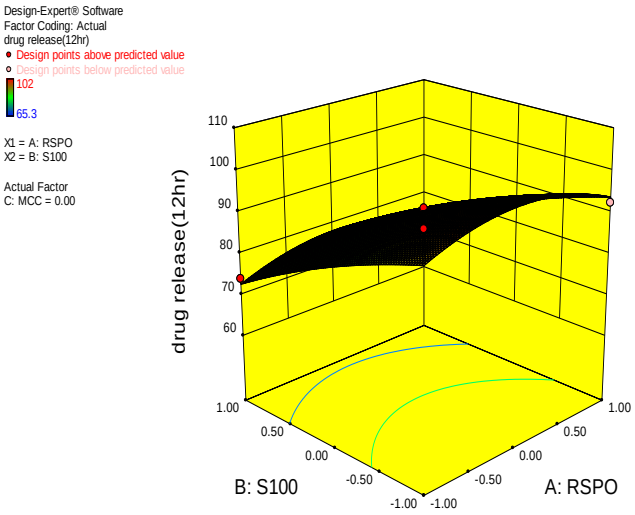

Figure 5. 4 Response surface plot showing the effect of Eudragit® S100 and Eudragit® RSPO on D4T release

The contour plot in which the effect of Eudragit® RSPO and Avicel® PH102 on % D4T release reveals a 'horse shoe' pattern (Figure 5.5). The responses observed are relatively complex and difficult to interpret. There is however no significant effect on D4T release when Eudragit® RSPO or Avicel® PH102 levels are increased while keeping the other exicipent level constant as can be seen from the response surface plot (Figure 5.6).

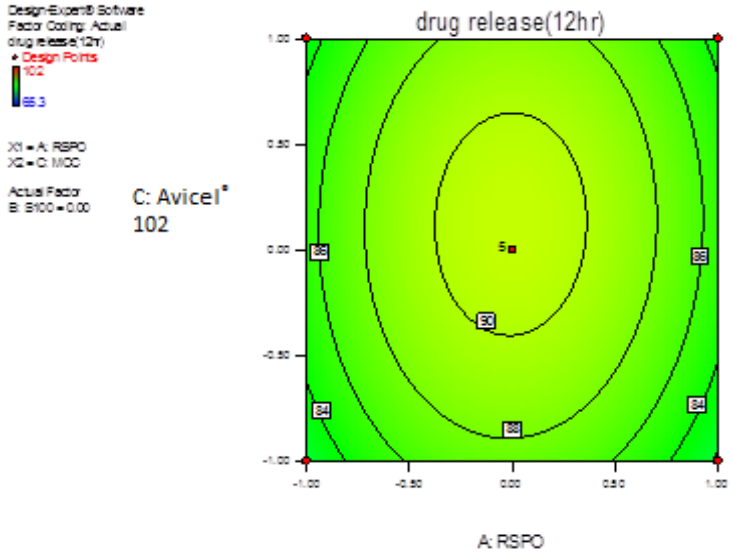

Figure 5. 5 Contour plot showing the effect of Eudragit® RSPO and Avicel® PH102 on D4T release

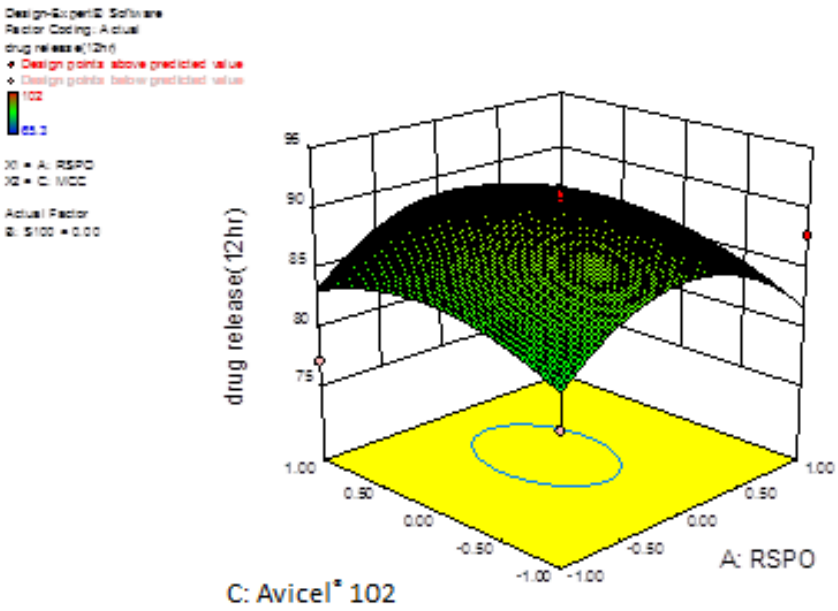

Figure 5. 6 Response surface plot showing the effect of Eudragit® RSPO and Avicel® PH102 on D4T release

The % D4T released decreases when the Eudragit® S100 content is increased and Avicel® PH102 levels are held constant. Simlarly an increase in Avicel® PH102 content when Eudragit® S100 levels are held constant results in a decrease in the amount of D4T released, although the effect is not pronounced (Figures 5.7-5.8).

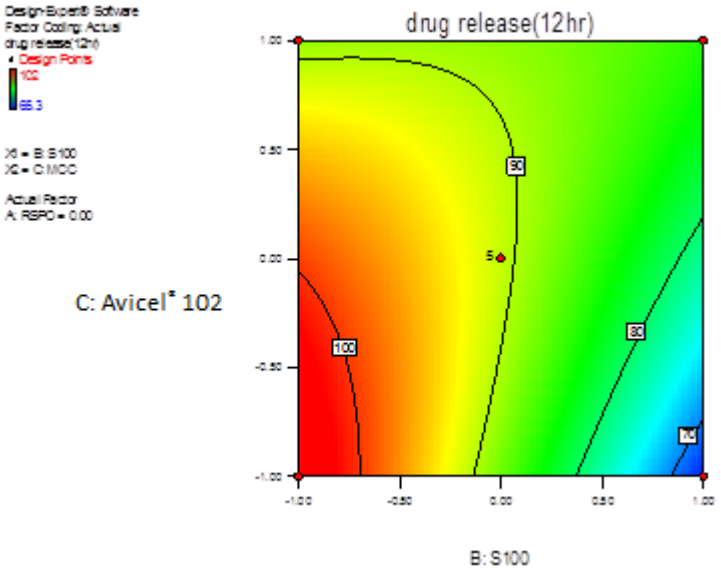

Figure 5. 7 Contour plot showing the effect of Eudragit® S100 and Avicel® PH102 on D4T release

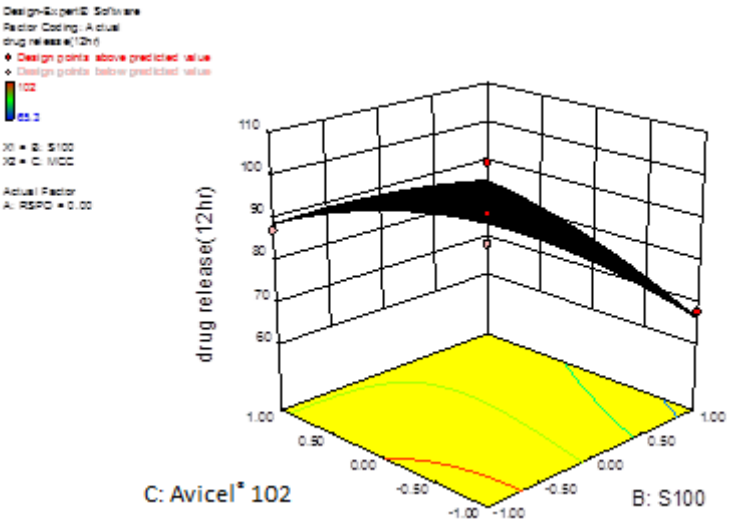

Figure 5. 8 Response surface plot showing the effect of Eudragit® S100 and Avicel® PH102 on D4T release

5.3.2 Encapsulation efficiency

The ANOVA table for the Response Surface Quadratic Model for % EE is listed in Table 5.5.

Table 5. 5 ANOVA Table for Response Surface Quadratic Model for %EE

Source	Sum of squares	Df	Mean square	f-value	p-value prob>F	
MODEL	**877.17**	**9**	**97.46**	**78.55**	**<0.0001**	**Significant**
A:RSPO	**73.81**	**1**	**73.81**	**59.49**	**0.0001**	**Significant**
B:S100	**750.78**	**1**	**750.78**	**605.09**	**<0.0001**	**Significant**
C:MCC	**14.05**	**1**	**14.05**	**11.32**	**0.0120**	**Significant**
AB	**12.60**	**1**	**12.60**	**10.16**	**0.0153**	**Significant**
AC	0.36	1	0.36	0.29	0.6068	
BC	2.89	1	2.89	2.33	0.1708	
A2	1.17	1	1.17	0.94	0.3636	
B2	**20.89**	**1**	**20.89**	**16.84**	**0.0046**	**Significant**
C2	0.26	1	0.26	0.21	0.6623	
Residual	8.69	7	1.24			
Lack of fit	5.60	3	1.87	2.42	0.2067	
Pure error	3.09	4	0.25			
Cor total	885.86	16	0.77			
Std dev.	1.11					
Mean	84.30					
C.V %	1.32					
Press	94.38					
R^2	0.9776					
Adj R^2	0.6392					
Pred R^2	0.8935					
Adeq Precision	29.79					

An adequate precision of 29.79 was generated and it was concluded that this model is significant and can be used to interpret the data. The R^2 value is close to 1, denoting a high degree of correlation between the observed and predicted values. The CV % of 1.32 indicates the degree of precision with which the experiments were performed and the reliability of an experiment is indicated by a % CV < 10. The normal probability plot and predicted vs actual plot reveals that the points lie on a straight line, which further confirms the adequacy of the model (Figure 5.9-5.10).

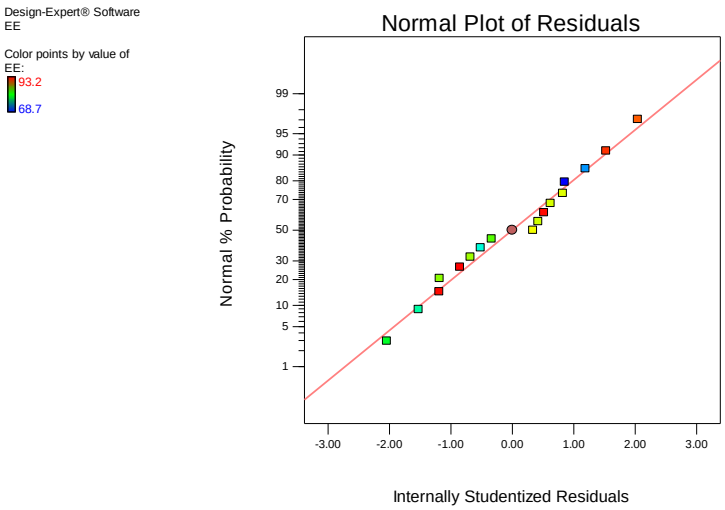

Figure 5. 9 Normal plot of residuals for %EE

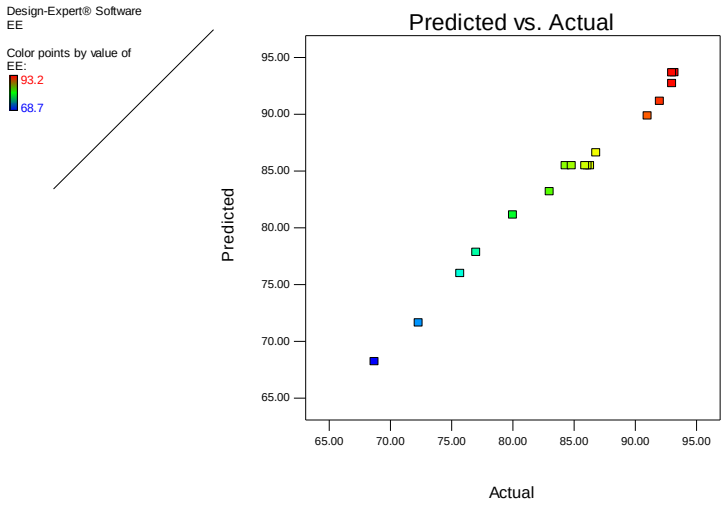

Figure 5. 10 Predicted versus actual plot for %EE

The Model F-value of 78.55 implies the model is significant and values of "Prob > F" < 0.0500 indicate that the model terms are significant. In this case the terms A (Eudragit® RSPO), B (Eudragit® S100), C (Avicel® PH102), AB (Eudragit® RSPO and Eudragit® S100), B^2 (Eudragit® S100) were considered significant model terms. From the contour plot and response surface plot depicted in Figures 5.11-5.12 it can be seen that an increase in Eudragit® S100 content at constant Eudragit® RSPO content resulted in an increase in %EE. Likewise an increase in Eudragit® RSPO content when Eudragit® S100 is held constant resulted in an increase in %EE.

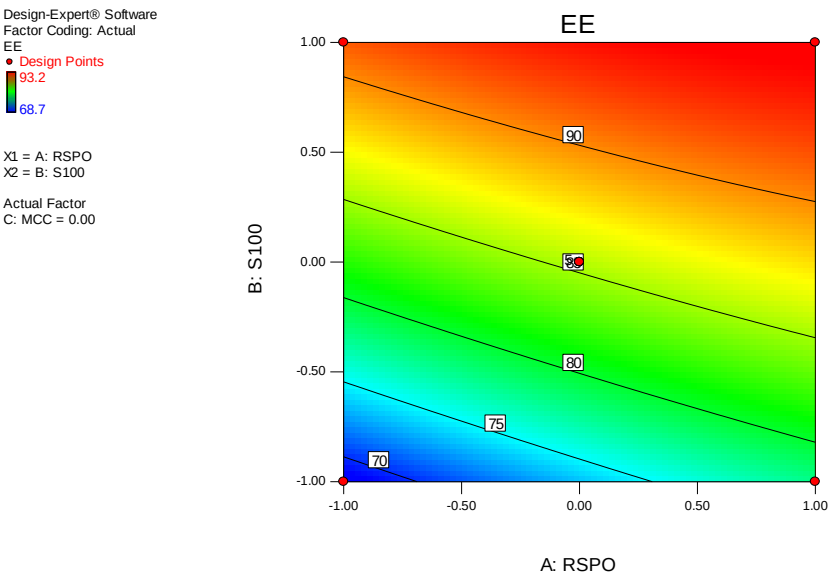

Figure 5. 11 Contour plot showing the effect of Eudragit® S100 and Eudragit® RSPO on %EE

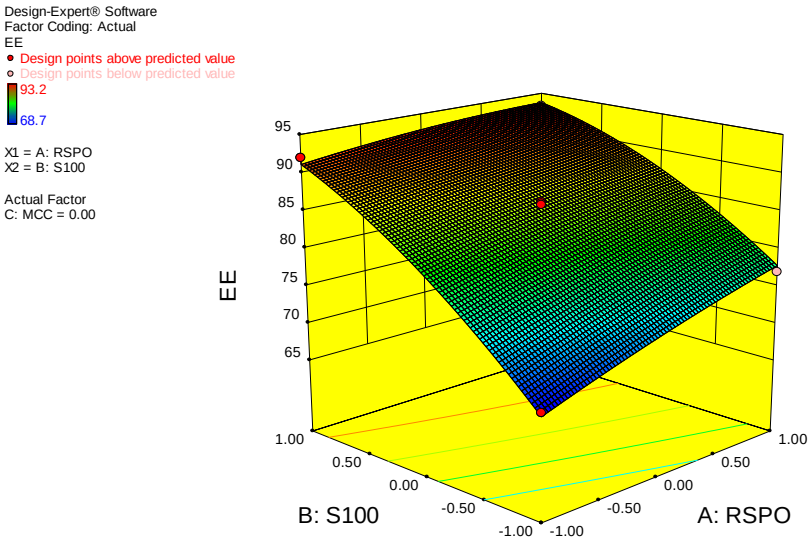

Figure 5. 12 Response surface plot showing the effect of Eudragit® S100 and Eudragit® RSPO on %EE

An increase in Eudragit® RSPO content at constant Avicel® PH102 content resulted in an increase in %EE and an increase in Avicel® PH102 at constant Eudragit® RSPO content also resulted in an increase in %EE (Figures 5.13-5.14).

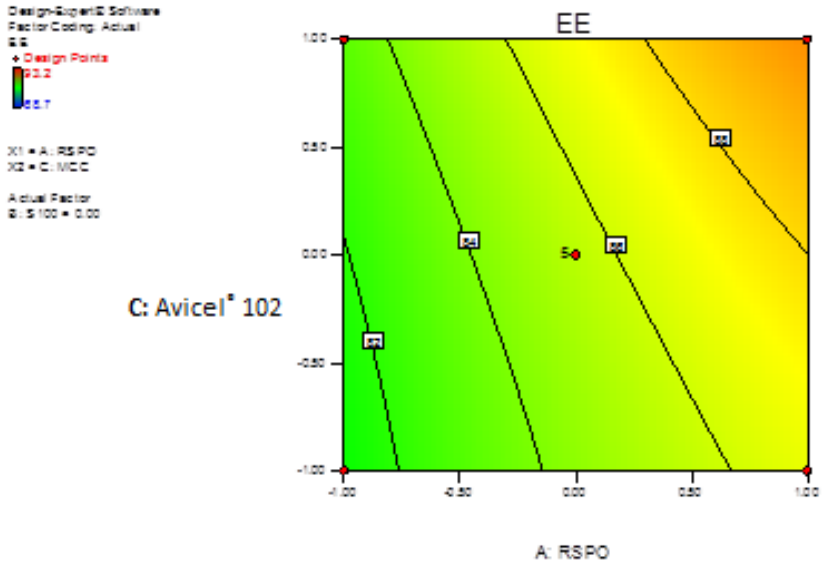

Figure 5. 13 Contour plot showing the effect of Eudragit® RSPO and Avicel® PH102 on %EE

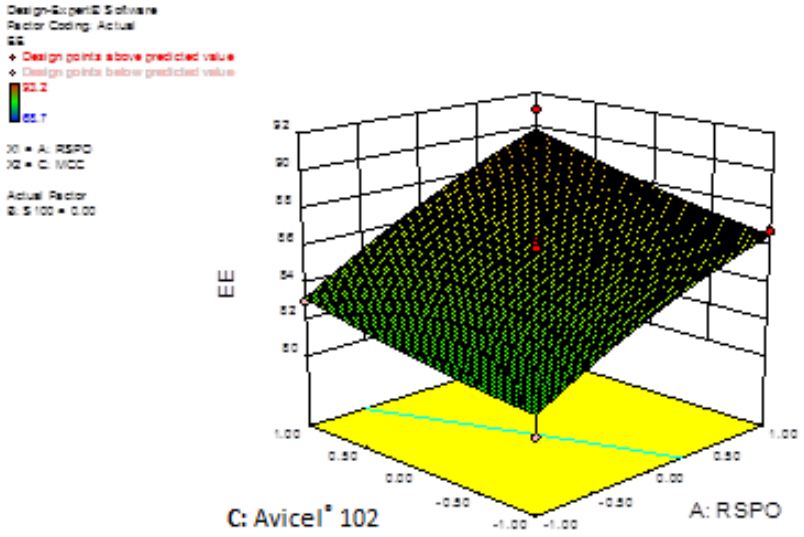

Figure 5. 14 Response surface plot showing the effect of Eudragit® RSPO and Avicel® PH102 on %EE

An increase in %EE was noted when Eudragit® S100 content was increased and the Avicel® PH102 content was held constant. There was no significant effect noted with an increase in Avicel® PH102 (Figures 5.15-5.16).

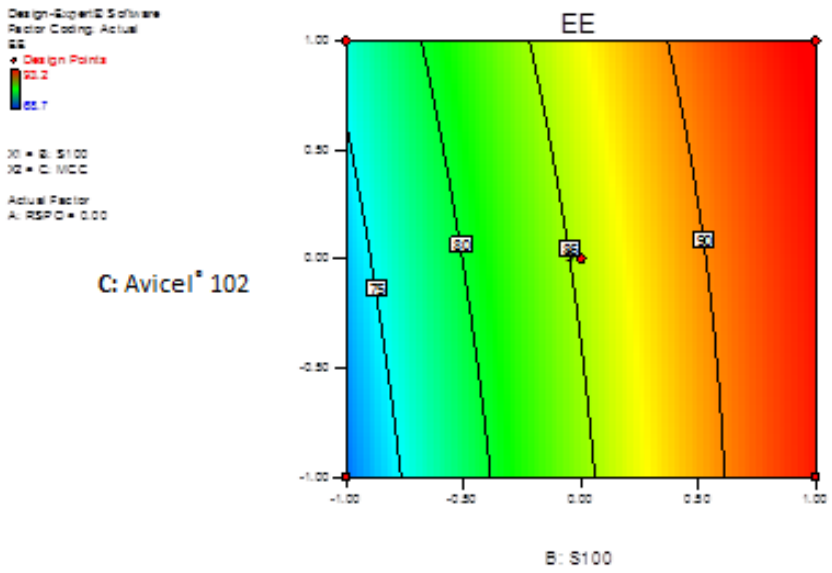

Figure 5. 15 Contour plot showing the effect of Eudragit® S100 and Avicel® PH102 on %EE

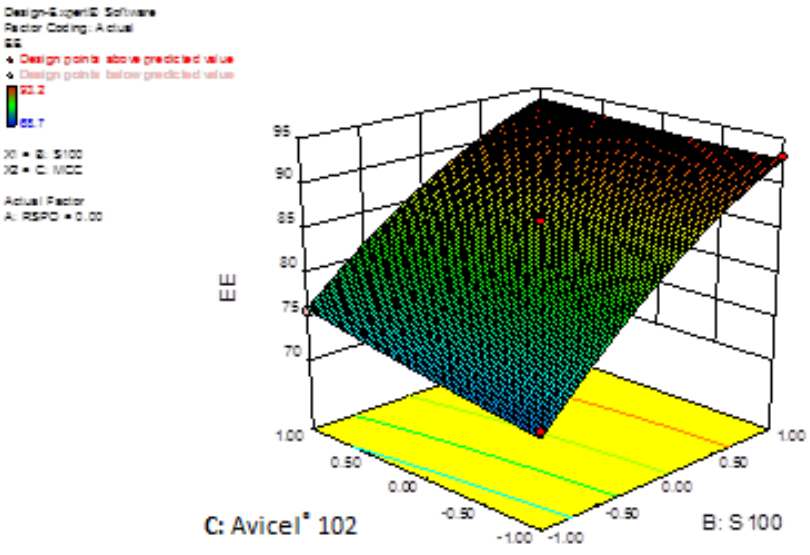

Figure 5. 16 Response surface plot showing the effect of Eudragit® S100 and Avicel® PH102 on %EE

An increase in polymer concentration results in an increase in viscosity of the solution in which the polymers are dissolved and consequently an increase in mean particle size is observed. This effect results in a decrease in surface area and a delay in diffusion of D4T from the particles, ultimately ensuring a high EE [173]. A high viscosity and rapid

solidification of the dispersed phase contributes significantly to a reduction in porosity of the microparticles and D4T release (Figure 5.17).

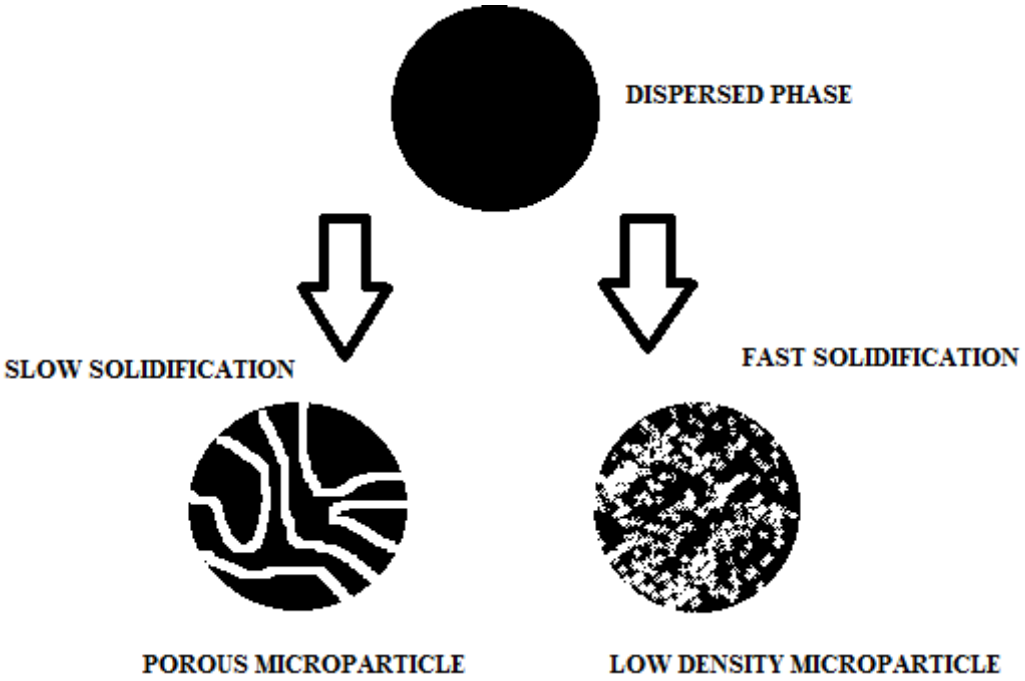

Figure 5. 17 Schematic representation of the relationship between solidification rate and particle morphology [174]

Highly concentrated polymer solution would permit rapid precipitation of the material onto the surfaces of dispersed phase nuclei preventing D4T diffusion across the phase boundary (Figure 5.18.) and delaying D4T diffusion within polymer droplets [173-175].

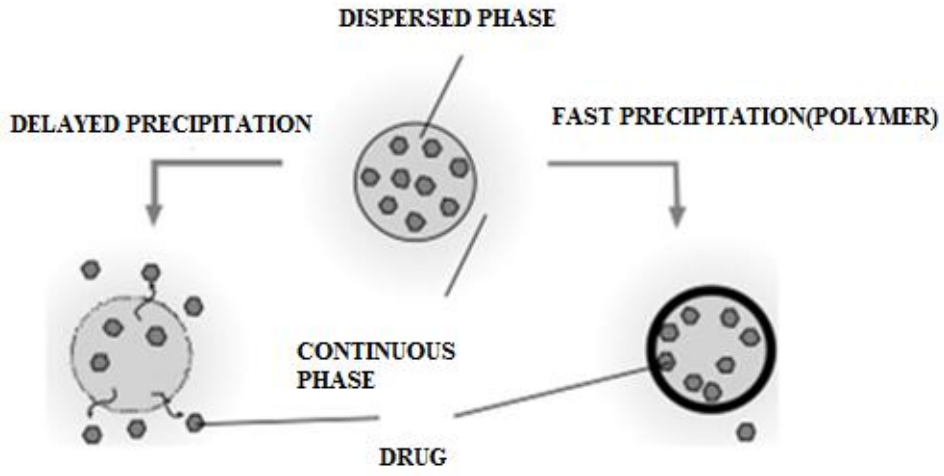

Figure 5. 18 Schematic representation of the rationale for high %EE [174]

D4T is a highly water soluble compound and the increased EE could be due to the limited solubility of D4T in liquid paraffin and acetone. Consequently D4T exhibited a greater affinity for the polymer matrix than for the continuous phase. The high EE could also be due to the relative volumes of the continuous and dispersed phases that were constant, as an increase in volume has been shown to produce small microparticles with a low EE [173, 175]. A low ratio of the dispersed to continuous phase also resulted in a high EE. It is likely that the large volume of continuous phase provides a steep concentration gradient for the organic solvent across the phase boundary by diluting the solvent, leading to rapid solidification of the microparticles [173, 174]. The agitation rate was maintained at 400rpm, because at faster homogenizing speeds small microparticles with a low EE were produced. The EE for these studies ranged between 78.7-103%.

5.3.3 Yield and particle size

The yield of microparticles was fairly high and ranged between 70.8-99.2%. In general an increase in polymer concentration increased the yield. Decreased yields were observed in some cases and may have been due to the fact that the microparticles were lost during manufacture. For example the polymer adhered to the homogenizer stirrer or during washing, polymer was lost and therefore the % yield was < 100%.

The size of the microparticles ranged between 523-822µm and their mean diameter of the microparticles was primarily influenced by the concentration of the polymers used. An increase in polymer concentration resulted in an increased viscosity and an increase in particle size. The homogenizing speed was set at 400rpm since higher agitation rates have been seen to produce very small microparticles due to high shear. Speeds < 400rpm do not result in microparticle formation since the polymer sediments and coalesces at the bottom of the beaker. This is as a result of inadequate agitation of the medium to maintain a highly dispersed inner phase of discrete droplets within the bulk phase [125].

5.3.4 Microencapsulation

Acetone has a dielectric constant of 20.7 and shows poor miscibility with liquid paraffin [176]. It has a low boiling point of 56-57 °C and is highly volatile [177]. Acetone is a class 3 organic solvent and has low toxicity potential to man and no health-based exposure limit is needed [149]. Acetone dissolves Eudragit® S100 and Eudragit® RSPO. Liquid paraffin was used as the continuous phase since D4T is insoluble in liquid paraffin, and therefore no D4T is lost into the continuous phase during production, with the result that the %EE is high. The

polymers used have poor miscibility in liquid paraffin and are soluble in acetone. Magnesium stearate was used as a droplet stabilizer to overcome droplet coalescence during solvent evaporation as it decreases the interfacial tension between the phases of the emulsion [124]. Hexane was used for washing the microparticles, as a stabilizer and to harden them. The process involves adding the dispersed phase to the continuous phase to form droplets after which agitation revealed the formation of a milky white emulsion. As the acetone diffuses into the continuous phase and evaporates the polymer precipitates onto the surface of the dispersed phase, forming a coating, after which solidification and precipitation of the microparticles can occur.

5.3.5 Flowability

Flowability is a very important parameter to evaluate as microparticles have the potential to be used in multi-particulate delivery systems where different drugs are encapsulated and filled into hard gelatine capsules [178]. Good flow properties and packability promote easy transfer of the microparticles into capsules resulting in uniform capsule fill. Flowability assessment includes the determination of the HR and the CI from the tapped and bulk densities of materials. A high HR indicates cohesion between particles, while a high CI is indicative of the tendency to form bridges [179]. The AOR is also used to assess flowability. These methods are based on an understanding of the flow process, and no one approach has an advantage over the other, however it is essential to perform more than one test for confirmation purposes. All formulations showed reasonably good flow properties, with no AOR > 40°, which is a limit indicative of poor flowability. The HR and CI ranged between 1.10-1.23 and 13.1-14.6 respectively, indicating good flow properties for the particles as the HR < 1.25 and the CI values < 15. An increase in flowability was noted with an increase in particle size. This is due to the absence of aggregation, which is usually evident with microparticles of small size due to high surface energy.

5.3.6 Scanning electron microscopy

The microparticles were generally spherical, discrete and uniform in shape, with no evidence of D4T on the surface for most formulations (Figures 5.19-5.20). These data are consistent with the high EE, showing that all the D4T had been encapsulated by the polymer. Some batches had rough surfaces that may have been the result of the addition of Avicel®PH102 (Figures 5.21-5.22). In addition the micropartilces were porous, which may be due to the high loading of D4T in the microparticles (Figures 5.23-5.24). An increase in the polymer

concentration also produced smooth surfaced microparticles (Figure 5.19-5.20). The scanning electron micrographs for all formulations are shown in Appendix 2 with all batch data.

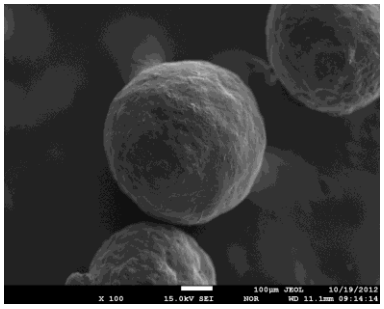

Figure 5. 20 SEM of a microparticle from Batch-006

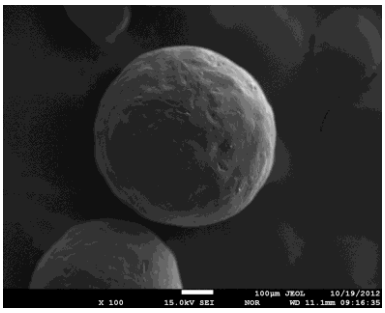

Figure 5. 19 SEM of a microparticle from Batch BB-008

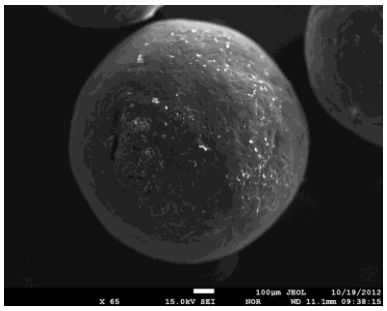

Figure 5. 22 SEM of a microparticle from Batch BB-009

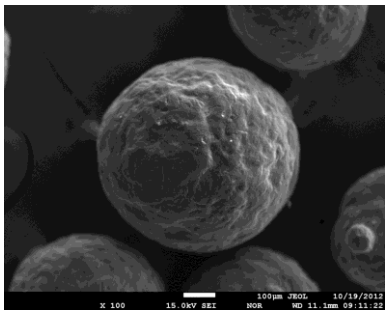

Figure 5. 21 SEM of a microparticle from Batch BB-016

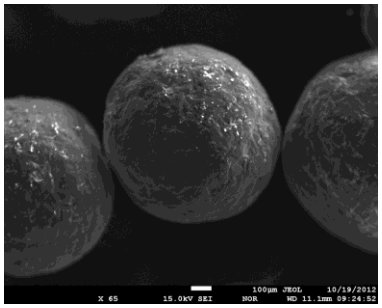

Figure 5. 23 SEM of a microparticle from Batch BB-012

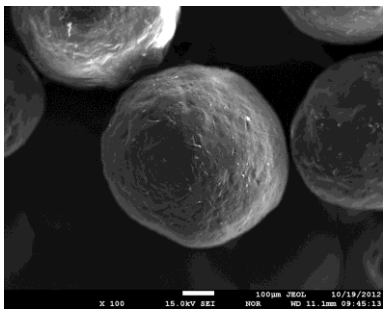

Figure 5. 24 SEM of a microparticle from Batch BB-014

5.3.7 *In vitro* D4T release

Dissolution testing was performed using USP Apparatus 3 for 12 hours with media of pH 1.6, 3.4, 4.7, 6.8 and 7.2. A few dissolution profiles were selected for discussion and are reported in order of manufacture. The data for all formulations are reported in Appendix 2 with all

relevant batch data. Eudragit® S100 was established as the primary polymer controlling D4T release. An increase in the polymer concentration increased particle size, thereby lengthening the diffusion pathlength for D4T and decreasing the surface area for D4T release. The retardant effect observed with an increase in polymer concentration and only 65% and 74% D4T released are depicted in Figures 5.25 and 5.26. Formulations BB-006 and BB-008 released the required amount of D4T in the first part of the dissolution but however failed to met the guidelines with less than 75% being release after 12 hours as depicted by the USP limits in Figures 5.25 and 5.26. Following dissolution testing mass balance analysis revealed that some D4T remained in the polymer matrix of the microparticles.

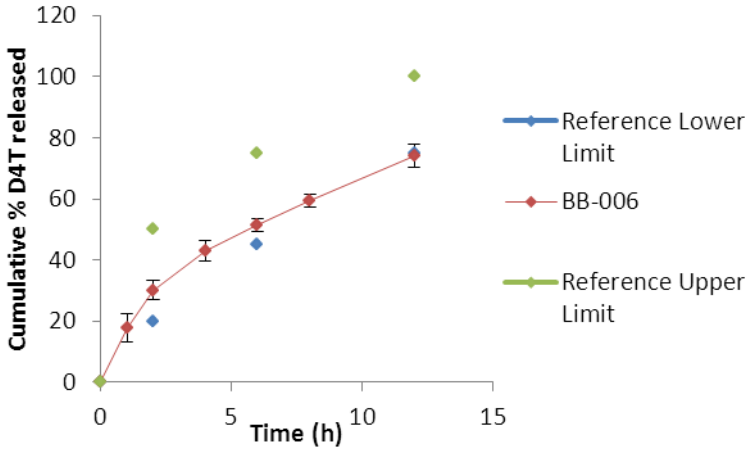

Figure 5. 25 Cumulative % D4T released from Batch BB-006

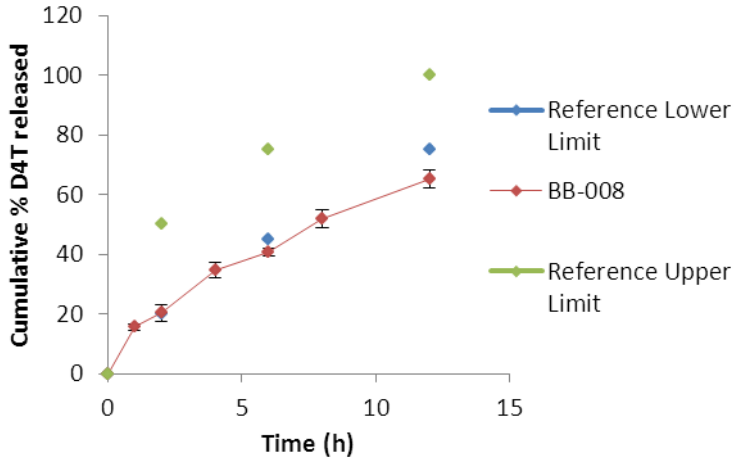

Figure 5. 26 Cumulative % D4T released from Batch BB-008

Where a low polymer concentration was used, up to 100% D4T was released after 12 hours with rapid release observed over the initial 2 hours of testing (Figures 5.27-5.28). The faster

rate and extent of release can be attributed to the porous nature of the microparticles. Despite the porosity formulation BB-004 met the required guidelines as depicted by the reference limits in Figures 5.27 and formulation BB-012 failed to meet the required guidelines with more than 50% D4T release after 3 hours (Figure 5.28).

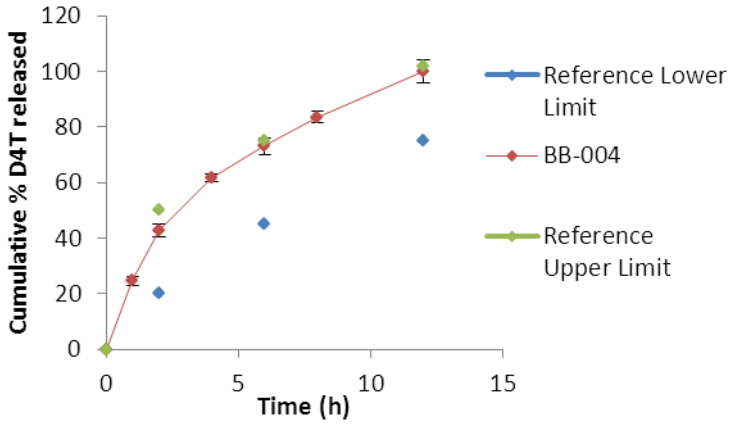

Figure 5. 27 Cumulative % D4T released from Batch BB-004

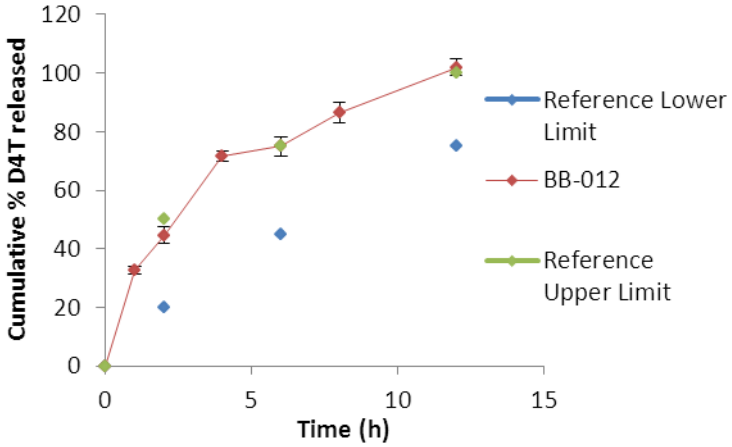

Figure 5. 28 Cumulative % D4T released from Batch BB-012

Eudragit® S100 is a copolymer of methacrylic acid and methyl methacrylate with a 1:2 ratio of carboxyl to ester groups and is soluble at pH > 7 [118]. Eudragit® S100 has been used in formulations for colon delivery. Eudragit® S100 was evaluated for its ability to sustain D4T release from microparticles in combination with Eudragit® RSPO since the pH varies along the GIT. Therefore a combination of polymers may facilitate manipulation of D4T release. The low ratio of carboxyl groups in Eudragit® S100 results in lower ionization in neutral to alkaline media and therefore slower solubilization of the anionic polymer resulting in control

of D4T release [180]. Microparticles containing Eudragit® S100 have low permeability due to hydrogen bonding between the hydroxyl groups of the carboxylic moiety and the carbonyl oxygen of the ester groups in the polymer molecules [118]. This bonding increases the degree of compactness of the polymer, decreases the porosity and therefore permeability of the material thereby minimizing the release of encapsulated drug. An increase in Eudragit® S100 content enhances this retarding effect.

Eudragit® RSPO is a copolymer of acrylic and methacrylic acid esters with 5% quartenary ammonium functional groups [118]. It is water insoluble and delivery systems manufactured using this polymer exhibit pH independent release. The low quartenary ammonium content plays an important role in sustaining release since these functional groups affect permeability of the film to water. Eudragit® RSPO exhibits low permeability and swells. The rough surface of some microparticles did not appear to have a significant effect on D4T release (Figures 5.29-5.30). Formulation BB-009 (Figure 5.29) did not fall within the required reference limits with more than 75% D4T release after 6 hours, formulation BB-016 fell within the required limits (Figure 5.30).

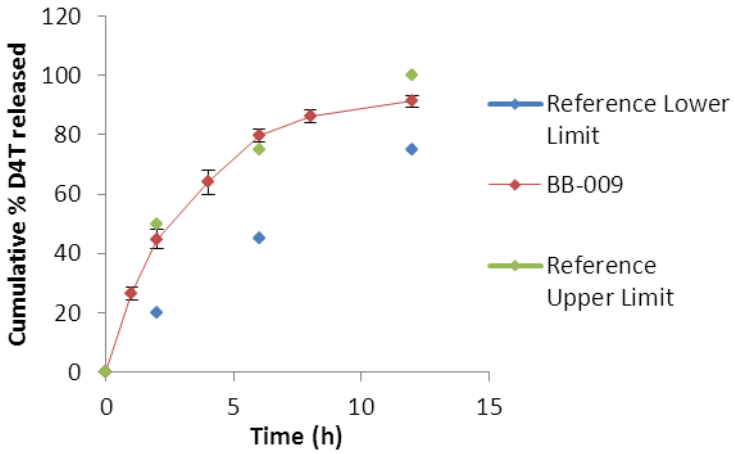

Figure 5. 29 Cumulative % D4T released from Batch BB-009

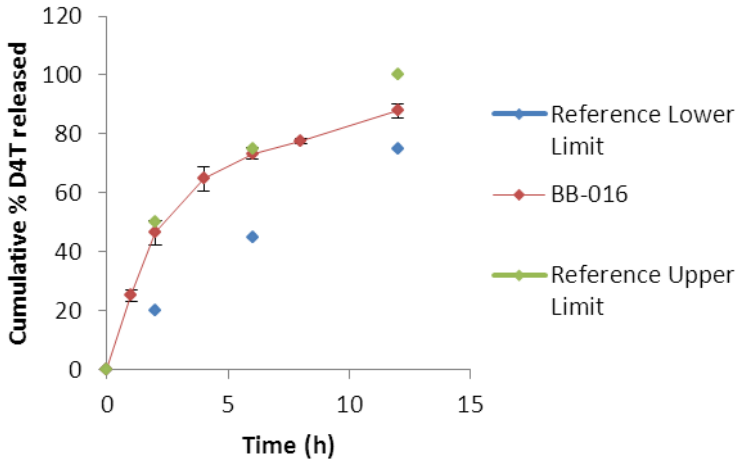

Figure 5. 30 Cumulative % D4T released from Batch BB-016

Burst release, defined as the release of more than 30% D4T within the first 2 hours, was observed for some formulations (Figures 5.31-5.32) .

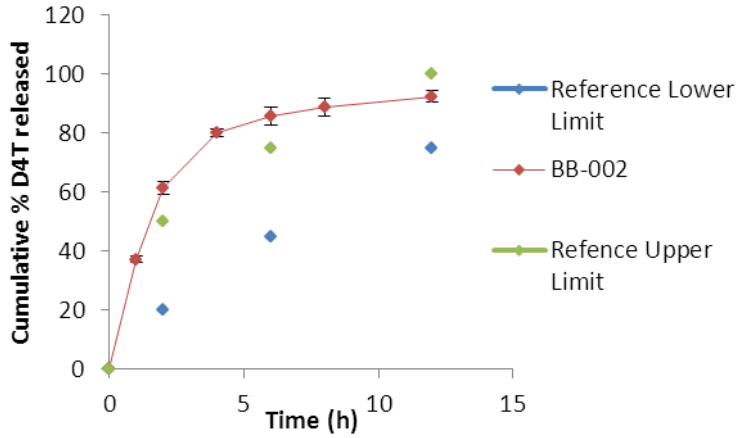

Figure 5. 31 Cumulative % D4T released from Batch BB-002

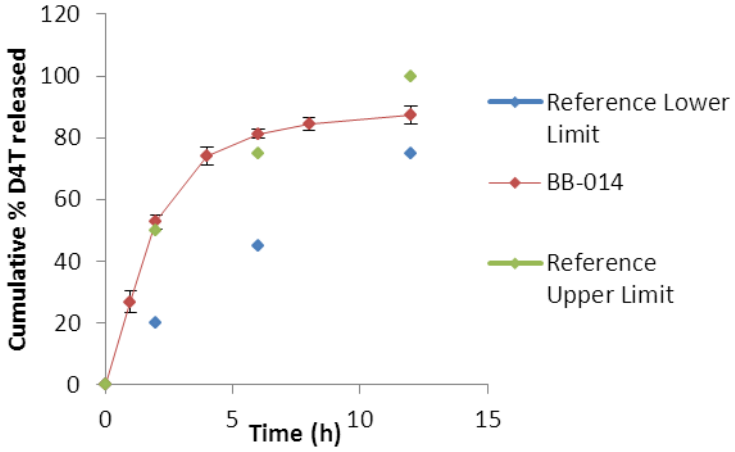

Figure 5. 32 Cumulative % D4T released from Batch BB-014

Despite the fact that rapid release of D4T occurs, burst release may be appropiate for some therapeutic strategies such as transdermal drug delivery systems for drugs that normally exhibit a considerable lag time between patch application and therapeutic effect [181]. However the negative effects brought about by burst release can be dangerous, and this approach is sometimes economically inefficient. Therefore a thorough understanding of the burst effect in controlled release systems is necessary [182]. One of the current difficulties with burst release is that it is unpredictable, and even when the burst is desired, the amount released often cannot be controlled. Although the significance of burst release in controlled delivery systems has not been ignored, no successful theories have been developed to describe the phenomenon completely. Several considerations for decribing burst release have been postulated and it is thought that initial burst occurs due to processing conditions, surface characteristics of microparticles, sample geometry, morphology and porous structure of materials [174, 182].

In this case the burst effect was attributed to the presence of D4T located on the surface of the microparticles, and dissolution through pre-existing pores and channels that formed during the solvent evaporation process, whilst the remaining D4T was released due to slow erosion of the polymer [183]. The pores at the surface of the microparticles were filled with dissolution media to form a non-porous layer around the microparticles that acts as a diffusion barrier and burst release was observed to decrease with increasing polymer concentration [184].

USP Apparatus 3 was used for dissolution testing as it permits the use of buffers over a wide pH range thereby mimicking *in vivo* conditions with dissolution environments close to that observed for pH in the gastro-intestinal tract. When manufacturing a generic product the goal is to produce a product that would release D4T in a manner similar to a commercially available product. No SR formulation of D4T is available and therefore FIP and USP guidelines were used to establish an appropriate release profile for the optimized formulation described in § 4.2.2.6 [156]. The curvelinear nature of most cumulative D4T release versus time plots suggest that D4T release did not follow a zero-order kinetic model.

The plots for responses Y_3, Y_4, Y_5, Y_6 and Y_7 are reported in Appendix 3. A summary of all optimization results is listed in Table 5.6.

Table 5. 6 Responses for each batch of microparticles

Standard Run Number	Run	RSPO	S100	MCC	Yield	EE	D4T released	PS	HR	CI	AOR
		%	%	%	%	%	%	µm			^{0}
5	1	40	15	24	93	93	79.3	664	1.23	14.6	39
2	2	50	10	29	89.3	94.3	92.5	658	1.12	13.3	24
15	3	45	15	29	81.3	96.3	90.8	633	1.18	14	30
9	4	45	10	24	77.1	103	100.2	594	1.21	14.4	37
12	5	45	20	34	98.1	87	89.7	677	1.10	13.1	22
3	6	40	20	29	83.8	85.7	74.1	743	1.17	13.9	29
16	7	45	15	29	78.3	94.8	89.9	642	1.15	13.6	27
4	8	50	20	29	79.4	103.2	65.3	523	1.12	13.3	24
17	9	45	15	29	81.4	96.1	91.2	635	1.16	13.8	28
8	10	50	15	34	99.2	101	86.2	621	1.10	13.1	22
14	11	45	15	29	83.2	96.8	90.6	624	1.18	14	30
1	12	40	10	29	70.8	103	102	562	1.20	14.3	36
10	13	45	20	24	71.5	90	67.8	669	1.13	13.4	25
11	14	45	10	34	86.4	102	87.3	615	1.17	13.9	29
13	15	45	15	29	80.9	95.9	91	638	1.16	13.8	28
6	16	50	15	24	71.6	78.7	87.8	822	1.12	13.3	24
7	17	40	15	34	89.5	82.3	77.1	777	1.14	13.5	26

EE: Encapsulation efficiency
PS: Particle Size
HR: Hausner Ratio
CI: Carr Index
AOR: Angle of Repose

5.3.8 Optimized formulation

A set of desired responses was selected and an optimized formulation composition was predicted, manufactured and tested. The results of testing the optimized formulation reveal that 85% D4T was released after 12h, and the dissolution profile fell within the acceptable limits as depicted in Figure 5.33. The microparticles exhibited a relatively smooth surface morphology as depicted in Figure 5.34. The particles were free flowing and a high %EE and yield were observed.

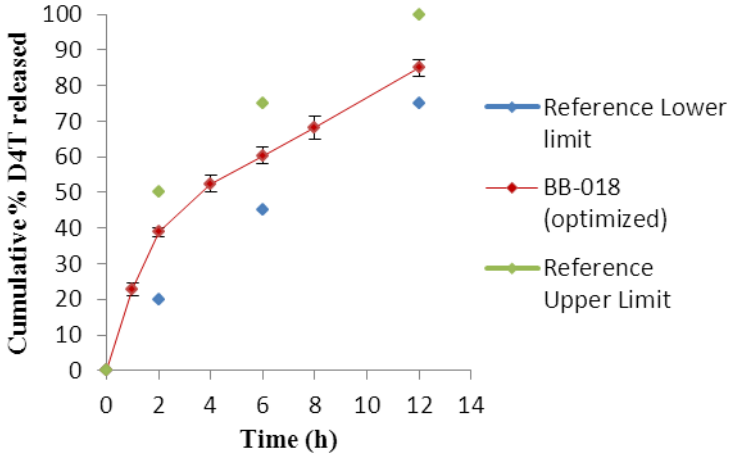

Figure 5. 33 Cumulative % D4T released for Batch BB-018 (optimized)

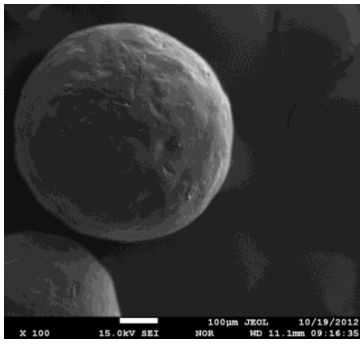

Figure 5. 34 SEM of a microparticle from Batch BB-018 (optimized)

The percent error was calculated to determine the deviation between predicted and observed values using Equation 5.9, and the results are summarised in Table 5.7. The % error for all responses was found to be within an acceptable limit of <5% and it was concluded that this method was efficient for statistical analysis of the data and also for predicting an optimized formulation.

$$\left[\frac{\text{Predicted} - \text{Observed}}{\text{Predicted}}\right] \text{X } 100$$

Equation 5.9

Table 5. 7 Predicted versus observed data for optimized formulation

Response	Predicted	Observed	% Error
% Yield	85	83.9	1.3
% D4T released	88.7	85	4.17
Encapsulation efficiency	97.6	94	3.8
Particle size	708	698	1.4
HR	1.15	1.18	2.6
CI	13.6	14	2.9
AOR	27	28	3.7

5.4 CONCLUSIONS

The development of SR D4T microparticles by solvent evaporation required careful selection of excipients and manufacturing parameters in order to get the safest possible route of production that resulted in the manufacture of a product with the desired target product profile. The physicochemical properties of D4T are also important factors to consider. D4T microparticles manufactured using copolymers of methacrylic acid and methyl methacrylate viz., Eudragit® S100 and RSPO have the potential to be used for the manufacture of a twice-daily dosing oral capsule product for D4T. These microparticles can be titrated to the required dose in pharmacy settings, depending on the dose required by a patient and this may be a solution to reduce dose dependant side effects of D4T. The flowability properties of the particles facilitates filling into hard gelatine capsules.

BBD is a useful statistical tool for the optimization of pharmaceutical dosage forms and permits manipulation of multiple variables simultaneously to perform fewer experiments than if a CCD were used, as CCD requires evaluation at extreme points. With the aid of a BBD microparticles with a high %EE that released approximately 85% D4T in 12 hours were produced. The optimized formulation meets the guidelines of the USP, FIP and FDA, which state that for SR dosage forms 20-50% of the labelled content should be released at 25% of the dosing interval, 45-75% of the labelled content should be released at 50% of the interval and at least 75% should be released at the full dosing interval.

Dissolution testing using USP Apparatus 3 was successfully used to monitor D4T release from microparticles in solutions of different pH and to mimic the GI tract environment. SR

D4T microparticles that have appropriate flow, release characteristics, loading capacity and %EE have been successfully manufactured using a solvent evaporation approach, and the formulation was optimized using BBD. The microparticles have the potential to be used to improve treatment of HIV positive patients and require further investigation in respect of stability that must be conducted according to ICH guidelines.

CHAPTER SIX

MODELING OF D4T RELEASE FROM MICROPARTICLES AND DISSOLUTION PROFILE COMPARISON

6.1 INTRODUCTION

The release of an API from solid pharmaceutical dosage forms is necessary to ensure therapeutic efficacy [185]. Important information relating to the mechanism of release of API and dosage form effects on release kinetics can be undertaken using mathematical modelling of dissolution profiles of SR dosage forms [156, 157]. A number of methods for the analysis of dissolution data as a function of time exist, however the impact of dosage form characteristics can best be explained mathematically by use of standard equations that translate dissolution curves into a function of other parameters related to the delivery device [186].

Dissolution from immediate release and SR dosage forms has been described by several kinetic models and the release kinetics are influenced by a variety of factors including temperature, nature of the API, dissolution medium, particle size of the API, polymorphic form, crystallinity, solubility, excipients and composition of polymers used to control API release [156, 186]. Common release mechanisms include diffusion, swelling and erosion controlled systems [156].

Diffusion controlled release may occur through a polymer matrix, water-filled cavities or both and occurs in parallel or sequentially [187]. Swelling controlled systems can be defined as a device in which swelling occurs and in which other mass transport systems such as dissolution, diffusion and polymer dissolution are involved [188, 189]. In such systems as the length of the diffusion pathway increases there is a corresponding decrease in the concentration gradient that is the driving force for diffusion [190]. Consequently there is a potential for a decrease in the rate of release of API. If the mobility of macromolecules in a delivery technology increases API mobility may increase and increased release rates may be observed. One of these phenomena usually dominate and is a consequence of the type of polymer used in the delivery system [191, 192].

Erosion controlled release is the process of material loss from a device or bulk polymer or the degradation of water-insoluble polymers as part of an erosion process. Two extreme types of erosion occur that is dependent on the rate at which water penetrates into the technology and/or rate of polymer chain cleavage. These are heterogeneous erosion parameters, and also known as surface erosion whereas homogenous erosion is known as bulk erosion [189]. In technologies that exhibit surface erosion polymer chain cleavage is much faster than water penetration into the system [193]. Consequently the degradation process is restricted to the outermost layers of polymer and the erosion predominantly affects the surface and not the inner parts of the device. Bulk erosion occurs when water penetration is more rapid than polymer chain cleavage and the entire system is rapidly wetted and degradation occurs throughout the device [189, 192-194].

The quantitative interpretation of dissolution data is described mathematically (Equation 6.1) and translates the dissolution curve into a function of parameters related to pharmaceutical dosage forms. The fundamentals of kinetics of API release were first proposed by Noyes and Whitney and the relationship is depicted mathematically in Equation 6.1[195, 196].

$$\frac{dM}{dt} = KS\,(Cs - Ct)$$

Equation 6.1

Where,

M = the mass transferred with respect to time, t, by dissolution from an instantaneous surface of a solid particle of, S, under the effect of the prevailing concentration driving force (Cs - Ct)
Ct = the concentration at time t
Cs = the equilibrium solubility of the solute at the experimental temperature
dM/dt = the amount dissolved per unit area per unit time and for most solids can be expressed in units of g x cm^{-2} x s^{-1}
K= dissolution rate constant
S = the area of dissolving surface or area of the diffusion layer

When Ct < 15% of the saturation solubility, Cs, Ct has a negligible influence on the dissolution rate of a solid. Under such circumstances the dissolution of the solid is said to occur under sink conditions. In general the surface area, S is not constant except when the quantity of material present exceeds the saturation solubility or initially when small quantities of drug have dissolved [186, 192, 195].

Fick's 1st law of diffusion (Equation 6.2) was used to establish a relationship between the constant in Equation 6.1 and the diffusion coefficient of a solute [186].

$$\mathbf{K = \frac{DS}{h\gamma}}$$

Equation 6.2

Where,

D = the diffusion coefficient
S = the area of dissolving surface or area of the diffusion layer
γ =the solution volume
h = the diffusion layer thickness
K= dissolution rate constant

The process that occurs at the surface of solid proceeds much faster than the transport process and a linear concentration gradient that is confined to a layer of solution that adheres to the surface of the solid exists. Ideal conditions can never be achieved as the actual surface changes as dissolution proceeds. The Noyes-Whitney equation describes the dissolution process as a first order reaction [195].

6.2 MATHEMATICAL MODELS

There are a number of kinetic models that can be used to describe the overall release of an API from a dosage form [197, 198]. The methods used to investigate the kinetics of API release from controlled release formulations include statistical methods such as ANOVA, model dependent methods that include but are not limited to Zero order, First order, Higuchi, Korsmeyer-Peppas or the Hixson-Crowell models and model independent methods such as the difference, f_1 and similarity factor, f_2 [192, 195].

6.2.1 Statistical methods

6.2.1.1 ANOVA

Methods based on the ANOVA can be distinguished as one-way analysis of variance (ANOVA) or multivariate analysis of variance (MANOVA). The statistical methods assess the difference between the means of two sets of data at a single time point (ANOVA or Student-t test) or from multiple time point dissolution (MANOVA) [186, 199].

6.2.2 Model dependent methods

Model dependent methods are based on different mathematical functions that can be used to describe a dissolution profile. Once a suitable function has been selected the dissolution profiles can be evaluated depending on the model parameters that have been derived [186].

6.2.2.1 Zero order

Mathematical modelling using a zero-order release model describes API dissolution from several types of modified release dosage forms including coated, membrane controlled and osmotic dosage forms. Zero-order release kinetics describe a profile in which a constant amount of API is released per unit of time and can be described mathematically using Equation 6.3 [199, 200].

$$\mathbf{Q_t = Q_0 + K_0 t}$$

Equation 6.3

Where,

Q_0 = initial amount of drug in the pharmaceutical dosage form and most times (Q_0=0)
Q_t = the amount of drug in the pharmaceutical dosage form at time t
K_0 = zero order release rate constant

API release in which the same amount of API per unit of time is delivered is ideal to achieve a prolonged pharmacological action. These dosage forms do not disaggregate and release the API slowly. To study the kinetics of release generated from *in vitro* release studies the data are plotted as the cumulative amount of API released versus time [186, 192, 195].

6.2.2.2 First order

The first-order model has been used to describe homogeneous dissolution in which release is independent of the amount of API in the dosage form. The release of the API that follows first order kinetics can be expressed mathematically using Equation 6.4.

$$\mathbf{Log\ C = Log\ C_0 - \frac{Kt}{2.303}}$$

Equation 6.4

Where,

C= amount of drug released
C_0 = initial concentration of drug

K= first order rate constant
t = time.

This relationship can be used to describe API dissolution from pharmaceutical dosage forms that contain water-soluble molecules dispersed in porous matrices that release the API in a manner that is proportional to the amount of API remaining in the technology. Consequently the amount of API released over time diminishes. It is difficult to conceptualize this mechanism on a theoretical basis and the data generated are plotted as log cumulative percent API remaining versus time to yield a straight line with a slope of -K/2.303 [186, 192, 195].

6.2.2.3 Higuchi model

The Higuchi model is the first mathematical model that was used to describe the release of water soluble and low solubility molecules from a uniform polymeric matrix system. Initially the model was used to describe release from planar systems and was then extended to include systems of different geometry and porosity [198]. This Higuchi model is based on the hypotheses that the initial API concentration in the matrix is much higher than the solubility of the molecule, that API diffusion occurs in only one dimension, that particles of the API are much smaller than the thickness of the device, that swelling and dissolution of the matrix are negligible, that the diffusivity of the API is constant and that perfect sink conditions are always maintained.

Mathematical expressions were obtained for drug particles dispersed in a uniform matrix behaving as the diffusion medium. In order to study dissolution from a planar system in which API is homogeneously distributed the mathematical relationship described in Equation 6.5 can be used [199, 201].

$$\mathbf{Q = A\sqrt{D(2C - Cs)Cs\ t}}$$

Equation 6.5

Where,

Q = the amount of drug released in time t per unit area
C = the drug initial concentration
C_S = the drug solubility in the matrix media
A= loading of solute
t= time
D = the diffusivity of the drug molecules (diffusion constant) in the matrix substance

This expression was first proposed by Higuchi [202] to describe the dissolution of an API suspended in ointment bases but can be applied to dissolution from other pharmaceutical dosage forms. Higuchi [202] described API release as a diffusion controlled process based on Fick's first law and that diffusion was square root time dependant. In general, it is possible to simplify the Higuchi model to the form described in Equation 6.6 [186, 192, 195],

$$\mathbf{F_t = K_H \, x \, t^{1/2}}$$

Equation 6.6

Where,

F_t = amount of drug released in time t
t= time
K_H = Higuchi dissolution constant

The dissolution data are plotted as cumulative percent API released versus square root of time.

6.2.2.4 Hixson-Crowell model

The Hixon-Crowell model is used to describe the release kinetics of water-soluble API from porous matrices. The release rate is limited by the dissolution rate of the API and not by diffusion through the polymeric matrix [198]. Hixson and Crowell recognized that the regular area of a particle is proportional to the cube root of its volume and they derived a relationship that can be described mathematically as Equation 6.7.

$$\mathbf{W_0^{1/3} - W_t^{1/3} = K_s t}$$

Equation 6.7

Where,

W_0 = the initial amount of drug in the pharmaceutical dosage form
Wt = the remaining amount of drug in the pharmaceutical dosage form at time t
Ks = a constant incorporating the surface–volume relation.

The data generated from *in vitro* API release studies are plotted as the cube root of percent API remaining in the matrix versus time. This expression applies to pharmaceutical dosage form such as tablets where dissolution occurs in planes that are parallel to the surface of the

API, if the tablet dimensions diminish proportionally and the initial geometrical form is constant over time [192, 195].

6.2.2.5 Korsmeyer-Peppas model

This model is also known as the Power Law and is a semi-empirical relationship that is used to describe the release of API from polymeric systems exponentially. The Power Law is mathematically described in Equation 6.8 [191, 201].

$$\frac{Mt}{M\infty} = Kt^n$$

Equation 6.8

Where,

K = a constant incorporating structural and geometric characteristics of the drug dosage form
n = the release exponent indicative of the drug release mechanism
$\frac{Mt}{M\infty}$ = fractional release of drug at time t

The Power Law is a model that is commonly used to determine the mechanism of release of an API. The release exponent, n, is used to characterize different release mechanisms. The Power Law us used to model swelling and API release from polymeric based dosage forms in situations when the release mechanism is not well known or when more than one release mechanism contributes to API release [203]. If diffusion is the main release mechanism, a graphical representation of the API released versus the square root of time should produce a straight line [191, 201, 204]. Under some experimental conditions the release mechanism deviates from Fick's law suggesting that anomalous behaviour or non-Fickian mechanisms control release. Peppas [203] used the value for n to characterise the release mechanisms from thin films, cylinders and spheres in order to determine whether diffusion occurs via Fickian, anomalous case II, or super case II transport. An interpretation of the diffusional release mechanisms from polymeric films, cylinders and spheres is summarized in Table 6.1.

Table 6. 1 An interpretation of diffusional release mechanisms from polymeric films, cylinders and spheres [195, 204]

Release exponent (n)			Drug transport mechanism	Rate as a function of time
Thin films	**Cylinder**	**Sphere**		
0.5	0.45	0.43	Fickian diffusion	$t^{-0.5}$
0.5<n<1.0	0.45<n<0.89	0.43<n<0.85	Anomalous transport	t^{n-1}
1.0	0.89	0.85	Case II transport	Zero order release
higher			Super case II transport	T^{n-1}

Fickian diffusion and Case-II relaxation release are the limits for this approach. Fickian diffusion occurs according to the usual molecular diffusion of API due to a potential concentration gradient. Case-II relaxation describes a transport mechanism associated with the stresses and state-transition in hydrophilic glassy polymers that swell in the presence of water [185]. To study the kinetics of release from data generated from *in vitro* release studies, the log cumulative percent API released versus log time profiles were plotted. This model requires that modelling be undertaken up to the point at which a maximum of 60% API has been released [186, 195, 199].

6.3 Model independent methods

Traditionally model-independent pharmacokinetic analysis methods have been successfully used to characterize the *in vitro* release kinetics of drugs [205]. The f_1 and f_2 difference and similarity factors are known as pair-wise procedures. The procedure includes a simple approach that uses the difference, f_1 and similarity, f_2 factors to compare dissolution profiles [205]. The difference factor is based on the percent difference between two mean dissolution curves at each time point and expresses the relative error between the two curves and is calculated using Equation 6.9 [205]:

$$f_1 = \frac{\sum_{j=1}^{n} Rj - Tj}{\sum_{j=1}^{n} Rj} \text{ x } 100$$

Equation 6.9

Where,

n = the sampling number
Rj and Tj = the percent dissolved of the reference and test products at each time point j.

The percent error is zero when the test and reference profiles are identical and increase proportionally with dissimilarity between the two dissolution profiles. The similarity factor, f_2 is a logarithmic transformation of the sum-squared error of differences between two curves and is calculated using Equation 6.10,

$$f_2 = 50 \text{ x } \log [1 + (1/n)\sum_{j=1}^{n} Wj\ (Rj - Tj)^2]^{-0.5} \text{ x } 100$$

Equation 6.10

Where,

All the variables are the same as for the difference factor,
Wj = an optional weight factor.

The profiles are considered similar when the difference factor is close to 0 and the similarity factor is close to 100. In general, dissolution profiles are considered similar if $f_1 \leq 15$ and $f_2 \geq 50$ (50-100) [192, 205]. This method is used to compare dissolution profiles when data from three or four dissolution time points have been generated. The similarity factor has been adopted by the CDER at FDA and by Human Medicines Evaluation Unit of The European Agency for the Evaluation of Medicinal Products (EMEA), as a criterion for the assessment of similarity between two *in, vitro* dissolution profiles. The similarity factor was first defined by Moore and Flanner [206] and is a logarithmic reciprocal square root transformation of one plus the mean squared (the average sum of squares) differences in percent API dissolved between a test and a reference product [192, 195].

However some relevant statistical issues relating to the similarity factor have been reported and include the invariant property of f_2 with respect to location change and the consequence of failure to take into account the shape of the curve and the unequal spacing between sampling time points. The similarity factor is a sample statistic that cannot be used to formulate a statistical hypothesis for the assessment of dissolution similarity and results from simulation studies suggest that the similarity factor is too liberal in concluding similarity between dissolution profiles and that the true range of f_2 is from $-\infty$ to 100 and it is not symmetrical about zero [195, 200, 205].

The f_2 is a convenience criterion and not a criterion based on scientific facts [195]. Although model-independent methods are easy to apply they often lack scientific justification.

However despite obvious limitations, model-independent methods are an important tool for the comparison of *in vitro* dissolution profiles and provide useful information to formulation scientists [185, 192, 200, 205].

6.4 MODEL SELECTION CRITERIA

The best way to establish a model that best describes dissolution or release phenomena of an API is the coefficient of determination, R^2. However, when comparing models with different numbers of parameters the adjusted coefficient of determination may be more meaningful and can be calculated using Equation 6.11 [192, 195],

$$R^2_{adjusted} = 1 - \frac{(n-1)}{(n-p)}(1-R^{2)}$$

Equation 6.11

Where,

n = the number of dissolution data points
p = the number of parameters in the model

6.5 METHODS

6.5.1 Model fitting

For the purposes of this research, the cumulative amount of D4T released from microparticles was analysed using model dependent and model independent approaches and the data for API release from all 18 formulations were modelled. The R^2 value was used to determine the goodness of fit or the best fit solution and a very high R^2 value indicated best fit. The f_1 and f_2 factors were used to compare D4T release from the optimized formulation, viz., Batch BB-018 and Batches BB-001- BB-017 to establish if all formulations satisfy the guidelines for API release from SR dosage forms. The mathematical equations that describe the models that were used for dissolution data for D4T microparticle formulations are summarized in Table 6.2.

Table 6. 2 Summary of equations used for modelling

Model	Equation
Zero order	$Q_t = Q_0 + K_0t$
First order	$\text{Log } C = \text{Log } C_0 - \frac{Kt}{2.303}$
Higuchi	$F_t = K_H \times t^{1/2}$
Korsmeyer-Peppas	$\frac{Mt}{M\infty} = Kt^n$
Hixson-Crowell	$W_0^{1/3} - W_t^{1/3} = K_st$

6.6 RESULTS AND DISCUSSION

6.6.1 Mathematical modelling

The formulations were modelled using the Higuchi, Korsemeyer-Peppas, Zero-order, First-order and Hixson-Crowell models and a high correlation coefficient of > 0.9 was used to indicate the goodness of fit. The curvilinear nature of some of the cumulative percent D4T released versus time plots indicate that D4T release from the microparticles did not follow zero-order kinetics (Section 5.3.7). This was confirmed by the low correlation coefficient obtained in most cases when these data were fitted to the zero-order model (Table 6.3). Modelling *in vitro* dissolution study confirmed that the majority of test formulations viz., BB-001-BB-008, BB-010, BB-012- BB-017 followed Higuchi release patterns and this model was considered the best to describe the release kinetics of D4T from microparticles with R^2 values approaching 0.99. However D4T release from the optimized formulation (BB-018) deviated from Higuchi type release to zero-order release with an R^2 value of 0.9940 for this model (Table 6.3) indicating that same amount of D4T was released per unit time. In general the First order and Hixson-Crowell models did not describe the mechanism of D4T release from the microparticles adequately as confirmed by the low correlation coefficients of <0.9 observed for these models. A summary of the mathematical modelling data for these studies is listed in Table 6.3.

Table 6. 3 A summary of the results obtained after mathematical modelling of D4T release

Model	Zero order		First order		Higuchi		Hixson-Crowell	
Formulation	**R^2**	**k**	**R^2**	**k**	**R^2**	**k**	**R^2**	**k**
BB-001	0.9201	3.0575	0.8710	0.0216	0.9778	13.9750	0.8955	0.0653
BB-002	0.7118	4.3450	0.6312	0.0295	0.8300	20.9500	0.6378	0.0874
BB-003	0.8425	5.5257	0.7452	0.0422	0.9364	25.8310	0.7795	0.1223
BB-004	0.9358	6.5196	0.8073	0.0489	0.9893	29.7200	0.8546	0.1442
BB-005	0.9661	5.9690	0.8441	0.0516	0.9976	26.8940	0.8940	0.1450
BB-006	0.9607	4.8565	0.8440	0.0501	0.9962	21.9300	0.8861	0.1331
BB-007	0.8488	5.6192	0.7607	0.0421	0.9393	26.2100	0.7954	0.1254
BB-008	0.9822	4.5659	0.8929	0.0540	0.9907	20.3320	0.9379	0.1383
BB-009	0.8362	5.7006	0.7317	0.0437	0.9327	26.6940	0.7693	0.1272
BB-010	0.9312	4.5920	0.9045	0.0333	0.9561	20.6320	0.9113	0.0992
BB-011	0.8409	5.6228	0.7395	0.0430	0.9343	26.2800	0.7731	0.1254
BB-012	0.9150	6.0620	0.8009	0.0411	0.9724	27.7100	0.9113	0.0992
BB-013	0.9824	4.5848	0.8715	0.0549	0.9980	20.4900	0.9124	0.1393
BB-014	0.6972	4.8257	0.5962	0.0375	0.8276	23.3000	0.6317	0.1089
BB-015	0.8468	5.5072	0.7483	0.0412	0.9393	25.7170	0.7890	0.1212
BB-016	0.8322	5.1282	0.7000	0.0410	0.9287	24.0200	0.7473	0.1179
BB-017	0.7864	3.6350	0.7032	0.0293	0.8958	17.2020	0.7298	0.0840
BB-018 (optimized)	**0.9940**	**5.2243**	**0.8222**	**0.0449**	**0.9877**	**23.687**	**0.8616**	**0.1280**

The fact that the mechanism of release of D4T from microparticles followed Higuchi release was confirmed by evaluation of the value for n following fitting of data to the Korsmeyer-Peppas model and the R^2 values observed. The values for n for most of the D4T microparticle formulations were $0.5<n<1.0$ suggesting that anomalous transport had occurred and that diffusion was not the only mechanism controlling D4T release, as the values were beyond the limits of the model. This is indicative of D4T release by other mechanisms such as polymer swelling and relaxation. *In vitro* release profiles for D4T for all manufactured formulations were modelled using the Korsmeyer-Peppas model and the data are summarised in Table 6.4.

Table 6. 4 Korsmeyer-Peppas data for in vitro release of D4T

Formulation	R^2	n	Mechanism
BB-001	0.9386	0.2333	*
BB-002	1.0000	0.7333	Anomalous
BB-003	0.9850	0.6000	Anomalous
BB-004	0.9871	0.6650	Anomalous
BB-005	0.9874	0.5952	Anomalous
BB-006	0.9851	0.5599	Anomalous
BB-007	1.0000	0.5850	Anomalous
BB-008	0.9880	0.5797	Anomalous
BB-009	0.9894	0.6500	Anomalous
BB-010	0.9231	0.2000	*
BB-011	0.9647	0.6233	Anomalous
BB-012	0.9868	0.5833	Anomalous
BB-013	0.9963	0.5990	Anomalous
BB-014	1.0000	0.9667	Anomalous
BB-015	0.9924	0.5817	Anomalous
BB-016	0.9608	0.6667	Anomalous
BB-017	0.9753	0.4833	*
BB-018 (optimized)	0.9945	0.7262	Anomalous

* Diffusion not the only mechanism controlling D4T release (not within the limits of the model)

When the f_1 and f_2 factors were used to compare the release profile for the optimized formulation to the other dissolution profiles it was noted that formulations BB-005 and BB-016 were similar to that observed for the optimized formulation as the f_1 values < 15 and f_2 values were > 50 and they fell within the acceptable limits set for this study. The similarity of release may be attributed to the formulation composition based on quantities of rate retarding polymers used. A variation in Eudragit® S100 content resulted in lower ionization and therefore slower solubilisation. Consequently a significant effect on D4T release was observed. The data generated from formulations with Eudragit® S100 exhibited a p-value of < 0.05 which showed its statistical significance at determining D4T release and using Equation 5.2 in § 5.3.1 its effect on D4T release is of a negative magnitude suggesting that at slightly lower concentrations of 13-20% w/w a similar dissolution profile is observed when the polymer is combined with Eudragit® RSPO at 42-50% w/w and Avicel®PH102 at 24-34% w/w levels. In conclusion, this shows the importance of investigating potential interactive effects when developing formulations, as different compositions may produce similar results. Formulations BB-004 and BB-010 were not statistically similar to the optimized formulation but also fell within the acceptable limits set for this study with approximately 43 and 40% D4T being released initially, respectively, 73 and 72% D4T release after 6 hours, respectively and 100.2 and 86% being released after the total test period of 12 hours. A summary of the results is listed in Table 6.5.

Table 6. 5 Summary of a comparison of the optimized and the other formulations using model independent methods (f_1 and f_2)

Formulation	f_1	f_2
1	19	45.8
2	36.1	34
3	19.9	45.7
4	17.8	47.7
5	**6.8**	**64.6**
6	15.9	52.9
7	18.1	46.9
8	30.2	38.3
9	19.8	45.3
10	13.4	50.9
11	18.8	46.4
12	25.9	41.3
13	28.3	40
14	24.2	40.8
15	20.6	45.2
16	**14.5**	**52.3**
17	15.8	52.5

Similar if $f_1 \leq 15$ and $f_2 \geq 50$

6.7 CONCLUSIONS

Microparticles containing D4T were manufactured using polymethacrylate copolymers and have been assessed using mathematical approaches to study mechanisms of release. The mechanism of release of D4T from test formulations was established by evaluating correlation co-efficients and a high correlation coefficient indicates the best fit model for these data. The use of model dependant mathematical approaches permitted identification of the mechanism of D4T release from the microparticles. It appears that D4T release from microparticles was predominantly controlled by diffusion through the polymethacrylate copolymer matrix as Higuchi release kinetics with $R^2 > 0.9$ were observed. The mechanism of release was further confirmed by the use of the Korsemeyer-Peppas model. The Higuchi release kinetics observed for most test formulations facilitates the identification of the mechanism of release for hydrophilic API from this formulation. D4T diffusion occurred with constant diffusivity and the D4T particles were much smaller than the thickness of the microparticles. However D4T release from the optimized formulation occurred via a zero-order process and this is desirable for therapeutic success.

The Korsmeyer-Peppas model was successfully used to elucidate the mechanism of D4T release from the test formulations. Most of the microparticles released D4T via an anomalous transport mechanism and the release exponent, n ranged between $0.5<n<1.0$ indicating that diffusion was not the only mechanism controlling D4T release from the microparticles.

Consequently the release process may also be controlled by swelling, stress, structural changes and/or polymer relaxation. Model independent models were used to compare D4T release from the optimized formulation and test formulations to provide an indication of how different the optimized and test profiles were and to establish if other formulations fell within the acceptable limits for API release from a SR dosage form. Formulations BB-005 and BB-016 were similar to the optimized formulation as the f_1 values < 15 and f_2 values were > 50 and they fell within the acceptable limits of the USP. The similarity was attributed to the formulation compositions of the retarding polymers and it was concluded that investigation of interactive effects on D4T release was important as different combined effects may produce similar dissolution profiles. D4T release from batches BB-005 and BB-016 occurred by a zero order process, however Higuchi release kinetics were predominant for most batches. Formulations BB-004 and BB-010 were not statistically similar to the optimized formulation but also fell within the acceptable limits set for this study.

An understanding of the limitations and assumptions of the different mathematical models is essential for an appropriate decision on which models to use. The models provide guidance in respect of transport mechanisms for D4T release from SR formulations. Furthermore the goodness of fit should be established using a number of approaches as the correlation coefficient alone is not always reliable.

CHAPTER SEVEN

CONCLUSIONS

The ongoing challenge of HIV/AIDS has led to continued research and development in an attempt to improve the quality of life of individuals suffering from this disease. At present, there is no cure for HIV/AIDS and it is therefore beneficial to develop dosage forms and formulations that are suitable for use by patients. SR dosage forms have increased patient adherence through decreased dosing frequency and convenience. SR dosage forms help maintain constant drug levels in the body and consequently reduce the side effects observed when immediate release formulations are used and dose dumping occurs.

D4T is a potent ARV commonly used in first-line combination therapy to treat HIV infection. D4T is highly water soluble with a solubility of 83mg/ml and has a short half-life of 1.5 hours suggesting that it is a suitable candidate for inclusion in SR dosage forms. There have been many issues relating to the use of D4T as it exhibits dose dependent side effects and at high doses it may cause life threatening adverse events such as lactic acidosis, peripheral neuropathy and lipodystrophy that is commonly referred to as the 'buffalo hump'. These side effects are likely to lead to poor patient adherence. D4T has been discontinued in developed countries due to the prevalence of adverse events. Nonetheless it is still used in resource limited settings since it is affordable when compared to other ARV. In this study SR D4T microparticles were manufactured to contain a low dose of the molecule and the microparticles have the potential to be administered as a 'twice-a-day' formulation when enclosed in capsules. In this way it may be possible to minimize dose dependent side effects and increase patient adherence.

A sensitive, selective, accurate, precise stability indicating RP-HPLC method for the analysis of D4T in pharmaceutical dosage forms was developed and validated following ICH guidelines. RSM using CCD was used to optimize the method in terms of flow rate, column temperature and mobile phase composition to produce a separation with R_t of less than 10 minutes. The method was found to be linear over the range 1-60µg/ml. D4T and AZT that was used as the internal standard were separated with R_t of 4 and 8 minutes, respectively. The method was accurate and precise with % RSD and % Bias values < 5%. The method was successfully applied to the analysis of commercially available D4T containing dosage forms on the South African market and for all formulation development studies

Pre-formulation studies were conducted and potential excipients such as Kollidon® VA64, Klucel®, Methocel®K4M, Eudragit® RSPO, Eudragit® EPO, Eudragit® S100, Eudragit® RLPO, Avicel®102 and magnesium stearate were evaluated for use in manufacturing microparticles. DSC was used to establish whether any drug-excipient and excipient-excipient interactions may occur. It was concluded that there was no evidence of any incompatibility as DSC thermograms for D4T revealed a melting endotherm peak at 175.5°C which corresponds to the melting point of the stable polymorph of D4T. DSC analyses of D4T in 1:1 ratio with excipients also revealed no potential interactions. IR spectroscopy was used to confirm the absence of any interactions between D4T and excipients and the results suggest that no interactions were likely to occur. IR spectroscopy revealed that all principal bands of D4T molecule were present in the binary mixtures of the API and excipients. The presence of interactions is usually revealed by the absence or appearance of frequency bands and this was not obvious. TGA was conducted to establish whether D4T would degrade under manufacturing conditions. It was concluded that D4T would be stable under the manufacturing conditions used to produce the microparticles and D4T undergoes degradation in three distinct steps over different temperature ranges with the initial degradation commencing at a temperature of approximately 190°C leaving no residue after 300^{0}C. These temperatures are much higher than those used during manufacture of the microparticles.

SR D4T microparticles were successfully manufactured using the oil-in-oil non aqueous solvent evaporation microencapsulation approach. Kollidon® VA64, Klucel®, Methocel®K4M, Eudragit® RSPO, Eudragit® EPO, Eudragit® S100 and Eudragit® RLPO were polymers that were evaluated for their ability to form microparticles and their ability to sustain D4T release based on a trial and error basis during screening. Microparticles manufactured using Kollidon® VA64, Klucel® and Methocel®K4M exhibited a poor surface morphology and some of the microparticles showed clustering and 'dough-like' structures with poor flow properties. Microparticles manufactured using Eudragit® RSPO, Eudragit® EPO, Eudragit® S100 and Eudragit® RLPO had a better surface morphology, were spherical, free-flowing and discrete. Dissolution studies revealed that microparticles manufactured using Eudragit® RSPO and Eudragit® S100 had the potential to sustain D4T release as Eudragit® RSPO is a copolymer of acrylic and methacrylic acid esters substituted with 5% quartenary ammonium functional groups. The low content of quartenary ammonium functional groups in Eudragit® RSPO play an important role in sustaining D4T release since

the permeability of the polymer to water is a function of this substitution and the polymer is less permeable and swells. Eudragit® S100 had a pronounced SR effect due in part to the fact that Eudragit® S100 is a copolymer of methacrylic acid and methyl methacrylate with a 1:2 ratio of carboxyl to ester functional groups and it is soluble at pH > 7. Following the manufacture and assessment of different drug-polymer ratios and compositions a final formulation was identified and then further optimized.

Optimization of the microparticle formulation was achieved using RSM and a BBD approach in which the amount of Eudragit® RSPO, Eudragit® S100 and Avicel®PH102 were varied. The optimized formulation was identified, manufactured and dissolution studies revealed that Eudragit® loaded microparticles have the potential to release D4T over a 12h period making it a potential 'twice-a-day' formulation. The microparticles were assessed in terms of yield, particle size, encapsulation efficiency, flow properties and *in vitro* release characteristics. Microparticles with good flow properties were manufactured and the values for the HR (1.10-1.23), CI (13.1-14.6) and AOR (22-39) were within the limits for good flow properties. The encapsulation efficiency ranged between 78.9 and 99.2%. D4T is a hydrophilic drug and does not dissolve in the lipophilic continuous phase used for solvent evaporation manufacture and therefore high values for encapsulation efficiency were achieved. It was established that an increase in polymer concentration resulted in an increase in encapsulation efficiency and an increase in viscosity resulted in an increased mean particle size. This results in a decreased surface area that delays diffusion of D4T from the microparticles. High yields of microparticles were achieved and yields < 100% can be attributed to the fact that some of microparticles stuck to the homogenizer blade or were lost during washing of the microparticles.

In vitro release studies were initially performed using USP Apparatus I for the screening formulations but was not ideal as it does not readily permit *in vitro* testing in media of different pH. Consequently USP Apparatus III was used to evaluate D4T release *in vitro* for formulations manufactured during the optimization process. An increase in the concentration of Eudragit® S100 had a significant impact on D4T release and an increase in Eudragit® RSPO levels also sustained D4T release. Avicel®PH102 did not have a significant effect on D4T release. Optimization studies enabled the determination of the effect of combinations of parameters on a particular response. The combination effect of Eudragit® S100 and Eudragit® RSPO resulted in significant decrease in D4T release. It was concluded that Eudragit® S100 was the primary polymer controlling D4T release as seen from the dissolution profiles for

batches BB-002 and BB-008 in which the Eudragit® S100 content was increased from 10% to 20% and reveal reduced D4T release from the microparticles. After two hours of testing approximately 20% D4T only had been released when the high concentration of Eudragit® S100 (BB-008) was used whereas approximately 61.5% was released in the same time from microparticles produced using the low concentration of polymer.

The optimized composition was identified and the formulation was successfully manufactured. The microparticles had good flow properties, and the yield was approximately 85 %. The encapsulation efficiency was 95 % and after 12 hours approximately 85% of the D4T had been released. The optimized formulation met the specification for the USP, FIP, FDA guidelines for SR dosage forms. The guidelines state that 20-50% of the labelled content should be released at 25% of the dosing interval, 45-75% of the labelled content should be released at 50% of the dosing interval and at least 75% D4T should be released at the full dosing interval. The % error for all responses was <5% and it was concluded that this method was efficient for analysis of data for predicting an optimized formulation.

The *in vitro* release kinetics of D4T from the microparticles was successfully elucidated using model-dependent and model-independent mathematical approaches. The data generated from *in vitro* release studies were modelled using Zero-order, First-order, Higuchi, Hixson-Crowell and the Korsmeyer-Peppas models. The mechanism of D4T release was primarily diffusion controlled and most of the microparticle formulations exhibited Higuchi release kinetics with correlation coefficients for the model > 0.9. This was confirmed using the Korsemeyer-Peppas model. Most of the formulations released D4T by an anomalous transport mechanism and the release exponent, n, ranged between $0.5<n<1.0$. Batch BB-018, the optimized formulation was manufactured and tested and the release of D4T from this batch appeared to follow a Zero-order model which was desirable. The Korsmeyer-Peppas model was used successfully to establish the mechanisms for D4T release from the microparticles. It was concluded that D4T release may be due to swelling, stress, structural changes and polymer relaxation. Diffusion was not the only mechanism controlling D4T release and the optimized formulation exhibited anomalous transport kinetics with the release exponent, n of 0.7262.

Model independent f_1 and f_2 factors were used to determine if D4T release from test formulations was similar to that of optimized formulation and D4T release from batches BB-005 and BB-016 were found to be similar to the optimized formulation as they had f_1 values that were less than 15 and f_2 values that were greater than 50. The similarity was attributed to

the formulation compositions of the retarding polymers and it was concluded that investigation of interactive effects on D4T release were important as different combined effects may produce similar dissolution profiles. Formulations BB-004 and BB-010 were not statistically similar to the optimized formulation but also fell within the acceptable limits set for this study.

In conclusion spherical, discrete SR microparticles of D4T have been successfully manufactured using copolymers of methacrylic acid and methyl methacrylate, Eudragit® S100 and RSPO. The microparticles have good flow properties and can be titrated to the required dose in pharmacy settings depending on the dose required to treat patients. This approach may reduce dose dependant side effects of D4T as these particles have the potential to be used for a 'twice-a-day' oral capsule dosage form. This manufacturing approach can be used as a basis for further development of D4T SR formulations in an attempt to improve the quality of life of patients by minimising side effects. Furthermore this approach can be used for the development of SR formulations for hydrophilic API. The microparticles produced in these studies can be further investigated in respect of scale up manufacture. Furthermore approaches to improving the manufacturing process to increase the yield may be required. In addition long term stability and in *vivo* bioavailability and bioequivalence studies would be necessary.

REFERENCES

1. E. Ojewole, I. Mackraj, P. Naidoo, and T. Govender. Exploring the use of novel drug delivery systems for antiretroviral drugs. *European Journal of Pharmaceutics and Biopharmaceutics*, Vol. 70, No. 3, 2008, pp. 697-710.

2. J. Starrett, M. M. Mansuri, J. C. Martin, C. E. Fuller, and H. G. Howell. Production of 2',3'-dideoxy-2',3'-didehydronucleosides. 07/173473[4904770]. 1990. Ref Type: Patent

3. R. W. Buckheit, T. L. Hartman, K. M. Watson, S. Chung and E. Cho. Comparative Evaluation of the Inhibitory Activities of a Series of Pyrimidinedione Congeners That Inhibit Human Immunodeficiency Virus Types 1 and 2. *Antimicrobial Agents and Chemotherapy*, Vol. 52, No. 1, 2008, pp. 225-236.

4. J. C. Liddy. Stavudine 20mg BID or less versus stavudine 30mg BID or more as a component of combination antiretroviral therapy for HIV infection. 2009, pp. 2-23, http://www.who.int/hiv/topics/treatments/stavudine_art.pdf [cited 5 March 2012].

5. A. C. Justice, D. S. Stein, G. P. Fusco, B. H. Sherrill, J. S. Fusco, S. C. Danehower, S. L. Becker, N. I. Hansen, N. M. H. Graham, and the CHORUS Program Team. Disease progression in HIV-infected patients treated with stavudine vs. zidovudine. *Journal of Clinical Epidemiology*, Vol. 57, No. 1, 2004, pp. 89-97.

6. K. Brinkman, H. J. M. ter Hofstede, D. M. Burger, J. A. M. Smeitink, and P. P. Koopmas. Adverse effects of reverse transcriptase inhibitors: mitochondrial toxicity as common pathway. *AIDS*, Vol. 12, 1988, pp. 1735-1744.

7. W. Lewis and M. C. Dalakas. Mitochondrial toxicity of antiviral drugs. *Nature Medicine 1*, 1995, pp. 417-422.

8. C. H. Chen and Y. C. Cheng. Delayed cytotoxicity and selective loss of mitochondrial DNA in cells treated with the anti-human immunodeficiency virus compound 2', 3' - dideoxycitidine. *Journal of Biological Chemistry*, Vol. 264, 1989, pp. 11934-11937.

9. D. J. Medina, C. H. Tsai, G. D. Hsiuna, and Y. C. Cheng. Comparison of mitochondrial morphology, mitochondrial DNA content and cell viability in cultured cells treated with three anti-human immunodeficiency virus deoxynucleosides. *Antimicrobial Agents Chemotherapy*, Vol. 38, 1994, pp. 1824-1828.

10. C. H. Chen, P. M. Vazquez, and Y. C. Cheng. Effect of anti-human immunodeficiency virus nucleoside analogs on mitochondrial DNA and its implication for delayed toxicity. *Journal of Molecular Pharmacology*, Vol. 39, 1991, pp. 625-628.

11. M. Garg, T. Dutta, and N. K. Jain. Reduced hepatic toxicity, enhanced cellular uptake and altered pharmacokinetics of stavudine loaded galactosylated liposomes. *European Journal of Pharmaceutics and Biopharmaceutics*, Vol. 67, No. 1, 2007, pp. 76-85.

12. South African Medicines Formulary. South African Medical Association, Health and Medical Publishing Group, Pinelands, SA. 2010, 9th Ed, pp. 334-335.

13. British Pharmacopoeia. The Stationery Office, London. 2011, Vol. II, pp. 2029-2030.

14. United States Pharmacopeia. United States Pharmacopeial Convention, Inc, Twinbrook Parkway, Rockville, MD, USA. 2012, 29th Edition, pp. 4273-4276

15. Drugbank: Showing Stavudine (DB00649). 2012, http://www.drugbank.ca/drugs/DB00649 [cited 5 March 2012].

16. STAVUDINE. 2012, http://chemicalland21.com/lifescience/UH/STAVUDINE.htm [cited 15 April 2012].

17. B. Radatus, M. Mirmehrabi, K. S. K. Murthy, and S. Rohani. Polymorphic Behaviour and Crystal Habit of an Anti-Viral/HIV Drug: Stavudine. *Journal of Crystal Growth & Des*, Vol. 6, No. 1, 2006, pp. 141-149.

18. K. Prakash, P. N Raju, K. S Kumari, and M. L Narasu. Solubility and dissolution rate determination of different antiretroviral drugs in different pH media using UV visible spectrophotometer. *E-J Chem*, Vol. 5, No. 2, 2008, pp. 1159-1164.

19. Food and Drug Administration (FDA). Guidance for Industry: Bioanalytical Method Validation,2001, http://www.accessdata.fda.gov/drugsatfda_docs/label/2009/020412s034,020413s026lbl.pdf. [cited 20 November 2011].

20. The Merck Index, Merck Sharp & Dohme Corp. Whitehouse Station, NJ, USA. 1996, 12 ed.

21. A. Barth, Infrared spectroscopy of proteins. *Biochimica et Biophysica Acta (BBA) - Bioenergetics*, Vol. 1767, No. 9, 2007, pp. 1073-1101.

22. R. B. Gandhi, J. B. Bogardus, D. E. Bugay, R. K. Perrone and M. A. Kaplan. Pharmaceutical relationships of three solid state forms of stavudine. *International Journal of Pharmaceutics*, Vol. 201, No. 2, 2000, pp. 221-237.

23. Horwitz. Synthetic Procedures in Nucleic Acid Chemistry. Vol. 1, 1968, pp. 344.

24. R. Paramashivappa, P. Phani Kumar, P. V. Subba Rao, and R. A. Srinivasa. Simple and efficient method for the synthesis of 2,3-didehydro-3-deoxythymidine (d4T). *Tetrahedron Letters*, Vol. 44, No. 5, 2003, pp. 1003-1005.

25. P. M. Skonezny. Process for large-scale preparation of 2'3,'-dideoxy-2',3'-didehydronucleosides. 309636[5539099]. 23-7-1996. New York. 23-9-1994. Ref Type: Patent

26. M. Mansuri. A highly potent and selective anti-HIV agent. 32, 461-466. *Journal of Medicinal Chemistry*, No. 32, 1989, pp. 461-466.

27. J. C. Martin, M. J. M. Hitchcock, E. De Clercq, and W. H. Prusoff. Early nucleoside reverse transcriptase inhibitors for the treatment of HIV: A brief history of stavudine (D4T) and its comparison with other dideoxynucleosides. *Antiviral Research*, Vol. 85, No. 1, 2010, pp. 34-38.

28. S. A. Riddler, R. E. Anderson, J. W. and Mellors. Antiretroviral activity of stavudine (2,3-didehydro-3-deoxythymidine, D4T). *Antiviral Research*, Vol. 27, No. 3, 1995, pp. 189-203.

29. K. Kunisuke and H. Shiragami. Practical syntheses of antiviral nucleosides. Vol. 70, No. 2 1998, pp. 313-318.

30. T. Adachi. Synthesis of Uracil and Thymine Nucleosides of Unsaturated 5-Aminopentafuranoses. *Carbohydrate Research*, No. 113, 1979.

31. Cosford. Selenium Nucleophiles for the preparation of Antiviral Nucleosides. *Journal of Organic Chemistry*, 1991, pp. 2161.

32. K. C. Chu, R. Schinazi, M. K. Ahn, G. V. Ullas, and Z. P. Gu. Structure-Activity Relationships of pyrimidine nucleosides as antiviral agents for human immunodeficiency virus type 1 in peripheral blood mononuclear cells. *Journal of Medicinal Chemistry*, Vol. 32, No. 3, 1989, pp. 612-617.

33. T. Cihlar, and A. S. Ray. Nucleoside and nucleotide HIV reverse transcriptase inhibitors: 25 years after zidovudine. *Antiviral Research*, Vol. 85, No. 1, 2010, pp. 39-58.

34. A. Dunge, A. K. Chakraborti, and S. Singh. Mechanistic explanation to the variable degradation behaviour of stavudine and zidovudine under hydrolytic, oxidative and photolytic conditions. *Journal of Pharmaceutical and Biomedical Analysis*, Vol. 35, No. 4, 2004, pp. 965-970.

35. E. Livni, M. Berker, S. Hillier, S. C. Waller, M. D. Ogan, R. P. Discordia, J. K. Rienhart, R. H. Rubin, and A. J. Fischman. Preparation and pharmacokinetics of 11C labeled stavudine (d4T). *Nuclear Medicine and Biology*, Vol. 31, No. 5, 2004, pp. 613-621.

36. S. C. Sweetman. Martindale: The complete drug reference, Pharmaceutical Press, London. 1999. 33rd Edition. pp. 625-626.

37. E. De Clercq. Antiviral drug discovery and development: Where chemistry meets with biomedicine. *Antiviral Research*, Vol. 67, No. 2, 2005, pp. 56-75.

38. Stavudine. Micromedex Healthcare Series. 2012. http://0-www.thomsonhc.com.wam.seals.ac.za/micromedex2/librarian/ND_T/evidencexpert/ND_PR/evidencexpert/CS/ED96DD/ND_AppProduct/evidencexpert/DUPLICATIONSHIELDSYNC/C9B14B/ND_PG/evidencexpert/ND_B/evidencexpert/ND_P/evidencexpert/PFActionId/evidencexpert.DoIntegratedSearch?SearchTerm=stavudine [cited 6 April 2012].

39. B. D. Herman and N. Sluis-Cremer. Molecular Pharmacology of Nucleoside and Nucleotide HIV-1 Reverse Transcriptase Inhibitors. *Pharmacology*. University of Pittsburgh, Department of Medicine, Division of Infectious Diseases, Pittsburgh, USA, 2008, pp. 63-80.

40. J. Lennerstrand, D. K. Stammers and B. A. Larder. Biochemical Mechanism of Human Immunodeficiency Virus Type 1 Reverse Transcriptase Resistance to Stavudine. *Antimicrobial Agents and Chemotherapy*, Vol. 45, No. 1, 2001, pp. 2144-2146.

41. D. R. Kuritzkes, R. L. Bassett, J. D. Hazelwood, and V. A. Johnson. Rate of Thymidine Analogue Resistance Mutation Accumulation with Zidovudine- or Stavudine-Based Regimens. *Journal of Acquired Immune Deficiency Syndrome*, Vol. 36, 2004, pp. 600-603.

42. M. Pernas, and Lipez-Galndez. An HIV-1 215V mutant shows increased phenotypic resistance to d4T. *Virus Research*, Vol. 135, No. 2, 2008, pp. 340-344.

43. J. H. Knox, J. N. Done, A. F. Fell, A. Pryde, and R. A. Wall. High Perfomance Liquid Chromatography. Edinburgh University Press, Edinburgh, Scotland, 1978, pp. 1-138.

44. C. F. Simpson. Practical HPLC. The Whitefriars Press, London, UK, 1976, 30th Ed, pp. 624-641.

45. J. R. Dean, A. M. Jones, D. Holmes, R. Reed, J. Weyers, and A. Jones. Practical Skills in Chemistry. Pearson Education Ltd publishers, Essex, UK, 2002, pp. 205-208.

46. R. J. Hamilton, P. A. Sewell, Chapman, and Hall. Introduction to HPLC. 2nd Ed, London, UK, 1982, pp. 1-12.

47. L. Snyder , J. Kirkland, and J. Glajch. Practical HPLC Method Development. John Wiley and Sons Inc, USA. 1997. 2nd Ed, pp. 233-350.

48. D. J. Rusner. Maintaining and Troubleshooting HPLC Systems, John Wiley and Sons, New York, USA. 1981, pp. 4-95.

49. J. C. Berridge. Techniques for the Automated optimisation of HPLC Separation. John Wiley and Sons, New York, USA, 2012.

50. D. Watson. Pharmaceutical Analysis, Reader in Pharmaceutical Sciences, School of Pharmacy, University of Strathclyde, Glasglow, UK. 2005. 2nd Ed, pp. 267-311.

51. R. Raghavan and J. Joseph. Chromatographic methods of Analysis-High Performance Liquid chromatography. *Encyclopedia of Pharmaceutical Technology*, Marcel Decker, Inc, New York, 2002, 2 Ed, pp. 414-428.

52. W. Lough and I. Wainer. High Performance Liquid Chromatography: Fundamental Principles and Practice. Chapman and Hall, UK. Vol. 239, 1996, pp. 240.

53. Y. V. Kazakevich, HPLC for pharmaceutical scientists, John Wiley and Sons Inc. USA, 2007, pp. 2-20.

54. B. Karcher, M. Davies, E. Delaney, and J. Venit. A 21st Century HPLC Workflow for Process R&D. *Journal of the Association for Laboratory Automation*, Vol. 10, No. 6, 2005, pp. 381-393.

55. G. J. Dorsey, and K. A. Dill. Molecular Mechanism of Retention in RPLC. *Chemical Review*, Vol. 89, 1989, pp. 331-346.

56. S. N. Lanin and Y. S. Nikitin. The model of retention in HPLC with binary mobile phase. P*ure and Applied Chemistry*, Vol. 65, No. 10, 1993, pp. 2281-2286.

57. J. L. Rafferty, J. I. Siepmann, M. R. Schure and L. Zhang. Retention mechanisms in Reversed Phase Liquid Chromatography: A molecular perspective. *Analytical Chemistry*, Vol. 79, 2007, pp. 6551-6558.

58. C. Horvath. High-Performance Liquid Chromatography, Advances and perspectives. Department of Engineering and Applied Science, Yale University, New haven, Connecticut. 1980, Vol. 1, pp. 76-95.

59. C. Horvath. High-Performance Liquid chromatography. Department of engineering and Applied Science, Yale University, New Haven, Connecticut, 1980, Vol. 2, pp. 57-220.

60. Reversed Phase Chromatography, Principles and Methods. Amersham Biosciences, Amersham Place, Little Charlfont, Buckinghamshire, England HP7 9NA. 1999, pp. 1-85.

61. T. Wattananat, I. O. Prasanchaimontri and W. Akarawut. Simultaneous determination of stavudine and lamivudine in human plasma by high performance liquid chromatography and its application to a bioavailability study. *Southeast Asian Journal of Tropical Medicine Public Health*, Vol. 41, No. 2, 2010, pp. 369-377.

62. M. V. Basaveswara, A. V. D. Nagendrakumar, R. G. Venkata, and S. Arikati. Validated RP-HPLC method for the estimation of stavudine in formulation and serum. *Research Journal of Pharmaceutical, Biological and Chemical Sciences*, Vol. 2, No. 2, 2011, pp. 872-879.

63. S. Weerasak, S. Paron, R. Suwannaratana, C. Sornchaithawatwong, S. Vorarat and S. Ongart. Simultaneous determination of lamivudine, stavudine, and nevirapine in presence of their acid degradation products by HPLC. *Thai Pharmaceutical Health Sciences*, Vol. 2, No. 1, 2007, pp. 39-45.

64. S. Verma, P. Mullick, S. Bhatt, N. Siddiqui, O. Alam, and S. A. Khan. Bioanalytical method development and validation for the simultaneous estimation of lamivudine and stavudine in human plasma by HPLC. *Acta Poloniae Pharmaceutica-Drug Research*, Vol. 67, No. 4, 2010, pp. 429-437.

65. M. Sarkar, S. Khandavilli, and R. Panchagnula. Development and validation of RP-HPLC and ultraviolet spectrophotometric methods of analysis for the quantitative estimation of antiretroviral drugs in pharmaceutical dosage forms. *Journal of Chromatography B*, Vol. 830, No. 2, 2006, pp. 349-354.

66. A. Dunge, N. Sharda, B. Singh, and S. Singh. Establishment of inherent stability of stavudine and development of a validated stability-indicating HPLC assay method. *Journal of Pharmaceutical and Biomedical Analysis*, Vol. 37, No. 5, 2005, pp. 1115-1119.

67. V. Wissen, R. E. Aarnoutse, and D.M.Burger. Simultaneous determination of the HIV nucleoside analogue reverse transcriptase inhibitors lamivudine, didanosine, stavudine, zidovudine and abacavir in human plasma by reversed phase high performance liquid chromatography. *Journal of Chromatography B*, Vol. 816, 2005, pp. 121-129.

68. S. Anbazhagan, N. Indumathy, P. Shanmugapandiyan and S. K. Sridhar. Simultaneous quantification of stavudine, lamivudine and nevirapine by UV spectroscopy, reverse phase HPLC and HPTLC in tablets. *Journal of Pharmaceutical and Biomedical Analysis*, Vol. 39, No. 34, 2005, pp. 801-804.

69. J. Contreras, H. M. Gonztílez, R. Mentendez, and M. Lipez. Development and validation of a reversed-phase liquid chromatographic method for analysis of D4T (Stavudine) in rat plasma. *Journal of Chromatography B*, Vol. 801, No. 2, 2004, pp. 199-203.

70. N. Kapoor, S. Khandavilli, and R. Panchagnula. Simultaneous determination of lamivudine, stavudine and nevirapine in antiretroviral fixed dose combinations by high performance liquid chromatography. *Analytica Chimica Acta*, Vol. 570, 2006, pp. 41-45.

71. C. Josegnanababu and V. Kumar. Validated RP-HPLC method for the quantitation of stavudine in bulk and capsule dosage forms. *Journal of Pharmacy Research*, Vol. 4, No. 2, 2011, pp. 335-337.

72. S. Jayaseelan, S. Ganesh, M. Rajasekar, V. Sekar and P. Perumal. A New Analytical Method Development and Validation for the Simultaneous Estimation of Lamivudine and Stavudine in Tablet Dosage Form by Rp-Hplc Method. *International Journal of PharmTech Research*, Vol. 2, No. 2, 2010, pp. 1539-1542.

73. C. Balasekareddy, B. Awen, C. Baburao, N. Sreekanth and P. Ramalingam. Validated HPLC method for determination of lamivudine and stavudine in their formulations. *International Journal of Advances in Pharmaceutical Sciences*, Vol. 1, No. 1, 2010, pp. 22-28.

74. N. Kapoor, S. Khandavilli and R. Panchagnula. Simultaneous determination of lamivudine and stavudine in antiretroviral fixed dose combinations by first derivative spectrophotometry and high performance liquid chromatography. *Journal of Pharmaceutical and Biomedical Analysis*, Vol. 41, No. 3, 2006, pp. 761-765.

75. Waters HPLC column hardware. 2013, http://www.waters.com/waters/nav.htm?cid=10049068&locale=en_US [cited 28 January 2013].

76. Reviewer Guidance: Validation of Chromatographic Methods. 1994, http://fda/cder/guidance/cmc3.pdf [cited 29 October 2011].

77. M. A. Bezerra, R. E. Santelli, E. P. Oliveira, L. S. Villar, and L. A. I. Escaleira. Response surface methodology (RSM) as a tool for optimization in analytical chemistry. *Talanta*, Vol. 76, No. 5, 2008, pp. 965-977.

78. N. Aslan. Modeling and optimization of Multi-Gravity Separator to produce celestite concentrate. *Powder Technology*, Vol. 174, No. 3, 2007, pp. 127-133.

79. N. Aslan. Application of response surface methodology and central composite rotatable design for modeling and optimization of a multi-gravity separator for chromite concentration. *Powder Technology*, Vol. 185, No. 1, 2008, pp. 80-86.

80. N. Aslan. Application of response surface methodology and central composite rotatable design for modeling the influence of some operating variables of a Multi-Gravity Separator for coal cleaning. *Fuel*, Vol. 86, No. 56, 2007, pp. 769-776.

81. V. Hosseinpour, M. Kazemini and A. Mohammadrezaee. An experimental design approach to determine effects of the operating parameters on the rate of Ru promoted Ir carbonylation of methanol. *World Academy of Science, Engineering and Technology*, Vol. 73, 2011, pp. 598-603.

82. R. V. Lenth. Response-Surface Methods in R, Using rsm. *Journal of Statistical Software*, Vol. 32, No. 7, 2009, pp. 1-17.

83. S. Khandavilli, R. Panchagnula. Simultaneous determination of lamivudine, stavudine and nevirapine in antiretroviral fixed dose combinations by high performance liquid chromatography. *Analytica Chimica Acta*, Vol. 570, No. 1, 2006, pp. 41-45.

84. G. Openhaim and E. Grushka. Temperature-dependent refractive index issues using a UV-visible detector in high-performance liquid chromatography. *Journal of Chromatography A*, Vol. 942, No. 12, 2002, pp. 63-71.

85. M. Karmakar and R. R. Ray. Optimization of endoglucanase production in liquid state fermentation from waterhyacinth by *Rhizopus oryzae* using response surface methodology. *Australian Journal of Basic and Applied Sciences*, Vol. 5, No. 3, 2011, pp. 713-720.

86. S. M. M. Khamanga and R. B. Walker. The use of experimental design in the development of an HPLC-ECD method for the analysis of captopril. *Talanta*, 2011, 1037-1049.

87. C. P. W. G. Verweij-van, R. E. Aarnoutse and D. M. Burger. Simultaneous determination of the HIV nucleoside analogue reverse transcriptase inhibitors lamivudine, didanosine, stavudine, zidovudine and abacavir in human plasma by reversed phase high performance liquid chromatography. *Journal of Chromatography B*, Vol. 816, No. 12, 2005, pp. 121-129.

88. ICH Harmonised Tripartite Guideline: Validation of Analytical Procedures: Methodology, Q2 (R1). 2005.

89. N. Toomula, A. Kumar, S. Kumar and V. S. Bheemidi. Development and Validation of Analytical Methods for Pharmaceuticals. *Analytical & Bioanalytical Techniques*, Vol. 2, No. 5, 2011, pp. 1-4.

90. G. Ngwa. Forced Degradation as an Integral Part of HPLC Stability-Indicating Method Development. *Journal of Drug Delivery Technology*, Vol. 10, No. 5, 2010, pp. 1-5.

91. D. W. Reynolds, K. L. Facchine, J. F. Mullaney, K. M. Alsante, T. D. Hatajik and M. G. Motto. Available Guidance and Best Practices for Conducting Forced Degradation Studies. *Journal of Pharmaceutical Technology*, 2002, pp. 48-56.

92. International Conference on Harmonisation of Technical Requirements for Registration of Pharmaceuticals for Human Use. Stability testing: Photostability Testing of New Drug substances and products (Q1B). 2003, http://www.ich.org/LOB/media/MEDIA412.pdf [cited 22 May 2012].

93. M. Bakshi, S. Singh. Development of validated stability-indicating assay methods critical review. *Journal of Pharmaceutical and Biomedical Analysis*, Vol. 28, No. 6, 2002, pp. 1011-1040.

94. M.Gibson. Pharmaceutical Preformulation and Formulation. Informa Healthcare USA, Inc.52 Vanderbilt AvenueNew York, NY 10017. 2009, pp. 367.

95. M. C. Adeyeye and H. G. Brittain. Preformulation in Solid Dosage Form Development. Informa HealthCare. 2008, 1st Ed.

96. K. N. Gohil ,P. M. Patel, and N. M. Patel. Application of analytical techniques in preformulation study: a review. *International Journal of Pharmaceutical and Biological Archives*, Vol. 2, No. 5, 2005, pp. 1319-1326.

97. A. Burger . Differential thermal analysis and differential scanning calorimetry: basis, methods and use. *Pharm Unserer Zeit*, Vol. 11, No. 6, 1982, pp. 177-189.

98. S. P. Stodghill. Thermal Analysis – A Review of Techniques and Applications in the Pharmaceutical Sciences. *American Pharmaceutical Review*, Vol. 13, No. 2, 2010.

99. A. Li Wan Po. Application of Differential Scanning Calorimetry in Pharmacy: Prediction of Solid State Stability of Drugs. 1986, Vol. 23, pp. 391.

100. A. Smith. Use of Thermal Analysis in Predicting Drug-Excipient Interactions. 1982, Vol. 19, No. 12 pp. 559-561.

101. M. J. Hardly. Drug-Excipient Compatibility Prediction by DSC. 1982, Vol. 19, No. 12 pp. 559-561.

102. S. D. Clas, C. R. Dalton, and B. C. Hancock. Differential scanning calorimetry: applications in drug development. *Pharmaceutical Science Technology Today*, Vol. 2, No. 8, 1999, pp. 311-320.

103. F. Balestrieri, A. D. Magri, A. L. Magri, D. Marini, and A. Sacchini. Aplication of Differential Scanning Calorimetry to the study of Drug-Excipient compatibility. 1996, Vol. 285, No. 2 pp. 337-345.

104. J. L. Ford and P.Timmins. *Pharmaceutical Thermal Analysis: Techniques and Applications*, Halsted Press, New York. 1989.

105. F. I. Khattab. Thermal analysis of pharmaceutical compounds: The use of differential scanning calorimetry in the analysis of certain pharmaceuticals. *Thermochimica Acta*, Vol. 61, 1983, pp. 253-268.

106. J. H. Flynn. Thermodynamic properties from differential scanning calorimetry by calorimetric methods. *Thermochimica Acta*, Vol. 8, No. 12, 1974, pp. 69-81.

107. D. Q. M. Craig. A review of thermal methods used for the analysis of the crystal form, solution thermodynamics and glass transition behaviour of polyethylene glycols. *Thermochimica Acta*, Vol. 248, 2005, pp. 189-203.

108. D.Giro. Applications of thermal analysis and coupled techniques in pharmaceutical industry," *Journal of Thermal Analysis and Calorimetry*, 2002, Vol. 68, pp. 335-357.

109. M. Yoshida, E. Gomes, C. Soares, A. Cunha, and M. Oliveira. Thermal Analysis Applied to Verapamil Hydrochloride Characterization in Pharmaceutical Formulations. *Molecules*, Vol. 15, 2010, pp. 2439-2452.

110. C. P. S. Hsu. Infrared Spectroscopy. Handbook of instrumental techniques for analytical chemistry Separation sciences, Research and Product Development Mallinckrodt, Inc. Mallinckrodt Baker Division. 2012, pp. 247-283.

111. C. Gendrin, Y. Roggo and C. Collet. Pharmaceutical applications of vibrational chemical imaging and chemometrics: A review. *Journal of Pharmaceutical and Biomedical Analysis*, Vol. 48, No. 3, 2008, pp. 533-553.

112. J. Coates. Interpretation of Infrared Spectra, A Practical Approach. *Encyclopedia of Analytical Chemistry*. John Wiley and Sons Ltd, Chichester. 2000, pp. 10815-10837.

113. A. K. Burrell, G. R. Clark, J. G. Jeffrey, C. E. F. Rickard, and W. R. Roper. Migration of a hydride ligand to a difluorocarbene ligand bound to rhodium. The synthesis and crystal structure of RhCl2(CF2H)(PPh3)2. *Journal of Organometallic Chemistry*, Vol. 388, No. 3, 1990, pp. 391-408.

114. G. Peyronel, A. Pignedoli and W. Malavasi. Infrared spectra recorded on dry powder spread over KBr pellets. A comparison of the spectrum of thiourea with those recorded in KBr pellets and as Nujol mulls. *Spectrochimica Acta Part A: Molecular Spectroscopy*, Vol. 40, No. 1, 1984, pp. 63-64.

115. H. Kanai, V. Inouye, and R. Goo. Anomalous infrared spectra of diazepam in potassium bromide pellets prepared from chloroform solutions. *Analytica Chimica Acta*, Vol. 162, No. 0, 1984, pp. 427-430.

116. T. Nortia and E. Kontas. An improved potassium bromide pellet method for the measurement of i.r. spectra of hygroscopic compounds. *Spectrochimica Acta Part A: Molecular Spectroscopy*, Vol. 29, No. 7, 1973, pp. 1493-1495.

117. A. Mondal, N. Mukherjee, S. Kumar Bhar and D. Banerjee. An electrochemical technique to deposit thin films of PbTe. *Thin Solid Films*, Vol. 515, No. 4, 2006, pp. 1255-1259.

118. R. C. Rowe, S. C. Owen and P. J. Sheskey. *Handbook of pharmaceutical excipients*, London, Greyslake, IL, Washington, DC: Pharmaceutical Press, American Scientists Association. 2006, 5th Ed, pp. 196, 525, 314, 326, 404, 129.

119. T. Tsujiyama, N. Suzuki, T. Kuriki, M. Kawata and S. Goto. Pharmacological evaluation of hydroxypropylcellulose-ethylcellulose microcapsules containing pinetanide. *Journal of Pharmacobiodynamics*, Vol. 13, No. 1, 1990, pp. 1-9.

120. Y. Guan, Y. Zhang, T. Zhou and S. Zhou. Stabilty of hydrogen-bonded hydroxypropylcellulose/ poly (acrylic acid) microcapsules in aqueous solutions. *Journal of Royal Society of Chemistry*, Vol. 5, 2009, pp. 842-849.

121. K. Kim and S. J. Park. Influence of glyceryl palmitostearate on release behaviours of hydroxypropylcellulose microcapsules containing Indomethacin by W/O emulsion. *Macromolecular research*, Vol. 19, No. 11, 2013, pp. 1121-1126.

122. S. M. Khamanga and R. B. Walker. Formulation and evaluation of captopril loaded polymethacrylate and hydroxypropyl methycellulose microcapsules. 2010. PhD thesis, Rhodes University, Grahamstown, South Africa.

123. Eudragit. Technical Information. Rohm Pharma, Darmstadt, Germany. 2013.

124. S. Haznedar and B. Dortunto. Preparation and in vitro evaluation of Eudragit microspheres containing acetazolamide. *International Journal of Pharmaceutics*, Vol. 269, No. 1, 2004, pp. 131-140.

125. S. M. Khamanga, N. Parfitt, T. Nyamuzhiwa, H. Haidula and R. B. Walker. The evaluation of Eudragit^{Ò} microcapsules manufactured by solvent evaporation using USP apparatus 1. *Dissolution Technologies*, Vol. 5, No. 22, 2009, pp. 15-22.

126. K. Tahara, K. Yamamoto and T. Nishihata. Overall Mechanism Behind Matrix Sustained Release (SR) Tablets Prepared with Hydroxypropylmethycellulose. *Journal of Controlled Release*, Vol. 35, No. 1, 1995, pp. 59-66.

127. A. Maschke, U. Klumpp and K. Kolter. *Effect of Copovidone on the release profile of theophylline SR Kollidon® SR matrices*. BASF SE, Development Pharma Ingredients, 67055, Ludwigshafen, Germany. 2008.

128. V. Buhler. Pharmaceutical Technology of BASF excipients, The Chemical Company, Germany. 2008, pp. 71-151.

129. M. Saravanakumar, N. Venkateswaramurthy, D. Dhachinamoorthi and P. Perumal . Extended release matrix tablets of Stavudine: Formulation and in vitro evaluation. *Asian journal of pharmaceutics*, Vol. 4, No. 3, 2010, pp. 219-223.

130. K. D. Wagh, K. Sundaramoorthy and T. Vetrichelvan. Formulation and In-vitro evaluation of stomach specific drug delivery system of stavudine. *Research Journal of Pharmaceutical, Biological and Chemical Sciences*, Vol. 1, No. 4, 2010, pp. 240-251.

131. K. Dhirendra, D. Vivek, L. Shaila, P. Brajesh, R. Kavita and P. Sarvesh. Design and evaluation of sustained release matrix once daily formulation of stavudine. *International Journal of Drug Delivery*, Vol. 2, 2010, pp. 125-134.

132. S. K. Sahoo, A. A. Mallick, B. B. Barik and P. C. Senapati. Formulation and in vitro evaluation of Eudragit® Microspheres of stavudine. *Tropical Journal of Pharmaceutical Research,* Vol. 4, No. 1, 2005, pp. 369-375.

133. P. R. Narayana, K. Prakash, C. S. R. Bonepally, B. Krishnaveni, K. Shantakumari and N. M. Lakshmi. Stavudine loaded microcapsules using various cellulose polymers: preparation and in-vitro evaluation. *International Journal of Pharmaceutical Sciences and Nanotechnology*, Vol. 2, No. 2, 2009, pp. 551-556.

134. B. Mazumder, M. K. Sarkar, S. Dey and N. Roy. Effect of formulation and process variables on the characteristics of microspheres of anti-viral drug stavudine prepared by oil-in-oil solvent evaporation technique. *International Journal of Pharmacy and Pharmaceutical Sciences,* Vol. 2, No. 2, 2010, pp. 52-59.

135. V. A. Sawant, R. B. Unhlale, V. S. Shende, S. N. Borkar and V. K. Chatap. Formulation and in-*vitro* release kinetic study of stavudine from sustained release matrix tablet containing hydrophilic and hydrophobic polymers. *Indian Journal of Novel Drug Delivery*, Vol. 1, No. 1, 2009, pp. 36-41.

136. M. C. Dalakas. Peripheral neuropathy and antiretroviral drugs. *Journal of the Peripheral Nervous System*, Vol. 6, No. 1, 2001, pp. 14-20.

137. W. Lewis, B. J. Day and W. C. Copeland. Mitochondrial toxicity of NRTI antiviral drugs: an integrated cellular perspective. *Nature Reviews*, Vol. 2, 2003, pp. 812-822.

138. S. Innes, L. Levin and M. Cotton. Lipodystrophy syndrome in HIV infected children on HAART. *The South African Journal of HIV Medicine*, 2009, pp. 76-80.

139. M. Caron, C. Vigouroux, J. P. Bastard and J. Capeau. Antiretroviral-related adipocyte dysfunction and lipodystrophy in HIV-infected patients: alteration of the PPAR dependent pathways. *PPAR research*, 2009, pp. 1-10.

140. S. Innes, M. Cotton and F. Venter. Why should we still care about the stavudine dose. *The South African Journal of HIV Medicine*, 2011.

141. R. Scherzer, M. Estrella, Y. Li, S. G. Deeks, C. Grunfeld and M. G. Shlipak. Association of tenofovir exposure with kidney disease risk in HIV infection. *AIDS*, Vol. 26, 2012, pp. 1-9.

142. A. Hill. D4T: Keep it or abandon it. *Asian biomedicine*, Vol. 4, No. 4, 2010, pp. 541-546.

143. K. N. Khachane. Novel sustained release drug delivery system: review. *International Journal of Pharmaceutical Research and Development*, Vol. 3, No. 12, 2012, pp. 1-14.

144. P. Venkatesan, R. Manavalan and K. Valliappan. Microencapsulation: A vital technique in novel drug delivery system. *Journal of Pharmaceutical Sciences and Research*, Vol. 1, No. 4, 2009, pp. 26-35.

145. M. N. Singh, K. S. Y. Hemant, M. Ram and H. G. Shivakumar. Microencapsulation: A promising technique in controlled drug delivery. *Journal of Research in Pharmaceutical Sciences*, Vol. 5, No. 2, 2010, pp. 65-35.

146. S. S. Bansode, S. K. Banarjee, D. D. Gaikwad, S. L. Jadhav and R. M. Thorat. Microencapsulation: A review. *International Journal of Pharmaceutical Sciences Review and Research*, Vol. 1, No. 2, 2010, pp. 38-43.

147. S. Freitas, H. P. Merkle and B. Gander. Microencapsulation by solvent extraction/evaporation: reviewing the state of the art of microsphere preparation process technology. *Journal of Controlled Release*, Vol. 102, No. 2, 2005, pp. 313-332.

148. M. Li, O. Rouaud and D. Poncelet. Microencapsulation by solvent evaporation: State of the art for process engineering approaches. *International Journal of Pharmaceutics*, Vol. 363, No. 12, 2008, pp. 26-39.

149. ICH Topic Q3C (R4) Impurities: Guidelines for residual solvents. 2009, pp. 1-22.

150. P. B. O'Donnell and J. W. McGinity. Preparation of microspheres by the solvent evaporation technique. *Advanced Drug Delivery Reviews*, Vol. 28, No. 1, 1997, pp. 25-42.

151. T. K. Mandal and S. Tenjarla. Preparation of biodegradable microcapsules of zidovudine using solvent evaporation: Effect of the modification of aqueous phase. *International Journal of Pharmaceutics*, Vol. 137, No. 2, 1996, pp. 187-197.

152. K. Elkharraz, A. R. Ahmed, A. Dashevsky and R. Bodmeier. Encapsulation of water-soluble drugs by an o/o/o-solvent extraction microencapsulation method. *International Journal of Pharmaceutics*, Vol. 409, No. 12, 2011, pp. 89-95.

153. D. S. Jones and K. J. Pearce. An investigation of the effects of some process variables on the microencapsulation of propranolol hydrochloride by the solvent evaporation method. *International Journal of Pharmaceutics*, Vol. 118, No. 2, 1995, pp. 199-205.

154. D, Perumal. Microencapsulation of ibuprofen and Eudragit RS 100 by the emulsion solvent diffusion technique. *International Journal of Pharmaceutics*, Vol. 218, No. 12, 2001, pp. 1-11.

155. United States Pharmacopeia: USP 29-NF 24, United States Pharmacopeial Convention, Inc, Twinbrook Parkway, Rockville, MD, USA. 2012, 29 Ed, pp. 3017.

156. A. H. Kibbe, W. E. Brown, G. B. Crist, M. M. deVilliers, E. Swanepoel , A. P. Lotter and W. Liebenberg. Dissolution theory, methodology, and testing. Dissolution technologies, Inc, 9 yorkridge trail, Hockessin, DE 19707 USA, 2007, 1st Ed, pp. 1-224.

157. U. V. Banakar, W. A. Hanson, C. D. Lathia, P. M. Albertha, S. J. Vetticaden and J. H. Wood. Pharmaceutical dissolution testing, Informa Healthcare 2010, Vol. 49, pp. 1-299.

158. J. M. Aiache, N. Aoyagi, H. Blune, J. Dressman, H. D. Friedel, L. T. Grady and V. Gray. FIP Guidance for dissolution testing of solid oral products. *Dissolution Technologies*, Vol. 4, No. 4, 1997, pp. 5-14.

159. S. M. Khamanga and R. B. Walker. The Effects of Buffer Molarity, Agitation Rate, and Mesh Size on Verapamil Release from Modified-Release Mini-Tablets Using USP Apparatus 3. *Dissolution Technologies*, 2007, pp. 19-23.

160. L. X. Yu, J. T. Wang and A. S. Hussain. Evaluation of USP apparatus 3 for dissolution testing of immediate release products. *AAPS Pharmaceutical Science Technology*, Vol. 4, No. 1, 2002, pp. 1-5.

161. I. Borst, S. Ugwa and A. H. Bekett. New and extended application for USP drug release apparatus 3. *Dissolution technology*, Vol. 4, No. 1, 1997, pp. 11-16.

162. M. C. Gohel and A. F. Amin. Formulation optimization of controlled release diclofenac sodium microspheres using factorial design. *Journal of Controlled Release*, Vol. 51, No. 2, 1998, pp. 115-122.

163. J. B. Schwartz and R. E. O'Connor. Modern Pharmaceutics. Marcel Dekker, New York, 1997, 3rd Ed, pp. 727.

164. S. L. C. Ferreira, R. E. Bruns, H. S. Ferreira, G. D. Matos, J. M. David, G. C. Brandúo, E. G. P. da Silva, L. A. Portugal, P. S. dos Reis,A. S. Souza and W. N. L. dos Santos. Box-Behnken design: An alternative for the optimization of analytical methods. *Analytica Chimica Acta*, Vol. 597, No. 2, 2007, pp. 179-186.

165. N. Aslan and Y. Cebeci. Application of box-Behnken and response surface methodology for modeling of some Turkish coals. *Fuel*, Vol. 86, No. 1-2, 2007, pp. 90-97.

166. A. S. Souza, W. N. L. dos Santos and S.L.C.Ferreira. Application of box-Behnken design in the optimization of an online pre-concentration system using knotted reactor for cadmium determination by flame atomic absorption spectrometry. *Spectrochimica Acta Part B: Atomic Spectroscopy*, Vol. 60, No. 5, 2005, pp. 737-742.

167. G. E. P. Box and D. W. Behnken. Some new three level designs for the study of quantitative variables. *Technometrics*, Vol. 2, No. 4, 1960, pp. 455.

168. S. Ozgen, A. Yildiz, A. Caliskan and E. Sabah. Modeling and optimization of hydrocyclone processing of low grade bentonites. *Applied Clay Science*, Vol. 46, No. 3, 2009, pp. 305-313.

169. J. M. Bosque-Sendra, S. Pescarolo, L. Cuadros-Rodríguez , E. M. Almansa-López and A. M. García-Campaña. Optimizing analytical methods using sequential response surface methodology, Application to the pararosaniline determination of formaldehyde. *Fresenius Journal of Analytical Chemistry*, Vol. 369, No. 7, 2001, pp. 715-718.

170. G. Annadurai and R. Y. Sheeja. Use of Box-Behnken design of experiments for the adsorption of verofix red using biopolymer. *Bioprocess Engineering*, Vol. 18, 1998, pp. 463-466.

171. N. Motlekar and B. Youan. Optimization of experimental parameters for the production of LMWH-loaded polymeric microspheres. D*rug Design, Development and Therapy*, Vol. 2, 2008, pp. 39-47.

172. A. B. Solanki, J. R. Parikh and R. H. Parikh. Formulation and optimization of piroxicam proniosomes by 3-factor, 3-level Box-Behnken design. *AAPS PharmSciTech*, Vol. 8, No. 4, 2007, pp. E1-E7.

173. N. Jyothi, M. Prasanna, S. Prabha, P. S. Ramaiah, G. Srawan and S. N. Sakarkar. Microencapsulation Techniques, Factors Influencing Encapsulation Efficiency: A Review. *The Internet Journal of Nanotechnology*, Vol. 3, No. 1, 2009.

174. Y. Yeo and K. Park. Control of Encapsulation Efficiency and Initial Burst in Polymeric Microparticle Systems. *Arch Pharm Res*, Vol. 27, No. 1, 2004, pp. 1-12.

175. S. Freiberg and X. X. Zhu. Polymer microspheres for controlled drug release. *International Journal of Pharmaceutics*, Vol. 282, No. 1-2, 2004, pp. 1-18.

176. A. Biswal, D. Dinda, S. Das, K. A. Chowdary and S. Si. Encapsulation Protocol for Highly Hydrophilic Drug Using Non- Biodegradable Polymer. *International Journal of Pharmacy and Pharmaceutical Sciences*, Vol. 3, No. 2, 2011, pp. 256-259.

177. H. H. Amer, R. R. Paxton and M.Van Winkle. Methanol-Ethanol-Acetone vapor-liquid equilibria. *Industrial Engineering Chemistry*, Vol. 48, No. 1, 1956, pp. 142-146.

178. N. S. Dey, S. Majumdar and M. Rao. Multiparticulate drug delivery system for controlled release. *Tropical Journal of Pharmaceutical Research*, Vol. 7, No. 3, 2008, pp. 1067-1075.

179. R. Tanvi and D. Anupana. Novel Polymeric Combinations for Gastroretentive Microspheres of Stavudine. *International Journal of Drug Development & Research*, Vol. 3, No. 2, 2011, pp. 211-216.

180. A. Akhgari, G. Frasiabi, F. Sadeghi and M. Azimaie. Statistical optimization of indomethacin pellets coated with pH-dependent methacrylic polymers for possible colonic drug delivery. *International Journal of Pharmaceutics*, Vol. 305, No. 1GÇô2, 2005, pp. 22-30.

181. R. Mehta. Topical and transdermal Drug delivery: What a Pharmacist needs to know. 2000, http://inetce.com/articles/pdf/221-146-04-054-H01.pdf.

182. X. Huang and C. S. Brazel. On the importance and mechanisms of burst release in matrix-controlled drug delivery systems. *Journal of Controlled Release*, Vol. 73, No. 23, 2001, pp. 121-136.

183. A. S. Hasan, M. Socha, A. Lamprecht, F. E. Ghazouani, A. Sapin, M. Hoffman, P. Maincent and N. Ubrich. Effect of microencapsulation of nanoparticles on the reduction of burst release. *International Journal of Pharmaceutics*, Vol. 344, No. 1-2, 2011, pp. 53-61.

184. K. Elkharraz, A. R. Ahmed, A. Dashevsky and R. Bodmeier. Encapsulation of water-soluble drugs by an o/o/o-solvent extraction microencapsulation method. *International Journal of Pharmaceutics*, Vol. 409, No. 12, 2011, pp. 89-95.

185. P. Costa and J. M. S. Lobo. Modeling and comparison of dissolution profiles. *European Journal of Pharmaceutical Sciences*, Vol. 13, 2001, pp. 123-133.

186. H. Lokhandwala, A. Deshpande and S. Deshpande. Kinetic modeling and dissolution profiles comparison: An overview. *International Journal of Pharmaceutics and BioSciences*, Vol. 4, No. 1, 2013, pp. 728-737.

187. J. Siepmann, F. Siepmann and R. A. Siegel. Diffusion controlled drug delivery systems. *Application of controlled drug delivery, Advances in delivery Science and Technology* 2012, pp. 127-152.

188. J. Siepmann and F. Siepmann. Advances in Delivery Science and Technology. *Fundamentals and Applications of controlled release drug delivery*, 2012, pp. 153-154.

189. R. A. Siegel and M. J. Rathbone. Overview of controlled release mechanisms. Fundamentals and Applications of controlled release drug delivery. University of Minnesota, Minneapolis, USA, MN55419, 2012, pp. 19-42.

190. S. A. Chime, G. C. Onunkwo and I. Onyishi. Kinetics and Mechanisms of Drug Release from Swellable and Non Swellable Matrices: A Review. *Research Journal of Pharmaceutical, Biological and Chemical Sciences*, Vol. 4, No. 2, 2014, pp. 97-103.

191. C. S. Brazel and N. A. Peppas. Modeling of drug release from swellable polymers. *European Journal of Pharmaceutics and Biopharmaceutics*, Vol. 49, 2000, pp. 47-58.

192. J. Siepmann and F. Siepmann. Mathematical modeling of drug delivery. *International Journal of Pharmaceutics*, Vol. 364, 2008, pp. 328-343.

193. A. Gopferich and R. Langer. Modeling of polymer erosion. *Macromolecules*, Vol. 30, No. 9, 1993, pp. 4105-4112.

194. J. Siepmann and F. Gopferich. Mathematical modeling of bioerodible, polymeric drug delivery systems. *Advanced Drug Delivery Reviews*, Vol. 48, 2001, pp. 229-247.

195. S. Dash, M. N. Padala, N. Lilakanta and C. Prasanta. Kinetic modeling on drug release from controlled drug delivery systems. *Acta Poloniae Pharmaceutical and Drug Research*, Vol. 67, No. 3, 2010, pp. 217-223.

196. A. Dokoumetzidis, V. Papadopoulou and P. Macheras. Analysis of dissolution data using modified versios of Noyess-Whitney equation and the Weibull function. *Pharmaceutical Research*, Vol. 23, No. 2, 2006, pp. 256-261.

197. G. Singhvi and M. Singh. Review: in-vitro drug release characterization models. *International Journal of Pharmaceutical Studies and Research*, Vol. 2, No. 1, 2011, pp. 77-84.

198. B. S. Mahat. Mathematical models used in drug release studies. Thesis, Kathmandu University Dhulikhel, Nepal. 2010, pp 1-26

199. N. Yukson, A. E. Kanik and T. Baykara. Comparison of in-*vitro* dissolution profiles by ANOVA-based, model dependent and model independent methods. *International Journal of Pharmaceutics*, Vol. 209, 2000, pp. 57-67.

200. T. O'Hara, A. Dunne, J. Butler and J. Devane. A review of methods used to compare dissolution data. *Plasmo Sounrces Science and Technology*, Vol. 1, No. 5, 1998, pp. 214-222.

201. J. Siepmann and N. A. Peppas. Modeling of drug release from delivery systems based on hydroxypropyl methycellulose. *Advanced Drug Delivery Reviews*, Vol. 48, 2001, pp. 139-157.

202. M. A. Kalam, M. Humayun, N. Parvez, S. Yadav, A. Garg, S. Amin, Y. Sultana and A. Ali. Release kinetics of modified pharmaceutical dosage forms:A review. *Continental Jornal of Pharmaceutical Sciences*, Vol. 1, 2007, pp. 30-35.

203. J. Siepmann and N. A. Peppas. Higuchi equation: Derivation, applications, use and misuse. *International Journal of Pharmaceutics*, Vol. 418, No. 1, 2011, pp. 6-12.

204. S. K. Ei-Arini and H. Leuenberger. Modelling of drug release from polymer matrices: Effect of drug loading. *International Journal of Pharmaceutics*, Vol. 121, No. 2, 1995, pp. 141-148.

205. C. Moderuelo, A. Zarzuelo, and J. M. Lanao. Optimization of release kinetics from sustained release formulations using model-independent simulation. *Journal of Pharmaceutical Science*, Vol. 100, No. 8, 2011.

206. J. W. Moore and H. H. Flanner. Mathematical comparison of curves with an emphasis on in vitro dissolution profiles. *Journal of Pharmaceutical Technology*, Vol. 20, No. 6, 1996, pp. 64-67.

APPENDIX 1

BATCH PRODUCTION RECORD

Only a sample of one solvent evaporation record for ST-001 is included for this study. The production record for the other formulations manufactured and assessed are available on request.

RHODES UNIVERSITY, FACULTY OF PHARMACY, GRAHAMSTOWN, SOUTH AFRICA

BATCH PRODUCTION RECORD

Product name	Stavudine
Batch	ST-001
Batch size	5g

MANUFACTURING APPROVALS

Batch record issued by:	**Date:**
Master record issued by:	**Date:**

RHODES UNIVERSITY, FACULTY OF PHARMACY, GRAHAMSTOWN, SOUTH AFRICA

BATCH PRODUCTION RECORD

Product name	Stavudine
Batch	ST-001
Batch size	5g

MASTER FORMULA AND BATCH FORMULA

Material	% m/m (v/m)	Amount dispensed	Dispensed by	Checked
D4T	0.5g			
Eudragit® EPO	1.5g			
Avicel® 102	2.95g			
Magnesium stearate	0.05g			
Liquid paraffin	135ml			
Hexane	15ml			
Acetone	20ml			

RHODES UNIVERSITY, FACULTY OF PHARMACY, GRAHAMSTOWN, SOUTH AFRICA

BATCH PRODUCTION RECORD

Product name	Stavudine
Batch	ST-001
Batch size	5g

EQUIPMENT VERIFICATION

Description	Type	Verified by	Confirmed by
Scale	Mettler® Toledo Model AG135		
Homogenizer	Virtis®		

RHODES UNIVERSITY, FACULTY OF PHARMACY, GRAHAMSTOWN, SOUTH AFRICA

BATCH PRODUCTION RECORD

Product name	Stavudine
Batch	ST-001
Batch size	5g

MANUFACTURING DIRECTIONS

Step	Procedure	Time	Done by	Checked by
1	Weigh out the different quantities of D4T, Eudragit® EPO, Avicel® 102 and magnesium stearate			
2	Place acetone in a 100ml beaker and liquid paraffin and n-hexane in a 250ml beaker			
3	Dissolve the Eudragit® EPO in the acetone to make a polymer solution and then add the D4T, Avicel® 102 and magnesium stearate to the polymer solution			
4	Mix the acetone dispersion with the contents in the 400ml beaker			
5	Agitate at 400rpm with a three blade stirrer for 3 hours			
6	Collect the microparticles in a funnel, washed 2-3 times with n-hexane and dried at room temperature overnight. Microparticles placed in airtight container until analysis			
7	Mean particle size, microparticle flowability; encapsulation efficiency and dissolution studies were conducted.			

RHODES UNIVERSITY, FACULTY OF PHARMACY, GRAHAMSTOWN, SOUTH AFRICA

BATCH PRODUCTION RECORD

Product name	Stavudine
Batch	ST-001
Batch size	5g

SIGNATURE AND INITIAL REFERENCE

Full name (Print)	Signature	Initials	Date

APPENDIX TWO

BATCH SUMMARY

RHODES UNIVERSITY, FACULTY OF PHARMACY, GRAHAMSTOWN, SOUTH AFRICA

BATCH SUMMARY

Formulator	Chiedza Zindove	**Batch size**	5g
Product	Stavudine	**Microencapsulation time (start)**	10:00
Batch ID	ST-001	**(end)**	13:00
Microencapsulation date	20/06/2012		

Material	**Amount added**	**Rhodes #**
D4T	0.5g	RM000270
Eudragit® EPO	1.5g	RM000015
Avicel® 102	2.95g	X061882
Magnesium stearate	0.05g	RM000200
Liquid paraffin	135ml	
Hexane	15ml	
Acetone	20ml	

Production	**Model**
Top load balance	Mettler® Toledo
Homogenizer	Virtis® at 400rpm
Analysis	**Model**
SEM	Tescan, VEGA LMU
Dissolution	USP I
Temperature	21^{o}C

Dissolution and surface morphology

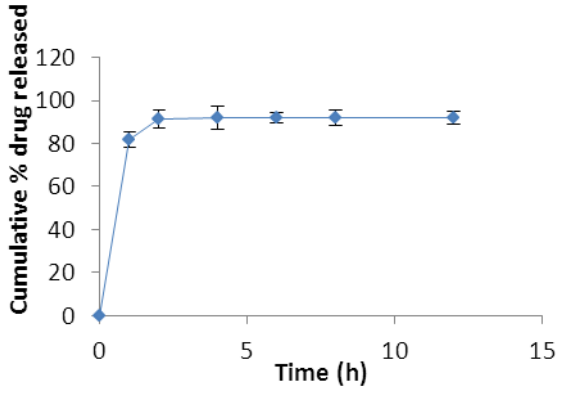

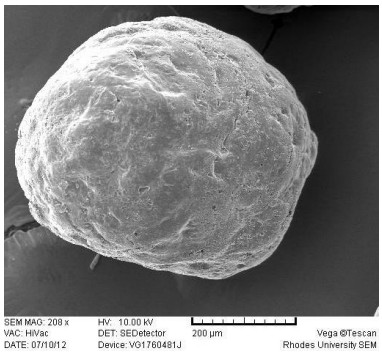

- Rough surface, reasonable flowability white microparticle.

RHODES UNIVERSITY, FACULTY OF PHARMACY, GRAHAMSTOWN, SOUTH AFRICA

BATCH SUMMARY

Formulator	Chiedza Zindove	**Batch size**	5g
Product	Stavudine	**Microencapsulation time (start)**	10:00
Batch ID	ST-002	**(end)**	13:00
Microencapsulation date	21/06 /2012		

Material	**Amount added**	**Rhodes #**	**Production**	**Model**
D4T	0.5g	RM000270	Top load balance	Mettler® Toledo
Eudragit® RSPO	1.5g	RM000023	Homogenizer	Virtis® at 400rpm
Avicel®102	2.95g	X061882		
Magnesium stearate	0.05g	RM000200	**Analysis**	**Model**
Liquid paraffin	135ml		SEM	Tescan, VEGA LMU
Hexane	15ml		Dissolution	USP I
Acetone	20ml		**Temperature**	21^{0}C

Dissolution and surface morphology

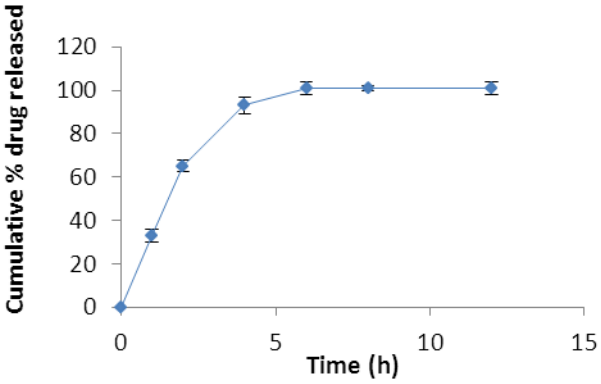

- Reasonably spherical, rough surface, reasonable flow properties and white

RHODES UNIVERSITY, FACULTY OF PHARMACY, GRAHAMSTOWN, SOUTH AFRICA

BATCH SUMMARY

Formulator	Chiedza Zindove	**Batch size**	5g
Product	Stavudine	**Microencapsulation time (start)**	10:00
Batch ID	ST-003	**(end)**	13:00
Microencapsulation date	21/06 /2012		

Material	**Amount added**	**Rhodes #**	**Production**	**Model**
D4T	0.5g	RM000270	Top load balance	Mettler® Toledo
Eudragit® RLPO	1.5g	RM000022	Homogenizer	Virtis® at 400rpm
Avicel® 102	2.95g	X061882		
Magnesium stearate	0.05g	RM000200	**Analysis**	**Model**
Liquid paraffin	135ml		SEM	Tescan, VEGA LMU
Hexane	15ml		Dissolution	USP I
Acetone	20ml		**Temperature**	21^{0}C

Dissolution and surface morphology

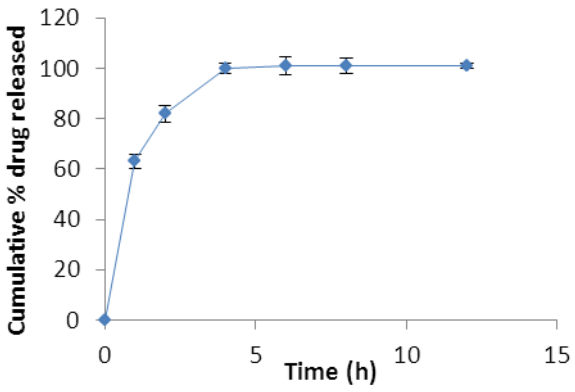

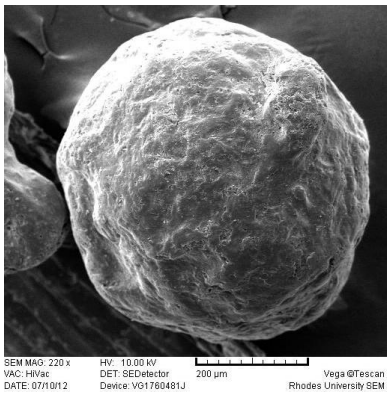

- Rough surface, reasonable flowability and white

RHODES UNIVERSITY, FACULTY OF PHARMACY, GRAHAMSTOWN, SOUTH AFRICA

BATCH SUMMARY

Formulator	Chiedza Zindove	**Batch size**	5g
Product	Stavudine	**Microencapsulation time (start)**	10:00
Batch ID	ST-004	**(end)**	13:00
Microencapsulation date	23/06 /2012		

Material	**Amount added**	**Rhodes #**	**Production**	**Model**
D4T	0.5g	RM000270	Top load balance	Mettler® Toledo
Eudragit® S100	1.5g	RM000017	Homogenizer	Virtis® at 400rpm
Avicel® 102	2.95g	X061882		
Magnesium stearate	0.05g	RM000200	**Analysis**	**Model**
Liquid paraffin	135ml		SEM	Tescan, VEGA LMU
Hexane	15ml		Dissolution	USP I
Acetone	20ml		**Temperature**	21^{0}C

Dissolution and surface morphology

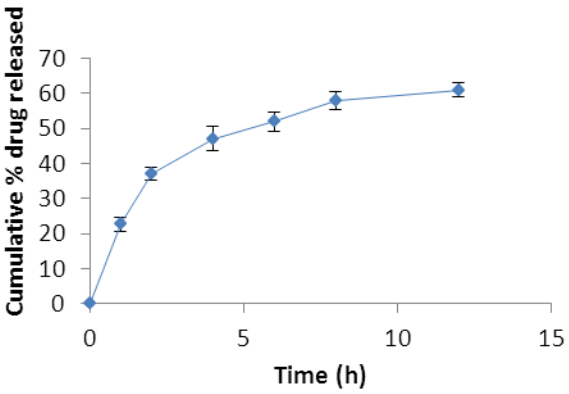

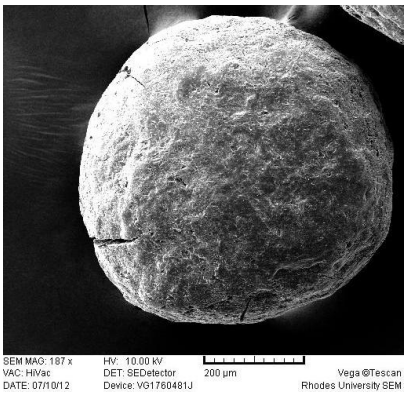

- Rough, porous, spherical, white with reasonable flow properties

RHODES UNIVERSITY, FACULTY OF PHARMACY, GRAHAMSTOWN, SOUTH AFRICA

BATCH SUMMARY

Formulator	Chiedza Zindove	**Batch size**	5g
Product	Stavudine	**Microencapsulation time (start)**	10:00
Batch ID	D4T-005	**(end)**	13:00
Microencapsulation date	24/06 /2012		

Material	**Amount added**	**Rhodes #**	**Production**	**Model**
D4T	0.5g	RM000270	Top load balance	Mettler® Toledo
Kollidon® VA 64	1.5g	RM000214	Homogenizer	Virtis® at 400rpm
Avicel® 102	2.95g	X061882		
Magnesium stearate	0.05g	RM000200	**Analysis**	**Model**
Liquid paraffin	135ml		SEM	Tescan, VEGA LMU
Hexane	15ml		Dissolution	USP I
Acetone	20ml		**Temperature**	21^{0}C

Surface morphology

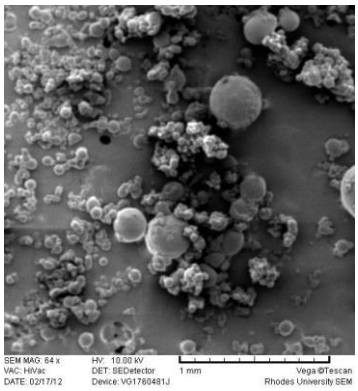

- Clustered microparticles, poor flowability, irregular shape

RHODES UNIVERSITY, FACULTY OF PHARMACY, GRAHAMSTOWN, SOUTH AFRICA

BATCH SUMMARY

Formulator	Chiedza Zindove	**Batch size**	5g
Product	Stavudine	**Microencapsulation time (start)**	10:00
Batch ID	ST-006	**(end)**	13:00
Microencapsulation date	25/06 /2012		

Material	**Amount added**	**Rhodes #**	**Production**	**Model**
D4T	0.5g	RM000270	Top load balance	Mettler® Toledo
Klucel®	1.5g	RM000064	Homogenizer	Virtis® at 400rpm
Avicel® 102	2.95g	X061882		
Magnesium stearate	0.05g	RM000200	**Analysis**	**Model**
Liquid paraffin	135ml		SEM	Tescan, VEGA LMU
Hexane	15ml		Dissolution	USP I
Acetone	20ml		**Temperature**	21^{o}C

Surface morphology

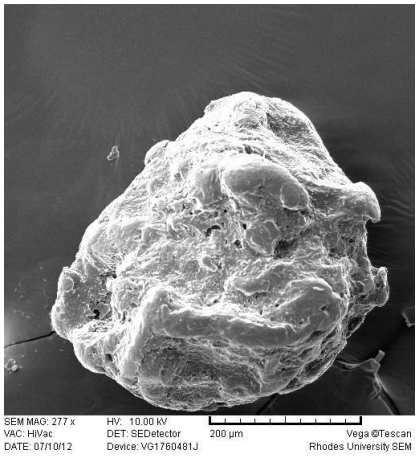

- Dough like appearance, poor flow properties, irregular shape

RHODES UNIVERSITY, FACULTY OF PHARMACY, GRAHAMSTOWN, SOUTH AFRICA

BATCH SUMMARY

Formulator	Chiedza Zindove	**Batch size**	5g
Product	Stavudine	**Microencapsulation time (start)**	10:00
Batch ID	ST-007	**(end)**	13:00
Microencapsulation date	26/06 /2012		

Material	**Amount added**	**Rhodes #**	**Production**	**Model**
D4T	0.75g	RM000270	Top load balance	Mettler® Toledo
Methocel®K4M	2.77g	RM000227	Homogenizer	Virtis® at 400rpm
Avicel® 102	0.5g	X061882		
Magnesium stearate	0.05g	RM000200	**Analysis**	**Model**
Liquid paraffin	135ml		SEM	Tescan, VEGA LMU
Hexane	15ml		Dissolution	USP I
Acetone	20ml		**Temperature**	21^{0}C

Surface morphology

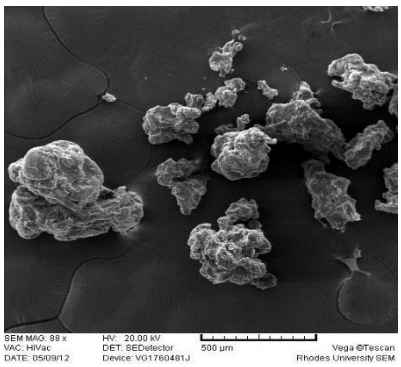

- Irregular shaped, clustered, poor flow properties

RHODES UNIVERSITY, FACULTY OF PHARMACY, GRAHAMSTOWN, SOUTH AFRICA

BATCH SUMMARY

Formulator	Chiedza Zindove	**Batch size**	5g
Product	Stavudine	**Microencapsulation time (start)**	10:00
Batch ID	ST-008	**(end)**	13:00
Microencapsulation date	27/06 /2012		

Material	**Amount added**	**Rhodes #**	**Production**	**Model**
D4T	0.5g	RM000270	Top load balance	Mettler® Toledo
Eudragit® RSPO	2.25g	RM000023	Homogenizer	Virtis® at 400rpm
Avicel® 102	2.2g	X061882		
Magnesium stearate	0.05g	RM000200	**Analysis**	**Model**
Liquid paraffin	135ml		SEM	Tescan, VEGA LMU
Hexane	15ml		Dissolution	USP I
Acetone	20ml		**Temperature**	21^{0}C

Dissolution and surface morphology

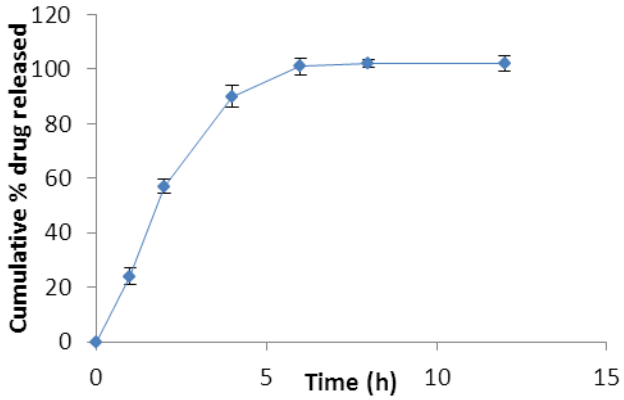

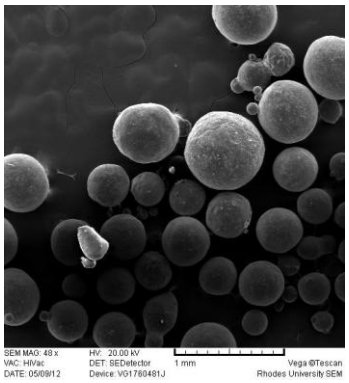

- Spherical, free-flowing, rough microparticles

RHODES UNIVERSITY, FACULTY OF PHARMACY, GRAHAMSTOWN, SOUTH AFRICA

BATCH SUMMARY

Formulator	Chiedza Zindove	**Batch size**	5g
Product	Stavudine	**Microencapsulation time (start)**	10:00
Batch ID	ST-009	**(end)**	13:00
Microencapsulation date	28/06 /2012		

Material	**Amount added**	**Rhodes #**	**Production**	**Model**
D4T	0.5g	RM000270	Top load balance	Mettler® Toledo
Eudragit® RSPO	2.25g	RM000023	Homogenizer	Virtis® at 400rpm
Eudragit®RLPO	0.75g	RM000022		
Avicel® 102	1.45g	X061882		
Magnesium stearate	0.05g	RM000200	**Analysis**	**Model**
Liquid paraffin	135ml		SEM	Tescan, VEGA LMU
Hexane	15ml		Dissolution	USP I
Acetone	20ml		**Temperature**	21^0C

Dissolution and surface morphology

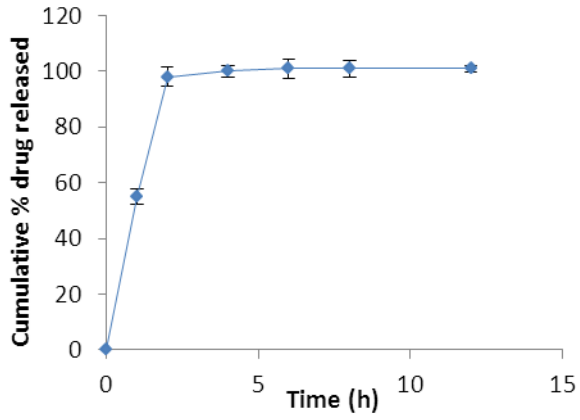

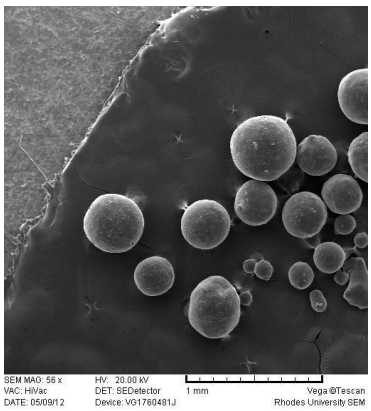

- Irregular shaped, rough, free-flowing

RHODES UNIVERSITY, FACULTY OF PHARMACY, GRAHAMSTOWN, SOUTH AFRICA

BATCH SUMMARY

Formulator	Chiedza Zindove	**Batch size**	5g
Product	Stavudine	**Microencapsulation time (start)**	10:00
Batch ID	ST-010	**(end)**	13:00
Microencapsulation date	29/06 /2012		

Material	**Amount added**	**Rhodes #**	**Production**	**Model**
D4T	0.5g	RM000270	T op load balance	Mettler® Toledo
Eudragit® S100	0.75g	RM000017	Homogenizer	Virtis® at 400rpm
Eudragit® RSPO	2.25g	RM000023		
Avicel® 102	1.45g	X061882		
Magnesium stearate	0.05g	RM000200	**Analysis**	**Model**
Liquid paraffin	135ml		SEM	Tescan, VEGA LMU
Hexane	15ml		Dissolution	USP I
Acetone	20ml		**Temperature**	21^{o}C

Dissolution and surface morphology

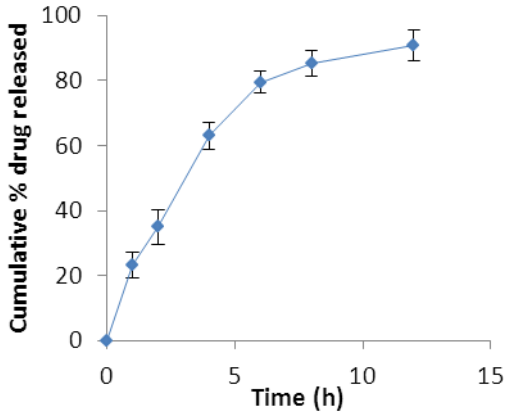

- Spherical, free-flowing, porous microparticles

RHODES UNIVERSITY, FACULTY OF PHARMACY, GRAHAMSTOWN, SOUTH AFRICA

BATCH SUMMARY

Formulator	Chiedza Zindove	**Batch size**	10g
Product	Stavudine	**Microencapsulation time (start)**	11:30
Batch ID	BB-001	**(end)**	14:30
Microencapsulation date	13/08/2012		

Material	**Amount added**	**Rhodes #**	**Production**	**Model**
D4T	1.11g	RM000270	Top load balance	Mettler® Toledo
Eudragit® RSPO	4.4g	RM000023	Homogenizer	Virtis® at 400rpm
Eudragit® S100	1.67g	RM000017		
Avicel® 102	2.67g	X061882		
Magnesium stearate	0.1g	RM000200	**Analysis**	**Model**
Liquid paraffin	135ml		SEM	Tescan, VEGA LMU
Hexane	15ml		Dissolution	Vankel® Bio-Dis® dissolution tester
Acetone	20ml		**Temperature**	21°C

Dissolution and surface morphology

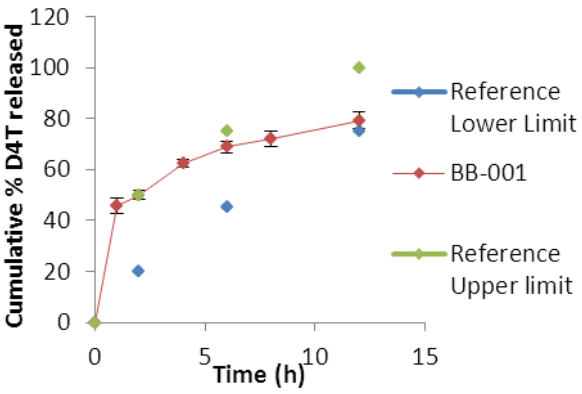

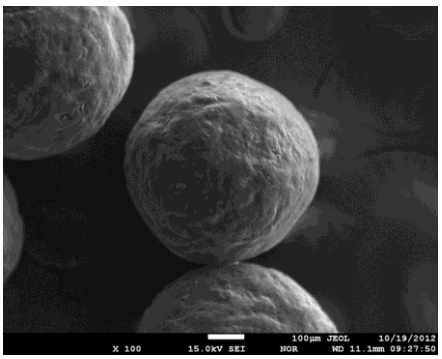

- Rough, discrete, spherical microparticles

RHODES UNIVERSITY, FACULTY OF PHARMACY, GRAHAMSTOWN, SOUTH AFRICA

BATCH SUMMARY

Formulator	Chiedza Zindove	**Batch size**	10g
Product	Stavudine	**Microencapsulation time (start)**	11:30
Batch ID	BB-002	**(end)**	14:30
Microencapsulation date	14/08//2012		

Material	**Amount added**	**Rhodes #**	**Production**	**Model**
D4T	1g	RM000270	Top load balance	Mettler® Toledo
Eudragit® RSPO	5g	RM000023	Homogenizer	Virtis® at 400rpm
Eudragit® S100	1g	RM000017		
Avicel® 102	2.9g	X061882		
Magnesium stearate	0.1g	RM000200	**Analysis**	**Model**
Liquid paraffin	135ml		SEM	Tescan, VEGA LMU
Hexane	15ml		Dissolution	Vankel® Bio-Dis® dissolution tester
Acetone	20ml		**Temperature**	21 ^{0}C

Dissolution and surface morphology

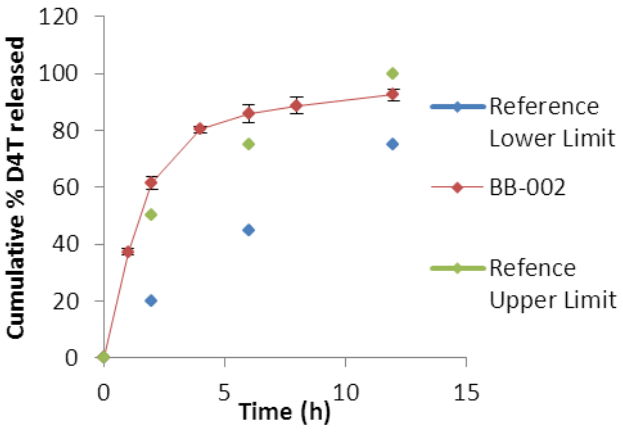

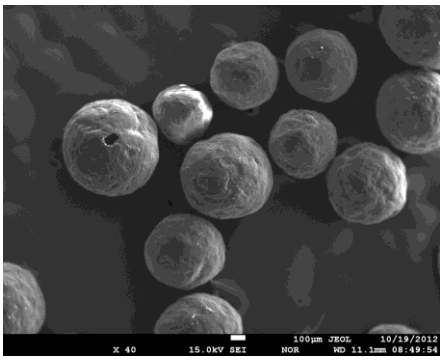

- Rough, porous, discrete and spherical microparticles

RHODES UNIVERSITY, FACULTY OF PHARMACY, GRAHAMSTOWN, SOUTH AFRICA

BATCH SUMMARY

Formulator	Chiedza Zindove	**Batch size**	10g
Product	Stavudine	**Microencapsulation time (start)**	11:30
Batch ID	BB-003	**(end)**	14:30
Microencapsulation date	15/08//2012		

Material	**Amount added**	**Rhodes #**	**Production**	**Model**
D4T	1g	RM000270	Top load balance	Mettler® Toledo
Eudragit® RSPO	4.5g	RM000023	Homogenizer	Virtis® at 400rpm
Eudragit® S100	1.5g	RM000017		
Avicel® 102	2.9g	X061882		
Magnesium stearate	0.1g	RM000200	**Analysis**	**Model**
Liquid paraffin	135ml		SEM	Tescan, VEGA LMU
Hexane	15ml		Dissolution	Vankel® Bio-Dis® dissolution tester
Acetone	20ml		**Temperature**	21 ^{0}C

Dissolution and surface morphology

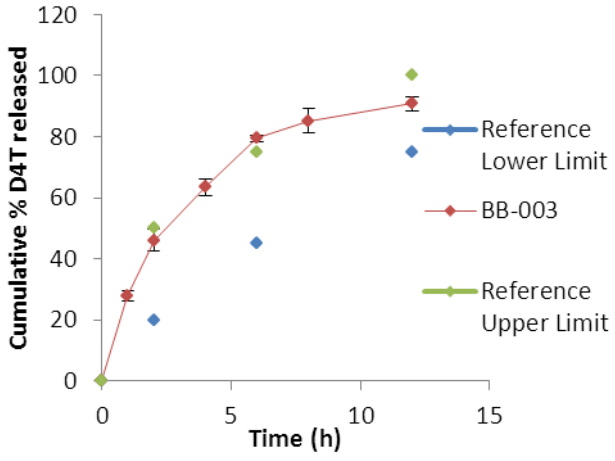

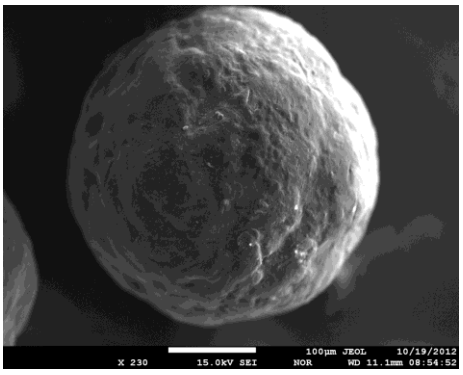

- Rough, discrete, spherical microparticles

RHODES UNIVERSITY, FACULTY OF PHARMACY, GRAHAMSTOWN, SOUTH AFRICA

BATCH SUMMARY

Formulator	Chiedza Zindove	**Batch size**	10g
Product	Stavudine	**Microencapsulation time (start)**	11:30
Batch ID	BB-004	**(end)**	14:30
Microencapsulation date	16/08/2012		

Material	**Amount added**	**Rhodes #**	**Production**	**Model**
D4T	1.11g	RM000270	Top load balance	Mettler® Toledo
Eudragit® RSPO	5g	RM000023	Homogenizer	Virtis® at 400rpm
Eudragit® S100	1.11g	RM000017		
Avicel® 102	2.67g	X061882		
Magnesium stearate	0.11g	RM000200	**Analysis**	**Model**
Liquid paraffin	135ml		SEM	Tescan, VEGA LMU
Hexane	15ml		Dissolution	Vankel® Bio-Dis® dissolution tester
Acetone	20ml		**Temperature**	21 ^{0}C

Dissolution and surface morphology

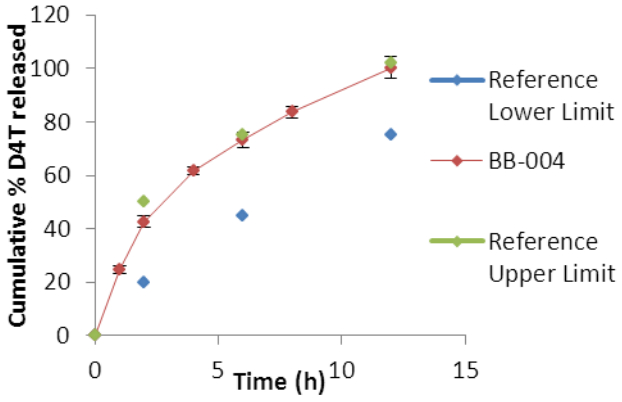

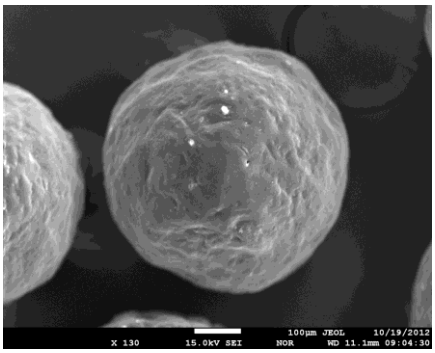

- Discrete, spherical, porous and rough microparticle

RHODES UNIVERSITY, FACULTY OF PHARMACY, GRAHAMSTOWN, SOUTH AFRICA

BATCH SUMMARY

Formulator	Chiedza Zindove	**Batch size**	10g
Product	Stavudine	**Microencapsulation time (start)**	11:30
Batch ID	BB-005	**(end)**	14:30
Microencapsulation date	17/08 /2012		

Material	**Amount added**	**Rhodes #**	**Production**	**Model**
D4T	0.91g	RM000270	Top load balance	Mettler® Toledo
Eudragit® RSPO	4.09g	RM000023	Homogenizer	Virtis® at 400rpm
Eudragit® S100	1.82g	RM000017		
Avicel® 102	3.09g	X061882		
Magnesium stearate	0.1g	RM000200	**Analysis**	**Model**
Liquid paraffin	135ml		SEM	Tescan, VEGA LMU
Hexane	15ml		Dissolution	Vankel® Bio-Dis® dissolution tester
Acetone	20ml		**Temperature**	21^{0}C

Dissolution and surface morphology

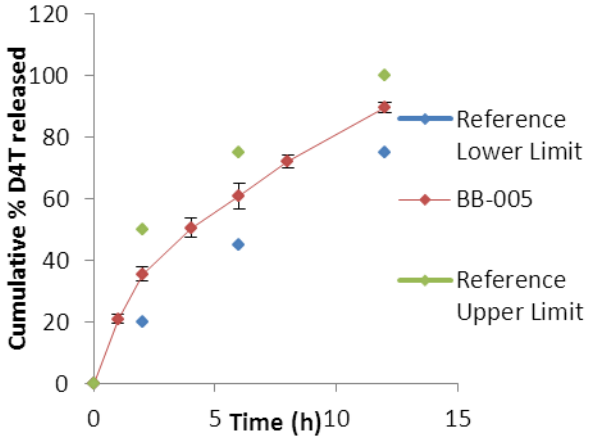

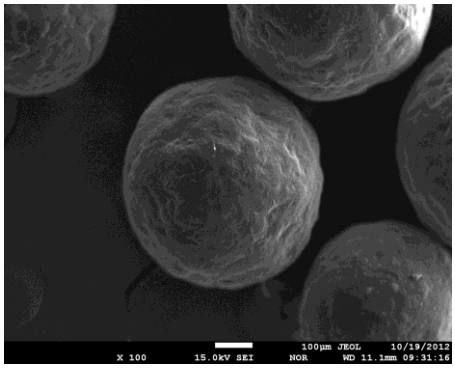

- Rough, porous, discrete and spherical microparticles

RHODES UNIVERSITY, FACULTY OF PHARMACY, GRAHAMSTOWN, SOUTH AFRICA

BATCH SUMMARY

Formulator	Chiedza Zindove	**Batch size**	10g
Product	Stavudine	**Microencapsulation time (start)**	11:30
Batch ID	BB-006	**(end)**	14:30
Microencapsulation date	18/08/2012		

Material	**Amount added**	**Rhodes #**	**Production**	**Model**
D4T	1g	RM000270	Top load balance	Mettler® Toledo
Eudragit® RSPO	4g	RM000023	Homogenizer	Virtis® at 400rpm
Eudragit® S100	2.g	RM000017		
Avicel® 102	2.9g	X061882		
Magnesium stearate	0.1g	RM000200	**Analysis**	**Model**
Liquid paraffin	135ml		SEM	Tescan, VEGA LMU
Hexane	15ml		Dissolution	Vankel® Bio-Dis® dissolution tester
Acetone	20ml		**Temperature**	21^0C

Dissolution and surface morphology

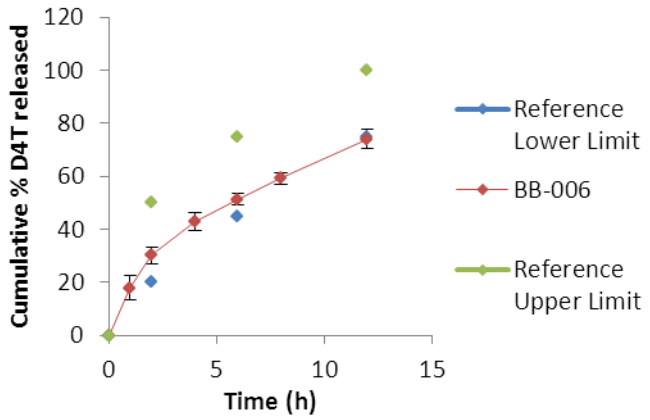

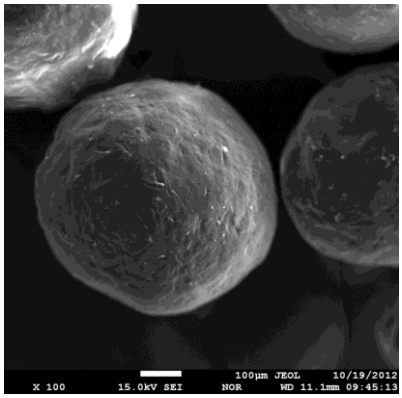

- Porous, discrete and rough microparticles

RHODES UNIVERSITY, FACULTY OF PHARMACY, GRAHAMSTOWN, SOUTH AFRICA

BATCH SUMMARY

Formulator	Chiedza Zindove	**Batch size**	10g
Product	Stavudine	**Microencapsulation time (start)**	11:30
Batch ID	BB-007	**(end)**	14:30
Microencapsulation date	19/08 /2012		

Material	**Amount added**	**Rhodes #**	**Production**	**Model**
D4T	1g	RM000270	Top load balance	Mettler® Toledo
Eudragit® RSPO	4.5g	RM000023	Homogenizer	Virtis® at 400rpm
Eudragit® S100	1.5g	RM000017		
Avicel® 102	2.9g	X061882		
Magnesium stearate	0.1g	RM000200	**Analysis**	**Model**
Liquid paraffin	135ml		SEM	Tescan, VEGA LMU
Hexane	15ml		Dissolution	Vankel® Bio-Dis® dissolution tester
Acetone	20ml		**Temperature**	21^{0}C

Dissolution and surface morphology

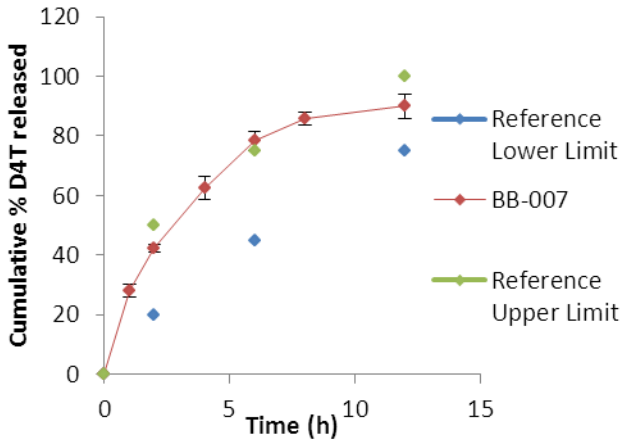

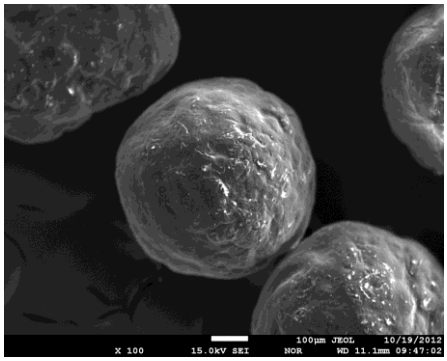

- Rough, porous, and discrete microparticles

RHODES UNIVERSITY, FACULTY OF PHARMACY, GRAHAMSTOWN, SOUTH AFRICA

BATCH SUMMARY

Formulator	Chiedza Zindove	**Batch size**	10g
Product	Stavudine	**Microencapsulation time (start)**	11:30
Batch ID	BB-008	**(end)**	14:30
Microencapsulation date	20/08 /2012		

Material	**Amount added**	**Rhodes #**	**Production**	**Model**
D4T	0.91g	RM000270	Top load balance	Mettler® Toledo
Eudragit® EPO	4.55g	RM000023	Homogenizer	Virtis® at 400rpm
Eudragit® RSPO	1.36g	RM000017		
Avicel® 102	2.64g	X061882		
Magnesium stearate	0.1g	RM000200	**Analysis**	**Model**
Liquid paraffin	135ml		SEM	Tescan, VEGA LMU
Hexane	15ml		Dissolution	Vankel® Bio-Dis® dissolution tester
Acetone	20ml		**Temperature**	21^0C

Dissolution and surface morphology

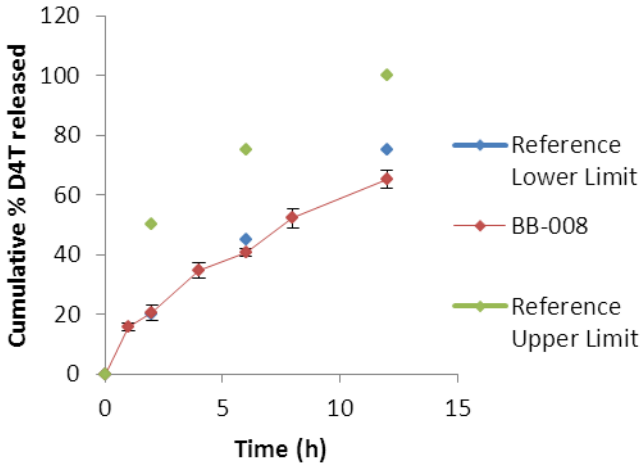

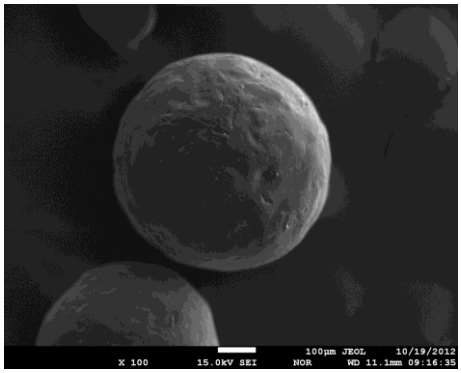

- Smooth, discrete, spherical microparticles

RHODES UNIVERSITY, FACULTY OF PHARMACY, GRAHAMSTOWN, SOUTH AFRICA

BATCH SUMMARY

Formulator	Chiedza Zindove	**Batch size**	10g
Product	Stavudine	**Microencapsulation time (start)**	11:30
Batch ID	BB-009	**(end)**	14:30
Microencapsulation date	21/08 /2012		

Material	**Amount added**	**Rhodes #**	**Production**	**Model**
D4T	1g	RM000270	Top load balance	Mettler® Toledo
Eudragit® RSPO	4.5g	RM000023	Homogenizer	Virtis® at 400rpm
Eudragit® S100	1.5g	RM000017		
Avicel® 102	0.5g	X061882		
Magnesium stearate	0.1g	RM000200	**Analysis**	**Model**
Liquid paraffin	135ml		SEM	Tescan, VEGA LMU
Hexane	15ml		Dissolution	Vankel® Bio-Dis® dissolution tester
Acetone	20ml		**Temperature**	21^0C

Dissolution and surface morphology

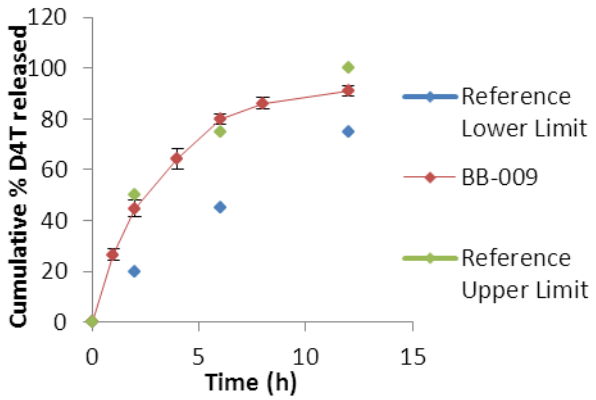

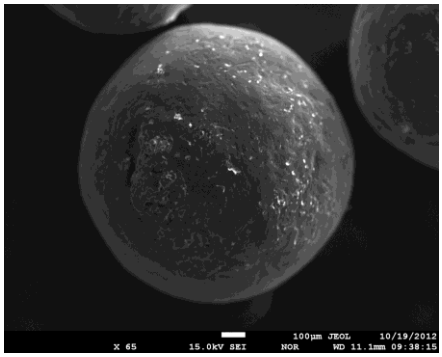

- Rough, spherical and porous microparticle

RHODES UNIVERSITY, FACULTY OF PHARMACY, GRAHAMSTOWN, SOUTH AFRICA

BATCH SUMMARY

Formulator	Chiedza Zindove	**Batch size**	10g
Product	Stavudine	**Microencapsulation time (start)**	11:30
Batch ID	BB-010	**(end)**	14:30
Microencapsulation date	22/08/2012		

Material	**Amount added**	**Rhodes #**	**Production**	**Model**
D4T	0.91g	RM000270	Top load balance	Mettler® Toledo
Eudragit® RSPO	4.55g	RM000023	Homogenizer	Virtis® at 400rpm
Eudragit® S100	1.36g	RM000017		
Avicel® 102	3.09g	X061882		
Magnesium stearate	0.1g	RM000200	**Analysis**	**Model**
Liquid paraffin	135ml		SEM	Tescan, VEGA LMU
Hexane	15ml		Dissolution	Vankel® Bio-Dis® dissolution tester
Acetone	20ml		**Temperature**	21^{0}C

Dissolution and surface morphology

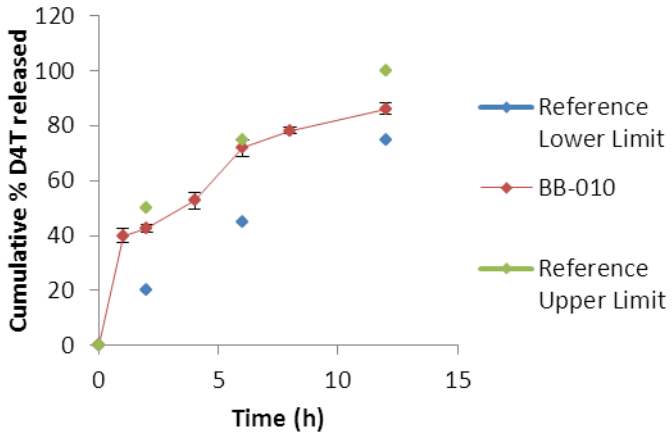

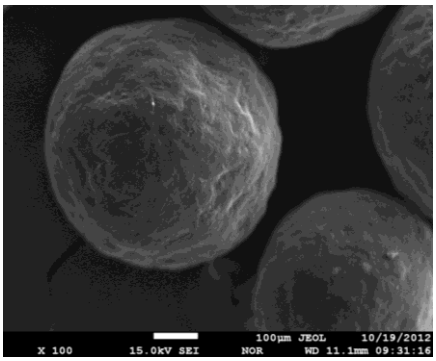

- Rough, porous, spherical and discrete microparticles

RHODES UNIVERSITY, FACULTY OF PHARMACY, GRAHAMSTOWN, SOUTH AFRICA

BATCH SUMMARY

Formulator	Chiedza Zindove	**Batch size**	10g
Product	Stavudine	**Microencapsulation time (start)**	11:30
Batch ID	BB-011	**(end)**	14:30
Microencapsulation date	23/08 /2012		

Material	**Amount added**	**Rhodes #**	**Production**	**Model**
D4T	1g	RM000270	Top load balance	Mettler® Toledo
Eudragit® RSPO	4.5g	RM000023	Homogenizer	Virtis® at 400rpm
Eudragit® S100	1.5g	RM000017		
Avicel® 102	2.9g	X061882		
Magnesium stearate	0.1g	RM000200	**Analysis**	**Model**
Liquid paraffin	135ml		SEM	Tescan, VEGA LMU
Hexane	15ml		Dissolution	Vankel® Bio-Dis® dissolution tester
Acetone	20ml		**Temperature**	21^0C

Dissolution and surface morphology

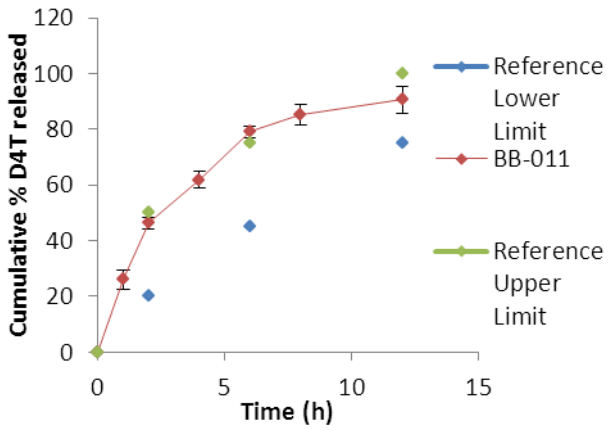

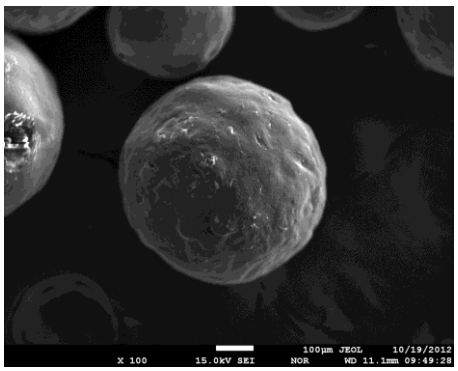

- Rough, porous, spherical and discrete microparticles

RHODES UNIVERSITY, FACULTY OF PHARMACY, GRAHAMSTOWN, SOUTH AFRICA

BATCH SUMMARY

Formulator	Chiedza Zindove	**Batch size**	10g
Product	Stavudine	**Microencapsulation time (start)**	11:30
Batch ID	BB-012	**(end)**	14:30
Microencapsulation date	24/08 /2012		

Material	**Amount added**	**Rhodes #**	**Production**	**Model**
D4T	1.11g	RM000270	Top load balance	Mettler® Toledo
Eudragit® RSPO	4.44g	RM000023	Homogenizer	Virtis® at 400rpm
Eudragit® S100	1.11g	RM000017		
Avicel® 102	3.22g	X061882		
Magnesium stearate	0.1g	RM000200	**Analysis**	**Model**
Liquid paraffin	135ml		SEM	Tescan, VEGA LMU
Hexane	15ml		Dissolution	Vankel® Bio-Dis® dissolution tester
Acetone	20ml		**Temperature**	21^{0}C

Dissolution and surface morphology

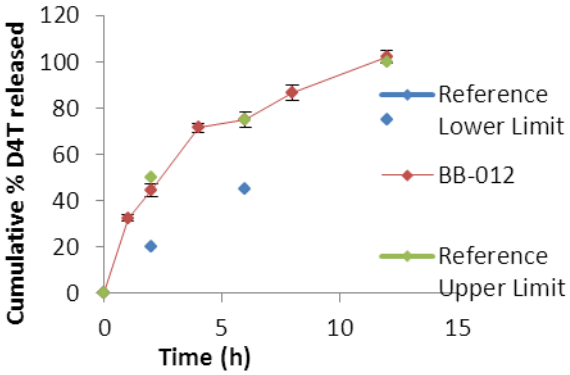

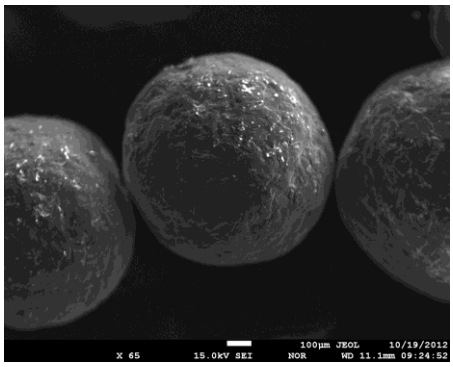

- Rough, spherical, porous and discrete microparticles

RHODES UNIVERSITY, FACULTY OF PHARMACY, GRAHAMSTOWN, SOUTH AFRICA

BATCH SUMMARY

Formulator	Chiedza Zindove	**Batch size**	10g
Product	Stavudine	**Microencapsulation time (start)**	11:30
Batch ID	BB-013	**(end)**	14:30
Microencapsulation date	25/08 /2012		

Material	**Amount added**	**Rhodes #**	**Production**	**Model**
D4T	1g	RM000270	Top load balance	Mettler® Toledo
Eudragit® RSPO	4.5g	RM000023	Homogenizer	Virtis® at 400rpm
Eudragit® S100	2.0g	RM000017		
Avicel® 102	2.4g	X061882		
Magnesium stearate	0.1g	RM000200	**Analysis**	**Model**
Liquid paraffin	135ml		SEM	Tescan, VEGA LMU
Hexane	15ml		Dissolution	Vankel® Bio-Dis® dissolution tester
Acetone	20ml		**Temperature**	21^0C

Dissolution and surface morphology

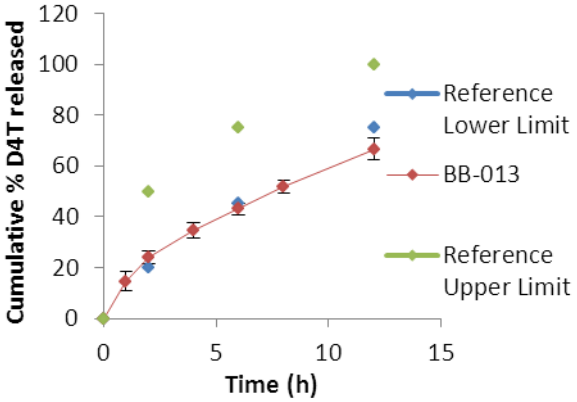

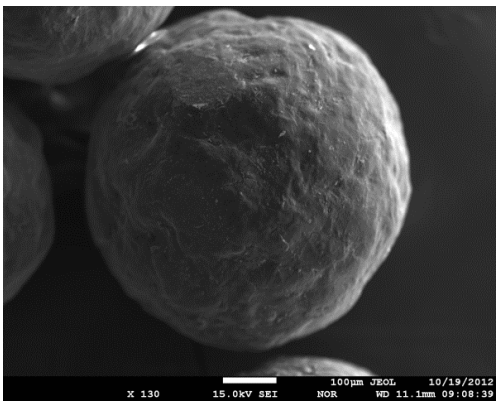

- Rough, spherical and discrete microparticle

RHODES UNIVERSITY, FACULTY OF PHARMACY, GRAHAMSTOWN, SOUTH AFRICA

BATCH SUMMARY

Formulator	Chiedza Zindove	**Batch size**	10g
Product	Stavudine	**Microencapsulation time (start)**	11:30
Batch ID	BB-014	**(end)**	14:30
Microencapsulation date	26/08 /2012		

Material	**Amount added**	**Rhodes #**	**Production**	**Model**
D4T	1g	RM000270	Top load balance	Mettler® Toledo
Eudragit®RSPO	4.5g	RM000023	Homogenizer	Virtis® at 400rpm
Eudragit® S100	1g	RM000017		
Avicel® 102	3.4g	X061882		
Magnesium stearate	0.1g	RM000200	**Analysis**	**Model**
Liquid paraffin	135ml		SEM	Tescan, VEGA LMU
Hexane	15ml		Dissolution	Vankel® Bio-Dis® dissolution tester
Acetone	20ml		**Temperature**	21^0C

Dissolution and surface morphology

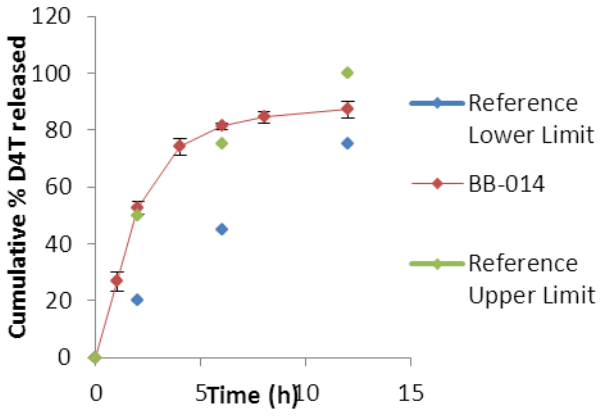

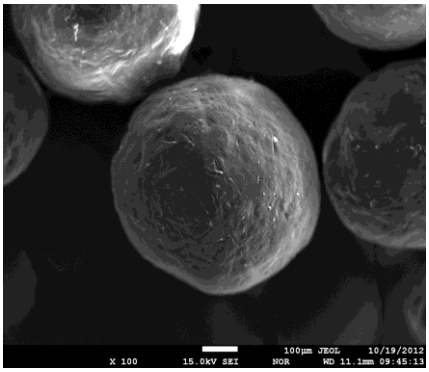

- Porous, discret, and spherical microparticles

RHODES UNIVERSITY, FACULTY OF PHARMACY, GRAHAMSTOWN, SOUTH AFRICA

BATCH SUMMARY

Formulator	Chiedza Zindove	**Batch size**	10g
Product	Stavudine	**Microencapsulation time (start)**	11:30
Batch ID	BB-015	**(end)**	14:30
Microencapsulation date	27/08 /2012		

Material	**Amount added**	**Rhodes #**	**Production**	**Model**
D4T	1g	RM000270	Top load balance	Mettler® Toledo
Eudragit® RSPO	4.5g	RM000023	Homogenizer	Virtis® at 400rpm
Eudragit® S100	1.5g	RM000017		
Avicel® 102	2.9g	X061882		
Magnesium stearate	0.1g	RM000200	**Analysis**	**Model**
Liquid paraffin	135ml		SEM	Tescan, VEGA LMU
Hexane	15ml		Dissolution	Vankel® Bio-Dis® dissolution tester
Acetone	20ml		**Temperature**	21^{0}C

Dissolution and surface morphology

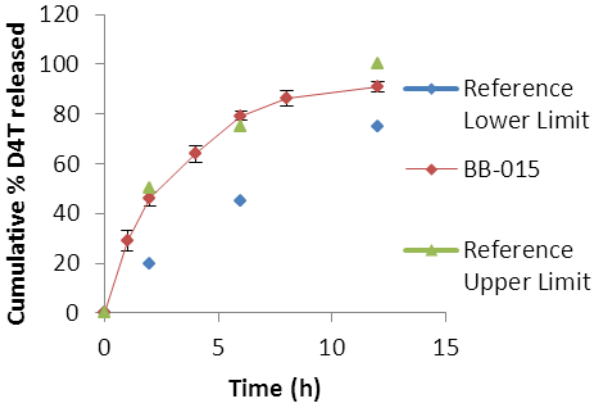

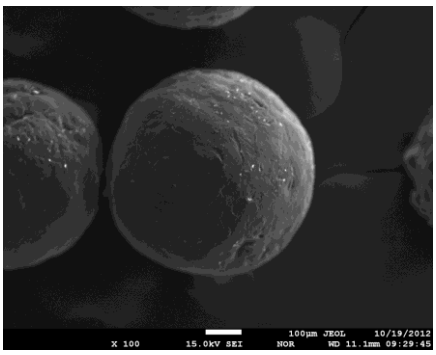

- Spherical, discrete and porous microparticles

RHODES UNIVERSITY, FACULTY OF PHARMACY, GRAHAMSTOWN, SOUTH AFRICA

BATCH SUMMARY

Formulator	Chiedza Zindove	**Batch size**	10g
Product	Stavudine	**Microencapsulation time (start)**	11:30
Batch ID	BB-016	**(end)**	14:30
Microencapsulation date	28/08/2012		

Material	**Amount added**	**Rhodes #**	**Production**	**Model**
D4T	1g	RM000270	Top load balance	Mettler® Toledo
Eudragit® RSPO	5g	RM000023	Homogenizer	Virtis® at 400rpm
Eudragit® S100	1.5g	RM000017		
Avicel® 102	2.4g	X061882		
Magnesium stearate	0.1g	RM000200	**Analysis**	**Model**
Liquid paraffin	135ml		SEM	Tescan, VEGA LMU
Hexane	15ml		Dissolution	Vankel® Bio-Dis® dissolution tester
Acetone	20ml		**Temperature**	21^{0}C

Dissolution and surface morphology

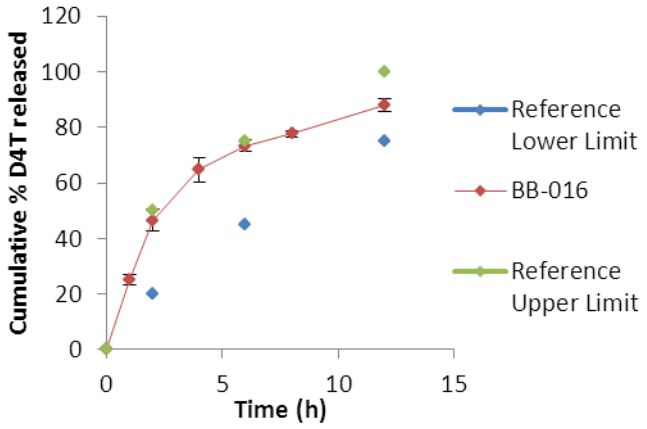

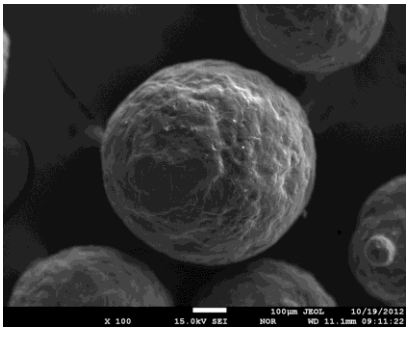

- Very rough, spherical, porous microparticles

RHODES UNIVERSITY, FACULTY OF PHARMACY, GRAHAMSTOWN, SOUTH AFRICA

BATCH SUMMARY

Formulator	Chiedza Zindove	**Batch size**	10g
Product	Stavudine	**Microencapsulation time (start)**	11:30
Batch ID	BB-017	**(end)**	14:30
Microencapsulation date	29/08 /2012		

Material	**Amount added**	**Rhodes #**	**Production**	**Model**
D4T	1g	RM000270	Top load balance	Mettler® Toledo
Eudragit® RSPO	4g	RM000023	Homogenizer	Virtis® at 400rpm
Eudragit® S100	1.5g	RM000017		
Avicel® 102	3.4g	X061882		
Magnesium stearate	0.1g	RM000200	**Analysis**	**Model**
Liquid paraffin	135ml		SEM	Tescan, VEGA LMU
Hexane	15ml		Dissolution	Vankel® Bio-Dis® dissolution tester
Acetone	20ml		**Temperature**	21^{0}C

Dissolution and surface morphology

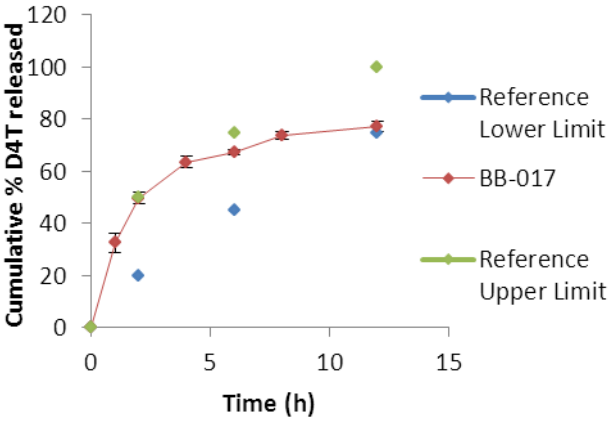

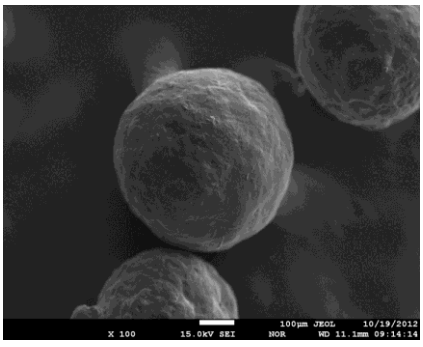

- Spherical, discrete microparticles

RHODES UNIVERSITY, FACULTY OF PHARMACY, GRAHAMSTOWN, SOUTH AFRICA

BATCH SUMMARY

Formulator	Chiedza Zindove	**Batch size**	10g
Product	Stavudine	**Microencapsulation time (start)**	11:30
Batch ID	BB-018	**(end)**	14:30
Microencapsulation date	06/09 /2012		

Material	**Amount added**	**Rhodes #**	**Production**	**Model**
D4T	1.04g	RM000270	Top load balance	Mettler® Toledo
Eudragit®RSPO	4.41 g	RM000023	Homogenizer	Virtis® at 400rpm
Eudragit® S100	1.43g	RM000017		
Avicel® 102	3.02g	X061882		
Magnesium stearate	0.1g	RM000200	**Analysis**	**Model**
Liquid paraffin	135ml		SEM	Tescan, VEGA LMU
Hexane	15ml		Dissolution	Vankel® Bio-Dis® dissolution tester
Acetone	20ml		**Temperature**	21^{0}C

Dissolution and surface morphology

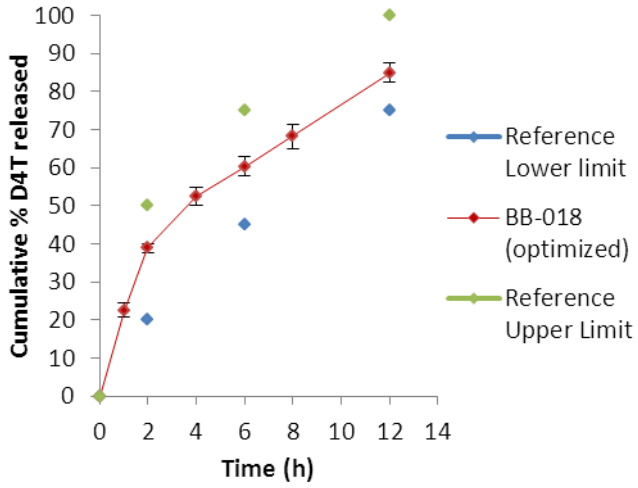

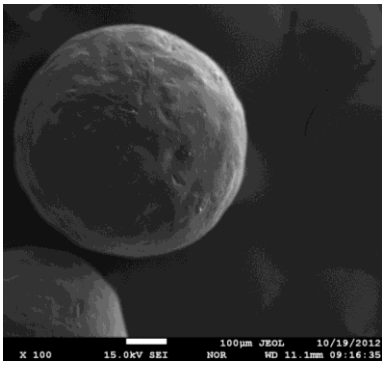

- Smooth, spherical, discrete microparticles with good flow properties

APPENDIX THREE

DIAGNOSTICS AND CONTOUR AND RESPONSE SURFACE PLOTS FOR RESPONSES MONITORED IN BOX BEHNKEN DESIGN OPTIMIZATION PROCESS

1.Diagnostic plots for response Y_3 (yield)

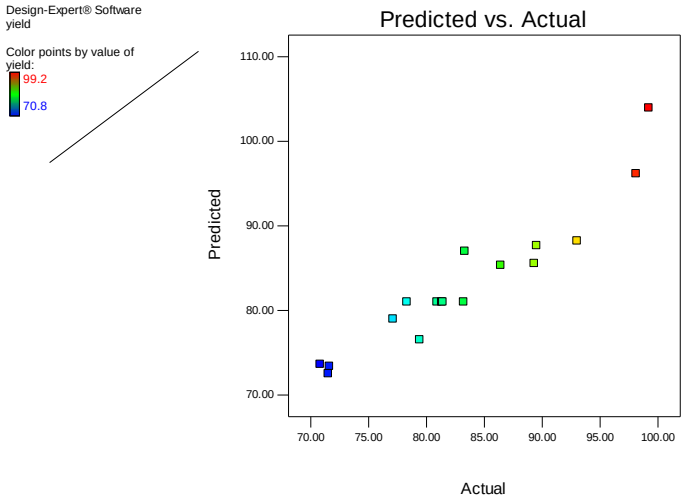

Figure Ap 3.1 Normal plot of residuals for yield

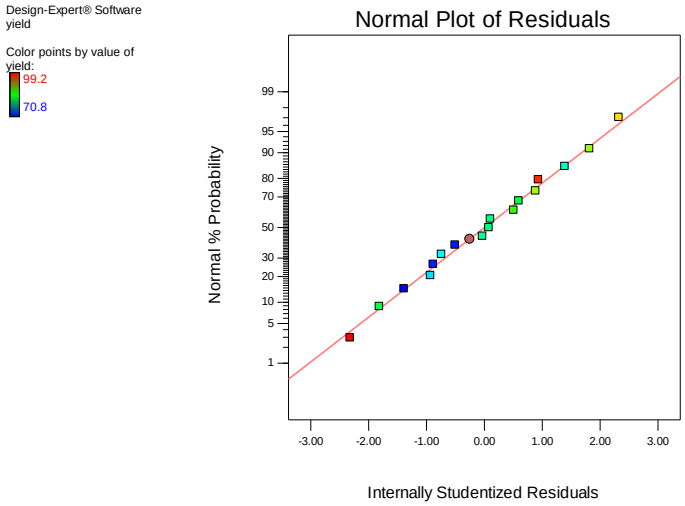

Figure Ap 3.2 Predicted versus actual plot for yield

Contour and response surface plots for response Y_3 (yield)

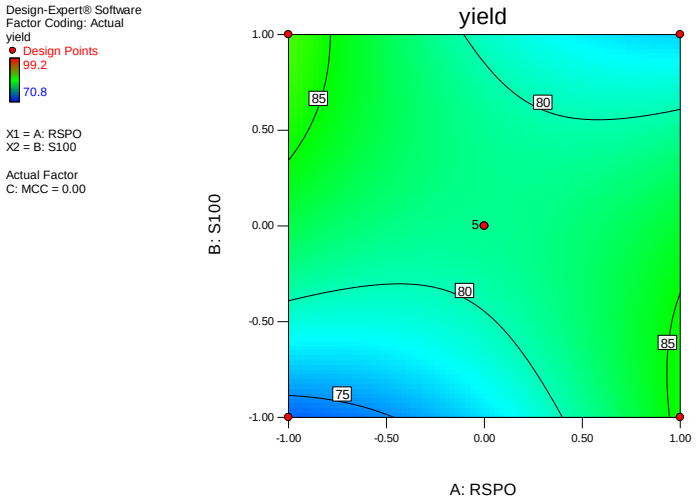

Figure Ap 3.3 Contour plot showing the effect of Eudragit® S100 and Eudragit® RSPO on yield

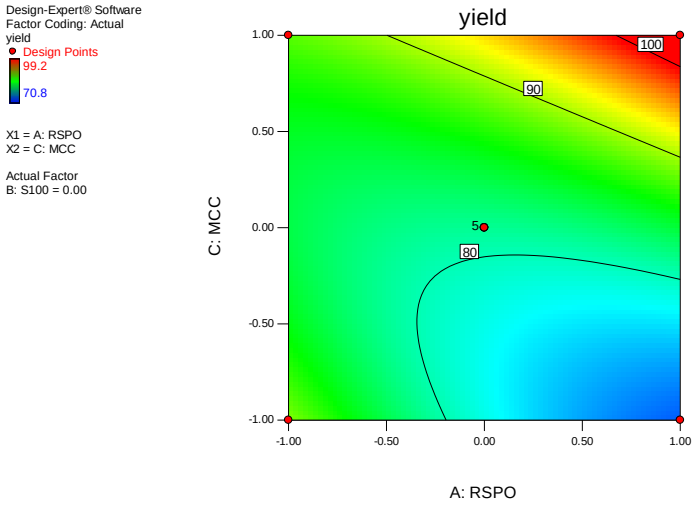

Figure Ap 3.4 Contour plot showing the effect of Eudragit® RSPO and Avicel® PH102 on yield

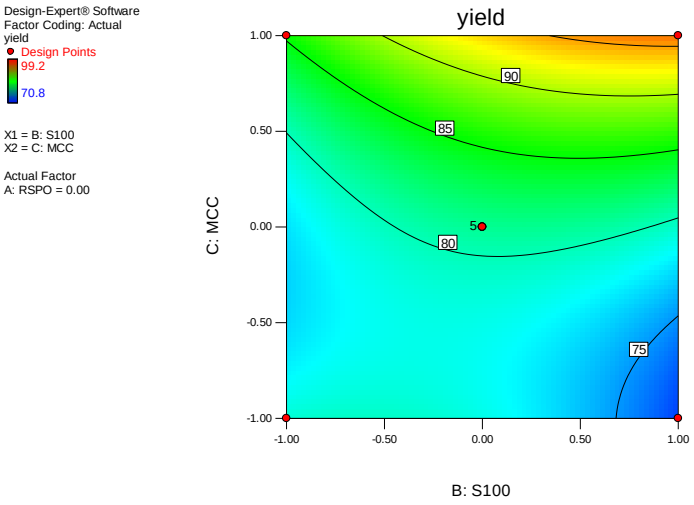

Figure Ap 3.5 Contour plot showing the effect of Eudragit® S100 and Avicel® PH102 on yield

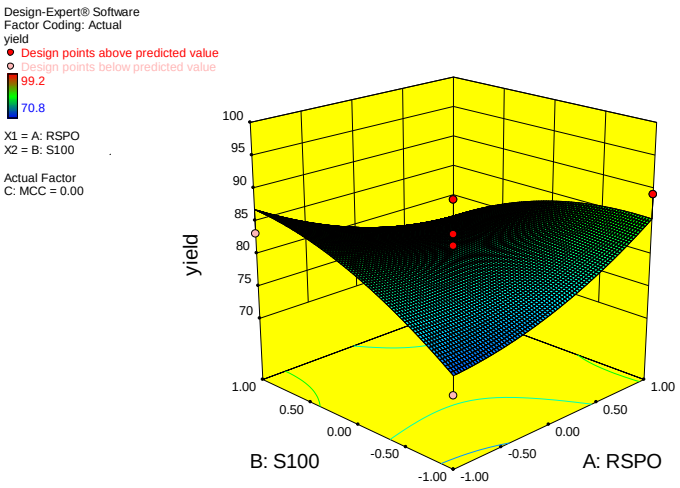

Figure Ap 3.6 Response surface plot showing the effect of Eudragit® S100 and Eudragit® RSPO on yield

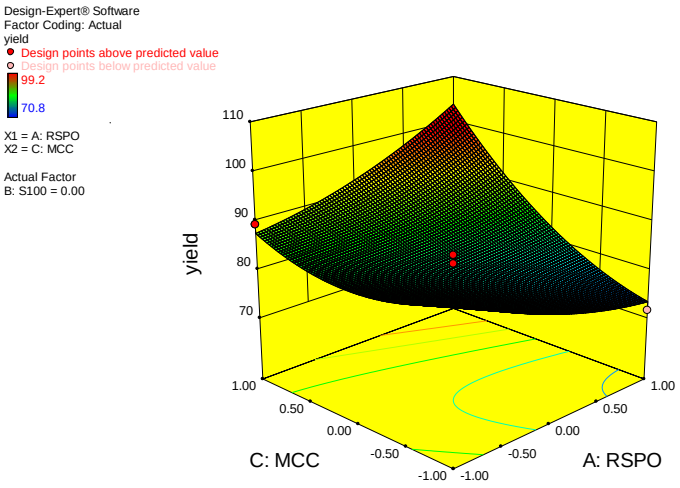

Figure Ap 3.7 Response surface plot showing the effect of Eudragit® RSPO and Avicel® PH102 on yield

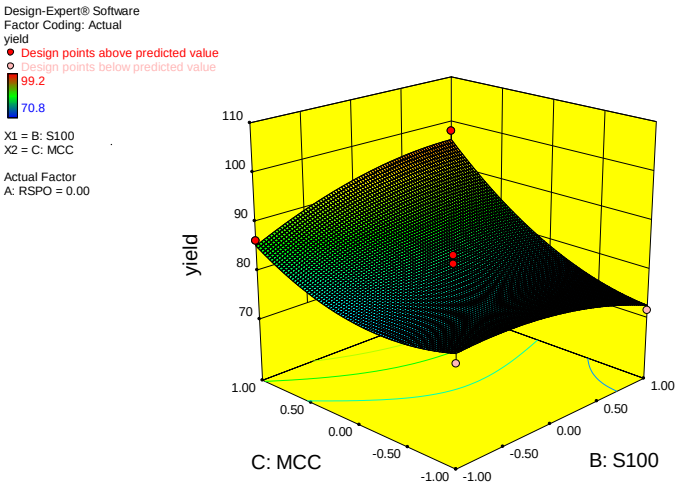

Figure Ap 3.8 Response surface plot showing the effect of Eudragit® S100 and Avicel® PH102 on yield

2.Diagnostic plots for response Y_4 (particle size)

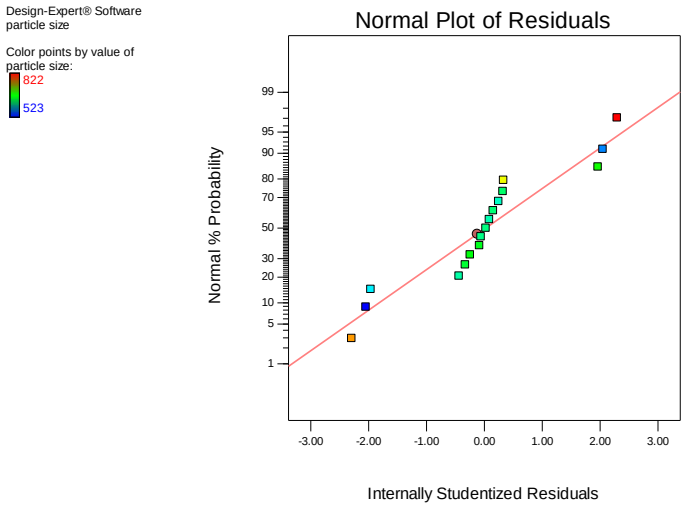

Figure Ap 3.9 Normal plot of residuals for particle size

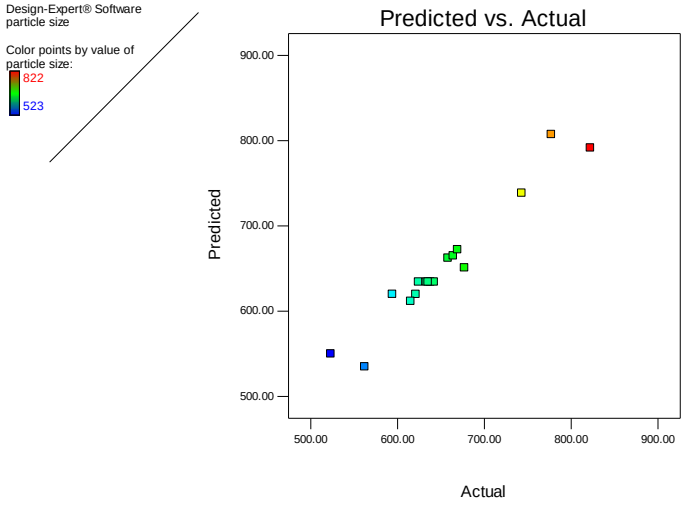

Figure Ap 3.10 Predicted versus actual plot for particle size

Contour and response surface plots for response Y_4 (particle size)

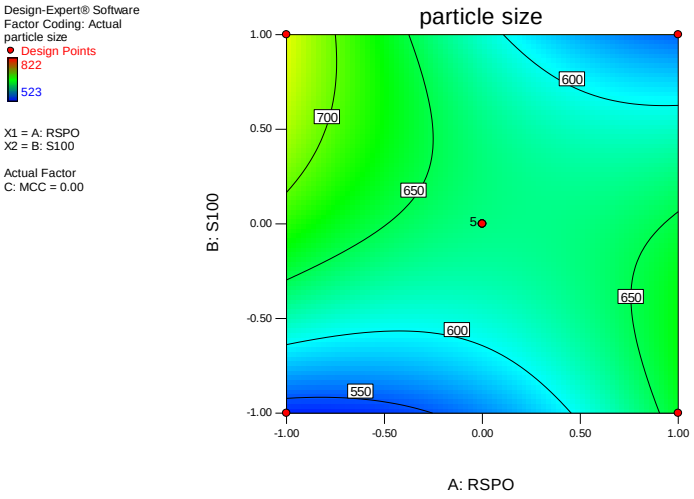

Figure Ap 3.11 Contour plot showing the effect of Eudragit® S100 and Eudragit® RSPO on particle size

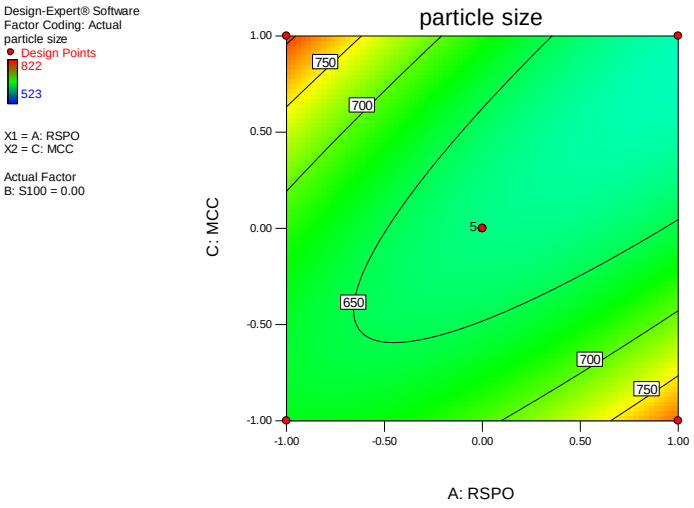

Figure Ap 3.12 Contour plot showing the effect of Eudragit® RSPO and Avicel® PH102 on particle size

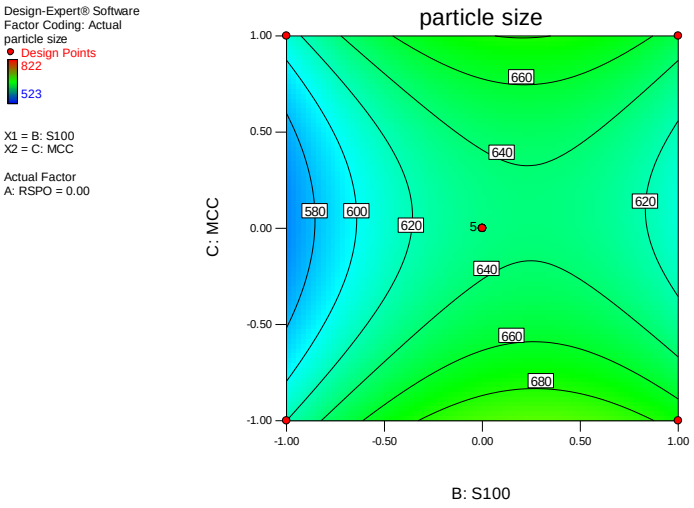

Figure Ap 3.13 Contour plot showing the effect of Eudragit® S100 and Avicel® PH102 on particle size

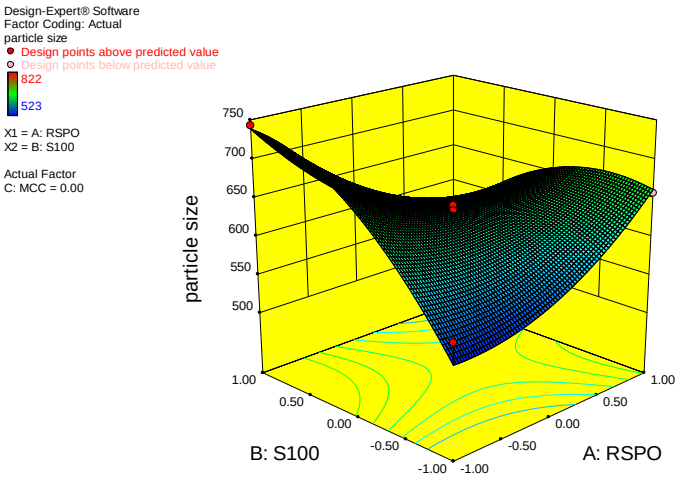

Figure Ap 3.14 Response surface plot showing the effect of Eudragit® S100 and Eudragit® RSPO on particle size

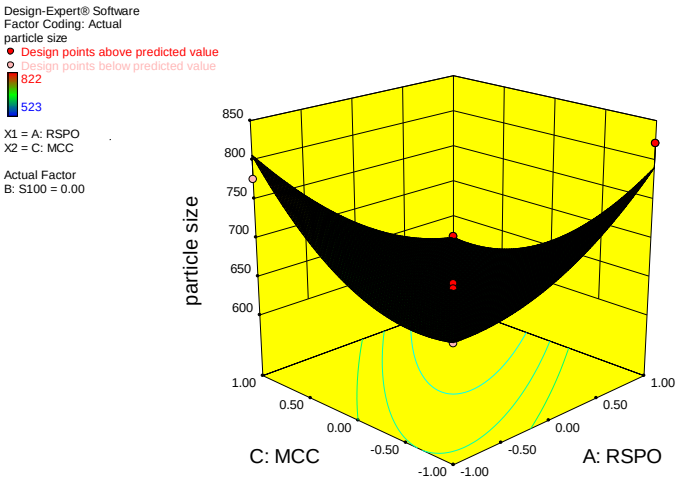

Figure Ap 3.15 Response surface plot showing the effect of Eudragit® RSPO and Avicel® PH102 on particle size

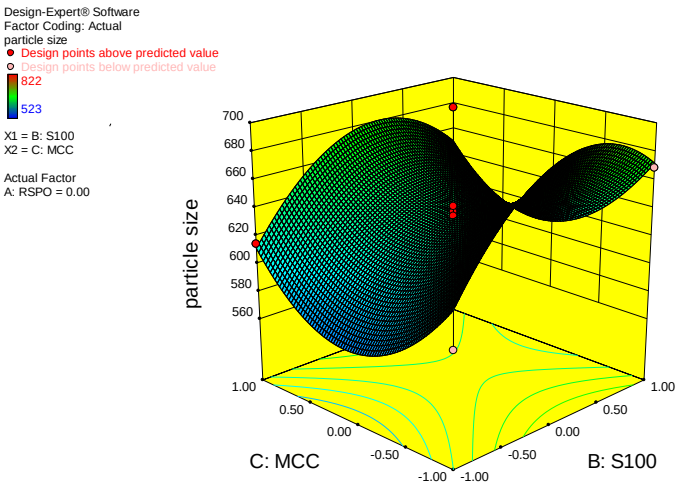

Figure Ap 3.16 Response surface plot showing the effect of Eudragit® S100 and Avicel® PH102 on particle size

3.Diagnostic plots for response Y_5 (HR)

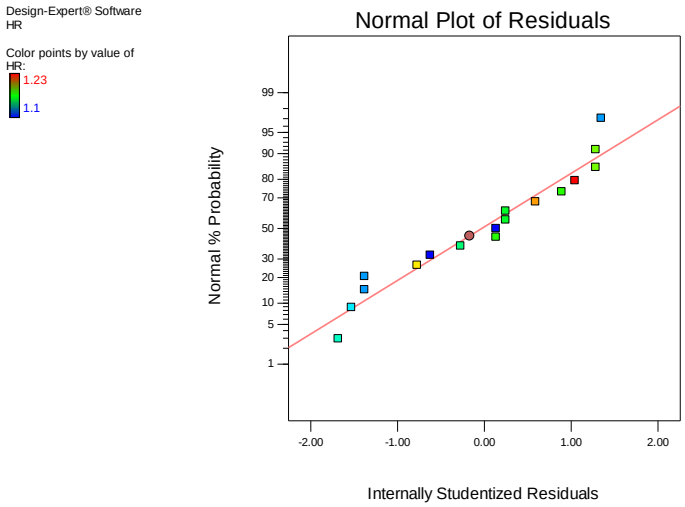

Figure Ap 3.17 Normal plot of residuals for HR

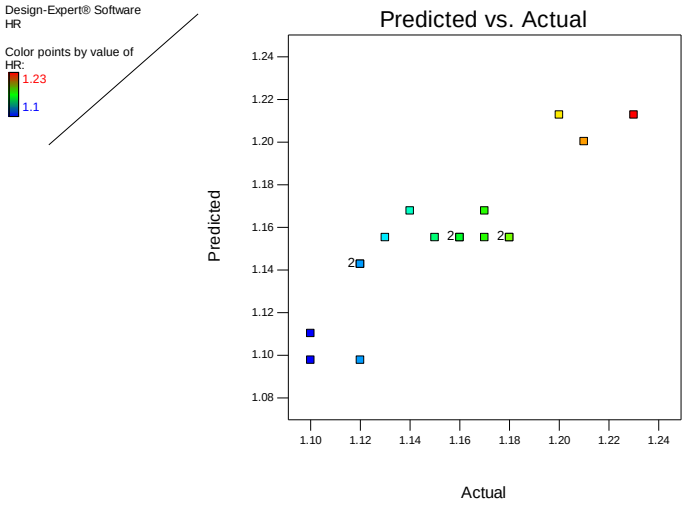

Figure Ap 3.18 Predicted versus actual plot for HR

Contour and response surface plots for response Y_5 (HR)

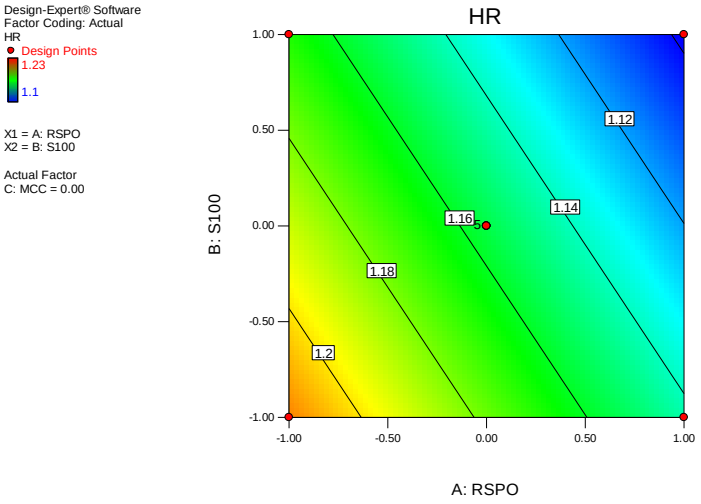

Figure Ap 3.19 Contour plot showing the effect of Eudragit® S100 and Eudragit® RSPO on HR

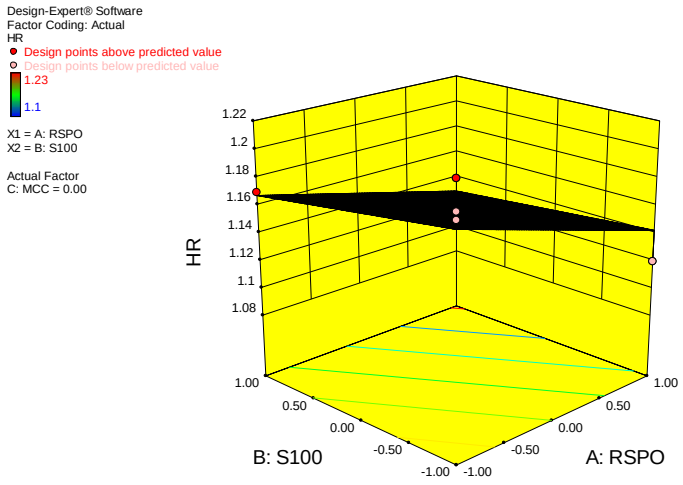

Figure Ap 3.20 Response surface plot showing the effect of Eudragit® S100 and Eudragit® RSPO on HR

4.Diagnostic plots for response Y_6 (CI)

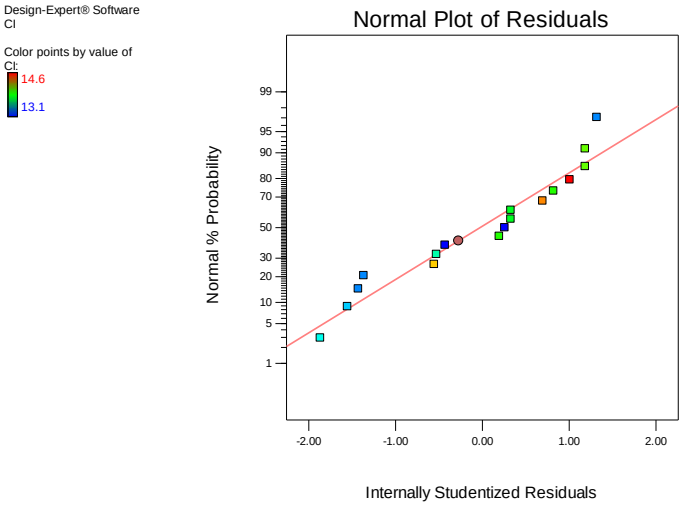

Figure Ap 3.21 Normal plot of residuals for CI

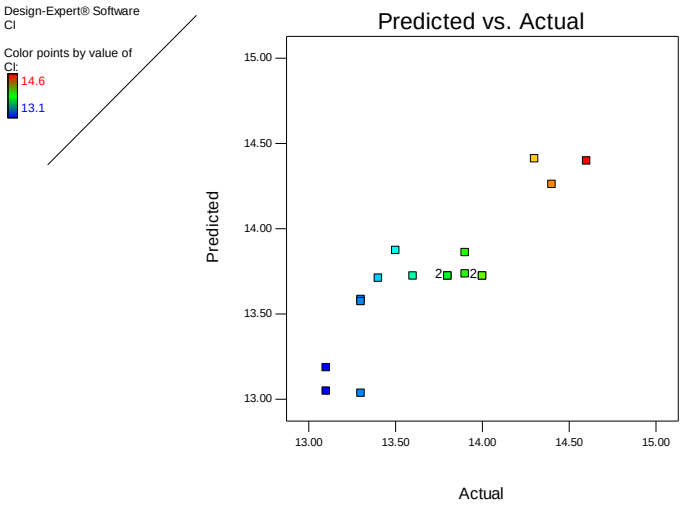

Figure Ap 3.22 Predicted versus actual plot for CI

Contour and response surface plots for response Y_6 (CI)

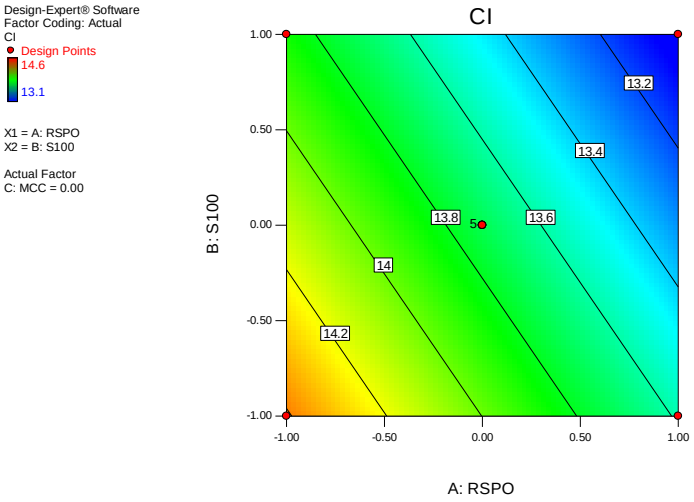

Figure Ap 3.23 Contour plot showing the effect of Eudragit® S100 and Eudragit® RSPO on CI

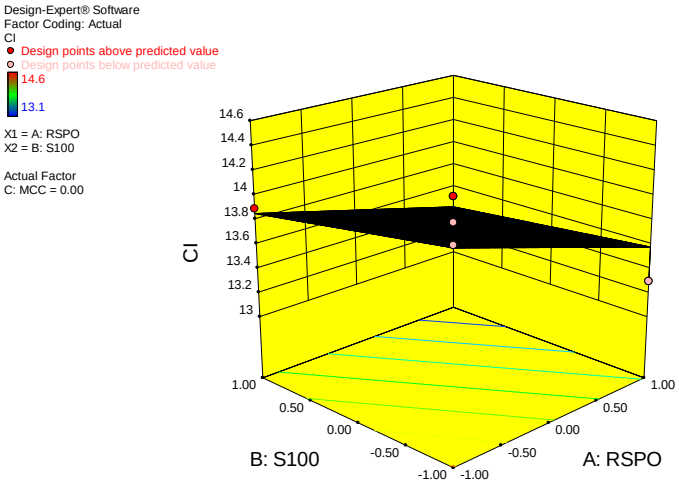

Figure Ap 3.24 Response surface plot showing the effect of Eudragit® S100 and Eudragit® RSPO on CI

5.Diagnostic plots for response Y_7 (AOR)

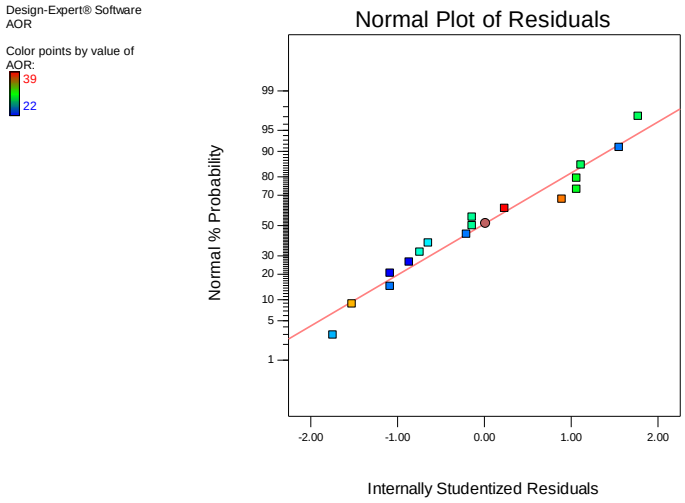

Figure Ap 3.25 Normal plot of residuals for AOR

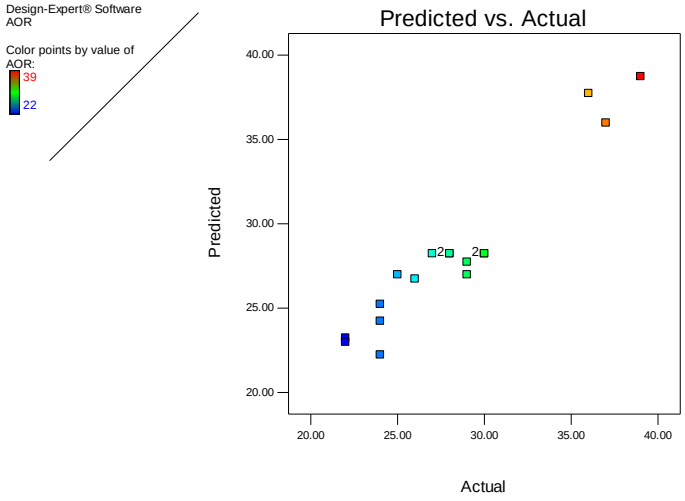

Figure Ap 3.26 Predicted versus actual plot for AOR

Contour and response surface plots for response Y_7 (AOR)

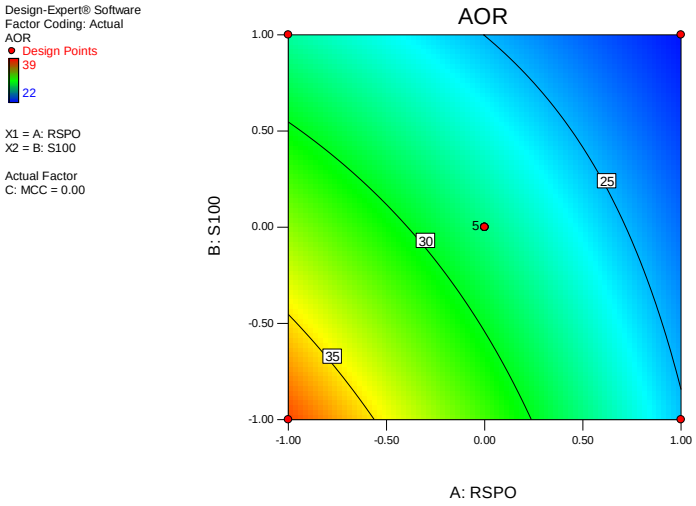

Figure Ap 3.27 Contour plot showing the effect of Eudragit® S100 and Eudragit® RSPO on AOR

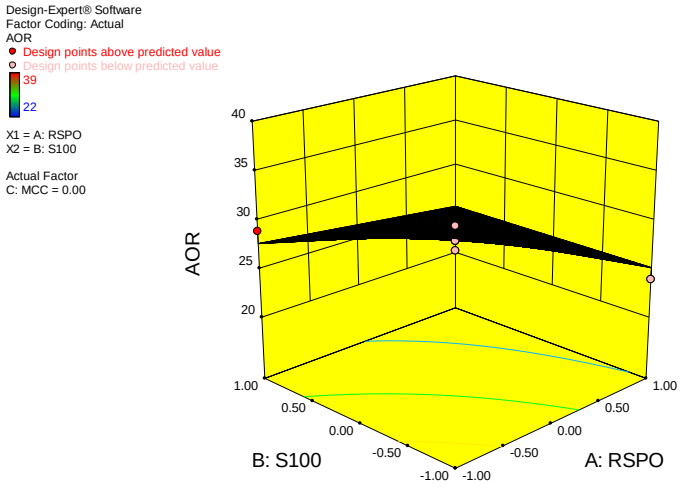

Figure Ap 3.28 Response surface plot showing the effect of Eudragit® S100 and Eudragit® RSPO on AOR

APPENDIX FOUR

HPLC OPTIMIZATION DATA

Table Ap 4.1 HPLC optimization response results

Run	Type	A Mobile Phase Concentration	B Flow rate	C Column Temperature	R_t	Peak symmetry
		% v/v	ml/min	°C	min	
1	Fact	1	-1	-1	6.4	1.3
2	Fact	-1	1	1	6.4	1.2
3	Fact	-1	-1	1	7.8	1.2
4	Axial	0	0	1.68	4	1.2
5	Axial	0	1.68	0	4.4	0.95
6	Center	0	0	0	4.8	0.95
7	Fact	-1	-1	-1	12	1.3
8	Fact	1	1	1	3.2	1
9	Fact	1	-1	1	3.6	1
10	Axial	0	0	-1.68	6.8	1.1
11	Axial	1.68	0	0	4.4	1.1
12	Axial	0	-1.68	0	4.8	1.1
13	Fact	1	1	-1	6.4	1.3
14	Center	0	0	0	4.4	1
15	Center	0	0	0	4.4	1
16	Center	0	0	0	4.4	1
17	Fact	-1	1	-1	10.4	1.3
18	Center	0	0	0	4.4	1
19	Axial	-1.68	0	0	10	1.3
20	Center	0	0	0	4.4	1

Table 4.2 Predicted versus observed data for optimized HPLC method

Response	Predicted	Observed	% Error
R_t	4.2	4	4.76
Peak symmetry	1	1	0